Universidade de Aveiro Departamento de Química
Ano 2020

IRAM MOHMOOD

CONTAMINAÇÃO DA ÁGUA COM ELEMENTOS POTENCIALMENTE TÓXICOS: PROCESSO DE REMEDIAÇÃO COM NANOPARTÍCULAS E AVALIAÇÃO DA ECOTOXICIDADE

WATER CONTAMINATION WITH POTENTIAL TOXIC ELEMENTS: REMEDIATION PROCESS WITH NANOPARTICLES AND ECOTOXICITY ASSESSMENT

Universidade de Aveiro Departamento de Química
Ano 2020

IRAM MOHMOOD

CONTAMINAÇÃO DA ÁGUA COM ELEMENTOS POTENCIALMENTE TÓXICOS: PROCESSO DE REMEDIAÇÃO COM NANOPARTÍCULAS E AVALIAÇÃO DA ECOTOXICIDADE

Tese apresentada à Universidade de Aveiro para cumprimento dos requisitos necessários à obtenção do grau de Doutor em Química, realizada sob a orientação científica do Doutor Doutora Maria Eduarda da Cunha Pereira, Professora associada do Departamento de Química da Universidade de Aveiro, da Doutora Isabel Lopes, Investigadora Principal do Departamento de Biologia da Universidade de Aveiro e da Doutora Cláudia Batista Lopes, Investigadora Doutorada do Departamento de Química da Universidade de Aveiro.

Apoio financeiro da FCT e do FSE no âmbito do QREN-POPH.Tipologia 4.1 Apoio via Bolsa de Doutoramento SFRH/ /BD/74410/2010.

I dedicate this work to my family for their continued support.

o júri

Presidente

Prof. Doutor Tito de Silva Trindade
professor Catedrático do Departamento de Química da Universidade de Aveiro

Prof. Doutor Miguel Ângelo do Carmo Pardal
professor Catedrático do Departamento de Ciências da Vida Faculdade de Ciências e Tecnologia Universidade de Coimbra

Prof.Doutor Miguel Alberto Fernandes Machado e Santos
professor Auxiliar do Departamento de Biologia da Universidade do Porto

Prof. Doutor João Carlos Mano Castro Loureiro
professor Auxiliar, Universidade de Coimbra - Faculdade de Ciências e Tecnologia

Prof. Doutor José Lino Costa
professor Auxiliar, Universidade Nova de Lisboa - Faculdade de Ciências e Tecnologia

Doutora. Rosa de Fátima Lopes de Freitas
Investigador Doutorado (nível 1), Departamento de Biologia da Universidade de Aveiro

Prof. Doutora Maria Eduarda da Cunha Pereira (Orientadora)
professora Associada do Departamento de Química da Universidade de Aveiro

.

Agradecimentos

This work would not have been possible without the advice, encouragement and friendship of some persons, to whom I wish to express my deepest thanks:
To my supervisors Dr. Cláudia Batista Lopes, Dr. Isabel Lopes and Prof. Eduarda Pereira for their supervision, support, essential opinions, guidance and patience over the last few years.
To the director of Chemistry PhD programme and Honourable Vice-Rector Professor Artur Silva for his support in numerous ways.
To my labmates for their continuous support, friendship and providing a great work environment.
To my friends, you should know that your support and encouragement was worth more than I can express on paper.
To my sister and brother providing invaluable advice and consistent encouragement.
To my parents, for they are the ones always supporting and wishing the best.
To my dear husband for his steadfast support, patience, and encouragement during this process and my children Ayat and Saqaf. You both are an inspiration to me on a daily basis to be more than what I was the day before.
To those who are no longer among us but last forever in our memory, and warm our hearts.
Finally...I want to thank all of those people who, once upon a time, were my teachers and who helped me begin this long journey.

palavras-chave

Água do mar, Organismos marinhos, Alterações Climáticas, Mercúrio, Arsénio, Cádmio, Ecotoxicidade, Índices bioquímicos, Nano remediação

Resumo

O mercúrio é reconhecido como um elemento de elevada perigosidade. Devido à sua toxicidade e persistência no ambiente existe a necessidade de removê-lo dos diversos compartimentos ambientais e de promover o desenvolvimento de novos métodos para a sua remoção, nomeadamente para um dos compartimentos onde a sua presença causa maior preocupação, a água. Uma das lacunas neste campo, é que a grande maioria das metodologias de tratamento são especificas para água doce. No entanto, águas com salinidade são muitas vezes o último recetor dos poluentes, constituindo assim um risco para o ambiente e para a Saúde Humana. Neste contexto, o presente trabalho de investigação tem como principais objetivos: (a) avaliar a eficiência de nanopartículas (NPs) de magnetite revestidas com sílica e funcionalizadas com grupos ditiocarbamato para a descontaminação de mercúrio em água do mar, na ausência e presença de outros contaminantes (arsénio, As; e cádmio, Cd); (b) avaliar a influência de um aumento da temperatura da água na eficiência das NPs na remoção ou diminuição da toxicidade da água do mar contaminada com Hg, na ausência e presença de As e Cd; e (c) avaliar a possível toxicidade das NPs utilizadas para a remoção de Hg. Para responder ao objetivo (a), os níveis de Hg em água do mar fortificada antes (solução não-remediada) e depois do processo de remediação (solução remediada) foram determinados; foi também avaliada a toxicidade de água do mar contaminada com Hg e com Hg, As e Cd, antes (solução não-remediada) e depois (solução remediada sem e com NPs) do processo de remediação, para diferentes espécies aquáticas. Para responder ao objetivo (b), simulou-se um cenário de aumento da temperatura da água e realizou-se uma análise toxicológica *ex-vivo* utilizando guelras de *Anguilla anguilla* L. para diferentes temperaturas (20 ºC foi a temperatura escolhida para comparação de resultados). A influência da temperatura foi avaliada através de marcadores bioquímicos (peroxidação lipídica, LPO; oxidação da proteína carbonilo, PC; 8-hidroxi-2'-desoxiguanosina, 8-OHdG; e da proteção antioxidante: catálase; glutationa peroxidase; glutationa redutase; glutationa S-transferase; tiol não proteico; glutationa total) antes e depois do processo de remediação adotado, e para diferentes níveis de contaminação. Para dar resposta ao objetivo (c), os possíveis efeitos adversos provocados pelas NPs foram avaliados através de ensaios toxicológicos de curta exposição (2 - 72 h) de *A. anguilla* às NPs, e às NPs com Hg, em condições *in vitro*. Foram avaliados marcadores de genotoxicidade (LPO; 8-OHdG; anomalias nucleares eritrocíticas, ANE) e de imunotoxicidade (viabilidade; fagocitose; oxidação de neutrófilos, OBA; LPO). Os resultados obtidos referentes ao objetivo (a) indicam que as de nanopartículas de magnetite revestidas com sílica e funcionalizadas com grupos ditiocarbamato são eficientes na remoção de Hg(II) de soluções mono e multi elementares de água do mar.

Os resultados indicam também que o processo de remoção de Hg(II) pelas NPs é mais rápido para concentrações de metal mais baixas (50 μg/L), e a presença dos outros contaminantes não interfere na taxa de remoção de Hg(II) pelas NPs. Relativamente aos resultados ecotoxicológicos, as soluções não remediadas causaram maior toxicidade às espécies testadas, do que as soluções remediadas. Este resultado evidência a eficiência das NPs na descontaminação de água do mar com Hg. Os resultados obtidos referentes ao objetivo (b) permitem-nos concluir que um aumento da temperatura da água poderá resultar numa maior adsorção de Hg e no aumento de dano lipídico, proteico e no ADN, nas guelras de *A. anguilla*. Um possível aumento da temperatura da água, diminuirá também os benefícios do processo de remediação, uma vez que o dano observado nas soluções remediadas foi maior para a temperatura mais elevada testada. Relativamente, à proteção antioxidante, verificou-se que de um modo geral, as defesas antioxidantes existentes nas guelras de *A. anguilla* provavelmente foram suprimidas, levando ao aumento da acumulação de Hg e a uma maior toxicidade quando a temperatura foi aumentada. Para além disso, a modulação da proteção antioxidante em resposta à exposição de Hg ou à sua co-exposição com outros contaminantes, foi insuficiente para abolir o dano, como observado pelo aumento da LPO, 8-OHdG e oxidação da proteína carbonilo. Os resultados obtidos referentes ao objetivo (c) permitem-nos concluir que a formação do complexo NPs-Hg é eficiente para eliminar o dano de ADN induzido pela exposição individual às NPs ou Hg, durante o período inicial, mas os resultados da exposição de plasma apenas às NPs, evidenciaram um aumento relevante dos níveis de 8-OHdG após 2 e 48 horas de exposição. No entanto, os resultados da co-exposição de NPs e Hg revelaram um aumento nos níveis de 8-OHdG para todos os tempos de exposição (exceto 16 horas), sugerindo que tanto as NPs como o Hg oxidaram, independentemente o DNA. Em relação às respostas imunitárias, os fagócitos de *A. anguilla* isolados do peritónio (P-fagócitos), guelras (G-fagócitos), prónefros (HK-fagócitos) e baço (Fagocitos-S) revelaram sob ativação e produção de espécies reativas de oxigênio (ROS), como mecanismo indireto de imunotoxicidade. A resposta dos fagócitos seguiu a seguinte ordem: P-> S-> HK- = G-fagócitos G para a exposição apenas às NPs; S-> HK-> P- = Fagocitos G para exposição apenas a Hg; e HK-> G- = S-> P-fagócitos para a exposição a NPs-Hg.
Em geral, a eficiência das NPs (elevada percentagem de remoção de Hg e diminuição da toxicidade da água) em conjunto com as suas propriedades magnéticas, evidenciam um conjunto de vantagens que fazem deste material, um adsorvente promissor para aplicações de tratamento *in-situ* e/ou *ex-situ* em sistemas como lagoas costeiras, portos, estuários ou mesmo aquacultura. Considerando a associação do Hg e às NPs, bem como a probabilidade de que ela possa representar uma séria ameaça para os organismos aquáticos, os resultados atuais sugerem que o passo da remoção desse complexo, NPs-Hg, não deve ser subestimado e deverá ser sempre realizado.

Keywords Seawater, Marine organisms, Climate change, Mercury, Arsenic, Cadmium, Ecotoxicity, Biochemical indices, Nano-remediation.

Abstract

Mercury is a well-known hazardous element. Its toxicity and non-degradability in the environment has led to the necessity of its removal from the environmental compartments. Regarding the aquatic compartment, where its toxicity causes serious concerns due to bioaccumulation and biomagnification processes, several new techniques have been development for mercury removal. So far, most of the water treatment methodologies are intended to fresh water. Nevertheless, salt waters are often the last receptor of pollutants, which may constitute a risk, both to the environment and human health. In this perspective, the current study was executed with the following aims to: (a) assess the efficiency of dithiocarbamate functionalized silica coated magnetite nanoparticles (NPs) for mercury (Hg) decontamination, in the presence and absence of other hazardous chemicals (arsenic, As; and cadmium, Cd), in seawater; (b) assess the influence of increased water temperature on the NPs' efficiency in the toxicity removal or decrease of Hg-contaminated seawater in the absence and presence of As and Cd; and (c) evaluate the toxic effects caused by the NPs used in the removal of Hg. To address the objective (a), the residual levels of Hg in spiked seawater were assessed and the toxicity of seawater to aquatic biota contaminated with Hg or with Hg, As and Cd, before (non-remediated solutions) and after (remediated solutions with and without NPs) the sorption process, were compared. To address the objective (b), *Anguilla anguilla* L. gill *ex vivo* approach was considered taking into account a scenario of increased temperature and its comparison with temperature 20 ºC. The influence of temperature was assessed using biochemical endpoints (lipid peroxidation, LPO; protein carbonyl oxidation, PC; 8--Hydroxy-2'-deoxyguanosine, 8-OHdG; and antioxidants protection: catalase; glutathione peroxidise; glutathione reductase; glutathione S-transferase; non-protein thiol; total glutathione) before and after the remediation process adopted, and for the different degree of contamination. To address the objective (c), the eco-friendly nature of NPs was assessed conducting short-term exposure (2 to 72 h) of *A. anguilla* to NPs either alone or in combination with Hg under *in vitro* conditions profiling the responses of *A. anguilla* genotoxicity (LPO; 8-OHdG; erythrocytic nuclear abnormalities, ENA) and immunotoxicity (viability; phagocytosis; oxidative burst activity, OBA; LPO). The observations pertaining to objective (a) revealed that the NPs used in the current study were efficient to remove Hg from single- and multi-contaminated seawater. However, the removal of Hg by the NPs was faster for the lowest contamination scenario (50 µg/L). The presence of other contaminants displayed no interference on the rate of removal of Hg by the NPs. Concerning ecotoxicological profile, the non-remediated solutions caused higher toxicity than the remediated ones, highlighting the effectiveness of the magnetic NPs on the remediation of Hg-contaminated seawater. The observations related to objective (b) revealed that an increase in the water temperature results in higher Hg absorption and increased damage to lipid, protein and DNA in *A. anguilla* gill.

Moreover, the increase of temperature, decreased the benefits of the remediation process as the damage observed in remediated solutions was higher at the highest temperature. Regarding antioxidants protection, in general, the antioxidant defences were likely overwhelmed in fish gill, leading to increased Hg accumulation and exaggerated Hg toxicity when the temperature was increased. Despite the modulation of antioxidants protection in response to the exposure of Hg or its co-exposure with other hazardous contaminants, their insufficiency to abolish damage as observed by increase in LPO, 8-OHdG and PC oxidation. On the aspect of the objective (c), the results concluded that NP-Hg complex formation is efficient to eliminate the DNA damage-induced by individual exposure to NPs or Hg at early hour, whereas plasma exposure to NPs alone displayed a significant increase in 8-OHdG levels at both 2 and 48-hour of exposure. Nevertheless, NPs in combination with Hg co-exposure revealed an increase in 8-OHdG levels at all the exposure length (except 16 hours), suggesting that both NPs and Hg independently oxidized DNA. At the aspect of immune responses, *A. anguilla* phagocytes isolated from peritoneum (P-phagocytes), gill (G-phagocytes), head-kidney (HK-phagocytes) and spleen (S-phagocytes) revealed overactivation and reactive oxygen species (ROS) production as an indirect mechanism of immunotoxicity. The phagocytes responded in the following manner: P- > S- > HK- = G-phagocytes for NP exposure alone; S- > HK- > P- = G-phagocytes for Hg exposure alone; and HK- > G- = S- > P-phagocytes for NPs-Hg exposure.

Overall, the efficiency of NPs (high Hg removal percentage and decrease of water toxicity) combined with its magnetic property proved this material a very promissory adsorbent and can be applied for both *in-situ* and/or *ex-situ* treatment applications in systems like coastal lagoons, harbours, estuaries, or even aquacultures. Considering Hg and its association with NPs, as well as the likelihood that it could pose a serious threat to aquatic organisms, current results suggest that the step of NPs-Hg complex removal must not be underrated and should be processed without any more ado.

.

Table of Contents

CHAPTER 1

Introduction

1. GENERAL INTRODUCTION

1.1. SALTWATER ECOSYSTEMS – IMPORTANCE AND PRESSURES

Saltwater ecosystems are among the largest of earth's aquatic ecosystems and are essential for the overall health of both marine and terrestrial environments (Barange et al., 2010). Humans depend, socially and economically, on the services that saltwater ecosystems provide (Liquete et al. 2013), including provisioning services such as the production of food and regulating services such as the maintenance of hydrological cycles (TEEB 2010). Terrestrial ecosystems provide an estimated US$12 trillion of goods and services (Costanza et al. 1997, 2014), while marine habitats, from the intertidal zone to open ocean systems, are estimated to provide over US$14–21 trillion per year (Costanza et al. 1997; Harley et al. 2006). Such services are provided and maintained by ecosystem functions that create flows of carbon, water, mineral nutrients as well as fluxes of energy and matter within and between trophic levels and the environment. To ensure the continuing provision of these services, we must ensure the sustainability of the ecosystem functions that underpin them.

Saltwater ecosystems are subjected to pressures directly or indirectely associated with a variety of human activities (Tornero and Hanke 2016). The critical functions of these ecosystems, such as productivity, are increasingly threatened by some of these pressures (e.g. intensive exploration, pollution or presence of contaminants, and climate change) that have impact on different parts of the saltwater ecosystems in different ways (Vitousek et al. 1997; Barbier et al. 2011). Some pressures are direct, and their impacts are easy to observe, whereas others are far less obvious and therefore more difficult to understand. For example, fisheries and shipping directly influence populations of fish and marine mammals, and sediment extraction causes localised habitat destruction. However, saltwater ecosystems are also affected by the on going global climate change, along with chemical contamination, although the mechanisms involved and the possible consequences are still the topic of current research.

On the perspective of chemical contaminants, which are ubiquitous and can alter ecosystem functioning (McMahon et al. 2012; Johnston et al., 2015), the extent of this threat is large and has been increasing (Johnston et al., 2015). There is a vast array of commonly used chemical contaminants such as metals, pesticides and hydrocarbons that are found in coastal and marine ecosystems. The complete number of chemicals currently in use makes it difficult to predict effects for any one contaminant. However, chemicals have particular modes of toxic action and an analysis of impact within classes of contaminants may identify clear patterns of effect on structure and functioning. Johnston and Roberts (2009) did this for contaminant impacts on marine biodiversity, identifying major diversity losses associated with toxic chemicals, but a similar synthesis is yet to be carried out for chemical impacts on ecosystem function (Hector & Bagchi 2007).

The impact of pressure of contaminants on saltwater ecosytem may also be potentiated by climate changes, as it is predicted that oceans will be highly affected by sea level rise and increased water temperatures, which ultimately lead to change in pH, salinity and other water physico-chemical properties. Recent assessments of the global climate have concluded that ocean temperature, sea level and acidity have been increasing (IPCC 2013). Further, summaries of recent climatic data indicate that the intensity and frequency of ocean storms are increasing as well. Climate induced changes and other less-understood anthropogenic changes will be superimposed on other impacts resulting from human activities such as over fishing, pollution, damming of rivers and habitat loss in coastal areas (Chen CAT 2008). Consequently, the fundamental characteristics of saltwater ecosystems, some already under stress, will be altered

1.2. CONTAMINATION OF SALTWATER ECOSYSTEMS

The major contaminants of saltwater ecosystem include several classes of contaminants such as organic and inorganic (Tornero and Georg Hanke 2016), and jeopardize the environment and organisms, at a same way and scale, regardless of the source of contamination. However, Among the diverse range of chemicals being release to the environment by Humans, mercury (Hg) is one of the priority environmental contaminant because of its pervasive nature in the environment and known toxicity/carcinogenicity inducing potential (Tchounwou et al., 2012; WFD 2008/105/EC) and thus generates a need of scientific attention in this direction.

1.2.1. MERCURY

Mercury (Hg) is a well-known hazardous element and widely spread around the world. It is one of the priority environmental contaminants according to European water framework directive (Directive 2008/105/EC, European Parliament 2008; OSPAR 2009) due to its high toxicity and known carcinogenic potential (Yabanli and Alparslan, 2015). In water, Hg undergoes a set of chemical and biological transformations, with a part being reduced and volatized back into the atmosphere, while the other either enters the food chain or settles into sediments (Mason et al., 1994). This sedimentary compartment functions as an important Hg reservoir in aquatic systems (Pereira, 1996; Kim et al., 2004; Hung and Chmura, 2006; De Marco et al., 2006). Mercury entrance in food chain starts with bacterial methylation of the inorganic Hg in water (Spry and Wiener, 1991). This is the most important step in the environmental Hg cycle since it greatly increases Hg toxicity and bioaccumulation potential (Scudder et al., 2009). Methylmercury biotransfer will occur afterwards to higher trophic levels, both via benthic and pelagic pathways (Chen et al., 2009). Mercury levels in biota has been extensively assessed and reported in considerable high amount in organisms from lower (primary producers to invertebrates) to higher (e.g. fish, birds and mammals) trophic levels (Abreu et al., 2000; Coelho et al., 2005; Coelho et al., 2007; Coelho et al., 2008; Tavares et al., 2008; Young et al., 2010; Dietz et al., 2011). Mercury bioaccumulation in aquatic organisms may occur via direct exposure (in the water) and/or trophic exposure (in the diet) (Boudou and Ribeyre, 1985). The contribution of each route is species-specific and depends on the Hg bioavailability in water and diet (Rainbow, 2002), as well as on the chemical form of Hg, which can exhibit different abilities to cross the biological barriers (Boudou and Ribeyre, 1985). In this perspective, some authors estimated the bioaccumulation potential for Hg forms in aquatic biota, demonstrating that methylmercury's bioaccumulation potential is 1000 times higher than that of the inorganic form (Scudder et al., 2009). Furthermore, the bioaccumulation factor from water to edible fish tissues is thought to exceed 10 million times, indicating that even small environmental levels have the potential to accumulate in biota at harmful concentrations (Clarkson, 1992).

The toxic effects of Hg have been reported since the primordial of its use by society (UNEP 2002). The first recorded case of Hg poisoning occurred as early as 50 BC, when the Greeks and Romans used Hg as a component in ointments and cosmetics (Leon

Brimer 2011). In recent times, a high number of scientific works reported the toxic effects of Hg at different taxonomic/functional groups and levels of biological organization (from molecular/biochemical to population/community level) (Wolfe et al., 1998; Boening 2000; Sandheinrich and Wiener 2011; Rice et al., 2014). Mercury may cause adverse effects ranging from sub-lethal to lethal effects at concentrations as low as 30 µg/L (Boening, 2000). It has also been recognised that humans may be affected, namely through fish and shell-fish consumption, although, the exposure to areas with high Hg levels (in organic and inorganic forms) in multiple environmental compartments may also represent a risk to human health (Baeyers et al., 2003; Donkor et al., 2006). Many countries regulate Hg intake though commercial sale and consumption advisories. For example, the Canadian Food Inspection Agency's (CFIA) guideline for the commercial sale of fish (CSFG), both freshwater and marine, is 0.5 µg Hg/g wet weight (ww) in muscle tissue and Health Canada has established a guideline of 0.2 µg Hg/g ww for the consumers of fish (FCFG) (CFIA, 2002; Shilts and Coker, 1995; Stephens, 1995). In Europe, the European Commission set the maximum levels of Hg to crustaceans, excluding the brown meat of crab and excluding head and thorax meat of lobster and similar large crustaceans (*Nephropidae and Palinuridae*), as 0.5 µg/g ww and for fishes as 1.0 µg/g ww (EC 1881/2006) for the frequent consumers of seafood. Thus, its toxicity and non-degradability in the environment has led to the necessity of its removal from the environmental compartments and promoted the development of new techniques for its removal from one of the environmental compartments *i.e.* water, where its toxicity causes more concern due to its higher bioavialabity to the aquatic organisms considering water as an ultimate reservoir (Schartup et al., 2015).

History, sources and forms of mercury in the environment and its biogeochemical cycle

Since ancient times, the Chinese, Indian, Greek, and Roman civilizations have recognized Hg's properties and had used it in different applications. For instance, Egyptians used Hg to form amalgams in 1500 BC, Greeks used it in ointments, and Romans used it in cosmetics (D'Itri, 1977). Mercury has also been used in the extraction of gold because of its ability to combine with other metals and to form amalgams. In addition,

of being widely used in the past, Hg has still many current applications with approximately 2,300 metric tonnes of Hg mining production in year 2015 to supply global requirements (USGS, 2016).

Mercury is an element naturally present in the earth's crust. It occurs as a liquid at room temperature and atmospheric pressure, and evaporates easily into the atmosphere at temperatures above 20 ºC. Mercury is emitted to the environment naturally through volcanic eruptions and seismic activity, the weathering of rocks and soils, photo-reduction of divalent Hg in natural waters and biological formation from methylation of elemental or dimethylmercury (UNEP, 2013). In addition to these natural phenomena, high amounts of this element are also released through human activity; and since industrialization, the amount of Hg found in the environment has increased by a factor of three (Porcella et al., 1996). Mercury is released through many industrial processes including energy production (coal-fired power plants), base metal smelting, gold mining, and waste incineration (Neimi, 1998; USA ATSDR, 2001). Therefore, the highest Hg levels are found in industrial areas where these processes are occurring (Churchill, 1999; Hunerlach et al., 1999). Nevertheless, the released Hg is transported through the air, where it can travel long distances, and is eventually deposited on water and land either as dry particles, or through wet precipitation (UNEP, 2002). It is also transported over the earth's surface through effluent discharge into flowing rivers and via ocean currents (Driscol et al., 2013). Experimental studies have also shown that reservoir creation can increase the total mercury (T-Hg) and methylmercury (MeHg) yields by 40-fold (Montgomery et al., 2000; St. Louis et al., 2004). Also, sediments can act as source and sink of Hg. Sediment cores collected from central and northern Canada show an increase in Hg deposition over time, possibly due to increased anthropogenic release of Hg to the atmosphere (Lockhart et al., 1998; Fitzgerald et al., 2007).

Mercury has three valence states (Hg^0, Hg^+, and Hg^{2+}), which are easily interconvertible. The natural Hg biogeochemical cycle involves degassing of Hg from soils and surface waters, atmospheric transport, deposition of Hg back to land and surface water, sorption of Hg onto soil or sediment particles, and re-release back to the water column and atmosphere (Figure 1.1) (NRC, 2000).

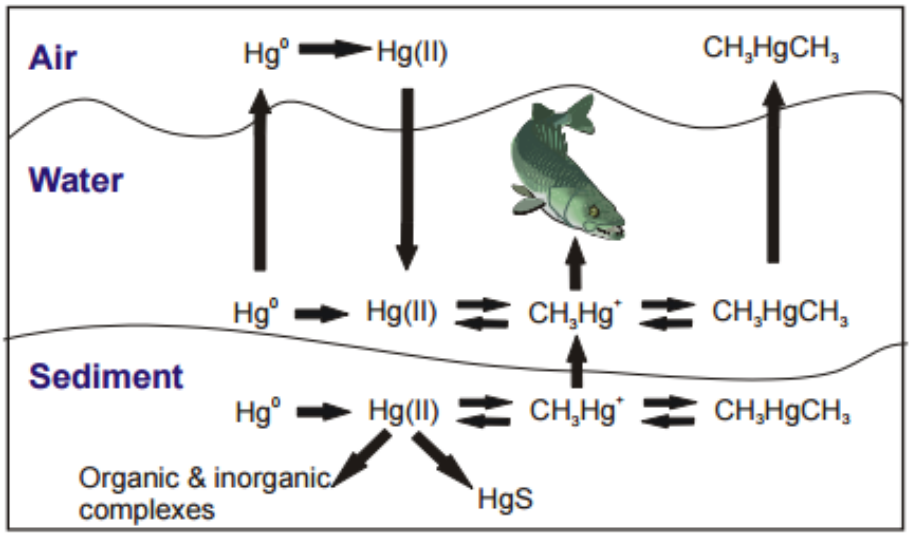

Figure 1.1. Mercury biogeochmical cycle (adapted from Winfrey and Rudd 1990).

This complex cycle, including mixing of Hg from various sources, makes it difficult to trace mercury in a given region back to its original source (USA ATSDR, 2001). Different forms and oxidation states of mercury are interchangeable in atmospheric, aquatic, and terrestrial environments, and the proportions of the different Hg species depend on the combined effects of numerous physicochemical and biological variables (Jackson, 1997).

1.2.2. OTHER AQUATIC CONTAMINANTS

Mercury is not the only hazardous contaminant in the aquatic environment, and usually the aquatic organisms are exposed to a broad spectrum of toxicants, including organics and inorganics (Ghani, 2015; Pastorinho et al., 2012). Hence, it is important to evaluate the toxic effects of Hg to the orgamisms, in the presence of other hazardous contaminants, to identify synergies or antagonic behaviours between contaminants. In this perspective, metals and metalloids are among the most common hazardous substances found in the aquatic environment (Gautam et al., 2014), and so far most of the studies available in literature have been done with single or individual elements lacking some attention to understand the interactive toxic effects between contaminants at ecologically relevant concentrations.

Like Hg, arsenic (As) and cadmium (Cd) are non-essential elements and due to their persistent nature and tendency toward bioaccumulation are also rated among the most hazardous potentially toxic elements (Vinodhini and Narayanan, 2008; Mishra et al., 2008; Gutierrez-Mejia et al., 2009). Cadmium is classified as "priority hazardous substance" by the European Union water framework directive (http://ec.europa.eu/environment/water/water-framework/index_en.html) as well as by OSPAR https://www.ospar.org/work-areas/hasec/chemicals/priority-action and As occupies the first position in the Agency for Toxic Substances and Disease Registry (ATSDR, 2011) Substance Priority List (http://www.atsdr.cdc.gov/spl/index.html).

Arsenic is a naturally occurring element that ubiquitously exists in both organic and inorganic form in the environment. In aquatic environments, arsenic is usually found in the form of arsenate or arsenite. (Kumari et al., 2016; Hughes et al., 2011). The unrestricted application of As pesticides, industrial activities, and mining operations has led to the global occurrence of soluble As above permissible levels of 0.010 mg/L (Kumari et al., 2016; Kovendan et al., 2013). Continuous exposure of aquatic organisms to low concentrations of As results in bioaccumulation, notably in liver and kidney, and as a consequence As induces hyperglycemia, depletion of enzymatic activities, various acute and chronic toxicity, and immune system dysfunction (Kumari et al., 2016).

Cadmium is one of the metals that occur naturally in ores and enters the environment as a result of both natural processes (weathering and erosion of rock and soils, natural combustion from volcanoes and forest fires) and anthropogenic sources (mining, agriculture, urban activities, and waste streams from industrial processes, manufacturing, coal ash ponds/pits, fossil fuel combustion, incineration and municipal effluent) (Shevchenko et al., 2003; U.S. EPA, 2016; WHO, 2010). As mentioned previously, cadmium is a non-essential metal (NRC, 2005) with no biological function in aquatic animals (Shanker, 2008; McGeer et al., 2012). In one study comparing the acute toxicity of all 63 atomically stable metals in the periodic table, Cd was found to be the most acutely toxic metal to the amphipod, *Hyalella azteca*, based on the results of seven-day acute aquatic toxicity tests (Borgmann et al. 2005). In addition to acute toxicity, Cd is a known teratogen and carcinogen and is known to induce a variety of other short- and long-term adverse physiological effects in fish and wildlife at both the cellular and individual level (ATSDR 2012; Okocha and Adedeji, 2011). Chronic exposure to cadmium

leads to adverse effects on growth, reproduction, immune and endocrine systems, development, and behavior in aquatic organisms (McGeer et al., 2012). Other toxic effects include histopathologies of the gill, liver and kidney in fish, renal tubular damage, alterations of free radical production and the antioxidant defense system, immunosuppression, and structural effects on invertebrate gills (McGeer et al., 2011; Okocha and Adedeji, 2011; Shanker, 2008). Cadmium can bioaccumulate in aquatic organisms, with total uptake depending on the environmental cadmium concentration, exposure route and the duration of exposure (Annabi et al., 2013; Francis et al., 2004).

Therefore, the contamination of aquatic ecosystems by As and Cd also causes serious environmental and human health concerns on a worldwide scale (Mahimairaja et al., 2005; Kapaj et al., 2006, Valavanidis and Vlachogianni, 2010).

1.3. CONVENTIONAL AND EMERGING METHODOLOGIES FOR THE REMOVAL OF CONTAMINANTS FROM SALTWATER

Keeping in view the previous toxicity aspect, it is equally important to study the complex phenomena controlling the transference of toxic elements to aquatic organisms and develop new techniques for their removal from saltwater. Various technologies such as ion exchange, reverse osmosis, electrolytic removal, reduction, adsorption, precipitation, membrane filtration and flocculation have been reported for the removal of metals and metalloids from waters and industrial effluents (Rengaraj et al., 2001; Lai and Lin 2003; Remoudaki et al., 2003; Cardoro et al., 2004; Mohammadi et al., 2004; Taty-Costodes et al., 2005; Lopes et al., 2007; Lopes et al., 2008; Baral et al., 2009; Lopes et al., 2009; Valderrama, et al., 2010; Lopes et al., 2011). Each of these processes has its advantages and disadvantages and, although some of these technologies are simple, rapid, quantitative and selective under proper conditions, some require high-energy or large quantities of chemicals, involving high operating and maintenance costs and expensive equipment, others produce large volumes of solid wastes (e.g. precipitation), generating toxic residual sludge, which give rise to another major problem that is the disposal of toxic sludge (Monteagudo et al., 2000; Pacheco et al., 2006), while others do not achieve the target concentrations after treatment since the removal of the toxic elements is incomplete.

Among conventional technologies, chemical precipitation, ion-exchange and adsorption are probably the three processes most used for the removal of metals from contaminated water.

Chemical precipitation is commonly employed for removal of metals, including Hg. Hydroxide (OH^-) and sulphide (S^{2-}) are the common precipitants, but in some cases carbonate (CO_3^{2-}) has also been used (Tchobanoglous et al., 2003). Precipitation is accompanied by flocculation or coagulation and one of the major disadvantaged of this technique is the production of a large amount of sludge, which contains metal ions (Dabrowski et al., 2004) and, in some cases, the effluent discharge limits are not achieved (Cruz-Olivares et al., 2010). For example, an effluent containing 0.1 g/L of Cu(II), Cd(II) or Hg(II) compounds originates 10-, 9- and 5-times larger amounts of sediments (Dabrowski et al., 2004).

Ion-exchange is one of the most effective and common methodology used for removal of metals, including Hg. The economic feasibility of this process improves when used for the recovery of valuable metals, like gold and silver (Tchobanoglous et al., 2003). Moreover, by ion-exchange either all ions can be removed from solutions or separated, allowing the complete deionization or selective removal of ionic contamination or of a valuable metal (Dabrowski et al., 2004). Several materials can be used as ion exchangers, but the most known and used include zeolites, weak and strong anion and cation resins, chelating resins and microbial and plant biomass (Tchobanoglous et al., 2003). However, further developments on new type of ion-exchangers are in progress and consequently the range of application of the ion-exchange process has been remarkably extended. The ion-exchange process is highly pH-dependent, since the solution pH has a strong impact on the metal speciation and on the interaction between ion exchanging ions and the resin (Tchobanoglous et al., 2003). Generally, the metals bind better a higher pH, due to the less competition with protons for the sorption sites. The performance of the ion exchange process is determined by the operating and wastewater conditions (pH, temperature, other ionic species and chemical background, e.g. oxidants, particles, solvents and polymers) (Tchobanoglous et al., 2003).

Adsorption is recognized as an effective and economic method for wastewater treatment (Fu and Wang, 2011). The adsorption process offers flexibility in design and operation and in many cases will produce high-quality treated effluents. Adsorption

consists in the separation of one or more components from a mixture by the addition of a solid material, the adsorbent. The widely used and known adsorbent is the activated carbon. Its usefulness derives mainly from its large micropores and mesopores volumes and the resulting high surface area. According with the nature of the interactions involved in the process, the adsorption can be chemical (formation of chemical bonds) or physical (Van der Waals intermolecular forces). In addition, because adsorption is sometimes reversible, adsorbents can be regenerated by suitable desorption process (Fu and Wang, 2011).

In adition to the conventional technologies, in the last decade nanotechnology arose as new field of study for many different areas, including its application for water and wastewater treatment. Nanotechnology is related to the preparation of materials at nanoscale. At this scale, materials show unique characteristics such as large surface area to volume ratio, potential for self-assembly, high specificity, high reactivity and catalytic potential, which make them excellent candidates for water treatment applications (Joo and Cheng, 2006; Mamalis, 2007; Zhua et al., 2009; Klabunde et al., 2010; Kaur and Gupta, 2008; Zhai et al., 2010; Sánchez et al., 2011). Consequently, nanoparticles (NPs) have emerged as new class of sorbents for recovery, separation and/or pre-concentration of metals. Ngomsik et al., (2005) wrote a mini review on the application of magnetic nano and microparticles in the removal of metals in wastewaters, and a review on the most common nanoscale materials and their use for water treatment will be explored more in details in the Chapter 2 of current thesis.

Among the huge variety of nanosorbents, magnetic iron oxides such as magnetite (Fe_3O_4) and maghemite (γ- Fe_3O_4) have been investigated intensively by our research group and other authors, for the removal of Hg from water (Girginova et al., 2010; Li et al., 2011; Hakami et al., 2012; Figueira et al., 2011; Tavares et al., 2013; Zhang et al., 2013; Rahbar et al., 2014; Shan et al., 2015; Zhang et al 2015; Mehdinia et al., 2015). Recently, Shan et al., (2015) reported the synthesis of Fe_3O_4@SiO_2 magnetic nanoparticles modified by grafting poly(1-vinylimidazole) oligomer as a novel adsorbent to remove Hg(II) from water. This material showed a high adsorption capacity toward the metal that was not inhibited with the increase of ionic strength. Tavares et al., (2013) explored the sorption efficiency of the synthesized magnetite particles coated with siliceous shells and

with different degree of dithiocarbamate functionalization in the removal of Hg ions from aqueous solutions by magnetic separation, while Figueira et al., (2011) also took advantage of the high affinity between Hg and sulphur, and used magnetite (Fe_3O_4) NPs functionalized with dithiocarbamate groups as a new type of sorbent to remove Hg(II) from synthetic and natural spiked waters.

In adition, to their high efficienty to uptake Hg, the magnetic NPs also have the advantage of being easly removed from water using an external magnetic field, taking the toxic elements associated and leaving the water with better quality (Ambashta et al., 2010; Kim et al., 2011).

These studies, like most of the approaches driven in the field of water treatment, aim only the quantification of the residual levels of metals and the amount of the metal effectively sorbed by the material applied (Lopes et al., 2009; Lopes et al., 2011; Girginova et al., 2010; Figueira et al., 2011; Tavares et al., 2013). However, the chemical analysis alone is not suitable to test for the water good quality status and, therefore, it is important to establish a cause-effect relationship between the remaining concentration of chemicals and consequent environmental damage. Thus, for a proper evaluation of the efficiency of a water treatment, an approach combining both chemical and ecotoxicological assays should be designed, and to the best of our knowledge, the studies following this approach about reducing or eliminating the toxicity of waters contaminated with metals are scarce (Mishra and Tripathi 2008; Lopes et al., 2014a; Rocha et al., 2014). Moreover, attention is also required to understand the efficiency of removal technologies under more realistic conditions, such as multi-contaminant scenarios. In addition, the assessment of NPs efficiency under the scenario of climate change makes this area of research completely unexplored. Besides, information on the environmental friendly nature of the material being used for the remediation of the contaminants are lacking, and so currently a considerable interest has been generated to assess the extent of aquatic pollution related to NPs and their impact on aquatic life and ultimately on humans. In an attempt, to recognize the environmental impact provoked by NPs, except few studies revealing the impact of NPs, it was found that the knowledge on NPs uptake, transport and exposure in the aquatic organisms is not sufficient for making accurate predictions. Hence more attention is needed to understand the full mechanism involved in the NPs toxicity. Another observation drawn from the literature revealed that there is a need to focus more

on the evaluation of NPs toxicity in fish, because of their virtual presence everywhere in the aquatic environment and playing a major ecological role in the aquatic food-webs. Fish sorb pollutants not only by the trophic chain, but also through the direct contact of gills and its scales, and thus affecting human health when ingested.

1.4. TOOLS TO EVALUATE THE EFFICIENCY OF WATER TREATMENT METHODOLOGIES – APPRASAL OF ECOTOXICOLOGICAL STUDIES AND INDUCED BIOCHEMICAL STRESS RESPONSES

Following the high bioaccumulation potential and toxicity of Hg, efforts have been carried out to minimise the use of Hg in many industrial processes and products, and, as well, to develop methodologies for preventing and/or reducing industrial discharges, and to remediate already Hg-impacted ecosystems. Within this framework, ecotoxicology have been playing an important role by generating relevant knowledge on the exposition, internalization pathways and toxic effects of Hg (Boeing, 2000; Ahmad et al., 2008, 2011a,b,). Moreover, literature revealed the use of ecotoxicology to evaluate the efficiency of several clean-up technologies such as biosorption, ion exchange and nano-remediation processes to remove contaminants from water (Rocha et al., 2014; Lopes et al., 2014a; Mohmood et al., 2016). A study done by Lopes et al. (2014a) reported the ecotoxicological efficiency of an ion-exchange process for Hg removal by assessing the water toxicity to organisms from different taxonomic groups that exhibit different key functions at the ecosystem level before and after the clean-up technology. In addition, Mohmood et al. (2016) also used a battery of bioassays to evaluate the efficiency of newly synthesised silica coated magnetite nanoparticles (NPs) in reducing the toxicity of saltwater either contaminated with Hg alone or with Hg in a mixture with As and Cd. These works highlight the importance of using a battery of bioassays with organisms from different trophic levels, to obtain an accurate assessment of toxicity removal by remediation processes. In this perspective, ecotoxicological assays (e.g. acute assays: usually with short-term exposure that assess mortality; or chronic assays: usually long-term assays that assess sub-lethal responses such as reproduction, growth), and the assays use to assess the early warning effects at biochemical level on lower concentrations are gaining considerations since a slight misappropriate functioning of the biochemical responses may predispose organisms towards pathogenicity or stress. Within this perspective, the oxidative stress resulting from the production of reactive oxygen species (ROS) has gained

considerable interest in the field of ecotoxicology (Lemaire et al., 1996; Ahmad et al., 2011a). Estimation of lipid peroxidation (LPO) in particular has been found to have high predictive importance as revealed from a credible number of research papers describing its use as a biomarker of effects (Ahmad et al., 2008; Oliveira et al., 2010a). Moreover, proteins are considered to be important targets of free radical attack in cells (Almroth et al., 2008; Lushchak, 2011) and thus, compromise antioxidant defense, cellular function, and survival (Padmini, 2010). Studies on cell lines exposed to peroxyl radicals showed that proteins can be oxidized before lipids or DNA in ROS exposed cells (Du & Gebicki, 2004). On the aspect of DNA oxidative damage, the formed free radicals attack not only on DNA bases but also on the deoxyribose backbone of DNA, reacting five times faster with nucleobases (Valavanidis et al., 2009). The oxidation of guanine in the C8 position results in the formation of 8-hydroxy-2′-deoxyguanosine (8-OHdG), a predominant and one of the most studied oxidative DNA lesions due to its easy formation and mutagenicity (Valko et al., 2004). The absence of base damage repair may lead to strand misreading, mutations, altered gene expression, strand breaks, microsatellite instability and loss of heterozygosity, chromosomal aberrations, cytostasis, cytotoxicity, or neoplastic growth (Croteau and Bohr 1997; Evans et al., 2004). On the perspective of antioxidants responses, both antioxidant enzymes and non-enzymatic antioxidants have also been successfully employed in aquatic biomonitoring studies (Oliveira et al., 2009). Nevertheless, the resultant immunotoxicity and genotoxicity has also been shown their utility in the environmental risk assessment (Mohmood et al., 2008; Ahmad et al., 2011b; Mohmood et al., 2014; Costa et al., 2015) in parallel to the antioxidants protections. In a critical review of the recent literature, Sandheinrich and Wiener (2011) concluded that changes in biochemical processes, damage to cells and tissues in fish occur at MeHg concentrations of about 0.5 to 1.2 μg Hg/g ww in axial muscle. Moreover, Fernández et al. (2010) used the antioxidant response to assess the effects of the main pollutants (Hg, Pb, Cd, Cu, Zn, As, PAH, PCB, and DDT) in wild mussels (*Mytilus galloprovincialis*) along the Mediterranean coast of Spain.

1.5. CLIMATE CHANGE AND ITS INFLUENCE ON WATER CONTAMINANTS AND TREATMENT METHODOLOGIES

Global climate change, which is largely driven anthropogenically, has become a dire reality in the past century, and its impacts are expected to increase in the near future (IPCC, 2013). Recent models predict that the mean global temperature increase by the end of the 21st century is likely to exceed 1.5 °C in all scenarios (IPCC, 2013). The U.N. Intergovernmental Panel on Climate Change (IPCC) has completed five assessments covering the evidence, impacts, and mitigation of climate change (IPCC, 2013). They report unequivocal global warming with evidence of increases in global mean air and ocean temperatures, widespread snow and ice melt, and rising global sea level. It is also expected that a rise in global temperature will be accompanied by increased temperature fluctuations and frequency of extreme temperatures (Trenberth et al., 2007). In addition to global warming, some regions, such as North and Southern America, northern Europe, and northern and central Asia are projected to experience increased precipitation, while others, including southern Africa and Asia and the Mediterranean, are expected to experience substantial droughts. Heat waves, precipitation and storm events are predicted to be more frequent and intense. The potential impacts of increasing temperatures on ocean ecosystems, as a consequence of rising levels of anthropogenically-generated carbon dioxide and other greenhouse gases, including methane, nitrous oxide, and chloroflourocarbons, is a growing threat to marine organisms and ecosystems.

Under this scenario, several studies have been done to predict, minimize and call the attention of decisors makers to the consequences of global climate change, in particular, the increase of water temperature. Recently, Velez et al. (2017) assessed the impact of rising temperatures on the native *Ruditapes decussatus* and introduced *R. philippinarum* bivalve species, through biochemical and mRNA transcription analyses. The findings showed that at 21 °C the electron transport system and antioxidant enzyme activity, as well as the expression of Hsp70 gene were induced in *R. decussatus* when compared with 17 °C. On the other hand, at 25 °C results suggested that *R. decussatus* closed their valves during short periods, as a behavioral strategy, down-regulating the expression of genes associated with mitochondrial metabolism (Cox-1 and 16S) and chaperone function (Hsp70) compared with organisms at 17 °C. In addition, the introduced species (*R. philippinarum*) increased the electron transport system and antioxidant

activities, as well as gene expression of antioxidant enzymes and molecular chaperone (Hsp70) at 21 °C. However, antioxidant mechanisms were not enough to prevent lipid membrane damages at 21 °C. At 25 °C *R. philippinarum* presented increased electron transport system and antioxidant activity, as well as the expression of genes associated with apoptosis regulation and molecular chaperone. Overall, the present findings indicate that in a global warming scenario both species are able to induce different mechanisms to mitigate the impacts of temperature increase. Moreira et al. (2017) studied the physiological and biochemical responses of native and introduced oyster species in a scenario of global temperature rise, in order to provide knowledge that may allow for better species management. Hence, the author compared biochemical alterations of the introduced *C. gigas* and the native *Crassostrea brasiliana*, the most important oyster species in Brazil, in response to different thermal regimes for 28 days (24, 28 and 32 °C). For this, metabolism (ETS), energy content (GLY), antioxidant system (SOD, CAT and GSH/GSSG) and cellular damage (LPO) were assessed in adult and juvenile specimens of both species. Juvenile *C. gigas* were the most affected by increased temperatures, presenting higher mortality, more pronounced antioxidant response (SOD), whereas adults were more tolerant than juveniles, showing no mortality, no significant changes in antioxidant enzymes activity neither energy expenditure. Native *C. brasiliana* juveniles presented lower mortality and less pronounced biochemical alterations were noted at higher temperature comparing to non-native *C. gigas* juveniles. Adult *C. brasiliana* were the least responsive to tested temperatures. Results obtained in this study bring interesting new insights on different oyster species life stages' physiological and biochemical tolerance towards thermal stress. The native species *C. brasiliana* showed ability to maintain biochemical performance at higher temperatures, with less pronounced biochemical changes than the non-native species. The introduced (*C. gigas*) showed to be more sensitive, presenting biochemical alterations to cope with the increase of temperature. Despite the lower observed fitness of the introduced species to temperatures closer to those naturally experienced by the native species, the ability of *C. gigas* to cope with higher temperatures should still raise concerns towards the native species *C. brasiliana* management and protection.

The increase of water temperature due to climate change can also affect sorption, distribution, storage and elimination of contaminants, including metals (Khan, 2006). It is

important to realize that interactions between natural stressors (e.g. temperature) and toxicants can occur at different levels. For example, physico-chemical properties of water have influence on the bioavailability of metals, meaning that the same total environmental concentration of a toxicant causes different effects in different exposure scenarios (Newman and Unger, 2003). Likewise, physical conditions (e.g. temperature) or nutritional status (influencing feeding activity) may influence toxicokinetics. Metals may interfere with the physiology of an organism, rendering it less tolerant to environmental stress caused by extreme levels of natural stressors. Also, the effect of climate change may influence the toxicity of the metals and rendering them more toxic to organisms (Højer et al., 2001; Noyes et al., 2009).

Several studies on the interactions of temperature and metals have been already performed. Khan et al., (2006) investigated the acute toxicity of four metals to juvenile crayfish *Orconectes immunis* (Hagen) (1-2 g wet body wt. each) at different room temperatures and the data indicated that rising global temperatures (currently 0.60 ºC) associated with climate change can have the potential to increase the sensitivity of aquatic animals to metals in their environment. Siscar et al. (2014) showed increased metal uptake in the Mediterranean fish *Solea senegalensis* and altered metallothionein levels and metal partitioning into liver and kidney at the increasing temperature from 15°C to 20°C. In addition, ectotherms have also been shown to have a reduced aerobic metabolism capacity at elevated temperatures (Pörtner, 2001), and oxygen limited effects have been demonstrated with Cd in the eastern oyster *Crassostrea virginica* (Lannig et al., 2006; Lannig et al., 2008). Increasing temperature from 20°C to 28°C significantly increased Cd toxicity as exhibited by increased oyster mortality and lipid peroxidation, and decreased condition index (Lannig et al., 2006). Hypoxemia occurred more rapidly in Cd-exposed oysters at high temperature (Lannig et al., 2008). In addition, metal detoxification mechanisms (glutathione levels and rate of protein synthesis) decreased at the higher temperature, reducing capacity for metal metabolism (Lannig et al., 2006). On the aspect of metalloids such as arsenic, McGeachy and Dixon (1989) investigated the influence of temperature (5 or 15 ºC) on the acute toxicity of waterborne arsenite and arsenate to rainbow trout. Trout exposed to arsenate at 5 ºC had a $LC_{50,144h}$ of 114.1 mg/L, twice the value of 58 mg/L evident in fish exposed at 15 ºC. Temperature had no effect on the toxicity of arsenite; $LC_{50,144h}$ at 5 and 15 ºC were 17.7 (16.5 to 18.9) and 20.7 (19.9 to

21.5) mg/L, respectively. When fish were exposed to 70 mg/L arsenate for 72 hours, those held at 15 ºC exhibited a mean whole-body of As levels that were five times higher than the levels in fish held at 5 ºC. There were, however, essentially no differences in the patterns of As uptake between 5 and 15 ºC when the fish were exposed to arsenate at 0.7 or 1.2 mg/L for the 144 hours LC_{50} at each temperature. Fish, which were held in arsenate-free water after the 72 hours after arsenate exposure depurated significantly more As at 15 ºC than at 5 ºC. Despite this, it is apparent that enhanced uptake at 15 ºC was the overriding factor controlling the differences in the expression of arsenate toxicity at the two temperatures.

A gap of information concerning the modulatory role of these exogenous factors on pollutant-induced physiological responses was found concerning aquatic animals. In general, oxidative damage to lipids and proteins, as well as reactive oxygen species generation have been reported to increase at higher temperatures, although exceptions are apparent. Hence, with few data available from fish, the expectation of broad applicability of such results may not be warranted. The up-regulation of oxidative stress response genes suggested that oxidative damage may be decreased in fish subject to temperature reduction (Malek et al., 2004). However, the mechanism by which temperature reduction serves to up-regulate oxidative stress response is not known.

On the perspective of water treatment methodologies, to the author's knowledge, no study in the literature has been reported screening the effect of climate change, in particular the increase of temperature, on the toxicity of contaminated water after its nano-remediation. Therefore, it is important to understand if the efficiency of the water treatment methodologies, usually developed under laboratory control temperature (approx. 20 ºC), would be sufficient enough to mitigate the water toxicity, when affected by climate change like the increase of water temperature. It may be postulated that an increase in water temperature may lead to higher uptake of chemicals and consequently to the increase of water toxicity (Sokolova et al., 2008; Khan et al., 2006). Thus, the residual low levels of contaminants after the water treatment could be toxic at higher temperatures, changing the efficiency (in terms of toxicity) of the treatment methodology, evaluated at laboratory control temperature.

1.6. ORIENTATION AND OBJECTIVES OF THE THESIS

As mentioned previously in the text, mercury is a priority hazardous substance and a global problem being subject of numerous studies, strategies and policies. Despite the large number of studies regarding Hg' knowledge concerning its toxicity in the presence of other hazardous contaminants (namely, As and Cd) and under predicted scenarios of increasing temperatures on saltwater organisms is still insufficient. Besides, the toxicity of Hg in the presence of As and Cd, and their removal using magnetite nanoparticles (NPs) has been dealt isolatedly either in terms of their ecotoxicity or remediation, giving the incomplete picture of the subject of reducing or eliminating the Hg toxicity of contaminated seawaters. Additionally, the evaluation of the toxic effects caused by the magnetite NPs used in the removal of Hg should also be considered important taking into account a key question of real advantage in their use.

Thus, the main aim of the current work was to: assess the effectiveness of magnetite NPs functionalized with dithiocarbamate groups for the removal of toxicity of seawater contaminated with mercury.

To achieve this major goal, the following specific objectives were established:

i. To assess the efficiency of dithiocarbamate functionalized silica coated magnetite NPs in the remediation of Hg - contaminated seawater in the absence and presence of other contaminants (As and Cd).

ii. To assess the influence of increased temperature on the efficiency of dithiocarbamate functionalized silica coated magnetite NPs in the toxicity removal of Hg-contaminated seawater in the absence and presence of other contaminants (As and Cd).

iii. To evaluate the toxic effects caused by the dithiocarbamate functionalized silica coated magnetite NPs used in the removal of Hg.

For this, the effect assessments were carried out with species from different taxonomic and functional groups, in order to have a better representativity of the sensitivity of biota, and at different levels of biological organization. As the legal limits established for Hg in wastewater to protect the environment is not expected to observe adverse effects at some of the individual responses, sub-individual endpoints (biochemical

stress responses) were also considered as early warning tools. The above mentioned aim and sub-objectives have been addressed in the following six chapters (Chapters 2 to 7) that constitute the focal point of this thesis and correspond to scientific articles published in peer-review journals. Chapter two describes the various remediation technologies used for the removal of contaminants in order to make a suitable choice of the material for the removal of the Hg in presence of other hazardous contaminants (As and Cd) from water. Chapter three describes the efficiency of dithiocarbamate functionalized silica coated magnetite NPs for the removal of Hg in absence and presence of As and Cd and as well the removal of ecotoxicity effects, by using species from different trophic levels (the bacterium *Vibrio fischeri*, representative of decomposers; the microalgae *Phaeodactylum tricornutum*, representative of producers; the crustacean *Artemia franciscana* and the rotifer *Brachionus plicatilis*, as consumers). In order to address the influence of increased temperature (as a consequence of climate change) in the Hg toxicity removal efficiency of magnetite NPs, biochemical parameters were considered using *ex vivo* study on *Anguilla anguilla* gill. Thus, chapter four and five focus on the *A. anguilla* gill *ex vivo* toxicity of the Hg plus As and Cd contaminated and nano-remediated seawater at three different temperature gradients. Chapter six and seven describe the toxicity aspect of the magnetite NPs used for Hg removal mainly focusing on the two major toxicity aspects *A. anguilla* genotoxicity and immunotoxicity in order to check the real advantage of NPs used in remediation. Moreover, these chapters were also intent to assess the probable risk to aquatic biota associated with the delay in the process of NPs removal from water. At the end, an overview of the results is presented, integrating the response to the previous questions, main conclusions and future research areas (Chapter 8).

This thesis led to the following scientific publications:

- **Nanoscale materials and their use in water contaminants removal—a review**.

  Iram Mohmood, Cláudia Batista Lopes, Isabel Lopes, Iqbal Ahmad, Armando C. Duarte, Eduarda Pereira. Environmental Science and Pollution Research (2013) 20:1239–1260

  DOI 10.1007/s11356-012-1415-x

- **Remediation of mercury contaminated saltwater with functionalized silica coated magnetite nanoparticles**

  Iram Mohmood, Cláudia B. Lopes, Isabel Lopes, Daniela S. Tavares, Amadeu M.V.M.Soares, Armando C. Duarte, Tito Trindade, Iqbal Ahmad, Eduarda Pereira. Science of the Total Environment (2016) 557–558: 712–721

  DOI 10.1016/j.scitotenv.2016.03.075

- **Influence of temperature on nanoparticles remediated seawater-induced biochemical stress responses in Anguilla *anguilla* L.: 1. Evaluation of lipid peroxidation, protein carbonyl oxidation and oxidative DNA lesions**

  Iram Mohmood, Iqbal Ahmad, Isabel Lopes, Cláudia Batista Lopes, Armando C. Duarte, Eduarda Pereira. To be submitted to Science and Pollution Research

- **Influence of temperature on nanoparticles remediated seawater-induced biochemical stress responses in *Anguilla anguilla* L.: 2. Evaluation of enzymatic and non-enzymatic antioxidants**

  Iram Mohmood, Iqbal Ahmad, Isabel Lopes, Cláudia Batista Lopes, Armando C. Duarte, Eduarda Pereira. To be submitted to Science and Pollution Research

- **The interference of the co-exposure of mercury with silica coated iron oxide nanoparticles can modulate genotoxicity induced by their individual exposures - A paradox depicted in fish under *in vitro* conditions**

  Iram Mohmood, Iqbal Ahmad, Mohammad Assim, Leonor Costa, Cláudia B. Lopes, Tito Trindade, Armando C. Duarte, Eduarda Pereira. Environmental Science and Pollution Research (2015) 22:3687–3696.

  DOI 10.1007/s11356-014-3591-3

- **Rescheduling process of nanoparticle removal used for water mercury remediation can increase the risk to aquatic organism: evidence of innate immune functions modulation in European eel (*Anguilla anguilla* L.)**

  Leonor Costa, Iram Mohmood, Tito Trindade, Mohammad Saleem, Armando C. Duarte, Eduarda Pereira, Iqbal Ahmad. Environmental Science and Pollution Research (2015) 22(23):18574-89.

  DOI: 10.1007/s11356-015-5375-9.

1.7. REFERENCE

Abreu SN, Pereira E, Vale C, Duarte AC. (2000) Accumulation of mercury in sea bass from a contaminated lagoon (Ria de Aveiro, Portugal). Marine Pollution Bulletin.40(4): 293-297.

Agency for Toxic Substances and Disease Registry (ATSDR), 2011 Substance Priority List (http://www.atsdr.cdc.gov/spl/index.html).

Agency for Toxic Substances and Disease Registry (ATSDR). 2012. Toxicological profile for cadmium. U.S. Department of Health and Human Services, Public Health Service. Atlanta, GA.

Ahmad I, Maria VL, Oliveira M, Serafim A, Bebianno MJ, Pacheco M, Santos MA.(2008) DNA damage and lipid peroxidation vs. protection responses in the gill of Dicentrarchus labrax L. from a contaminated coastal lagoon (Ria de Aveiro, Portugal). Sci. Tot. Environ. 406: 1-2, 298-307.

Ahmad I, Coelho JP, Mohmood I, Pacheco M, Santos MA, Duarte AC, Pereira E (2011a) Immunosuppression in the infaunal bivalve Scrobicularia plana environmentally exposed to mercury and association with its accumulation. Chemosphere. 82: 11, 1541-6.

Ahmad I, Mohmood I, Mieiro CL, Coelho JP, Pacheco M, Santos MA, Duarte AC, Pereira E (2011b) Lipid peroxidation versus antioxidant modulation in the bivalve Scrobicularia plana in response to environmental mercury–organ specificities and age effect. Aquatic Toxicology. 103: 3-4, 150-8.

Almroth BC, Sturve J, Stephensen E, Holth TF, Förlin L (2008) Protein Carbonyls and Antioxidant Defences in Corkwing Wrasse (Symphodus melops) from a Heavy Metal Polluted and a PAH Polluted Site. Marine Environmental Research 66: 271–277.

Annabi A, Said K, Messaoudi I (2013) Cadmium: bioaccumulation, histopathology and detoxifying mechanisms in fish. Amer. J. Res. Comm. 1(4): 60-79.

Baeyers W. Leermakers M. Papina T. Saprykin A. Brion N. Noyen J. et al. (2003). Bioconcentration and biomagnification of mercury and methylmercury in North Sea and

Scheldt estuary fish. Archives of Environmental Contamination and Toxicology, 45; 498–508.

Baral SS, Das N, Ramulu T S, Sahoo S K, Das SN, Chaudhury GR (2009) Removal of Cr(VI) by thermally activated weed Salvinia cucullata in a fixed-bed column. J. Hazard. Mat. 161(2-3): 1427-1435.

Barbier EB, Hacker SD, Kennedy C, Koch EW, Stier AC, Silliman BR (2011) The value of estuarine and coastal ecosystem services. Ecological Monographs 81: 169–193.

Boening DW. (2003) Ecological effects, transport, and fate of mercury: a general review. Chemosphere. 40:1335-1351.

Borgmann UY, Couillard P, Doyle. Dixon DG (2005) Toxicity of sixty-three metals and metalloids to Hyalella azteca at two levels of water hardness: Environ. Toxicol. Chem. 24(3): 641-652.

Boudou A, Ribeyre F (1985) Experimental Study of Trophic Contamination of Salmo gairdneri by two mercury compounds - HgCl2 And CH3HgCl - Analysis at the organism and organ levels. Water, Air, and Soil Pollution. 26: 137-148.

Brimer L (2011) Chemical Food Safety (Book). Technology & Engineering. pp143

Cardoro VA, Desoza AG, Sartoratto PPC, Numes LM (2004) The ionic exchange process of cobalt, nickel and copper (II) in alkaline and acid layered titanates, Colloids Surf. A 248: 145–149.

CFIA. (2002) Canadian Food Inspection Agency: Fact sheet on mercury and fish consumption. Accessible at: http://www.inspection.gc.ca/english/corpaffr/foodfacts/mercurye.shtml.

Chen CAT (2008) Effects of Climate Change on Marine Ecosystems. Fisheries for Global Welfare and Environment, 5th World Fisheries Congress 2008, pp. 307–316.

Chen CY, Dionne M, Mayes BM, Ward DM, Sturup S, Jackson BP (2009) Mercury bioavailability and bioaccumulation in estuarine food webs in the Gulf of Maine. Environmental Science & Technology. 43(6): 1804-1810.

Churchill R (1999) Insights into California mercury production and mercury availability for the gold mining industry from the historical record: Geological Society of America Abstracts with Programs. 31,6: 45.

Clarkson TW (1992) Mercury: Major issues in environmental health. Environmental Health Perspectives. 100: 31-38.

Coelho JP, Nunes M, Dolbeth M, Pereira ME, Duarte AC, Pardal MA (2008) The role of two sediment dwelling invertebrates on the mercury transfer from sediments to the estuarine trophic web. Estuar Coast Shelf Sci 78:516–523.

Coelho JP, Pereira ME, Duarte AC, Parda, MA (2005) Macroalgae response to a mercury contamination gradient in a temperate coastal lagoon (Ria de Aveiro, Portugal). Estuarine, Coastal and Shelf Science.65: 492-500.

Coelho JP, Policarpo E, Pardal MA, Millward GE, Pereira ME, Duarte AC (2007) Mercury contamination in invertebrate biota in a temperate coastal lagoon (Ria de Aveiro, Portugal). Marine Pollution Bulletin. 54: 4, 475 - 480.

Costa L, Mohmood I, Trindade T, Saleem M, Duarte AC, Pereira E, Ahmad I (2015) Rescheduling the process of nanoparticle removal used for water mercury remediation can increase the risk to aquatic organism: evidence of innate immune functions modulation in European eel (Anguilla anguilla L.) Environmental Science and Pollution Research 22(23):18574-89

Costanza R, dArge R, deGroot R, Farber S, Grasso M, Hannon B et al. (1997) The value of the world's ecosystem services and natural capital. Nature, 387, 253–260.

Costanza R, de Groot R, Sutton P, van der Ploeg S, Anderson SJ, Kubiszewski I, Farber S, Turner RK (2014) Changes in the global value of ecosystem services. Global Environmental Change 26: 152–158.

Croteau DL, Bohr VA (1997) Repair of oxidative damage to nuclear and mitochondrial DNA in mammalian cells. J Biol Chem 272: 25409–25412

Cruz-Olivares J. Pérez-Alonsoa C. Barrera-Díaz C. López G. Balderas-Hernández P. (2010) Inside the removal of lead(II) from aqueous solutions by De-Oiled Allspice Husk in batch and continuous processes. Journal of Hazardous Materials. Journal of Hazardous Materials 181; 1095–1101.

Dabrowski A, Hubicki Z, Podkoscielny P, Robens E (2004) Selective removal of the heavy metal ions from waters and industrial wastewaters by ion-exchange method. Chemosphere.56(2): 91-106.

Delorenzo ME (2015) Impacts of climate change on the ecotoxicology of chemical contaminants in estuarine organisms. Current Zoology 61 (4): 641–652.

De Marco SG, Botte SE, Marcovecchio JE (2006) Mercury distribution in abiotic and biological compartments within several estuarine systems from Argentina: 1980–2005 period. Chemosphere. 65(2): 213-223.

Dietz R, Born EW, Riget F, Aubail A, Sonne C, Drimmie R, Basuz N (2011) Temporal Trends and Future Predictions of Mercury Concentrations in Northwest Greenland Polar Bear (Ursus maritimus) Hair. Environ Sci Technol 45:1458-1465

D'Itri, P. (1997) Mercury contamination: A human tragedy. John Wiley & Sons, New York, 1977 NY, USA.

Donkor AK. Bonzongo JC. Nartey V K. Adotey DK (2006). Mercury in different environmental compartments of the Pra River Bay, Ghana. Science of the Total Environment 368:164–176.

Driscol CT, Chan HM, Jacob DJ, Pirrone N (2013) Mercury as a Global Pollutant: Sources, Pathways, and Effects. Environ Sci Technol 47: 4967–4983

Du J, Gebicki JM (2004) Proteins are major initial cell targets of hydroxyl free radicals. Int J Biochem Cell Biol. 36(11):2334-43.

EPA, Environmental Protection Agency. Mercury Update: Impact on Fish Advisories. EPA-823-F-01-011 June 2001

European commission, Commission Regulation (EC) No 1881/2006 of 19 December 2006

Evans MD, Dizdaroglu M, Cooke MS (2004) Oxidative DNA damage and disease: induction, repair and significance. Mutat Res/Rev Mutat Res 567:1–61.

Fernández B, Campillo JA, Martínez-Gómez C, Benedicto J (2010) Antioxidant responses in gills of mussel (Mytilus galloprovincialis) as biomarkers of environmental stress along the Spanish Mediterranean coast. Aquat. Toxi. 99: 186-197

Figueira P, Lopes C B, Daniel-da-Silva A L, Pereira E, Duarte AC, Trindade T (2011) Removal of mercury (II) by dithiocarbamate surface functionalized magnetite particles: Application synthetic and natural spiked waters. Water Res. 45: 5773-5784.

Fitzgerald WF, Lamborg CH, Hammerschmidt CR (2007) Marine biogeochemical cycling of mercury. Chemical Reviews. 107(2): 641-662.

Francis PC, Birge WJ, Black JA (2004) Effects of cadmium enriched sediment on fish and amphibian embryo-larval stages. Fish. Physiol. Biochem. 36: 403-409.

Fu F, Wang Q (2011) Removal of heavy metal ions from wastewaters: A review. Journal of Environmental Management. 92: 407-418.

Gautam RK, Sharma SK, Mahiya S, Chattopadhyaya MC (2014) Contamination of Heavy Metals in Aquatic Media: Transport, Toxicity and Technologies for Remediation, in *Heavy Metals In Water: Presence, Removal and Safety* CHAPTER 1 : 1-24

Ghani SA (2015) Trace metals in seawater, sediments and some fish species from Marsa Matrouh Beaches in north-western Mediterranean coast, Egypt. The Egyptian Journal of Aquatic Research. 2: 145–154

Girginova PI, Daniel-Da-Silva AL, Lopes CB, Figueira P, Otero M, Amaral VS, Pereira E, Trindade T (2010) Silica coated magnetite particles for magnetic removal of Hg(II) from water. J Colloid and Interface Sci. 2010; 345: 234-240.

Gutierrez-Mejia E, Lares ML, Sosa-Nishizaki O (2009)Hg and As in muscle and liver of the golden cownose ray, Rhinoptera steindachneri, Evermann and Jenkins, 1891, from the Upper Gulf of California, Mexico. Bull. Environ. Contam. Toxicol 83: 230–234.

Hakami O, Zhang Y, Banks CJ (2012) Thiol-functionalised mesoporous silica-coated magnetite nanoparticles for high efficiency removal and recovery of Hg from water. Water Res 2012; 46(12): 3913-3922.

Harley CDG, Hughes AR, Hultgren KM, Miner BG, Sorte CJB, Thornber CS, Rodriguez LF, Tomanek L, Williams SL (2006) The impacts of climate change in coastal marine systems. Ecology Letters 9: 228–241.

Hector A, Bagchi R (2007) Biodiversity and ecosystem multifunctionality. Nature 448: 188–196.

Højer R, Bayley M, Damgaard C, Holmstrup M. Stress synergy between drought and a common environmental contaminant: studies with the collembolan Folsomia candida. Glob Chang Biol 2001;7:485–94.

Hughes MF, Beck BD, Chen Y, Lewis AS, Thomas DJ (2011) Arsenic exposure and toxicology: a historical perspective. Toxicol Sci 123(2):305–332

Hunerlach MP, Rytuba JJ, Alpers CN (1999)Mercury contamination from hydraulic placer-gold mining in the Dutch Flat mining district, California: U.S. Geological Survey Water-Resources Investigations Report 99-4018B: 179-189.

Hung GA, Chmura GL (2006) Mercury accumulation in surface sediments of salt marshes of the Bay of Fundy. Environmental Pollution. 142: 418-431.

IPCC (United Nations Intergovernmental Panel on Climate Change), (2013) Climate Change 2013 The Physical Science Basis Working Group I Contribution to the Fifth Assessment Report of the Intergovernmental Panel on Climate Change. Available at https://www.ipcc.ch/report/ar5/

Jackson TA. (1997) Long-range atmospheric transport of mercury to ecosystems, and the importance of anthropogenic emissions – a critical review and evaluation of the published evidence. Environmental Reviews 5: 99 - 120.

Johnston EL, Roberts DA (2009) Contaminants reduce the richness and evenness of marine communities: a review and meta-analysis. Environmental Pollution 157: 1745–1752.

Johnston EL, Mayer-Pinto M, Crowe TP (2015) Chemical contaminant effects on marine ecosystem functioning. Journal of Applied Ecology 2015, 52, 140–149

Joo S, Cheng I. (2006) Nanotechnology for Environmental Remediation, Springer, New York, USA.

Kaur A, Gupta U (2008) Preconcentration Procedure Using 1-(2-Pyridylazo)-2-napthol Anchored to Silica Nanoparticle for the Analysis of Cadmium in Different Samples. E-Journal of Chemistry 5(4): 930-939.

Khan MAQ, Ahmed SA, Bogdon C, Khodadoust A, Ajayi O, Vaugh M (2006) Effect of Temperature on Heavy Metal Toxicity to Juvenile crayfish, Orconectes immunis (Hagen). Environ. Toxicol. 2006;5: 513-520

Kim BC, Lee J, Um W, Kim J, Joo J, Lee JH, Kwak JH, Kim JH, Lee C, Lee H, Addleman RS, Hyeon T, Gu MB, Kim J (2011) Magnetic mesoporous materials for removal of environmental wastes. Journal Hazard Mater 192: 1140–1147

Kim EH, Mason, RP, Porter ET, Soulen HL. (2004) The effect of resuspension on the fate of total mercury and methyl mercury in a shallow estuarine ecosystem: a mesocosm study. Marine Chemistry 86: 121-137.

Klabunde KJ, Erickson L, Koper O, Richards R. (2010) Review of Nanoscale Materials in Chemistry: environmental Applications, ACS Symp. Ser. 1045, American Chemical Society, Washington DC, USA.

Kumari B, Kumar V, Sinha AK, Ahsan J, Ghosh K, Wang H, DeBoec G (2016) Toxicology of arsenic in fish and aquatic systems Environ Chem Lett DOI 10.1007/s10311-016-0588-9

Kovendan K, Vincent S, Janarthanan S, Saravanan M (2013) Expression of metallothionein in liver and kidney of freshwater fish Cyprinus carpio var. communis (Linn) exposed to arsenic trioxide. Am J Sci Ind Res 4(1):1–10.

Lannig G, Flores JF, Sokolova IM (2006) Temperature-dependent stress response in oysters Crassostrea virginica: Pollution reduces temperature tolerance in oysters. Aquat. Toxicol. 79: 278–287.

Lannig G, Cherkasov AS, Pörtner HO, Bock C, Sokolova IM (2008) Cadmium-dependent oxygen imitation affects temperature tolerance in eastern oysters Crassostrea virginica Gmelin. Am. J. Physiol. Regul. Integr. Comp. Physiol. 294: R1338–R1346.

Lai CL, Lin SH. (2003) Electrocoagulation of chemical mechanical polishing (CMP) wastewater from semiconductor fabrication, Chem. Eng. J. ;95: 205–211

Lemaire P, Forlin L, Livingstone DR (1996) Responses of hepatic biotransformation and antioxidant enzymes to cypla-inducers (3-methylchloranthrene, β-naphthoflavone) in sea bass (Dicentrachus labrax), dab (Limanda limanda) and rainbow trout (Oncorhynchus mykiss). Aquat. Toxicol. 36: 141–160.

Liquete C, Piroddi C, Drakou EG, Gurney L, Katsanevakis S, Charef A, Egoh B (2013) Current status and future prospects for the assessment of marine and coastal ecosystem services: a systematic-review. PLoS ONE, 8, e67737.

Lopes C.B., Otero M., Coimbra J., Pereira E., Rocha J., Lin Z., Duarte A.C. (2007) Removal of low concentration Hg2+ from natural waters by microporous and layered titanosilicates. Microporous and Mesoporous Materials 103: 325-332.

Lopes C.B., Lito P.F., Otero M., Lin Z., Rocha J., Silva C.M., Pereira E., Duarte A.C. (2008). Mercury removal with titanosilicate ETS-4: Batch experiments and modelling. Microporous and Mesoporous Materials 115: 98-105.

Lopes CB, Otero M, Lin Z, Silva CM, Rocha J, Pereira E, Duarte AC. (2009) Removal of Hg^{2+} ions from aqueous solution by ETS-4 microporous titanosilicate--Kinetic and equilibrium studies. Chem Eng J 151:247-254.

Lopes CB, Pereira E, Lin Z, Pato P, Otero M, Silva CM, Duarte AC, Rocha J.(2011) Fixed-bed removal of Hg^{2+} from contaminated water by microporous titanosilicate ETS-4: experimental and theoretical breakthrough curves. Micropor Mesopor Mat 145: 32-40

Lopes CB, Lopes I, Duarte AC, Soares AMVM Rocha J, Pereira E(2014a) A Multidisciplinary Approach to Evaluate the Efficiency of a Clean-Up Technology to Remove Mercury from Water. Bull Environ Contam Toxicol 93(2):138-43.

Lopes CB, Oliveira JR Rocha LS, Tavares DS, Silva CM, Silva SP, Hartog N, Duarte AC, Pereira E. (2014b) Cork stoppers as an effective sorbent for water treatment: the removal of mercury at environmentally relevant concentrations and conditions. Environ Sci Pollut Res 21:2108–2121 DOI 10.1007/s11356-013-2104-0

Lockhart WL, Wilkinson P, Billeck BN, Danell RA, Hunt RV, Delaronde J, Brunskill GJ.(1998) Fluxes of mercury to lake sediments in central and northern Canada inferred from dated sediment cores. Biogeochemistry 40: 163 - 173.

Lushchak VI.(2011) Environmentally induced oxidative stress in aquatic animals. Aquatic Toxicology 101: 13-30

Mamalis AG. (2007) Recent advances in nanotechnology, J. Mater. Process. Technol. 2007;181: 52–58.

Mahimairaja S, Bolan NS, Adriano DC, Robinson B. (2005) Arsenic contamination and its risk management in complex environmental settings. Advances in Agronomy86: 21-34.

Malek, RL. et al., (2004) The effects of temperature reduction on gene expression and oxidative stress in skeletal muscle from adult zebrafish. Comp. Biochem. Physiol. C: Toxicol. Pharmacol. 363–373.

Mason RP, Fitzgerald WF, Morel FMM (1994) The biogeochemical cycling of elemental mercury. Geochimica et Cosmochimica Acta, 58 (15): 3191-3198.

McGeachy SM, Dixon DG (1998). The impact of temperature on the acute toxicity of arsenate and arsenite to rainbow trout (Salmo gairdneri). Ecotoxicol. Environ. Saf.17(1): 86-93

McGeer JC, Niyogi S, Smith D (2011) Cadmium. Fish Physiol. 31: 125-184.

McGeer JC, Niyogi S, Smith D (2012) Cadmium. In: C.M. Wood, A.P. Farrell and C.J. Brauner (Eds.), Homeostasis and Toxicology of Non-Essential Metals. Fish Physiol. 31 (Part B): 125–184.

McMahon TA, Halstead NT, Johnson S, Raffel TR, Romansic JM, Crumrine PW, Rohr JR (2012) Fungicide-induced declines of freshwater biodiversity modify ecosystem functions and services. Ecology Letters 15: 714–722.

Mehdinia A, Akbari M, Kayyal TB, Azad M (2014) High-efficient mercury removal from environmental water samples using di-thio grafted on magnetic mesoporous silica nanoparticles. Environ Sci Pollut Res 22(3):2155-2165.

Mishra A, Tripathi BD (2008) Utilization of fly ash in adsorption of heavy metals from wastewater. Toxicol Environ Chem 2008;90(6): 1091– 1097

Mishra VK, Upadhyay AR, Pathak V, Tripathi BD (2008) Phytoremediation of Hg and As from tropical opencast coalmine effluent through naturally occurring aquatic macrophytes. Water Air Soil Pollut.192: 303–314.

Mohammadi T, Moheb A, Sadrzadeh M, Razmi A (2004) Modeling of metal ion removal from waste water by electrodialysis, Sep. Purif. Technol. 41: 73–82.

Mohmood I, Lopes CB, Lopes I, Tavares DS, Soares AM, Duarte AC, Trindade T, Ahmad I, Pereira E (2016) Remediation of mercury contaminated saltwater with functionalized silica coated magnetite nanoparticles. Science of the Total Environment 557: 712-721

Mohmood I, Ahmad I, Asim M, Costa L, Lopes CB, Trindade T, Duarte AC, Pereira E (2014) Interference of the co-exposure of mercury with silica-coated iron oxide nanoparticles can modulate genotoxicity induced by their individual exposures—a paradox depicted in fish under in vitro conditions. Environmental Science and Pollution Research 22: 3687–3696

Mohmood I, Lopes CB, Lopes I, Ahmad I, Duarte AC, Pereira E (2013) Iram Mohmood, Cláudia Batista Lopes, Isabel Lopes, Iqbal Ahmad, Armando C. Duarte, Eduarda Pereira. Environmental Science and Pollution Research 20:1239–1260

Monteagudo J.M., Ortiz M.J. (2000) Removal of inorganic mercury from mine waste water by ion exchange. J. Chem. Technol. Biotechnol. 75: 767–772.

Montgomery S, Lucotte M, Rheault I (2000) Temporal and spatial influences of flooding on dissolved mercury in boreal reservoirs. Science of the Total Environment 260: 147 – 157

Moreira A., Figueira E., Pecora I.L., Soares A.M.V.M., Freitas R. (2017) Biochemical alterations in native and exotic oyster species in Brazil in response to increasing temperature. Comparative Biochemistry And Physiology C-toxicology & Pharmacology. 191, 183-193. (see details) Link: http://dx.doi.org/10.1016/j.cbpc.2016.10.008

National Research Council (NRC) (2000) Toxicological effects of methylmercury. Committee on the Toxicological Effects of Methylmercury, National Research Council, National Academy Press, Washington, DC, USA.

National Research Council (NRC) (2005) Mineral tolerance in animals. Second Revised Edition. Committee on Minerals and Toxic Substances in Diets and Water for Animals, National Academies Press. 496 page

Neimi D (1995) Hg Emission Notes. Environment Canada. Pollution Data Branch. Emission Inventory Task Group. 1998.Ottawa, Ontario, Canada

Newman MC, Unger MA (2003). Fundamentals of ecotoxicology. Second Edition. Boca Raton: Lewis Publishers 458.

Ngomsik AF, Bee A, Draye M, Cote G, Cabuil V. (2005) Magnetic nano-and microparticles for metal removal and environmental applications: A review. C. R. Chimie 8: 963–970.

Noyes PD, McElwee MK, Miller HD, Clark BW, Van Tiem LA et al., (2009) The toxicology of climate change: Environmental contaminants in a warming world. Environ. Int. 35(6): 971– 986.

Okocha RC, Adedeji OB (2011) Overview of cadmium toxicity in fish. J. Appl. Sci. Res.7(7): 1195-1207.

Oliveira M, Ahmad I, Maria VL, Pacheco M, Santos MA (2010a) Antioxidant responses versus DNA damage and lipid peroxidation in golden grey mullet liver – A field study at Ria de Aveiro (Portugal). Arch. Environ. Contam. Toxicol. 59: 3, 454-463.

Oliveira M, Ahmad I, Maria VL, Serafim A, Bebianno MJ, Pacheco M, Santos MA.(2010b) Hepatic metallothionein concentrations in the golden grey mullet (Liza aurata) – Relationship with environmental metal concentrations in a metal-contaminated coastal system in Portugal. Mar. Environ. Res. 69(4): 227-233.

OSPAR (2009) Convention for the protection of the Marine Environment of the North-East Atlantic. Document on mercury and organic mercury compounds. https://www.ospar.org/documents?v=7185

Pacheco S, Medina M, Valencia F, Tapia J (2006) Removal of inorganic mercury from polluted water using structured nanoparticles. J. Environ. Eng. ASCE342–349

Padmini E. (2010) Physiological Adaptations of Stressed Fish to Polluted Environments: Role of Heat Shock Proteins. Reviews of Environmental Contamination and Toxicology 2006: 1–27

Pastorinho RM, Telfer TC, Nogueira AJA, Soares AMV, Ranville JF.(2012) An evaluation of trace metal distribution, enrichment factors and risk in sediments of a coastal lagoon (Ria de Aveiro, Portugal). Environ Earth Sci 67: 2043–2052.

Patrick Lyn (2002) Mercury Toxicity and Antioxidants: Part I: Role of Glutathione and alpha-Lipoic Acid in the Treatment of Mercury Toxicity. Alternative Medicine Review 7(6) 456-471.

Pereira ME. (1996) Distribuição, reactividade e transporte do mercúrio na Ria de Aveiro. Aveiro, University of Aveiro. Tese de Doutoramento.

Pereira ME, Lillebø AI, Pato P, Válega M, Coelho JP, Lopes C, Rodrigues S, Cachada A, Otero M, Pardal MA, Duarte AC (2009) Mercury pollution in Ria de Aveiro (Portugal): a review of the system assessment. Environ. Monit. Assess. 155: 39-49.

Perez-Casanova JC, Rise ML, Dixon B, Afonso LO, Hall JR, Johnson SC, Gamperl AK (2008). The immune and stress responses of Atlantic cod to long-term increases in water temperature, Fish Shellfish Immunol. 2008; 24:600–609.

Peuranen S, Keinanen M, Tigerstedt C, Vuorinen PJ (2003) Effects of temperature on the recovery of juvenile grayling (Thymallus thymallus) from exposure to Al + Fe, Aquat. Toxicol.; 65: 73–84.

Porcella DB, Chu P, Allan MA (1996) Inventory of North American Hg emissions to the atmosphere. In W. Baeyens, R. Ebinghaus, and O. Vasiliev (eds), Global and regional

mercury cycles: Sources, fluxes and mass balances. NATO ASI Series, Series 2: Environment 21, Kluwer Academic Publishers, Dordrecht, The Netherlands.

Pörtner HO (2001). Climate change and temperature dependent biogeography: Oxygen limitation of thermal tolerance in animals. Naturwissenschaften 88: 137–146.

Rahbar N, Jahangiri A, Boumi S, Khodayar MJ. Mercury Removal From Aqueous Solutions With Chitosan-Coated Magnetite Nanoparticles Optimized Using the Box-Behnken Design. Jundishapur J Nat Pharm Prod. 2014: 9(2)

Remoudaki E, Hatzikioseyian A, Tsezos K, Tsezos M (2003)The mechanism of metals precipitation by biologically generated alkalinity in biofilm reactors. Water Res 37:3843–3854.

Rengaraj S, Ho YK, Hyeon MS (2001) Removal of chromium from water and waste water by ion exchange resin. J. Hazard. Mater.8:273–287.

Rice KM, Walker EM, Wu M, Gillette C, Blough ER (2014) Environmental Mercury and Its Toxic Effects 2014 J Prev Med Public Health 47:74-83.

Rocha L, Lopes CB, Borges JA, Duarte AC, Pereira E (2014) Valuation of unmodified rice husk waste as an eco-friendly sorbent to remove mercury: a study using environmental realistic concentrations. Water Air Soil Pollut 224(7):1–18. doi:10.1007/ s11270-013-1599-9

Sánchez A, Recillas S, Font X, Casals E, González E, Puntes V (2011) Ecotoxicity of, and remediation with, engineered inorganic nanoparticles in the environment. Trends in Analytical Chemistry 30:3.

Sandheinrich MB, Weiner JG (2010) Methylmercury in freshwater fish: recent advances in accessing toxicity of environmentally relevant exposures. In: Beyer WN, Meador JP (eds) Environmental contaminants in biota: interpreting tissue concentrations. Taylor and Francis, CRC Press, Boca Raton:169–190.

Schartup AT, Balcom PH, Mason RP, Sunderland EM (2015) Contrasting Effects of Marine and Terrestrially Derived Dissolved Organic Matter on Mercury Speciation and Bioavailability in Seawater. Environ Sci Technol 49 (10):5965–5972

Scudder BC, Chasar LC, Wentz DA, Bauch NJ, Brigham ME, Moran PW, Krabbenhoft DP.(2009) Mercury in fish, bed sediment, and water from streams across the United States, 1998–2005: U.S. Geological Survey Scientific Investigations Report 5109, 74

Shan C, Ma Z, Tong M, Ni J. Removal of Hg(II) by poly(1-vinylimidazole)-grafted Fe3O4@SiO2 magnetic nanoparticles. Water Res 2015: 69:256-260.

Shanker AK (2008) Mode of action and toxicity of trace elements. In: M.N.V. Prasad (Ed.), Trace Elements as Contaminants and Nutrients: Consequences in Ecosystems and Human Health, John Wiley & Sons, Inc., Hoboken, NJ.

Shevchenko V A, Lisitzin A, Vinogradova A (2003) Heavy metals in aerosols over the seas of the Russian Arctic. Sci. Total Environ. 306: 11-25.

Shilts WW, Coker WB (1995) Mercury anomalies in lake water and in commercially harvested fish, Kaminak lake area, District of Keewatin, Canada. Water, Air, and Soil Pollution 80: 881 - 884.

Siscar R, Torreblanca A, del Ramo J, Solé M (2014) Modulation of metallothionein and metal partitioning in liver and kidney of Solea senegalensis after long-term acclimation to two environmental temperatures. Environ. Res. 132: 197–205.

Spry DJ, Wiener JG. (1991) Metal bioavailability and toxicity to fish in low- alkalinity lakes: a critical review. Environmental Pollution.71: 243-304.

Stephens GR (1995) Mercury concentrations in fish in a remote Canadian arctic lake. Water, Air, and Soil Pollution 80: 633 - 636.

St. Louis VL, Rudd JWM, Kelly CA, Bodaly JWM, Paterson MJ, Beaty KG, Husslein RH, Heyes A, and Majewski AR (2004) The rise and fall of mercury methylation in an experimental reservoir. Environmental Science and Technology 38: 1348 - 1358.

Taty-Costodes V C, Fauduet H, Porte C, Ho Y-S (2005) Removal of lead (II) ions from synthetic and real effluents using immobilized Pinus sylvestris sawdust: Adsorption on a fixed-bed column. J Hazard Mat 123(1-3): 135-144.

Tavares DS, Daniel-da-Silva AL, Lopes CB, Silva NJO, Amaral VS, Rocha J, Pereira E, Trindade T. (2013) Efficient sorbents based on magnetite coated with siliceous hybrid shells for removal of mercury ions. J Mater Chem 1: 8134-8143.

Tavares PC, Kelly A, Maia R, Lopes RJ, Serrão Santos R, Pereira ME, Duarte AC, Furness RW. (2008) Variation in the mobilization of mercury into Black-winged Stilt Himantopus himantopus chicks in coastal saltpans, as revealed by stable isotopes. Estuar. Coast. Shelf Sci.77(1): 65-76.

Tchobanoglous G, Burton FL, Stensel HD (2003) Wastewater Engineering: Treatment and Reuse, Inc. McGraw-Hill.

Tchounwou PB, Yedjou CG, Patlolla AK, Sutton DJ (2012) Heavy metal toxicity and the environment. EXS. 101:133-64.

TEEB (2010) The Economics of Ecosystems and Biodiversity: Mainstreaming the Economics of Nature: A Synthesis of the Approach, Conclusions and Recommendations of TEEB. UNEP, Paris.

Tornero V, Hanke G (2016) Chemical contaminants entering the marine environment from sea-based sources: A review with a focus on European seas. Marine Pollution Bulletin 112: 17–38

Trenberth et al., (2007) Ch. 3. Observations: Atmospheric Surface and Climate Change, Section 3.2.2.2: Urban Heat Islands and Land Use Effects, p. 244, in IPCC AR4 WG1.

UNEP (2002) Chemicals. Global Mercury Assessment. United Nations Environmental Programme Chemicals, Geneva, Switzerland.

UNEP (2012). A Practical Guide: Reducing Mercury Use in Artisanal and Small-Scale Gold Mining. United Nations Environment Programme, Global Mercury Partnership.

UNEP (2013) Global Mercury Assessment. Sourse, emissions, releases and Environmental Transport. Geneva, Switzerland. United Nations Environment Programme,

USA ATSDR. (2001) Toxicological profile for mercury. Agency for Toxic Substances and Disease Registry, Atlanta, USA.

US Environmental Protection Agency (EPA). (2016) Coal ash basics. Office of Water, Washington, DC. Available at: http://www.epa.gov/coalash/coal-ash-basics (info accessed February 2016).

US Environmental Protection Agency (EPA). (2002) Method 1631, Revision E: Mercury in water by oxidation, purge and trap, and cold vapor atomic fluorescence spectrometry. Publication EPA-821-R-02-019.

US Geological Survey (2016), Mineral Commodity Summaries, January 2012

Valderrama C, Arévalo JA, Casas I, Martínez M, Miralles N, Florido A (2010)Modelling of the Ni(II) removal from aqueous solutions onto grape stalk wastes in fixed-bed column. J. Hazardous Mat 174(1-3): 144-150

Valavanidis A, Vlachogianni T, Fiotakis C. (2009) 8-Hydroxy-2'-deoxyguanosine (8-OHdG): a critical biomarker of oxidative stress and carcinogenesis. J Environ Sci Health Part C: Environ Carcinog Ecotoxicol 27: 120–139.

Valavanidis A, Vlachogianni T (2010) Metal Pollution in Ecosystems.Ecotoxicology Studies and Risk Assessment in the Marine Environment. Science advances on Environment, Toxicology and Ecotoxicology issue. 1: 1-14.

Valko M, Izakovic M, Mazur M, Rhodes CJ, Telser J (2004) Role of oxygen radicals in DNA damage and cancer incidence. Mol Cell Biochem 266: 37–56.

Velez C., Figueira E., Soares A.M.V.M., Freitas R. (2017) Effects of seawater temperature increase on economically relevant native and introduced clam species. Marine Environmental Research. 123, 62-70. (see details) Link: http://dx.doi.org/10.1016/j.marenvres.2016.11.010

Verlecar XN, Jena KB, Chainy GNB (2007) Biochemical markers of oxidative stress in Perna viridis exposed to mercury and temperature. Chemico-Biological Interactions 167: 219–226.

Vinodhini R., Narayanan M. (2008) Bioaccumulation of heavy metals in organs of fresh water fish Cyprinus carpio (Common carp) Int. J. Environ. Sci. Tech. 5 (2): 179 -182.

Vitousek PM, Mooney HA, Lubchenco J, Melillo JM (1997) Human domination of Earth's ecosystems. Science 277: 494–499.

World Health Organization (WHO). 2010. Cadmium- Environmental Aspects: Environmental Health Criteria 135. Geneva, World Health Organization.

Wolfe MF, Schwarzbach S, Sulaiman RA (1998) Effects of mercury on wildlife: A comprehensive review. Environ Chem Toxicol 17:146-160.

Zhai Y., Duan Q. He, Yang X., Han Q. (2010). "Solid phase extraction and preconcentration of trace mercury(II) from aqueous solution using magnetic nanoparticles doped with 1,5-diphenylcarbazide." Microchimica Acta 169(3): 353-360.

Wanga H. (2009). Removal of arsenic from water by supported nano zero-valent iron on activated carbon. J. Hazard. Mat. 172: 1591–1596

Zhang S, Zhang Y, Liu J, Xu Q, Xiao H, Wang X, Xu H, Zhou J (2013)Thiol modified Fe3O4@SiO2 as a robust, high effective, and recycling magnetic sorbent for mercury removal. Chem Eng J 226:30-38.

CHAPTER 2

Nanoscale materials and their use in water contaminants removal – a review

Abstract

Water scarcity is being recognized as a present and future threat to human activity and as a consequence water purification technologies are gaining major attention worldwide. Nanotechnology has many successful applications in different fields but recently its application for water and wastewater treatment has emerged as a fast–developing, promising area. This review highlights the recent advances on the development of nanoscale materials and processes for treatment of surface water, groundwater and industrial wastewater that are contaminated by toxic metals, organic and inorganic compounds, bacteria and viruses. In addition, the toxic potential of engineered nanomaterials for human health and the environment will also be discussed.

Keywords – *Nanotechnology, nanoscale material, nanoparticles, water purification, water remediation, toxicity.*

Environmental Science Pollution Research
(2013) 20:1239–1260

2.1. INTRODUCTION

Increasing pollution of groundwater and surface water from a wide variety of industrial, municipal and agricultural sources has seriously contaminated water quality in these water resources, effectively reducing the supply of freshwater for human use (Foley et al., 2005; Coetser et al., 2007; Sprenger et al., 2011; Delpla et al., 2011). Although the nature of pollution problems may vary, they are typically due to inadequate sanitation, algal blooms, detergents, fertilizers, pesticides, chemicals, potentially toxic metals, salinity caused by widespread and inefficient irrigation, and high sediment loads resulting from upstream soil erosion (Falconer and Humpage 2005; Foley et al., 2005; Rozell and Reaven 2011). Thus, water scarcity is being recognized as a present and future threat to human activity and as a consequence, water purification technologies are gaining major worldwide attention (Theron et al., 2008; Dankovich and Gray 2011; Zhai et al., 2012). In this perspective, nanotechnology has been identified as one of the most promising technologies that could play an important role in resolving many of the problems involving water purification and quality (Bottero et al., 2006; Theron et al., 2008; Warner et al., 2010; Chen et al., 2011; Sánchez et al., 2011). Most environmental applications of nanotechnology fall into three categories: (i) environmental–friendly and/or sustainable products (*e.g.* green chemistry or pollution prevention), (ii) treatment and remediation of materials contaminated with hazardous substances, and (iii) sensors and detectors for environmental protection (Rickerby and Morrison 2007; Vaseashta et al., 2007). Within the category of treatment and remediation, nanotechnology has the potential to contribute to long–term water quality, availability and viability of water resources such as through the use of advanced filtration materials that enable greater water reuse, recycling and desalinization. Within the category of sensing and detection, of particular interest, is the development of new and enhanced sensors to detect biological, chemical and emerging contaminants, present at very low concentration levels in the environment, including water. Moreover, nanotechnology has the potential to facilitate the development of continuous monitoring devices capable of yielding real–time measurements at a low cost and with improved specificity in this field (Riu et al., 2006; Vaseashta et al., 2007).

Nanomaterials have many properties, such as, strong adsorption, enhanced redox and photocatalytic properties providing unprecedented opportunities to treat contaminants

in water. It is emphasized that during the treatment of water contaminants using nanomaterials, the following four precedent conditions should be met: (1) environment security, (2) reuse of treatment agents, (3) low cost and (4) high treatment efficiency. The main highlights for the study and development of water treatments are design, synthesis and application of nanosorbents, nanocatalysts, redox active nanoparticles and nanostructures. Nanomaterials and nanostructures have at least one nanoscale dimensions that range from 1 to 100 nm. At nanoscale level, materials are characterized by different physical, chemical and biological properties instead of their normal size equivalents (Zhang and Fang 2010; Liu et al., 2011). For instance, metals, metal oxides, polymers and carbon derivatives (carbon nanotubes and fullerenes) have higher ratio of surface area to particle size at the nanoscale level than at their normal level. In other words, the surface area of particles increases with decreasing particle size and as such, nanoparticles exhibit different optical, electrical and magnetic properties from the properties exhibited by microscopic particles (Warner et al., 2010). These remarkable characteristics of particles, at the nanoscale level, possibly originated from the increase in the number of surface atoms with the decreasing of particle size. Thus, this review will highlight the uses of different nanoscale materials and their applications in water treatment contaminated by toxic metals, organic and inorganic compounds, bacteria and viruses. In addition, the toxic potential of engineered nanomaterials for human health and the environment will also be discussed.

2.2. NANOSCALE WATER TREATMENT APPLICATIONS

Recent advances on water treatment technology suggest that many of the issues involving water quality could be resolved or greatly ameliorated using nanoparticles, nanofiltration or other products resulting from the development of nanotechnology. Innovations in the development of novel technologies to desalinate water are among the most exciting and promising. The application of specific nanoparticles either embedded in membranes or on other structural media that can effectively, inexpensively and rapidly render unusable water potable is being explored at a variety of institutions. Innovative use of nanoparticles for treatment of industrial wastewater is another potentially useful application. Many factories generate large amounts of wastewater. Removal of

contaminants and reusing of the purified water would provide significant reductions in cost, time, and labor to industry, resulting in an improved environmental stewardship. Groundwater remediation is also a critical issue, becoming more important as water supplies steadily decrease and demand continues to increase. Most of the remediation technologies available today, while effective, very often are costly and time consuming, particularly pump–and–treat methods. The ability to remove toxic compounds from subsurface and other environments that are very difficult to access *in situ*, and doing so rapidly, efficiently and within reasonable costs is the ultimate goal. Below, we highlight the results of selected studies on the nano–based water treatment applications mainly divided into three category: nanoscale materials and water filtration (*e.g.* nanostructured and nanoreactive membranes), nanoscale materials for water remediation (*e.g.* zeolite, carbon nanotubes, magnetic nanomaterials, semiconductor photocatalysts, nanoscale zerovalent iron particles) and others nanoscale materials for water purification (*e.g.* bioactive nanoparticles for water disinfection).

2.2.1. Water Filtration

Membrane processes are playing an important role in water purification, since conventional water treatment techniques such as sedimentation, flocculation, coagulation and activated carbon are not able to remove organic pollutants to meet laid down specifications (Viessman 2008; Strathmann 2001). The types of membrane processes that are commonly used in water purification include microfiltration (MF), ultrafiltration (UF) and nanofiltration (NF) for water and wastewater treatment (Peltier et al., 2003; Ahmad et al., 2004; Qin et al., 2007) and nanofiltration and reverse osmosis (RO) for desalination and water reclamation (Mohsen et al., 2003; Walha et al., 2007). Because membrane processes are considered key components of advanced water purification and desalination technologies, there is a continuous search for new materials and water purification technologies. In this regard, nanomaterials (*e.g.*, carbon nanotubes, nanoparticles and dendrimers) are contributing to the development of more efficient and cost–effective water filtration processes (Table 2.1).

2.2.1.1. Nanostructured and nanoreactive membranes

Since sedimentation, flocculation, coagulation and activated carbon each remove a narrow spectrum of water pollutants, membrane filtration has played an important role in

reducing pollutants and producing high quality pure water (Strathmann 2001; Leiknes 2009; Kim and Buggen 2010). Van der Bruggen and Vandercasteele (2003) have reviewed the use of nanofiltration to remove cations, natural organic matter, biological contaminants, organic pollutants, nitrates and arsenic from groundwater and surface water. Favre–Reguillon et al., (2003) showed that nanofiltration can be used to remove small quantities of U(VI) from seawater. Mohsen et al., (2003) have evaluated the use of nanofiltration to desalinate water and found that nanofiltration in combination with reverse osmosis could effectively render brackish water potable. Peltier et al., (2003) demonstrated an improvement in water quality for a large water distribution system using nanofiltration. Substantial reductions in the quantities of both organic and biological contaminants (*e.g.*, bacteria and viruses) were achieved using this process. Cohen (2006) reported that a promising approach to improve membrane performance, while mitigating fouling, is to structure the membrane surfaces at nano– and molecular scale. Porous carbons have a great potential in adsorption and in membrane synthesis for water filtration as they are considered as "molecular sieve materials". Water filters from carbon nanotubes were synthesized by Srivastava et al., (2004). These new filtration membranes consist of hollow cylinders with radially aligned carbon nanotube walls effective at removing bacteria (*Escherichia coli* and *Staphylococus aureus*) and Poliovirus sabin 1 from contaminated water. These carbon nanotube filters were also re–usable and could be cleaned by ultrasonication or autoclaving.

Table 2.1. Examples of nanostructured and nanoreactive membranes for use in water purification

Membrane	Pollutant	Reference
Nanostructured membrane		
Carbon nanotubes	Bacteria and Viruses	Srivastava et al., (2004)
Nanoreactive membrane		
Alumina membrane formed from A-alumoxane	Synthetic dyes	DeFriend et al., (2003)
Alumina membranes functionalized with poly(styrene sulfonate) or poly(allylamine hydrochloride)	Divalent cations	Stanton et al., (2003)

Silica and cellulose-based membranes functionalized with amino acid homopolymers	Metal ions	Bhattacharayya et al., (1998); Ritchie et al., (2001)
Alumina or polymeric membranes with gold nanoparticles	4-nitrophenol	Dotzauer et al., (2006)
Polymer-impregnated ceramic TiO_2 filters	Polycyclic aromatic hydrocarbons (PAHs)	Arkas et al., (2006)
Polymer-impregnated ceramic alumina and silicon-carbon filters	Trihalogen methanes, PAHs, pesticide	Allabashi et al., (2007)
Nanosilver impregnate membranes	Bacteria	Zodrow et al., (2009)
Ag/TiO_2 nanofiber membrane	Bacteria	Liu et al., (2012)
TiO_2/Al_2O_3 composite membranes	Direct Black 168 dye	Zhang et al., (2006)
TiO_2 photocatalytic nanofiltration membrane	methyl orange, azo-dye	Romanos et al., (2011); Athanasekou et al., (2012)

The nanostructured manipulation of nanostructured membrane to produce a surface with salt rejection selectivity was achieved by Linder and Oren (2006). Membranes were prepared having 70% of rejection to NaCl and less than 40% of rejection to $CaCl_2$ in single solution. This monovalent/divalent cation selection is important to minimize the membrane fouling by calcium carbonates or sulphate salts and to keep the Na to Ca ratio to a proper level for agricultural purposes. In a similar approach, the nanostructure surface modification of microporous ceramics was achieved by Wegmann et al (2008) with the aim of efficient virus filtration. The procedure consisted of coating the internal surface area of highly porous elements with a colloidal nanodispersion hydrated yettrium oxide. It was then heated to obtain an electropositive yettrium oxide coated surface. Modified–nanostructure filters were able to remove 99.99% of 25 nm diameter MS2 bacteriophages from feed water of pH between 5 and 9. Recently, self–organized liquid–crystalline nanostructured membranes were achieved by Henmi et al., (2012), exhibiting the salt–rejection properties and unique ion selectivity. The membrane has self–organized pores of average size 0.60 nm. Self–organized nanostructured membranes have great potential for

removing a variety of solutes and afford high quality potable, agricultural, and industrial water. Scott et al., (2011) demonstrated that through the utilization of this reactive, nanostructured, two-membrane stacked system, harmful organic contaminants can be degraded through the addition of a substrate, glucose, which is enzymatically converted to H_2O_2, thereby eliminating the need for additional chemical reagents. To illustrate the effectiveness of this membrane platform in real–world applications, membrane–immobilized ferrihydrite/iron oxide nanoparticles were reacted with hydrogen peroxide to form free radicals for the degradation of a chlorinated organic contaminant in groundwater. These reactive, nanostructured multimembrane systems presents an opportunity for conducting other complex reaction sequences quickly and efficiently. Water filtration membranes fabricated from nanomaterials are already being promoted by water treatment companies. For instance, Argonide (*Pittsburgh*) has a product called *NanoCeram*, which is a purifier that uses 2 nm diameter alumina nanofibres to remove 99.9999% of bacteria, viruses and protozoan cysts from water (Smith 2006).

The use of nanostructured material for improving membrane filters will gain more attention in the near future, because of unlimited benefits that accrue from producing membranes with superior performance in terms of organic and biological contaminants removal, with metal selectivity, that are resistant to fouling, durable and cost effective.

In addition to the above nanostructured membranes, several reactive and functionalized membranes have also been developed for their use in water filtration processes. DeFriend et al (2003) reported the successful fabrication of alumina UF membranes, using alumina (A–alumoxane) nanoparticles that showed selectivity toward different synthetic dyes (*i.e.,* Direct Red 81, Direct Blue 71 and Direct Yellow 71). Subsequently, the fabrication of novel NF membranes by deposition of 4.5–5.0 layer pairs of poly(styrene sulfonate)/poly(allylamine hydrochloride) onto porous alumina has also been reported (Stanton et al., 2003). These NF membranes exhibited high water flux, high retention of divalent cations (Ca(II) and Mg(II)) and Cl^-/SO_4^{2-} selectivity ratios up to 80. Polyelectrolytes or polyamines, which contain multifunctional chelating groups (*e.g.*, amines, carboxylic acids or pyridines), form strong and stable interactions with metal ions (Rivas et al., 2003), and procedures for their attachment on membrane internal pore surfaces have been studied previously for their use in metal ions sorption (Bhattacharyya et

al., 1998; Ritchie et al., 2001). Amino acids are particularly interesting groups of chelating species, since a primary amine and a carboxylic acid are available for metal ion binding. Consequently, homopolymers of amino acids may be used effectively for metal sorption (Bhattacharyya et al., 1998; Ritchie et al., 2001). Novel membranes have been prepared by deposition of multilayers charged polypeptides (poly(L–glutamic acid) or poly(L–lysine)) inside the pores of functionalized polycarbonate track–etched membranes, which were subsequently shown to display enhanced metal ion retention and permeate flux (Hollman and Bhattacharyya 2004). Moreover, Dotzauer et al., (2006) described a method for modifying alumina and polymeric membranes with gold nanoparticles through layer–by–layer adsorption of polyelectrolytes and citrate–stabilized gold nanoparticles. The modified membranes were subsequently shown to reduce more than 99% of 0.4 mM 4–nitrophenol to 4–aminophenol. Polysulfonate ultrafiltration membranes impregnated with silver nanoparticles were found effective against *E. coli* K 12 and *P. mendocina* bacteria strain and showed a significant removal (Zodrow et al., 2009). Additionally, the nanosilver impregnate membranes were resistant to biofouling mainly because of the bacteria attachment to the membrane surface was prohibited by Ag^{+}. Recently, a novel membrane was synthesized by using facile polyol for the deposition of Ag nanoparticles on electrospun TiO_2 nanofibers for the subsequent fabrication of Ag/TiO_2 nanofiber membrane (Liu et al., 2012). These permeate flux of the Ag/TiO_2 nanofiber membrane was remarkably high compared to commercial P25 deposited membrane. The Ag/TiO_2 nanofiber membrane achieved 99.9% bacteria inactivation and 80.0% dye degradation under solar irradiation within 30 min. The Ag/TiO_2 nanofiber membrane also showed excellent antibacterial capability without solar irradiation. Considering the excellent intrinsic antibacterial activity and high–performance photocatalytic disinfection/degradation under solar irradiation, this novel membrane proved to have promising applications in water purification industry.

Composite photocatalytic membranes that combine the separation technology provided by the membrane process and the photocatalytic activity of catalysts, were studied by several researchers (Zhang et al., 2006; Yang and Li 2008; Romanos et al., 2011; Athanasekou et al., 2012). TiO_2/Al_2O_3 composite membranes fabricated by following the extrusion method and sol-gel/slip casting method effectively decomposed Direct Black 168 dye (82% removal) when photocatalysis is coupled with membrane

separation (Zhang et al., 2006). Similarly, Yang and Li (2008) have successfully employed the extrusion method and sol–gel/slip casting method to prepare inside–out tubular TiO_2/Al_2O_3 composite membranes to degrade a great amount of the concerned water pollutant from the target wastewater that had a final permeate turbidity of lower than 0.75 NTU. Recently, a novel composite TiO_2 photocatalytic nanofiltration membrane was developed by chemical vapour deposition (Romanos et al., 2011). The method involved pyrolytic decomposition of titanium tetraisopropoxide vapor and formation of TiO_2 nanoparticles through homogeneous gas phase reactions and aggregation of the produced intermediate species. The developed composite nanofiltration membranes were highly efficient in the decomposition of methyl orange exhibiting low adsorption–fouling tendency and high water permeability. Similarly, composite TiO_2 photocatalytic ultrafiltration membranes were developed through chemical vapour layer–by–layer deposition of TiO_2 (Athanasekou et al., 2012). The technique comprised chemisorption or physisorption of the titanium isopropoxide vapour and a subsequent oxidative treatment in order to promote the precursor condensation and generate new adsorption sites for the accomplishment of the successive adsorption/surface reaction steps. The membranes developed through the physisorption path were highly efficient in the decomposition of azo–dye pollutant.

2.2.1.2. Polymer supported filtration

Reverse osmosis (RO) membranes have pore sizes of 0.1–1.0 nm and thus are very effective at retaining dissolved inorganic and organic solutes with molar mass below 1000 Da (Zeman and Zydney 1996), whereas Nanofilter (NF) membranes remove hardness (*e.g.,* multivalent cations) and organic solutes with molar mass between 1000–3000 Da (*e.g.,* natural organic material) (Zeman and Zydney 1996). However, high pressures are required to operate both RO and NF membranes. Conversely, Ultrafine (UF) membranes require lower pressure (200–700 kPa) and unfortunately are not very effective at removing dissolved organic and inorganic solute with molar mass below 3000 Da. Advances in macromolecular chemistry such as the invention of dendritic polymers are providing unprecedented opportunities to develop effective UF processes for purification of water contaminated by toxic metal ions, radionuclide, organic solutes and inorganic ions, bacteria and viruses. Dendrimers are highly branched monodisperse macromolecules with well controlled composition and architecture consisting of a central core, repeating units

and terminal functional groups (Tully and Frechet 2001; Arkas 2010). The nature of the internal repeating units determines the microenvironment of the interior and consequently its solubilization properties, whilst the external groups determine the chemical behavior of dendrimers in the external medium (Frechet and Tomalia 2001; Klajnert and Bryszewska 2001). Hyperbranched polymers maintain many of the architectural features and properties of dendrimers, but they are synthesized by one–step reactions forming polydisperse polymers of a non–perfectly symmetric shape (Jikei et al., 2001; Gao and Yan 2004; Yates and Hayes 2004). In contrast, cyclodextrins are cyclic polysaccharide oligomers and have a truncated–cone shape that forms a well–defined cylindrical cavity (Schneiderman and Stalcup 2000; Tick et al., 2003; Del Valle 2004). The interior of the cavity is lipophilic and can encapsulate various different organic compounds with suitable geometry and polarity, forming stable inclusion complexes. The outer surface of cyclodextrins has multiple hydroxyl groups, which are susceptible to further functionalization, thus leading to diversified molecules suitable for various applications, including the removal of pesticides (Sawicki and Mercier 2006) and organic contaminants from water (Arkas et al., 2006; Arkas et al., 2010). Indeed, studies have established that modified poly(propylene imine) (Yates and Hayes 2004) and poly(amidoamine) dendrimers (Diallo et al., 2004), as well as polyethylene imine hyperbranched polymers (Arkas et al., 2005) can effectively remove various organic molecules from water. Moreover, dendritic polymers have also been used successfully as delivery vehicles or scaffolds for antimicrobial agents such as ionic silver (Ag(I)) and quaternary ammonium chlorides (Balogh et al., 2001; Chen and Cooper 2002).

A dendrimer–enhanced ultrafiltration (DEUF) process for recovering metal ions from aqueous solutions has been reported by Diallo et al (2004; 2005). Using poly(amidoamine) dendrimers, separation of dendrimer–Cu(II) complexes from aqueous solutions was achieved simply by UF membranes with the appropriate molecular weight cut–off (MWCO). The metal ion laden dendrimers could be regenerated by decreasing the solution pH to 4.0, thus enabling the recovery of the bound Cu(II) ions and recycling of the dendritic polymer (Diallo et al., 2005). Based on the very low tendency of the dendrimers to foul commercially available regenerated cellulose membranes and on their small intrinsic viscosities, it was concluded that a comparatively smaller operating pressure and energy consumption could be achieved with dendritic polymers in tangential/cross–flow UF systems, which are typically used in water purification (Diallo et al., 2005). The

development of a method that permits removal of organic pollutants by employing a simple filtration step has been described by Arkas et al., (2006). This was pursued by utilizing titanium dioxide (TiO_2) porous ceramic filters of which the pores were impregnated with an alkylated poly(propylene imine) dendrimer, poly(ethylene imine) hyperbranched polymer or β–cyclodextrin, thus resulting in hybrid organic/inorganic filter modules of high mechanical strength and high surface area. These filters were subsequently tested for the purification of water by continuous filtration experiments, employing a variety of water pollutants. Polycyclic aromatic hydrocarbons (PAHs) could be removed very efficiently (more than 95%). Moreover, representatives of different pollutant groups (*i.e.*, trihalogen methanes (THMs), monoaromatic hydrocarbons (benzene, toluene, xylene) and pesticides (simazine)) were also removed efficiently (in excess of 80%), but the filters became saturated considerably faster in such instances (Arkas et al., 2006; Arkas et al., 2010). These studies have been extended through the use of ceramic membranes made from alumina (A_2O_3) and silicon–carbon (SiC) impregnated with crosslinked silylated dendritic or cyclodextrin polymers (Allabashiet al., 2007). A comparison of the silylated polymers performance with the aforementioned alkyl substituted polymers revealed that the latter were better suited for PAH sorption, but that silylated cyclodextrins were able to remove a wide range of pollutants.

2.2.2. Water Remediation

The use of metals and chemicals in industrial processes has resulted in the generation of large quantities of effluent that contain high levels of toxic metals, furthermore mining and mineral processing operations also generate toxic liquid wastes into water bodies (Coetser et al., 2007). Moreover, groundwater is often contaminated by spills, agricultural practices, past waste disposal practices and leaking underground storage tanks (Foley et al., 2005; Rozemeijer et al., 2007). The presence of different organic and metal contaminants in these, as well as other environmental water sources has a large environmental, public health and economic impact. In addition, to highly toxic elements such as arsenic (As), lead (Pb), chromium (Cr), cadmium (Cd), and mercury (Hg) (Lee et al., 2005a), inorganic anions such as nitrate (NO_3^-) and perchlorate (ClO_4^-) are also of concern. Whereas high levels of nitrates in drinking water may be harmful to newborn babies and contribute to cancer (Yang and Lee 2005). Perchlorate, which has emerged as a

high profile contaminant and has consequently, received considerable regulatory attention (Urbansky and Schock 1999; Cheng et al., 2007) due to its leading role to hypothyroidism in adults (Blount et al., 2006). Moreover, almost all of the chlorinated aromatic compounds exhibit high toxicity and several of these compounds are carcinogenic (Xu et al., 2005b). Notably, trichloroethene (TCE) is considered to be one of the most common hazardous organic contaminants found in groundwater and has been linked to liver damage and impaired pregnancies in humans (Nutt et al., 2006). In addition, halogenated aromatic compounds have become a serious environment contamination problem because of their long life, chemical stability and non–biodegradablity (Keum and Li 2004). Most of the traditional technologies such as solvent extraction, activated carbon adsorption and common chemical oxidation, whilst effective, very often are costly and time–consuming (Langwaldt and Puhakka, 2000; Schwarzenbach et al., 2006). Biological degradation is environmentally friendly and cost-effective; but it is usually time–consuming (Ahluwalia and Goyal, 2007). Thus, the ability to remove toxic contaminants from these environments to a safe level and doing so rapidly, efficiently, and within reasonable costs is important (Savage and Diallo 2005). Nanotechnology could play an important role in this regard. An active emerging area of research is the development of novel nanomaterials with increased affinity, capacity and selectivity for metals and other contaminants. The benefits from the use of nanomaterials may derive from their enhanced reactivity, surface area and sequestration characteristics (Zhang 2003; Li et al., 2006b). A variety of nanomaterials are in various stages of research and development, each possessing unique functionalities that is potentially applicable to the remediation of industrial effluents, groundwater, surface water and drinking water (Table 2.2).

2.2.2.1. Zeolites

Zeolites are inorganic crystalline porous materials that have a highly ordered structure and are generally comprised of silicon (Si), aluminium (Al) and oxygen (Camblor et al., 1998). Their physicochemical characteristics such as high mechanical and chemical resistance in addition to their high surface area, have formed the basis for their widespread use in catalysis, separation and ion–exchange (Song et al., 2005a; Tavolaro et al., 2007; Margeta et al., 2011). Although conventional synthesis methods produce zeolites on the scale of 1 to 10 μm, nanoscale zeolites, which comprise discrete, uniform crystals with dimensions ranging from 5 to 100 nm, have been synthesized successfully (Camblor et al.,

1998; Song et al., 2004, 2005a; Ding and Zeng 2007). Compared to micron–scale zeolites, the nanocrystalline zeolites exhibit greater external surface areas, smaller diffusion path lengths and a greater aversion to coke formation (Song et al., 2005a). The Si/Al ratio of zeolites can be varied either during synthesis or post–synthetically and, in general, zeolites have a low Si/Al ratio and therefore a high ion–exchange capacity. Conversely, if the Al content decreases, the ion–exchange capacity of a zeolite is reduced and it becomes more hydrophobic or organophilic in its adsorptive characteristics (Tavolaro et al., 2007). In contrast to nanocrystalline zeolites, micron–scale zeolites have been tested for a variety of environmental applications. NaP1 zeolites, which can be synthesized inexpensively by alkaline hydrothermal activation of coal fly ash in 1–2 M NaOH solutions (Moreno et al., 2001), have been used successfully to remove metals from acid mine wastewaters (Moreno et al., 2001) and to remove Cr(III), Ni(II), Zn(II), Cu(II) and Cd(II) from metal electroplating wastewaters (Alvarez-Ayuso et al., 2003). Moreover, surfactant–modified zeolites (SMZ) have also been used, not only to remediate water containing the radioactive species ^{137}Cs and ^{90}Sr found in nuclear plant wastewater, but also to adsorb both tetrachloroethene and chromate (CrO_4^{2-}) from groundwater and to remove petroleum hydrocarbons such as benzene, toluene, ethylbenzene and xylene from oil field wastewater (Bowman 2002). In contrast, nanocrystalline zeolites appear to be in the research phase and no specific water remediation processes have been proposed. The synthesis of nanocrystalline NaY zeolites capable of absorbing *ca*. 10% more toluene and *ca.* 30% more nitrogen dioxide relative to commercial NaY zeolites have, however, been described (Song et al., 2005b). In addition, nanocrystalline ZSM–5 zeolites, with a particle size of 15 nm, have been reported to adsorb *ca.* 50% more toluene than ZSM–5 samples with larger particle sizes (Song et al., 2004), furthermore suggesting that such nanoscale zeolites may be potentially superior to traditional micron–scale zeolite sorbents. Recently, a study done by Orha et al (2011) concerning the sorption of humic acids (HA) from water on natural and synthetic zeolite envisaged the drinking water treatment. Synthetic zeolite nanoparticles were synthesized from natural clinoptilolite as Si source and sodium aluminate as Al source. The experimental results regarding the comparative adsorption capacities of natural and synthetic zeolite for HA removal showed that the synthetic zeolite exhibited a great capacity for HA adsorption from water. The exploratory experiments

showed the feasibility of this simple synthesis method in the area of nano–sized zeolite with enhanced sorption property for HA envisaging water treatment.

Table 2.2. Examples of nanoscale materials for use in water purification

Nanoparticle/Nanomaterial	Pollutant	Reference
Nanocrystalline zeolites	Toluene, nitrogen dioxide	Song et al., (2004, 2005b)
Synthetic zeolite nanoparticles	Humic acid	Orha et al., (2011)
Graphitized Carbon nanotubes (CNT)	1, 2-dichlorobenzene	Peng et al., (2003)
CeO_2 – CNTs	Metal ions	Di et al., (2006); Peng et al., (2005)
CNT functionalized with polymer	*p*-nitrophenol	Salipira et al., (2007)
Carbon nanoparticles conjugated with polyethylenimine	Metal ions	Khaydarov et al., (2010)
CNT–hydrite	Arsenate	Poinern et al., (2010)
CNT-sheets	Metal ions	Tofighy and Mohammadi (2011)
CNT functionalized with Fe	Benzene, toluene, dimethylbenzene, metal ions	Jin et al., (2007); Lu and Chiu (2006); Lu et al., (2005)
Single-walled carbon nanotubes and Multi-walled carbon nanotubes	Trihalomethanes (THMs), metal ions, roxarsone, ethylbenzene, herbicides, cyanobacterial toxins	Lu et al., (2005); Lu et al., (2006a); Li et al., (2003); Hu et al., (2012); Bina et al., (2012); Cai et al., (2005); Zhou et al., (2006a, 2006b); Zhou et al., (2007); Yan et al., (2008); Albuquerque et al., (2008); Yan et al., (2006)
Mesoporous aluminosilicate spheres with nanosized Fe_3O_4	Mercury	Guo et al., (2008)
Silica coated Fe_3O_4	Metal ions	Huang et al., (2008)
Fe_3O_4 particles encapsulated in thiol containing polymers	Metal ions	Shin et al., (2007)
Fe_3O_4 nanoparticles functionalized with dithiocarbamate groups	Mercury	Girginova et al., (2010); Figueira et al., (2011)
Fe_4O_3 magnetic nanoparticles coated with humic acid	Metal ions	Liu et al., (2008)

Zero-valent iron nanoparticles (nZVI)	Polychlorinated biphenyls (PCBs), inorganic ions, chlorinated organic compounds heavy metal ions	He and Zhao (2005); Choe et al., (2000); Cao et al., (2005); Yang and Lee (2005); Zhang et al.,(1998a); Cheng et al., (2007) Ponder et al., (2000); Kanel et al., (2005, 2006); Li and Zhang (2006); Xu and Zhao (2007); Uzum et al., (2009); Boparai et al., (2011)

2.2.2.2 Carbon nanotubes

Carbon nanotubes (CNTs) are cylinder–shaped macromolecules, made up of a hexagonal lattice of carbon atoms and are capped at their ends by one half of a fullerene–like molecule (Iijima 1991). CNTs can be divided essentially into single–walled carbon nanotubes (SWCNTs) and multi–walled carbon nanotubes (MWCNTs) based on the principle of hybridized carbon atom layers in the walls of CNTs. SWCNTs have diameters ranging from 0.3 to 3 nm, whereas the MWCNTs are composed of a concentric arrangement of many cylinders and can reach diameters of up to 100 nm (Iijima and Ichihashi 1993; Balasubramanian and Burghard 2005). Since their discovery, carbon nanotubes have attracted considerable attention, which stems from their outstanding structural, mechanical and chemical properties (Miyagawa et al., 2005). In addition to their potential application in electronics, chemical and biological sensing, catalysis and reinforced composite materials (Balasubramanian and Burghard 2005, 2006), their large surface area and tubular structure make CNTs a promising adsorbent material.

Carbon nanotubes (CNTs) have been evaluated for the sorption of 1,2–dichlorobenzene (DCB) and it was reported that they can be used in a wide pH range of 3 to 10 and that sorption of DCB onto the CNTs took 40 minutes to reach equilibrium with a maximum sorption capacity of 30.8 mg/g (Peng et al., 2003). Novel sorbents consisting of cerium oxide supported on either carbon nanotubes (CeO_2–CNT) (Peng et al., 2005) or on aligned carbon nanotubes (CeO_2–ACNTs) (Di et al., 2006) and which are characterized by having high surface areas (in excess of 189 m^2/g), have been developed. Although, the CeO_2–CNTs were effective sorbents for As (V), the addition of the divalent cations Ca(II) and Mg(II) at concentrations ranging between 1 and 10 mg/L increases the amount of sorbed As (V) from 10 to 82 mg/g (Peng et al., 2005). Other study showed that the CeO_2–

ACNTs exhibited high Cr(VI) adsorption efficiency from drinking water at a pH range of 3 to 7.4. The largest Cr(VI) adsorption capacity reached was 30.2 mg/g at pH 7.0, which was *ca*. two times higher than that of activated carbon and Al_2O_3 (Di et al., 2006). In this context, carbon nanoparticles (CNPs) conjugated with polyethylenimine were synthesized for removing metal ions from water (Khaydarov et al., 2010). A capacity of 4.0–5.7 mmol/g for most divalent metal ions was achieved. The adsorption rate of Zn^{2+}, Cd^{2+}, Cu^{2+}, Hg^{2+}, Ni^{2+} and Cr^{6+} ions was nearly 99%. A study done by Vuković et al., (2010) on the adsorption of Cd^{2+} by CNTs found that the adsorption property was greatly improved by oxidation and by amine–functionalization. Similarly, CNT–hydrite was synthesized through precipitation in ethyl alcohol media proved to be a good adsorbent for As(V) (Poinern et al., 2010). Recently, removal of some divalent metal ions (Cu^{2+}, Zn^{2+}, Pb^{2+}, Cd^{2+}, Co^{2+}) from aqueous solutions using CNT sheets was performed by Tofighy and Mohammadi (2011). CNT sheets were synthesized by chemical vapor deposition of cyclohexanol and ferrocene in nitrogen atmosphere at 750 °C, and oxidized with concentrated nitric acid at room temperature and then employed as adsorbent for water treatment. Results exhibit that by using the oxidized CNT sheets as adsorbent, economical wastewater treatment without CNT leakage into water is feasible. The oxidized CNT sheets are promising materials for pre–concentration and solidification of metal ions from large volume of solutions.

Pre–treated MWCNTs with nitric acid, have been used successfully for the sorption of different metal ions, including Pb(II) (97.08 mg/g), Cu(II) (24.49 mg/g) and Cd(II) (10.86 mg/g) from an aqueous solution. These sorption capacities were three and four times higher than those of powder and granular activated carbon, respectively (Li et al., 2003). In addition, SWCNTs and MWCNTs were shown to have better Ni(II) sorption properties following their oxidation with NaClO. The treatment improved the surface properties of the CNTs, *e.g.*, functional groups, total acidic sites and negatively charged carbons, thus resulting in them becoming more hydrophilic and therefore able to sorb more Ni(II) from aqueous solution (Lu and Liu 2006). Moreover, both SWCNTs (Lu et al., 2005) and MWCNTs (Lu et al., 2006) have been investigated for their ability to remove trihalomethanes (THMs; $CHCl_3$, $CHBrCl_2$, $CHBr_2Cl$ and $CHBr_3$) from water. These compounds, which are recognized as potentially carcinogenic substances (Bull et al., 1995), are formed during the chlorination of drinking water. Both CNTs displayed high

adsorption capacities for the respective THMs at 5 and 15ºC, which fluctuated very little in the pH range 3 to 7. Compared to activated carbon, the purified CNTs possessed two to three times higher adsorption capacities for $CHCl_3$, which accounts for a major portion of THMs in chlorinated drinking water (Lu et al., 2006). Recently, Bina et al., (2012) investigated the removal of ethylbenzene from aqueous solution by MWCNTs, SWCNTs and hybrid carbon nanotubes (HCNTs). The SWCNTs performed better for ethylbenzene sorption than the HCNTs and MWCNTs and possess good potential applications to maintain high–quality water. Another study done by Hu et al., (2012) demonstrated the adsorption of roxarsone, an organoarsenic compound, on MWCNTs. The results revealed that the high adsorption capacity in static and dynamic adsorption experiments implied that MWCNTs are promising adsorbents for the removal of roxarsone from water and wastewater. Salipira et al., (2007) reported that copolymerization of cross–linked nanoporous polymers with functionalized CNTs resulted in novel polymers capable of efficient removal of organic pollutants from water. These novel polymers removed p–nitrophenol by 99% from a 10 mg/L spiked water sample, whereas granular activated carbon removed only 47%. Moreover, these polymers removed trichloroethylene (10 mg/L spiked sample) to non–detectable levels (detection limit <0.01 ppb) compared to 55% for granular activated carbon (Salipira et al., 2007). In addition to their ability to sorb metals and organic compounds, CNTs may also be useful as adsorbents for toxins and herbicides in environmental water. Based on a report by Long and Yang (2001), indicating that significantly higher dioxin removal efficiency is found with CNTs than with activated carbon, MWCNTs have subsequently been used successfully as a new sorbent for the preconcentration and separation of chlorophenols (Cai et al., 2005) and different herbicides, including triazine herbicides (Zhou et al., 2006b; Yan et al., 2008), DDT and its metabolites (Zhou et al., 2006a), as well as sulfonylurea herbicides (Zhou et al., 2007), from river, tap and lake water samples. CNTs are an adsorbent media, able to remove wide range of biological contaminants including bacteria (Akasaka and Watari 2009; Deng et al., 2008; Srivatsava et al., 2004; Upadhyayula et al., 2009), viruses (Brady-Estevez et al., 2008; Mostafavi et al., 2009), natural organic matter (Hyung and Kim 2008; Saleh et al., 2008) and cyanobacterial toxins (Albuquerque et al., 2008; Yan et al., 2006). The success of CNTs as an adsorbent media in the removal of biological contaminants, especially

pathogens is mainly attributed to its unique physical, cytotoxic and surface functionalizing properties (Upadhyayula et al., 2009).

Whilst the above studies indicate that CNTs are potentially efficient adsorbents for a variety of pollutants in both drinking and environmental waters, their practical application may be hampered by their high cost, as well as their poor solubility and the difficulty in collecting them from their dispersing medium. It is therefore interesting to note that in a study, Lu et al., (2007) performed statistical analyses on the replacement cost of NaClO–oxidized SWCNTs and MWCNTs, both of which had been reported to be effective Zn(II) sorbents and could be reused through 10 cycles of water treatment and regeneration (Lu and Chiu 2006; Lu et al., 2006b). The results of their analyses revealed the use of such re–usable carbonaceous sorbents can indeed be cost–effective in spite of their high unit cost at the present time (Lu et al., 2007). In addition, Jin et al., (2007) reported a simple method for fabricating magnetic Fe nanoparticle functionalized MWCNTs, which not only displayed improved water solubility, but could also be recovered easily from the water by magnetic separation. The functionalized water–soluble MWCNTs (Fe–MWCNT–CH2COONa) were also tested as a sorbent using four model aromatic compounds. The results indicated that addition of 10 mg of Fe–MWCNT–CH_2COONa to aqueous solutions containing 8.6 ppb of the corresponding model compound, adsorbed benzene (79%), toluene (81%), dimethylbenzene (83%) and styrene (88%) very effectively. Notably, after being washed several times with methanol and dried in vacuum, the Fe–MWCNT–CH_2COONa could be re–used.

2.2.3. Nanoscale semiconductor photocatalysts

Since the discovery of photocatalytic water splitting on titatium(IV) dioxide (TiO_2) electrodes by Fujishima and Honda (1972), interest in applying TiO_2 as homogenous photocatalyst for the remediation of groundwater and wastewater has increased (Cho et al., 2005, 2006; Liu et al., 2006b; Chong et al., 2010), particularly due to its potential to degrade a wide range of organic and inorganic compounds (Kabra et al., 2004; Chong et al., 2010). The effective photoexcitation of TiO_2 photocatalysts requires the application of light with energy higher than its band–gap energy, thus resulting in the formation of

electrons (e^-) in the conduction band and positive holes (h^+) in the valence band. Hydroxyl ions and water are likely traps for holes, leading to the formation of hydroxyl radicals ($OH^\bullet$) that are strong oxidizing agents, whilst the traps for electrons are adsorbed oxygen species, leading to the formation of superoxide species ($O^\bullet_2$) that are unstable. The reactive oxygen species generated ($OH^\bullet$, $O^\bullet_2$) react with molecules adsorbed on the photocatalyst surface, resulting in its hydroxylation, oxidation and finally mineralization to carbon dioxide and water (Carp et al., 2004; Chong et al., 2010). Most of the semiconductor photocatalysts investigated are either metal oxides (*e.g.*, TiO_2, ZnO, SnO_2, WO_3) or chalcogenides (*e.g.*, CdS, ZnS, CdSe, ZnSe, CdTe) (Carp et al., 2004). Due to its physical and chemical stability, lower cost and resistance to corrosion, TiO_2 is the most commonly used photocatalyst for environmental applications. However, the wide technological usage of TiO_2 is hampered by its wide band–gap (rutile: 3.02 eV, anastase: 3.2 eV), which requires ultraviolet (UV) light irradiation for photocatalytic activation (Dvoranova et al., 2002; Chong et al., 2010). Since UV light accounts for only a small fraction (less than 5%) of solar irradiation compared to visible light (45%) (Romero et al., 1999), any shift in the optical response of TiO_2 from the UV ($\lambda \leq 385$nm) to the visible spectral range ($\lambda \geq 420$ nm) should have a beneficial effect on the photocatalytic efficiency of the material (Adesina 2004). Several approaches have therefore been used to lower the band–gap energy of TiO_2 photocatalysts, including reductive hydrogen plasma treatment (Palmer et al., 2002), sensitizing by adsorbed dyes (Moon et al., 2003) or by semiconductors having lower band–gaps (Yu et al., 2003), as well as transition metal doping (Dvoranova et al., 2002; Sakthivel et al., 2004; Barakat et al., 2005; Nahar et al., 2006). Although being a widely used approach, the photocatalytic activity of metal–doped TiO_2, depends, however on the nature and concentration of the dopant ion, preparation methods and calcination processes (Oh et al., 2003; Barakat et al., 2005). Consequently, anionic dopants such as nitrogen (Yang et al., 2004; Liu et al., 2006a), carbon (Irie et al., 2003; Neumann et al., 2005) and sulfur (Ohno et al., 2003; Yu et al., 2005; Jiang et al., 2006), have been investigated as an alternative approach. Commercially available TiO_2 Degussa P-25, consisting of 80% of anatase and 20% of rutile with an average particle size of 30 nm, is widely used in the treatment of contaminated wastewater and has become a research standard (Ohno et al., 2001; Kirchnerova et al., 2005). However, nanocrystalline TiO_2 (particle sizes of *ca.* 6–8 nm), synthesized mostly by using sol-gel techniques, has emerged as promising

photocatalysts for water remediation and purification. The decrease in semiconductor particle size has two significant benefits. The high surface density of active sites available for substrate adsorption, consistent with the high surface to volume ratio typical of nanosized particles, makes it possible to increase the overall photoreaction rate. Also, the band–gap of the nanosized semiconductor particle becomes size–dependent due to quantization effects, allowing for fine tuning of the band-gap and, thus, also the electron–hole pair redox potentials (Zhang et al., 1998b; Rao et al., 2002). Consequently, a measure of selectivity in the associated photoreactions can be achieved. Moreover, the presence of crystal defects, which can be associated to trap states for the photogenerated carriers, is generally less when high quality nanocrystals are synthesized, thus allowing the electron–hole separation yield to be maximized (Amal et al., 1999). In recent years, the synthesis of visible light–activated TiO_2 nanoparticles has attracted increasing interest. Bae and Choi (2003) have synthesized visible light–activated TiO_2 nanoparticles based on TiO_2 modified by ruthenium–complex sensitizers and platinum (Pt) deposits. The $Pt/TiO_2/RuIIL_3$ nanoparticles drastically enhanced the rate of reductive dehalogenation of trichloroacetate and carbon tetrachloride in aqueous solutions under visible light. Pena et al., (2005) reported that, in the presence of sunlight and dissolved oxygen, As(III) (2 mg/L) was completely converted to As(V) in a suspension containing 0.2 g/L TiO_2 nanocrystals through photocatalytic oxidation within 25 minutes. The adsorption capacity of the TiO_2 for As(V) and As(III) was much higher than Degussa P–25 and granular ferric oxide. Using three azo dyes, *i.e*., acid orange 7 (AO7), procion red MX–5B (MX–5B) and reactive black 5 (RB5), nitrogen (N) –doped TiO_2 nanoparticles were reported to exhibit substantial photocatalytic activity under direct sunlight irradiation, with 70% of the dye color removed in 1 hour and complete decolorization within 3 hours. In contrast, Degussa P–25 did not cause detectable dye decolorization under identical experimental conditions (Liu et al., 2005b). Furthermore, Fe(III)–doped TiO_2 nanoparticles were reported to degrade phenol in water and although the doped TiO_2 was more active than Degussa P–25 under solar light irradiation, it was less active than Degussa P–25 under UV light irradiation (Nahar et al., 2006). For water treatment, TiO_2 particles and nanocrystals can either be deposited as prepared or they can be incorporated in a suitable nanocomposite by using conventional grafting, precipitation and impregnation methods (Zhang et al., 2005; Yang et al., 2006). The latter is, however, preferred since it prevents not only

agglomeration of the TiO_2 particles, which can decrease the active surface area and thus reduce the efficiency of the photocatalytic reactions, but it also facilitates greatly the separation and recovery of the catalysts following treatment (Yang et al., 2006). López–Munoz et al., (2005) reported the use of tubular arrays of meso and microporous molecular sieves composed of TiO_2 nanoparticles, supported by mesoporous silica, for water remediation of aromatic pollutants in the presence of UV light. Photocatalysts composed of nanostructured TiO_2, uniformly deposited onto Fe_2O_3, have also been incorporated into ultrafiltration membranes, showing successfully reduce the fouling burden and improve the permeate flux (Sun et al., 2004). The ability to form films and nanotubes with semiconductor photocatalysts has also provided a means whereby photocatalytic structures with a high a surface area, can be obtained. Recently, the synthesis of TiO_2–based p–n junction nanotubes have been described of which the outside of the tubes is comprised of TiO_2 and the inside is comprised of platinum (Chen et al., 2005). The nature of the p–n junction allows the outside of the tube to act as an oxidizing surface, whilst the inside of the tube acts as a reductive surface. When these catalysts were exposed to UV light, they were able to degrade toluene and the photocatalytic destruction rates were higher compared to non–nanotube structured material and to nanotubes lacking a p–n junction (Chen et al., 2005). Recently, photocatalytic silver doped titanium dioxide nanoparticles (nAg/TiO_2) were investigated for their capability of inactivating Bacteriophage MS2 in aqueous media (Liga et al., 2011). The inactivation efficiency increased with increasing silver content. The increased production of hydroxyl free radicals was found to be responsible for the enhanced viral inactivation. In addition, the use of nanostructured ZnO semiconductor films for simultaneous sensing and degradation of organic contaminants has been demonstrated (Kamat et al., 2002). Using 4–chlorocatechol as model compound, its presence was detected from the quenching of visible emission of the ZnO semiconductor film. Not only was achieved a detection sensitivity of 1 ppm of 4–chlorocatechol in water, but it was also possible to photocatalytically degraded it, by the ZnO film under UV irradiation. The coupling of these two features may greatly facilitate the monitoring of the degradation process, because as decontamination occurs, a direct change in the emission intensity follows (Kamat et al., 2002). One–dimensional flat ZnO nanotower arrays were also fabricated, and the improved adsorption and photocatalytic abilities on a model pollutant, eosin B, were demonstrated (Deng et al., 2010). Ullah and

Dutta (2008) observed that the photodegradation of methylene blue using manganese-doped ZnO NPs was more efficient than using undoped ZnO in visible light. . In addition to TiO_2 and ZnO, other metal oxides such as bismuth oxide (Bi_2O_3), cerium dioxide (CeO_2) and tungsten trioxide WO_3 have been also used for water remediation (Table 2.3). In a recent study, it was found that the uniform Bi_2O_3 nanotubes synthesized by a facile solvothermal method without the need for any surfactants or templates provides a new promising adsorbent for the removal of chromium ions from water (Qin et al., 2012). Anandan et al (2010) also demonstrated the removal of Orange II dye from water using Bi_2O_3 and Au/Bi_2O_3 nanorods prepared by using microwave irradiation. Another metal oxide semiconductor CeO_2 showed high photoactivity towards the degradation of azodye and has been proven to be a promising alternative for dye–containing wastewater treatment under visible light irradiation (Zhai et al., 2007; Ji et al., 2009; Borker and Salker 2009). Based on the advantages of Ag nanoparticles and semiconductor CeO_2, a novel plasmonic photocatalyst $Ag\text{-}AgCl/CeO_2$ was prepared with a facile route (Wang et al., 2011) that exhibited a high visible–light photocatalytic activity and good stability for photocatalytic degradation of methyl orange in water. Nano tungsten trioxide (WO_3), synthesized by sol–gel method, showed a significant enhancement in the photo–catalytic activity in the process of disinfecting *Escherichia coli* microorganism in water (Gondal et al., 2009).

Some transition metal sulfides have been considered as photo–catalysts for the removal of organic pollutants from water and wastewater because they have narrow band gap and proper band potentials, which match well with the visible light photon energy and the thermodynamic conditions for the degradation of many compounds, respectively. Yang et al., (2009) prepared a stable and regenerable cadmium sulfide (CdS) photocatalyst by coating CdS nanoparticles incorporated in hexagonal mesoporous silica spheres with a polyelectrolyte layer. The coated catalyst completely degraded some dyes and phenolic compounds for over 22 runs without leakage of cadmium species into the solution. Other metal sulfides as bismuth sulfide (Bi_2S_3), zinc sulfide (ZnS) and molybdenum disulfide (MoS_2) have been tested for the photocatalytic degradation of organic pollutants. ZnS nanoporous nanoparticles composed of building blocks comprising hexagonal wurtzite ZnS nanocrystals of several nanometers in diameter were prepared by a solution–phase thermal decomposition route in the presence of poly(N–vinyl–2–pyrrolidone) (Hu et al.,

2005). The ZnS nanoporous nanoparticles showed much greater activity for the photodegradation of eosin B than that of P25 or ZnS nanocrystal–lites.

Table 2.3. Examples of nanoscale semiconductor photocatalyst for use in water remediation

Nanoparticle/Nanomaterial	Pollutant	Reference
Nanocrystalline TiO_2	Metal ions	Pena et al., (2005)
Nitrogen (N)-doped TiO_2	Azo dyes	Liu et al., (2005b)
Fe(III)-doped TiO_2	Phenol	Nahar et al., (2006)
Supported TiO_2 nanoparticles	Aromatic pollutants	Lópes-Munoz et al., (2005)
Silver doped titanium dioxide nanoparticles	Bacteria	Liga et al., (2011)
Manganese-doped ZnO NPs	Methylene blue	Ullah and Dutta (2008)
Nanotubes Bi_2O_3	Chromium ions	Qin et al., (2012)
Bi_2O_3 and Au/Bi_2O_3 nanorods	Orange II dye	Anandan et al., (2010)
CeO_2	Dyes	Zhai et al., (2007); Ji et al., (2009); Borker and Salker (2009)
Nanocomposite plasmonic photocatalyst Ag-AgCl/CeO_2	Methyl orange	Wang et al (2011)
Nano WO_3	*Escherichia coli*	Gondal et al (2009)
Photocatalyst CdS coated with CdS nanoparticles	Dyes and phenolic compounds	Yang et al., (2009)
ZnS nanoporous nanoparticles	Eosin	Hu et al., (2005)

2.2.4. Magnetic nanoparticles

Facilitated separation from the bulk medium by magnetic force is the most attractive property of magnetic nanoparticles. Among the magnetic nanosized materials, iron oxides play a major role in many areas of chemistry, physics and materials science. In particular, magnetic iron oxides such as magnetite (Fe_3O_4) and maghemite (Υ–Fe_3O_4) have been investigated intensively for environmental applications (Li et al., 2007; Daniel–da–Silva et al., 2008; Shen et al., 2009; Indira and Lakshmi 2010). In addition to convenient

magnetic properties and low toxicity and price, iron oxide (*e.g.* Fe_3O_4) nanoparticles exhibit high surface to volume ratios, depending on the particle size, which associated to their ability for surface chemical modification can show enhanced capacity for metals uptake in water treatment procedures. Surface modification achieved by the attachment of inorganic shells or/and organic molecules not only stabilizes the nanoparticles, eventually preventing their oxidation, but also provides specific functionalities that can be selective for ion uptake. For example, high selective hollow mesoporous aluminosilicate spheres with nanosized Fe_3O_4 cores are suitable for adsorption of Hg^{2+} (Guo et al., 2008). Iron oxide nanoparticles dispersed in chelating resins or coated with adequate chelating agents have been used for the removal of a wide range of metals ions from wastewater (Atia et al., 2007; Li et al., 2008; Sheha et al., 2008), overall displaying higher adsorption capacity than traditional materials such as activated carbon (Hu et al., 2005; Borai et al., 2007). Silica coated Fe_3O_4 functionalized with c–mercaptopropyltrimethoxysilane have been successfully applied for extraction of Cd^{2+}, Cu^{2+}, Hg^{2+} and Pb^{2+} in a wide pH range and even in the presence of foreign ions acting as interferents such as Al^{3+}, Fe^{3+} and Cl^{-} (Huang et al., 2008). Fe_3O_4 particles encapsulated in thiol containing polymers have also been reported and their efficiency to remove Ag^{+}, Hg^{2+} and Pb^{2+} ions has been evaluated (Shin et al., 2007). Also, Figueira et al., (2011) took advantage of the high affinity between mercury and sulphur, and synthesized magnetite (Fe_3O_4) nanoparticles functionalized with dithiocarbamate groups (Dtc) to be used as a new type of sorbent to remove Hg(II) from synthetic and natural spiked waters. The authors concluded that silica coated magnetite particles functionalized with Dtc groups are effective sorbents for Hg(II) removal from both types of water and the presence of higher concentrations of Cl^{-} and Na^{+} ions although did not affect the amount of Hg(II) removed per gram of sorbent at equilibrium, reduced the rate at which Hg(II) ions were removed from solution. Moreover, for application in surface–river water, the Hg(II) uptake efficiency of magnetite particles functionalized with Dtc groups is outstanding, achieving the quality criteria established by the Water Framework Directive, concerning Hg concentration in surface waters (Lopes et al., 2012). Similarly, the synthesis and the preliminary application of silica coated Fe_3O_4 particles functionalized with Dtc groups for the decontamination of synthetic waters with realistic Hg(II) levels (Girginova et al., 2010). Liu et al., (2008) developed humic acid coated Fe_3O_4 magnetic nanoparticles, which were used to remove metal ions from water. Over

99% of Hg^{2+} and Pb^{2+} and over 95% of Cu^{2+} and Cd^{2+} were removed in natural and tap waters. Maghemite (Υ–Fe_2O_3) nanoparticles were prepared to remove As(V) from water (Tuutijärvi et al., 2009). The adsorption capacity was as high as 50 mg/g. A novel magnetic nanosized adsorbent using hydrous aluminum oxide embedded with Fe_3O_4 nanoparticle (Fe_3O_4@$Al(OH)_3$ NPs), was prepared and applied to remove excessive fluoride (Zhao et al., 2010). This adsorbent combines the advantages of magnetic nanoparticle and hydrous aluminum oxide floc with magnetic separability and high affinity toward fluoride. About 98% of fluoride was removed when the initial concentration was 20 mg/L.

2.2.5. Nanoscale zerovalent iron (nZVI) particles

Nano zerovalent iron (nZVI) particles are effective for the transformation of a wide array of common environmental contaminants such as chlorinated organic compounds (Zhang et al., 1998a; Cheng et al., 2007), polychlorinated biphenyls (PCBs) (He and Zhao 2005), hexachlorocyclohexanes (Elliot et al., 2008), inorganic ions such as nitrate (NO_3^-) and perchlorate (ClO_4^-) (Choe et al., 2000; Cao et al., 2005) and metal and metalloid ions such as As(III), Pb(II), Cu(II), Ni(II), Ba(II), Co(II) and Cr(VI) (Ponder et al., 2000; Kanel et al., 2005; Li and Zhang 2006; Kanel et al., 2005; Li et al., 2007; Çelebi et al., 2007; Uzum et al., 2009; Boparai et al., 2011). It is assumed that the reactivity of core–shell nanoparticles of ZVI is driven by oxidation of the Fe^0 core (Liu et al., 2005a; Nurmi et al., 2005). Compared to their microscale counterparts, the higher reactivity of the nanoscale particles has been attributed to the greater density and higher intrinsic reactivity of their reactive surface sites (Zhang 2003; Nurmi et al., 2005). Over the last few years, various methods have been developed for the production of nZVI particles (Li et al., 2006a, 2006b; Sun et al., 2006) and the modification of their surface properties (Ponder et al., 2000; He and Zhao 2005).

Several field tests have demonstrated the promising prospective for *in situ* remediation (Li et al., 2006b; Zhang and Elliot 2006; Lin et al., 2010). Typically, nZVI particle–water slurries are injected under pressure and/or by gravity to the contaminated plume where treatment is needed. The nZVI particles can also remain in suspension for extended periods of time to establish an in situ treatment zone. As an alternative, nZVI particles may

also be anchored onto a solid matrix such as activated carbon and/or zeolite for enhanced treatment of water and wastewater (Zhang 2003).

Several studies have provided insights into nZVI particle properties associated with its potential to transform metal ions, as well as inorganic anions like perchlorate and nitrate. Recently, Boparai et al., (2011) used nZVI particles to investigate the removal of Cd^{2+} in the concentration range of 25–450 mg/L. The effect of temperature on kinetics and equilibrium of cadmium sorption on nZVI particles was thoroughly examined. Results suggested that nZVI could be employed as an efficient adsorbent for the removal of cadmium from contaminated water sources. Similar to results obtained with As(III) (Kanel et al., 2005), Kanel et al., (2006) reported that absorption of As(V) to nZVI particles was rapid, occurring within minutes. Approximately 25% of the As(V) was reduced to As(III) by the nZVI particles after 90 days. However, it was reported that in the presence of competing ions such as HCO_3^-, SiO_4^{2-} and PO_4^{3-}, the As(V) adsorption was reduced and thus a larger amount of nZVI particles may be required to remove As(III) and As(V) from aqueous solutions. While reduction appears to be the predominant mechanism for metal ion removal by nZVI particles, it was recently reported that for Ni(II) removal both reduction and surface complex formation (sorption) occurred (Li and Zhang 2006). At equilibrium, about 50% of Ni(II) is reduced as Ni(0) at the surface and 50% of Ni(II) remains adsorbed at the nZVI particle surface. Notably, the capacity (0.13 g Ni(II)/g nZVI) is more than 100% higher compared to sorbents such as zeolite. Cao et al., (2005) reported the near complete reduction of perchlorate to chloride in aqueous solutions by nZVI particles and no sequential degradation products were observed. In contrast, the reduction by microscale iron particles was negligibly slow. However, the high activation energy required for nZVI–mediated reduction of perchlorate (79 kJ/mol), suggests that the reaction is limited by slow kinetics. The use of nZVI particles for the chemical reduction of nitrate has also been investigated and, in contrast to microscale iron particles, which converted nitrate to ammonia, nZVI particles converted nitrate to nitrogen gas (Choe et al., 2000). Yang and Lee (2005) reported that chemical reduction of nitrate by nZVI particles is primarily an acid–driven surface mediated process. Thus, in addition to the requirement for a large surface area provided by the nanoparticles, both pH and dose of nZVI particles (*i.e.*, the stoichiometric ratio of nZVI to nitrate (as N)) were identified as being important for efficient reduction of nitrate. In general, acidic pHs were found to be favourable and

high doses of nZVI particles enhanced the reaction rate. Due to their extremely high reactivity, nanoparticles prepared using current methods tend to either react with surrounding media or agglomerate, resulting in the formation of much larger flocs and a significant loss in reactivity (Liu et al., 2004; He and Zhao 2005). Since efficient dispersion of the nZVI particles is thus a critical factor to improving their efficiency, various particle–stabilizing strategies have been reported. Ponder et al., (2000) tested a class of resin–supported nZVI particles (Ferragels) to reduce Cr(VI) in aqueous solutions. The resin supported nanoparticles had an average size of 10–30 nm and a specific surface area of 24m^2/g of nanoparticles. Notably, reduction of Cr(VI) was found to be 20–30 times faster than the commercial iron filings or iron powder per unit mass of Fe applied. In addition, stabilization of nZVI particles in cetylpyridinium chloride (CPC) has been described, resulting in a specific surface area of 25.4m^2/g of nanoparticles (Chen et al., 2004), whilst immobilizationof bimetallic Pd/Fe nanoparticles in water–soluble starch offered a surface area of 55 m^2/g of nanoparticles (He and Zhao 2005). The feasibility of using carboxymethyl cellulose (CMC) – stabilized nZVI particles for *in situ* reductive immobilization of Cr(VI) in water has recently been investigated by Xu and Zhao (2007). Batch kinetic tests indicated that 0.08 g/L of nZVI particles were able to rapidly reduce 34 mg/L of Cr(VI). Compared to non–stabilized nanoparticles, the stabilized nZVI particles displayed much greater reactivity and reaction kinetics for chromate reduction. When the dose was increased from 0.04 g/L to 0.12 g/L (*i.e.*, the Fe:Cr molar ratio was increased from 1.1 to 3.3), the reduction of Cr(VI) in water was increased from 24% to 90% (Xu and Zhao 2007). The above results suggest that the use of stabilized nZVI particles may represent an effective means for *in situ* remediation of groundwater or industrial effluents.

2.2.3. Water disinfection

Bioactive nanoparticles are playing an important role for water disinfection. A variety of strong oxidants (*e.g.*, chlorine) are used as disinfectants for pathogens (*e.g.*, bacteria and viruses) in water treatment. Because these compounds tend to generate toxic disinfection byproducts such as trihalomethanes, haloacetic acids and aldehydes, alternative disinfectants are critically needed to comply with the Stage 1 Disinfection

Byproduct Rule of the 1996 Safe Drinking Water Act Amendments (USEPA 1998). The mechanisms by which disinfectants such as chlorine inactivate waterborne pathogens include (1) impairment of pathogen cellular function by destruction of major constituents (*e.g.*, cell wall), (2) interference with the pathogen cellular metabolic processes and (3) inhibition of pathogen growth by blockage of the synthesis of key cellular constituents (*e.g.*, DNA, coenzymes and cell wall proteins) (USEPA 1999). Nanomaterials are also providing unprecedented opportunities to develop chlorine–free biocides.

Among the most promising nanomaterials with antimicrobial properties are metallic and metal-oxide nanoparticles, as well as TiO_2 photocatalysts.

Silver (Ag) ions and silver compounds have long been known to exhibit strong toxicity to a wide range of microorganisms (Zhao and Stevens 1998) and have thus been used as antimicrobial compounds in various biomedical products and applications (Fan et al., 2011). Consequently, several investigators have begun evaluating the use of Ag nanoparticles as biocides (Sondi and Salopek-Sondi 2004; Kim et al., 2007; Shrivastava et al., 2007; Mpenyana-Monyatsi et al., 2012). In general, the effect appears to be dose–dependent and is more pronounced against Gram-negative (*Escherichia coli*) than against Gram-positive (*Staphylococcus aureus*) bacteria, possibly as a consequence of the differences between the structure of their respective cell walls (Madigan and Martinko 2005). The bactericidal properties of the Ag nanoparticles appear to be dependent on both their size and shape (Morones et al., 2005; Pal et al., 2007). Analysis regarding the effect of silver nanoparticles in the range of 1–100 nm on the growth of four Gram–negative bacteria (*E. coli, Vibrio cholerae, Pseudomonas aeruginosa* and *Salmonella typhus*) indicated that growth of the bacterial cultures (5×10^7 colony forming units (cfu)/mL) was inhibited at concentrations above 75 μg/mL of the nanoparticles. However, subsequent characterization of the interactions of the Ag nanoparticles with the bacteria by high angle annular dark field (HAADF) scanning transmission electron microscopy (STEM) showed that nanoparticles attached to the surface of the cell membrane or located inside the bacteria were mainly in the range of 1–10 nm (Morones et al., 2005). Moreover, despite magnesium oxide (MgO) having been reported to be an effective biocide against *E. coli, Bacillus megaterium,* and *B. subtilis spores* (Koper et al., 2002; Stoimenov et al., 2002), it was subsequently shown that the antibacterial activities of MgO nanoparticles are also dependent on their size. Results indicated that smaller nanoparticles (8 nm) were the most

active in killing *E. coli* and *S. aureus*, whilst a gradual decrease in the bactericidal activity was observed with an increase in particle size (11–23 nm) (Makhluf et al., 2005). The shape dependence of the bactericidal activity of Ag nanoparticles against *E. coli* was recently investigated using Ag nanoparticles synthesized with different shapes (Pal et al., 2007). Although the respective nanoparticles were each capable of interacting with *E. coli*, the inhibition results indicated that truncated triangular silver nanoplates displayed the strongest biocidal action, compared with spherical and rod–shaped nanoparticles. It was proposed that differences in the effective surface areas in terms of active facets may influence the killing activity or relate to the bacterial killing capacity of the differently shaped Ag nanoparticles. The stabilization and immobilization of metallic nanoparticles in different matrixes has also gained increased importance since such nanoparticles purportedly present high antibacterial activity, low toxicity, chemical stability, a long–lasting action period and thermal resistance (Esteban-Cubillo et al., 2006). In this regard, Sondi and Salopek–Sondi (2004) have reported the preparation of stable Ag nanoparticles of narrow size distribution (12 nm) by reducing silver nitrate solutions with ascorbic acid in the presence of Daxad 19 (sodium salt of a high–molecular weight naphthalene sulfonate formaldehyde condensate) as stabilizing agent. The Ag nanoparticles were shown to be effective biocides against *E. coli*. In an alternative approach, Son et al., (2004) prepared ultrafine cellulose acetate (CA) fibers by direct electrospinning of a CA solution with 0.05 wt. % $AgNO_3$, followed by UV irradiation photoreduction. The CA fibers with embedded Ag nanoparticles (average diameters 15.4 nm) were reported to be effective biocides against Gram–positive (*S. aureus*) and Gram-negative (*E. coli, Klebsiella pneumoniae*, and *P. aeruginosa*) bacteria. Recently, copper monodispersed nanoparticles (2–5 nm) incorporated into sepiolite (a magnesium phylosilicate), which has a low ion exchange capacity but a large surface area (300 m^2/g), has been shown to be an effective biocide against *E. coli* and *S. aureus*, reducing their concentrations ($2.5–10\times10^5$ cfu/mL) by 99.9% after 24 hour of incubation (Esteban–Cubillo et al., 2006). Despite the above results indicating that stabilized nanoparticles display enhanced biocide activity, it may, however, not always be the case since a report by Top and Ülkü (2004) indicated that incorporation of Cu(II) into zeolite had negligible antibacterial activity.

Although the antibacterial activity of silver ions has been studied extensively, the effects of Ag nanoparticles on the bacteria and bactericidal mechanism are only partially

understood. Based on studies having shown that Ag nanoparticles anchor to and penetrate the bacterial cell wall (Sondi and Salopek–Sondi 2004; Morones et al., 2005), it is reasonable to suggest that the resultant structural changes in the cell membrane could cause an increase in cell permeability, leading to uncontrolled transport through the plasma membrane and ultimately cell death. It has also been proposed, based on electronspin resonance spectroscopy studies of Ag nanoparticles that damage of the bacterial membranes may furthermore be induced by the formation of free radicals (Danilczuk et al., 2006; Kim et al., 2007). Moreover, based on the greater tendency of silver (soft acid) to react with sulphur– and phosphorus–containing soft bases (Hatchett and Henry 1996) and on the presence of Ag nanoparticles inside the cells (Morones et al., 2005), it is likely that further damage could thus be caused by interactions with sulfur–containing proteins and phosphorus–containing compounds such as DNA. These interactions may prevent cell division and DNA replication from occurring, and also ultimately lead to cell death. In addition, evidence has recently been obtained suggesting that the Ag nanoparticles may modulate the phosphotyrosine profile of putative bacterial peptides that could affect cellular signaling and therefore inhibit the growth of the organisms (Shrivatava et al., 2007).

2.3. TOXIC POTENTIAL OF ENGINEERED NANOPARTICLES AND NANOMATERIALS

The growing use of engineered nanoparticles and nanomaterials for water purification, as highlighted in the previous sections, has raised concerns for human exposure which stems from the absence of specific technologies aimed at the removal of engineered nanomaterials from the water, and the safety of the new nanoparticles and nanomaterials that may be used by the water industry. These concerns are often based on the assumption that nanoparticles will be highly mobile in porous media because of their small size; thus implying a greater potential for exposure as they are dispersed over greater distances and their effective persistence in the environment increases. However, Wiesner et al., (2006) suggested that smaller nanoparticles should not be very mobile, since their relatively large diffusivity would enable them to produce more frequent contacts with the surfaces of porous media such as groundwater aquifers or the sand filters used in potable water treatment. Moreover, retention of nanoparticles by porous media has been reported

to be increased by conditions such as high ionic strength and the presence of small quantities of divalent ions (Brant et al., 2005). Since groundwater aquifers and surface waters typically have ionic strengths of greater than 10^{-4} M, in addition to significant concentrations of calcium or magnesium, conditions should thus favor deposition of the nanomaterial. Consequently, Wiesner et al., (2006) concluded that there is no evidence to support the scenario of a new nanoparticulate contaminant that current water treatment infrastructure cannot handle. Although the use of engineered nanoparticles and nanomaterials may have a positive health benefit on humans from the viewpoint of drinking water quality, various studies have nevertheless commented on their potential adverse effects on human health (Nel et al., 2006; Maynard 2007; Oberdörster et al., 2007; Aschberger et al., 2011; Simate et al., 2012; Sharifi et al., 2012) and the environment (Biswas and Wu 2005; Moore 2006; Farré et al., 2009; Aschberger et al., 2011). Since, it is likely that waste generated during the production and use of these nanoparticles will appear eventually in various environments, there is a possibility that humans could be exposed to these nanoparticles through inhalation, dermal contact or ingestion and absorption through the digestive tract. Several hypotheses concerning physiochemical characteristics of nanoparticles responsible for adverse health effects have been proposed (Lanone and Boczkowski 2006; Nel et al., 2006; Maynard 2007; Simate et al., 2012). These include properties such as surface area and reactivity (Oberdörster et al., 2000), particle size, shape and structure (Oberdörster et al., 2005; Donaldson et al., 2006; Lam et al., 2006; Farré et al., 2009; Sharifi et al., 2012), chemical composition (Donaldson et al., 2006; Harper et al., 2008), as well as surface treatments (coatings) and the degree to which nanoparticles aggregate or agglomerate (Ryman- Rasmussen et al., 2006; Wang et al., 2006; Zhao et al., 2010). In addition, the toxicity will also depend on whether they are persistent or cleared from the different organs of entry, and whether the host can generate an effective response to sequester or dispose of the particles (Card et al., 2008). In fact, the persistence or duration of the existence of the engineered nanomaterials in the body influences the long term effects of the engineered nanomaterials, and thus plays a major role in causing the disease (Som et al., 2011).

Despite the wide variety of different nanoparticles and nanomaterials, the toxicological effects, however, of only a limited range of nanomaterials have been investigated. Studies have focused mostly on the effects of carbon–based nanomaterials

and metal–oxide nanoparticles, including TiO_2 nanoparticles. Results from *in vivo* studies, which have focused on respiratory exposure in mostly laboratory rodents, raises concern about lung injury, inflammation and possible tumorgenesis, while the results from *in vitro* studies, using different tissue and cell cultures, suggest that oxidative stress (resulting from the production of reactive oxygen species) may be a possible mechanism of toxicity (Nel et al., 2006; Møller et al., 2010; Petersen et al., 2010). However, it should be noted that the doses or exposure concentrations of nanomaterials used in *in vitro* and *in vivo* toxicological studies are most often extraordinarily high, and also delivered as a bolus (extremely high dose rate), so as to have no or limited relevancy to real or anticipated human exposures (Oberdörster et al., 2007). Moreover, many of the *in vivo* studies have been conducted in rats, which are known to be especially sensitive when it comes to adverse lung responses (Donaldson and Tran 2004), thus furthermore complicating the extrapolation of rodent sensitivity to human responses. In addition, there is only limited information available regarding the uptake, translocation and distribution of nanoparticles in the body (Oberdörster et al., 2004; Elder et al., 2006; Singh et al., 2006). Without this basic knowledge, it becomes difficult to predict what all the major toxic effects might be. Despite the current lack of knowledge relating to which environments, and thus which organisms are most likely to be exposed to nanoparticles, some literature regarding the toxicological impact of nanoparticles on different aquatic organisms has started to emerge. Studies have been published regarding the effects of nanoparticles (Buckminster fullerenes (C60)) on fish such as the largemouth bass (Oberdörster 2004) and the fathead minnow (Zhu et al., 2006), as well as the effects of C60 and TiO_2 on aquatic invertebrates such as water fleas (*Daphnia magna*) (Oberdörster et al., 2006; Zhu et al., 2006; Kim et al., 2010b) and the bacteria *V. fisheri* (Pereira et al., 2011, Lopes et al., 2012). To aid solubilization of the nanoparticles used in these latter studies, they were prepared in the organic solvent tetrahydrofuran (THF), which is a neurotoxin. Consequently, it is unclear as to whether the high toxicity observed in these instances is due to increased particle dispersion or because of THF–induced toxicity. However, preparation of the nanoparticles by stirring in water only indicated a reduced toxicity in different aquatic species compared with THF–solubilized C60 (Oberdörster et al., 2006). Concerning metal and metal oxide engineered nanoparticles, nano–silver and nano–ZnO were more toxic to different fish life stages than nano-TiO_2 and to crustaceans in acute tests (Aschberger et al., 2011). The toxicity of

nanoparticles to microorganisms has been studied more extensively (*e.g.*, silver nanoparticles, MgO and TiO_2), although in relation to the development of biocidal agents, as highlighted previously. Since microorganisms are the foundation of all known ecosystems, serving as the basis of food webs and the primary agents for global biogeochemical cycles, an understanding of nanomaterial–microbe interactions, is especially important. Currently, there is insufficient evidence to suggest that all nanoparticles have antimicrobial effects or that all nanoparticles are toxic to any organism encountered in an exposed environment (Oberdörster et al., 2007). Thus, more research is needed before generalized statements can be made regarding nanoparticle ecotoxicology.

2.4. CRITICAL APPRAISAL, CONCLUSIONS AND PERSPECTIVES

Although water plays a critical role in every facet of human activity, it is becoming an increasingly scarce resource in many parts of the world. Besides utilization of non–traditional sources for production of high–quality water and the conservation and protection of water bodies from pollution, equally important is the development of innovative new technologies and materials whereby challenges associated with the provision of safe potable water can be addressed. It is widely recognized that nanotechnology and applications thereof may play an important role in resolving issues relating to water shortage and water quality. Due to their large surface areas and their size– and shape–dependent catalytic properties, considerable efforts are underway to explore uses of nanomaterials in applications such as membrane separations, catalysis and adsorption. Moreover, nanomaterials can be functionalized with various different chemical groups to increase their affinity toward a given compound, thus resulting in ligands that are not only recyclable but also have a high capacity and selectivity for organic and inorganic compounds, as well as toxic metal ions and inorganic anions in aqueous solutions. While much attention has been focused on the development and potential benefits of nanomaterials in water treatment processes, concerns have also been raised regarding their potential human and environmental toxicity. Indeed, studies have indicated that the selfsame properties of nanomaterials that make them attractive (*e.g.*, size, shape, structure, reactivity) may also cause them to be toxic. It is difficult, however, to assess the effect of nanomaterials on health and the environment because the methods and tools for such a task

have not been well developed yet. In addition, common frameworks for risk research, risk assessment and risk management are lacking at present. It is vital that these processes be developed and investigated to ensure that nanomaterials are as safe as possible, while reaching their full potential. Notwithstanding these information gaps, it is certain that new nanomaterials, particularly in water and wastewater treatment, will play key roles in ensuring sufficient and good quality water to meet the ever–increasing demand for potable water. New research should from the start include consideration of potential threats to health and the environment, while risk research should be linked to existing and future applications. In addition, also update test methods and guidelines on harmful properties and exposure of nanoscale materials should be considered.

2.5. REFERENCES

Adesina AA (2004) Industrial exploitation of photocatalysis: Progress, perspectives and prospects. Catal Surv Asia 8: 265–273.

Ahluwalia SS, Goyal D (2007) Microbial and plant derived biomass for removal of heavy metals fromwastewater. Bioresour Technol 98: 2243–2257.

Ahmad AL, Ooi BS, Mohammad AW, Choudhury JP (2004) Development of a highly hydrophobic nanofiltration membrane for desalination and water treatment. Desalination 168:215–221.

Akasaka T, Watari F (2009) Capture of bacteria by flexible carbon nanotubes. Acta Biomater 5:607–612.

Allabashi R, Arkas M, Hörmann G, Tsiourvas D (2007) Removal of some organic pollutants in water employing ceramic membranes impregnated with cross–linked silylated dendritic and cyclodextrin polymers. Water Res 41: 476–486.

Albuquerque JEC, Mendez MO, Coutinho ADR, Franco TT (2008) Removal of cyanobacterial toxins from drinking water by adsorption on activated carbon fibers. Material Res 11: 370–80.

Alvarez–Ayuso E, Garcia–Sanchez A, Querol X (2003) Purification of metal electroplating waste waters using zeolites. Water Res 37: 4855–4862.

Amal R, McEvoy S, Beydoun D, Low G (1999) Role of nanoparticles in photocatalysis. J Nanopart Res 1: 439–458.

Anandan S, Lee G-J, Chen P-K, Fan C, Wu JJ (2010) Removal of orange II dye in water by visible light assisted photocatalytic ozonation using Bi_2O_3 and Au/Bi_2O_3 nanorods. Ind Eng Chem Res 49: 9729–9737.

Arkas M, Tsiourvas D, Paleos CM (2010) Functional dendritic polymers for the development of hybrid materials for water purification. Macromol Mater Eng 295: 883–898.

Arkas M, Allabashi R, Tsiourvas D, Mattausch E–M, Perfler R (2006) Organic/inorganic hybrid filters based on dendritic and cyclodextrin "nanosponges" for the removal of organic pollutants from water. Environ Sci Technol 40: 2771–2777.

Arkas M, Paleos CM, Eleades L, Tsiourvas D (2005) Alkylated hyperbranched polymers as molecular nanosponges for the purification of water from polycyclic aromatic hydrocarbons. J Appl Polym Sci 97: 2299–2305.

Aschberger K, Micheletti C, Sokull-Klüttgen B, Christensen FM (2011) Analysis of currently available data for characterising the risk of engineered nanomaterials to the environment and human health — lessons learned from four case studies. Environ Inter 37: 1143–1156.

Athanasekou CP, Romanos Em G, Katsaros FK, Kordatos K, Likodimos V, Falaras, P (2012) Very efficient composite titania membranes in hybrid ultrafiltration/photocatalysis water treatment processes. J Memb Sci 392: 192–203.

Atia AA, Donia AM, El-Enein SA, Yousif AM (2007) Effect of chain length of aliphatic amines immobilized on a magnetic glycidyl methacrylate resin towards the uptake behavior of Hg(II) from aqueous solutions. Sep Sci Technol 42: 403–420.

Bae E, Choi W (2003) Highly enhanced photoreductive degradation of perchlorinated compounds on dye-sensitized metal/TiO_2 under visible light. Environ Sci Technol 37: 147–152.

Balasubramanian K, Burghard M, (2005) Chemically functionalized carbon nanotubes. Small 1:180–192.

Balasubramanian K, Burghard M (2006) Biosensors based on carbon nanotubes. Anal Bioanal Chem 385: 452–468.

Balogh L, Swanson DR, Tomalia DA, Hagnauer GL, McManus AT 2001. Dendrimer–silver complexes and nanocomposites as antimicrobial agents. Nano Lett 1:18–21.

Barakat MA, Schaeffer H, Hayes G, Ismat–Shah S (2005) Photocatalytic degradation of 2–chlorophenol by Co–doped TiO_2 nanoparticles. Appl Catal B Environ 57: 23–30.

Boparai HK, Joseph M, O'Carroll DM (2011) Kinetics and thermodynamics of cadmium ion removal by adsorption onto nano zerovalent iron particles. J Hazard Mater 186: 458–465.

Bina B, Pourzamani H, Rashidi A, Amin M (2012) Ethylbenzene removal by carbon nanotubes from aqueous solution. J Environ Public Health 817: 187-195.

Bhattacharyya D, Hestekin JA, Brushaber P, Cullen L, Bachas LG, Sikdar SK (1998) Novel poly–glutamic acid functionalized microfiltration embranes for sorption of heavy metals at high capacity. J Membr Sci 141:121–135.

Biswas P, Wu C–Y (2005) Nanoparticles and the environment. J. AirWaste Manage Assoc 55:708–746.

Blount BC, Pirkle JL, Osterloh JD, Valentin-Blasini L, Caldwell KL (2006) Urinary perchlorate and thyroid hormone levels in adolescent and adult men and women living in the United States. Environ Health Pers 114: 1865–1871.

Borai EH, El-Sofany EA, Morcos TN (2007) Development and optimization of magnetic technologies based processes for removal of some toxic heavy metals. Adsorption 13: 95–104.

Borker P, Salker AV (2007) Solar assisted photocatalytic degradation of Naphthol Blue Black dye using Ce1−xMnxO2. Mater Chem Phys 103: 366–370.

Bottero JY, Rose J, Wiesner MR, (2006) Nanotechnologies, Tools for sustainability in a new wave of water treatment processes. Integr. Environ Assess Manag 2: 391–395.

Bottini M, Bruckner S, Nika K, Bottini N, Bellucci S, Magrini A, Bergamaschi A, Mustelin T (2006) Multi-walled carbon nanotubes induce T lymphocyte apoptosis. Toxicol Lett 160:121–126.

Bowman RS (2002) Applications of surfactant–modified zeolites to environmental remediation. Micropor Mesopor Mater 61: 43–56.

Brant JA, Lecoanet H, Wiesner MR (2005) Aggregation and deposition characteristics of fullerene nanoparticles in aqueous systems. J Nanopart Res 7: 545–553.

Brady-Estevez AS, Kang S, Elimelech M (2008) A single walled carbon nanotube filter for removal of viral and bacterial pathogens. Small 4:481–484.

Bull RJ, Brinbaum LS, Cantor KP, Rose JB, Butterworth BE, Pegram R, Tuomisto J (1995) Water chlorination. Essential process and cancer hazard. Fund Appl Toxicol 28: 155–166.

Cai YQ, Cai Y, Mou SF, Lu YQ (2005) Multi-walled carbon nanotubes as a solid–phase extraction adsorbent for the determination of chlorophenols in environmental water samples. J chromatogr A 1081:245–247.

Camblor MA, Corma A, Valencia S (1998) Synthesis in fluoride media and characterization of aluminosilicate zeolite beta. J Mater Chem 8: 2137– 2145.

Cao J, Elliott D, Zhang W-X (2005) Perchlorate reduction by nanoscale iron particles. J. Nanopart Res 7: 499–506.

Card JW, Zeldin DC, Bonner JC, Nestmann ER (2008) Pulmonary applications and toxicity of engineered nanoparticles. Am J Physiol Lung Cell Mol Physiol 295: 400–511.

Carp O, Huisman CL, Reller A (2004) Photoinduced reactivity of titanium dioxide. Prog Solid State Chem 32: 33–177.

Celebi O, Uzum C, Shahwan T, Erten HN (2007) A radiotracer study of the adsorption behavior of aqueous Ba^{2+} ions on nanoparticles of zero-valent iron. J Hazard Mater 148: 761–767.

Chen CZS, Cooper S (2002) Interactions between dendrimer biocides and bacterial membranes. Biomateri 23: 3359–3368.

Chen L, Wang T, Tong J (2011) Application of derivatized magnetic materials to the separation and the pre-concentration of pollutants in water samples. Trends in Analy Chem 30: 207-215.

Chen Y, Crittenden J, Hackney S, Sutter L, Hand D (2005) Preparation of a novel TiO_2 -based p-n junction nanotube photocatalyst. Environ Sci Technol 39: 1201–1208.

Cheng R, Wang JL, Zhang WX (2007) Comparison of reductive dechlorination of p–chlorophenol using Fe^0 and nano-sized Fe^0. J Hazard Mater 144: 334–339.

Cho IH, Kim YG, Yang JK, Lee, NH, Lee SM (2006) Solar-chemical treatment of groundwater contaminated with petroleum at gas station sites: Ex situ remediation using solar/TiO_2 photocatalysis and solar photo-fenton. J Environ Sci Health A 4: 457–473.

Cho IH, Park JH, Kim YG (2005) Oxidative degradation and toxicity reduction of trichloroethylene (TCE) in water using TiO_2/solar light, Comparative study of TiO_2 slurry and immobilized systems. J Environ Sci Health A 40: 1033–1044.

Choe S, Chang YY, Hwang KY, Khim J (2000) Kinetics of reductive denitrification by nanoscale zero–valent iron. Chemosphere 41: 1307–1311.

Coetser SE, Heath RG, Ndombe N (2007) Diffuse pollution associated with the mining sectors in South Africa: A first–order assessment. Water Sci Technol 55: 9–16.

Cohen Y (2006) Membrane surface nano-structuring: Selective enhancement, fouling reduction and mineral scale formation. In US-Israeli Nanotechnology for water purification workshop, Arlington, Virginia, USA, March 13-16.

Chong MN, Jin B, Chow CWK, Saint C (2010) Recent developments in photocatalytic water treatment technology: A review. Water Res 44: 2997-3027.

Daniel-Da-Silva AL, Loio R, Lopes-Da-Silva JA, Trindade T, Goodfellow BJ, Gil AM (2008) Effects of magnetite nanoparticles on the thermorheological properties of carrageenan hydrogels. J Colloid Interface Sci 324: 205–211.

Danilczuk M, Lund A, Saldo J, Yamada H, Michalik J (2006) Conduction electron spin resonance of small silver particles. Spectrochim Acta A 63: 189–191.

Dankovich TA, Gray DG, (2011) Bactericidal paper impregnated with silver nanoparticles for point-of-use water treatment. Environ Sci Technol 45: 1992-1998.

DeFriend KA, Wiesner MR, Barron AR (2003) Alumina and aluminate ultrafiltration membranes derived from alumina nanoparticles. J Membr Sci 224: 11–28.

Del Valle EMM (2004) Cyclodextrins and their uses, A review. Process Biochem 39: 1033–1046.

Delpla I, Baures E, Jung AV, Clement M, Thomas O (2011) Issues of drinking water quality of small scale water services towards climate change. Water Sci Technol 63: 227-32.

Deng S, Upadhyayula VKK, Smith GB, Mitchell MC (2008) Adsorption equilibrium and kinetics of microorganisms on single walled carbon nanotubes. IEEE Sens 8: 954–62.

Deng S, Fan H, Wang M, Zheng M, Yi J, Wu R, Tan H, Sow C, Ding J, Feng Y, Loh K (2010) Thiol-capped ZnO nanowire/nanotube arrays with tunable magnetic properties at room temperature. ACS Nano 4: 495–505.

Di Z-C, Ding J, Peng X-J, Li Y-H, Luan Z-K, Liang J (2006) Chromium adsorption by aligned carbon nanotubes supported ceria nanoparticles. Chemosphere 62: 861–865.

Diallo MS, Christie S, Swaminathan P, Balogh L, Shi X, Um W, Papelis C, Goddard WA, Johnson JH (2004) Dendritic chelating agents 1. Cu(II) binding to ethylene diamine core poly(amidoamine) dendrimers in aqueous solutions. Langmuir 20: 2640–2651.

Diallo MS, Christie S, Swaminathan P, Johnson JH, Goddard WA (2005) Dendrimer-enhanced ultrafiltration. 1. Recovery of Cu(II) from aqueous solutions using Gx–NH2PAMAM dendrimers with ethylene diamine core. Environ Sci Technol 39:1366–1377.

Ding L, Zheng Y (2007) Nanocrystalline zeolite beta: The effect of template agent on crystal size. Mater Res Bull 42:584–590.

Donaldson K, Aitken R, Tran L, Stone V, Duffin R, Forrest G, Alexander A (2006) Carbon nanotubes: Are view of their properties in relation to pulmonary toxicology and workplace safety. Toxicol Sci 92: 5–22.

Donaldson K, Tran CL (2004) An introduction to the short–term toxicology of respirable industrial fibres. Mutat Res 553: 5–9.

Dotzauer DM, Dai J, Sun L, Bruening ML (2006) Catalytic membranes prepared using layer–by–layer adsorption of polyelectrolyte/metal nanoparticle films in porous supports. Nano Lett 6: 2268–2272.

Dvoranova D, Brezova V, Malati MA (2002) Investigations of metal–doped titanium dioxide photocatalysts. Appl Catal B Environ 37: 91–105.

Elder A, Gelein R, Silva V, Feikert T, Opanashuk L, Carter J, Potter R, Maynard A, Ito Y, Finkelstein J, Oberdörster G (2006) Translocation of inhaled ultrafine manganese oxide particles to the central nervous system. Environ Health Perspect 114: 1172–1178.

Elliott D, Lien H-L, Zhang W-X (2008) Zerovalent iron nanoparticles for treatment of ground water contaminated by hexachlorocyclohexanes. J Environ Quality 37: 2192–2201.

Esteban–Cubillo A, Pecharromán C, Aguilar E, Santarén J, Moya, JS (2006) Antibacterial activity of copper monodispersed nanoparticles into sepiolite. Mater Sci 41: 5208–5212.

Falcone IR, Humpage AR (2005) Health risk assessment of cyanobacterial (blue–green algal) toxins in drinking water. Int J Environ Res Public Health 2: 43–50.

Farré M, Gajda-Schrantz K, Kantiani L, Barceló D (2009) Ecotoxicity and analysis of nanomaterials in the aquatic environment. Anal Bioanaly Chem 393: 81–95.

Favre-Reguillon A, Lebuzit G, Fooz J, Guy A (2003) Selective concentration of uranium from seawater by nanofiltration. Ind Eng Chem Res 42: 5900–5904.

Figueira P, Lopes CB, Daniel-da-Silva AL, Pereira E, Duarte AC, Trindade T (2011) Removal of mercury (II) by dithiocarbamate surface functionalized magnetite particles: Application to synthetic and natural spiked waters. Water Res 45: 5773-5784.

Foley JA, DeFries R, Asner GP, Barford C, Bonan G, Carpenter SR, Chapin FS, Coe MT, Daily GC, Gibbs HK, Helkowski JH, Holloway T, Howard EA, Kucharik CJ, Monfreda C, Patz JA, Prentice IC, Ramankutty N, Snyder PK (2005) Global consequences of land use. Science 309: 570–574.

Frechet JMJ, Tomalia DA (2001) Dendrimers and other dendritic polymers. New York, Wiley and Sons Publishers.

Fujishima A, Honda K (1972) Electrochemical photolysis of water at a semiconductor electrode. Nature 238: 37–38.

Gao C, Yan D (2004) Hyperbranched polymers: From synthesis to applications. Prog Polym Sci 29: 183–275.

Girginova PI, Daniel-Da-Silva AL, Lopes CB, Figueira P, Otero M, Amaral VS, Pereira E, Trindade T (2010) Silica coated magnetite particles for magnetic removal of Hg(II) from water. J Colloid and Interface Sci 345: 234-240.

Gondal MA, Dastageer MA, Khalil A (2009) Synthesis of nano-WO_3 and its catalytic activity for enhanced antimicrobial process for water purification using laser induced photo-catalysis. Catal Commu 11: 214–219.

Guo LM, Li JT, Zhang LX, Li JB, Li YS, Yu CC, Shi JL, Ruan ML, Feng JW (2008) A facile route to synthesize magnetic particles within hollow mesoporous spheres and their performance as separable Hg^{2+} adsorbents. J Mater Chem 18: 2733–2738.

Harper S, Usenko C, Hutchison JE, Maddux BLS, Tanguay RL (2008) *In Vivo* Biodistribution and Toxicity Depends on Nanomaterial Composition, Size, Surface Functionalisation and Route of Exposure. J Exp Nanosciences 3: 195–206.

Henmi M, Nakatsuji K, Ichikawa T, Tomioka H, Sakamoto T, Yoshio M, Kato T (2012) Self-organized liquid-crystalline nanostructured membranes for water treatment: Selective permeation of ions. Adv Mater 24: 2238–2241.

He P, Zhao DY (2005) Preparation and characterization of a new class of starch–stabilized bimetallic nanoparticles for degradation of chlorinated hydrocarbons in water. Environ Sci Technol 39: 3314–3320.

Hollman AM, Bhattacharyya D (2004) Pore assembled multilayers of charged polypeptides in microporous membranes for ion separation. Langmuir 20: 5418–5424.

Huang CZ, Hu B, (2008) Silica-coated magnetic nanoparticles modified with gammamercaptopropyltrimethoxysilane for fast and selective solid phase extraction of trace amounts of Cd, CuHg, and Pb in environmental and biological samples prior to their determination by inductively coupled plasma mass spectrometry. Spectrochim Acta B 63: 437–444.

Hu J, Chen GH, Lo IMC (2005) Removal and recovery of Cr(VI) from wastewater by maghemite nanoparticles, Water Res 39: 4528–4536.

Hu J, Tonga Z, Hu Z, Chena G, Chenc T (2012) Adsorption of roxarsone from aqueous solution by multi-walled carbon nanotubes. J Colloid and Interface Sci 377: 355–361.

Hu JS, Ren LL, Guo YG, Liang HP, Cao AM, Wan LJ, Bai CL (2005) Mass production and high photocatalytic activity of ZnS nanoporous nanoparticles, Angew Chem Int Ed 44: 1269–1273.

Hyung H, Kim JH (2008) Natural organic matter (NOM) adsorption to multi walled carbon nanotubes: effect on NOM characteristics and water quality parameters. Environ Sci Technol 42: 4416–21.

Iijima S (1991) Helical microtubules of graphitic carbon. Nature 354: 56–58.

Iijima S, Ichihashi T (1993) Single–shell carbon nanotubes of 1-nm diameter. Nature 363: 603–605.

Indira TK, Lakshmi PK (2010) Magnetic nanoparticles- A review. Int J Pharm Sci Nanotec 3: 1035-1044.

Irie H, Watanabe Y, Hashimoto K (2003) Carbon-doped anatase as a visible light–sensitive photocatalyst. Chem Lett 32: 772–773.

Ji P, Zhang J, Chen F, Anpo M (2009) Study of adsorption and degradation of acid orange 7 on the surface of CeO_2 under visible light irradiation. Appl Catal B Environ 85: 148–154.

Jiang F, Zheng Z, Xu Z, Zheng S, Guo Z, Chen L (2006) Aqueous Cr(VI) photo–reduction catalyzed by TiO_2 and sulfated TiO_2. J Hazard Mater 134: 94–103.

Jikei M, Kakimoto M–A (2001) Hyperbranched polymers: A promising new class of materials. Prog Polym Sci 26: 1233–1285.

Jin J, Li R, Wang H, Chen H, Liang K, Ma J (2007) Magnetic Fe nanoparticle functionalized water-soluble multi-walled carbon nanotubules: Towards the preparation of sorbent for aromatic compounds removal. Chem Commun 4: 386–388.

Kabra K, Chaudhary R, Sawhney RL (2004) Treatment of hazardous organic and inorganic compounds through aqueous-phase photocatalysis: A review. Ind Eng Chem Res 43: 7683–7696.

Kamat P, Huehn R, Nicolaescu R (2002) A "sense and shoot" approach for photocatalytic degradation of organic contaminants in water. J Phys Chem B 106: 788–794.

Kanel SR, Greneche JM, Choi H (2006) Arsenic(V) removal from groundwater using nano–scale zero–valent iron as a colloidal reactive barrier material. Environ Sci Technol 40: 2045–2050.

Kanel SR, Manning B, Charlet L, Choi H (2005) Removal of arsenic (III) from groundwater by nanoscale zero-valent iron. Environ Sci Technol 39: 1291–1298.

Keum YS, Li QX (2004) Reduction of nitroaromatic pesticides with zerovalent iron. Chemosphere 54: 255–263.

Khaydarov RA, Khaydarov RR, Gapurova O (2010) Water purification from metal ions using carbon nanoparticle-conjugated polymer nanocomposites. Water Res 44: 1927–1933.

Kim JS, Kuk E, Yu KM, Kim J-H, Park SJ, Lee HJ, Kim SH, Park YK, Park YH, Hwang C-Y, Kim Y-K, Lee Y-S, Jeong D-H, Cho M-H (2007) Antimicrobial effects of silver nanoparticles. Nanomedicine 3: 95–101.

Kim J, Buggen BV (2010a) The use of nanoparticles in polymeric and ceramic membrane structures: Review of manufacturing procedures and performance improvement for water treatment. Environ Pollut 158: 2335-2349.

Kim KT, Klaine SJ, Cho J, Kim SH, Kim SD (2010b) Oxidative stress responses of Daphnia magna exposed to TiO(2) nanoparticles according to size fraction. Sci Total Environ 408: 2268-2272.

Kirchnerova J, Herrera Cohen M–L, Guy C, Klvana D (2005) Photocatalytic oxidation of n–butanol under fluorescent visible light lamp over commercial TiO2 (Hombicat UV100 and Degussa P25). Appl Catal A Gen 282: 321–332.

Klajnert B, Bryszewska M (2001) Dendrimers: Properties and applications. Acta Biochim Pol 48: 199–208.

Koper OB, Klabunde JS, Marchin GL, Klabunde KJ, Stoimenov P, Bohra L (2002) Nanoscale powders and formulations with biocidal activity towards spores and vegetative cells of Bacillus species, viruses, and toxins. Curr Microbiol 44: 49–55.

Langwaldt JH, Puhakka JA (2000) On-site biological remediation of contaminated groundwater: A review. Environ Pollut 107:187–197.

Lanone S, Boczkowski J (2006) Biomedical applications and potential health risks of nanomaterials: Molecular mechanisms. Curr Mol Med 6: 651–663

Lee J–S, Chon H–T, Kim K–W (2005a) Human risk assessment of As, Cd, Cu and Zn in the abandoned metal mine site. Environ Geochem Health 27: 185–191.

Leiknes T (2009) The effect of coupling coagulation and flocculation with membrane filtration in water treatment: a review. 21: 8–12.

Liga MV, Bryant BF, Colvin VL, Li Q (2011) Virus inactivation by silver doped titanium dioxide nanoparticles for drinking water treatment. Water Res 45: 535–544.

Linder C, Oren Y (2006) Relationships between materials parameters of nanofiltration membranes and the resultant membrane performance. In US-Israeli: Nanotechnology for water purification workshop, Arlington, Virginia, USA, March 13–16.

Li FB, Li XZ, Liu CS, Liu TX (2007) Effect of alumina on photocatalytic activity of iron oxides for bisphenol a degradation, J Hazard Mater 149: 199–207

Li HD, Li Z, Liu T, Xiao X, Peng ZH, Deng L (2008) A novel technology for biosorption and recovery hexavalent chromium in wastewater by biofunctional magnetic beads, Bioresour. Technol. 99: 6271–6279.

Li L, Fan M, Brown RC, Van Leeuwen J (2006a) Synthesis, properties, and environmental applications of nanoscale iron–based materials: A review. Crit Rev Environ Sci Tech 36: 405–431.

Li X–Q, Elliott DW, Zhang W–X (2006b) Zero–valent iron nanoparticles for abatement of environmental pollutants: Materials and engineering aspects. Crit Rev Solid State Mater Sci 31: 111–122.

Li Y–H, Ding J, Luan ZK, Di ZC, Zhu YF, Xu CL, Wu DH, Wei BQ (2003) Competitive adsorption of Pb2+, Cu2+ and Cd2+ ions from aqueous solutions by multi–walled carbon nanotubes. Carbon 41: 2787– 2792.

Li X–Q, Zhang W–X (2006) Iron nanoparticles, The core–shell structure and unique properties for Ni(II) sequestration. Langmuir 22: 4638–4642.

Liu L, Bai H, Sun D D (2012) Concurrent filtration and solar photocatalytic disinfection/ degradation using high-performance Ag/TiO2 nanofiber membrane. Water Res 46: 1102–1112.

Liu Y, Su G, Zhang B, Jiang G, Yan B (2011) Nanoparticle-based strategies for detection and remediation of environmental pollutants. Analyst 136: 872–877.

Liu Y, Li J, Qiu X, Burda C (2006a) Novel TiO2 nanocatalysts for wastewater purification – Tapping energy from the sun. Water Practice and Technology 1: 1–9.

Liu Y, Chen X, Li J, Burda C (2005b) Photocatalytic degradation of azo dyes by nitrogen–doped TiO2 nanocatalysts. Chemosphere 61: 11–18.

Liu Y, Majetich SA, Tilton RD, Sholl DS, Lowry GV (2005a) TCE dechlorination rates, pathways, and efficiency of nanoscale iron particles with different properties. Environ. Sci. Technol. 39:1338–1345.

Liu Z, He Y, Li F, Liu Y (2006b) Photocatalytic treatment of RDX wastewater with nano–sized titanium dioxide. Environ Sci Pollut Res Int 13: 328–332.

Liu J-F, Zhao ZS, Jiang G-B (2008) Coating Fe3O4 Magnetic Nanoparticles with Humic Acid for High Efficient Removal of Heavy Metals in Water Environ Sci Technol 42: 6949–6954.

Long QR, Yang RT (2001) Carbon nanotubes as superior sorbent for dioxin removal. J Am Chem Soc 123: 2058–2059.

Lopes CB, Figueira P, Tavares DS, Lin Z, Daniel-da-Silva AL, Duarte AC, Rocha J, Trindade T, Pereira E. (2012) Core–shell magnetite-silica dithiocarbamate-derivatized particles achieve the Water Framework Directive quality criteria for mercury in surface waters. Submitted to Water Res.

López-Munoz MJ, Van Grieken R, Aguado J, Marugán J (2005) Role of the support on the activity of silica-supported TiO_2 photocatalysts: Structure of the TiO_2/SBA–15 photocatalysts. Catal Today 101 307–314.

Lu, C., Chung, Y.-L., Chang, K.-F., 2005. Adsorption of trihalomethanes from water with carbon nanotubes. Water Res. 39, 183–189.

Lu C, Chung Y-L, Chang K-F (2006) Adsorption thermodynamic and kinetic studies of trihalomethanes on multiwalled carbon nanotubes. J Hazard Mater 138: 304–310.

Lu C, Liu L (2006) Removal of nickel(II) from aqueous solution by carbon nanotubes. J. Chem. Technol. Biotechnol. 81: 1932–1940.

Madigan M, Martinko J (2005) Brock Biology of Microorganisms, 11th ed. Englewood Cliffs, NJ, Prentice Hall Publishers.

Makhluf S, Dror R, Nitzan Y, Abramovich A, Jelinek R, Gedanken A (2005) Microwave–assisted synthesis of nanocrystalline MgO and its use as a bacteriocide. S Adv Funct Mater 15: 1708–1715.

Margeta1 K, Vojnovi B, Zabukovec L N (2011) Development of natural zeolites for their use in water-treatment systems. Recent Patents on Nanotech 5: 89-99.

Maynard AD (2007) Nanotechnology: The next big thing, or much ado about nothing? Ann Occup Hyg 51: 1–12.

Mitoraj D, Jánczyk A, Strus M, Kisch H, Stochel S, Heczko PB, Macyk W (2007) Visible light-inactivation of bacteria and fungi by modified titanium dioxide. Photochem. Photobiol. Sci 6: 642–648.

Miyagawa H, Misra M, Mohanty AK (2005) Mechanical properties of carbon nanotubes and their polymer nanocomposites. J Nanosci Nanotechnol 5: 1593–1615.

Mohsen MS, Jaber JO, Afonso MD (2003) Desalination of brackish water by nanofiltration and reverse osmosis. Desalination 157:167–177.

Møller P, Jacobsen NR, Folkmann JK, Danielsen PH, Mikkelsen L, Hemmingsen JG, Vesterdal LK, Forchhammer L, Wallin H, Loft S (2010) Role of oxidative damage in toxicity of particulates. Free Radic Res. 44:1-46.

Monteiro–Riviere NA, Nemanich RJ, Inman AO, Wang YYY, Riviere JE (2005) Multi–walled carbon nanotube interactions with human epidermal keratinocytes. Toxicol Lett 155: 377–384.

Montgomery MA, Elimelech M (2007) Water and sanitation in developing countries: Including health in the equation. Environ Sci Technol 41: 17–24.

Moon J, Yun CY, Chung K–W, Kang MS, Yi J (2003) Photocatalytic activation of TiO_2 under visible light using Acid Red 44. Catal. Today 87: 77–86.

Moore MN (2006) Do nanoparticles present ecotoxicological risks for the health of the aquatic environment? Environ Int 32: 967–976.

Moreno N, Querol X, Ayora C (2001) Utilization of zeolites synthesized from coal fly ash for the purification of acid mines water. Environ Sci Technol 35: 3526–3534.

Morones JR, Elechiguerra JL, Camacho A, Holt K, Kouri JB, Ramírez JP, Yacaman MY (2005) The bactericidal effect of silver nanoparticles. Nanotechnology 16: 2346–2353.

Mostafavi ST, Mehrnia MR, Rashidi AM (2009) Preparation of nanofilter from carbon nanotubes for application in virus removal from water. Desalination 238: 271–280.

Mpenyana-Monyatsi L, Mthombeni NH, Onyango MS, Momba MN (2012) Cost-effective filter materials coated with silver nanoparticles for the removal of pathogenic bacteria in groundwater. Int J Environ Res Public Health 9: 244-71.

Nahar S, Hasegawa K, Kagaya S (2006) Photocatalytic degradation of phenol by visible light–responsive iron–doped TiO_2 and spontaneous sedimentation of the TiO_2 particles. Chemosphere 65: 1976–1982.

Nel A, Xia T, Mädler L, Li N (2006) Toxic potential of materials at the nanolevel. Science 311: 622–627.

Neumann B, Bogdanoff P, Tributsch H, Sakthivel S, Kisch H (2005) Electrochemical mass spectroscopic and surface photovoltage studies of catalytic water photooxidation by undoped and carbon–doped titania. J Phys Chem B 109: 16579–16586.

Nurmi JT, Tratnyek PG, Sarathy V, Baer DR, Amonette JE (2005) Characterization and properties of metallic iron nanoparticles: Spectroscopy, electrochemistry, and kinetics. Environ Sci Technol 39: 1221–1230.

Nutt MO, Heck KN, Alvarez P, Wong MS (2006) Improved Pd-on- Au bimetallic nanoparticle catalysts for aqueous-phase trichloroethene hydrodechlorination. Appl Catal B Environ 69: 115–125.

Oberdörster E (2004) Manufactured nanomaterials (Fullerenes, C–60) induce oxidative stress in the brain of juvenile largemouth bass. Environ. Health Perspect. 112: 1058–1062.

Oberdörster G, Finkelstein JN, Johnston C, Gelein R, Cox C, Baggs R, Elder AC (2000) Acute pulmonary effects of ultrafine particles in rats and mice. Res. Rep. Health Eff. Inst. 96: 5–86.

Oberdörster G, Oberdörster E, Oberdörster J (2005) Nanotoxicology: An emerging discipline evolving from studies of ultrafine particles. Environ Health Perspect 113: 823–839.

Oberdörster G, Sharp Z, Atudorei V, Elder A, Gelein R, Kreyling W, Cox C (2004) Translocation of inhaled ultrafine particles to the brain. Inhalation Toxicol 16: 437–445.

Oberdörster G, Stone V, Donaldson K (2007) Toxicology of nanoparticles: A historical perspective. Nanotoxicology 1:2–25.

Oberdörster E, Zhu S, Blickley TM, McClellan-Green P, Haasch ML (2006) Ecotoxicology of carbon-based engineered nanoparticles: Effects of fullerene (C60) on aquatic organisms. Carbon 44:1112–1120.

Oh S-M, Kim S-S, Lee JE, Ishigaki T, Park D-W (2003) Effect of additives on photocatalytic activity of titanium dioxide powders synthesized by thermal plasma. Thin Solid Films 435: 252–258.

Ohno T, Mitsui T, Matsumura M (2003) Photocatalytic activity of S– doped photocatalyst under visible light. Chem Lett 32: 364–365.

Ohno T, Sarukawa K, Tokieda K, Matsumura M (2001) Morphology of a TiO_2 photocatalyst (Degussa P–25) consisting of anatase and rutile crystalline phases. J Catal 203: 82–86.

Orha C, Pop A, Lazau C, Grozescu I, Tiponut V, Manea F (2011) Structural characterization and the sorption properties of the natural and synthetic zeolite. Journal of Optoelectronics and Advanced Materials 13: 544-549.

Pal S, Tak YK, Song JM (2007) Does the antibacterial activity of silver nanoparticles depend on the shape of the nanoparticle? A study of the Gram– negative bacterium Escherichia coli. Appl Environ Microbiol 73: 1712–1720.

Palmer RA, Doan TM, Lloyd PG, Jarvis BL, Ahmed NU (2002) Reduction of TiO_2 with hydrogen plasma. Plasma Chem Plasma P 3: 335–350.

Peltier S, Cotte E, Gatel D, Herremans L, Cavard J (2003) Nanofiltration improvements of water quality in a large distribution system. Water Supply 3: 193–200.

Pena ME, Korfiatis GP, Patel M, Lippincott L, Meng X (2005) Adsorption of As(V) and As(III) by nanocrystalline titanium dioxide. Water Res 39: 2327–2337.

Peng XJ, Li YH, Luan ZK, Di ZC, Wang HY, Tian BH, Jia ZP (2003) Adsorption of 1,2–dichlorobenzene from water to carbon nanotubes. Chem. Phys. Lett. 376: 154–158.

Peng XJ, Luan ZK, Ding J, Di ZC, Li YH, Tian BH (2005) Ceria nanoparticles supported nanotubes for the removal of arsenate from water. Mater Lett 59: 399–403.

Pereira R, Rocha-Santos TAP, Antunes FE, Rasteiro MG, Ribeiro R, Gonçalves F, Soares AMVM, Lopes I (2012) Screening evaluation of the ecotoxicity and genotoxicity of soils contaminated with organic and inorganic nanoparticles: the role of ageing. J Haz Mat 194: 345-354.

Petersen EJ, Nelson BC (2010) Mechanisms and measurements of nanomaterial-induced oxidative damage to DNA. Analy Bioanaly Chem 398: 613–650.

Poinern GEJ, Parsonage D, Issa TB, Ghosh MK, Paling E, Singh P (2010) Preparation, characterization and As(V) adsorption behaviour of CNT-ferrihydrite composites. IJEST 8: 13–24.

Ponder SM, Darab JG, Mallouk TE (2000) Remediation of Cr(VI) and Pb(II) aqueous solutions using supported, nanoscale zero-valent iron. Environ Sci Technol 34: 2564–2569.

Qin F, Li G, Wang R, Wu J, Sun H, Chen R (2012) Template-free fabrication of Bi_2O_3 and $(BiO)_2CO_3$ nanotubes and their application in water treatment. Chem Eur J 00: 0 – 0.

Qin JJ, Oo MH, Kekre KA (2007) Nanofiltration for recoveringwastewater from a specific dyeing facility. Sep Pur Tech 56: 199–203.

Rao CNR, Kulkarni GU, Thomas PJ, Edwards PP (2002) Size– dependent chemistry: Properties of nanocrystals. Chem Eur J 8: 28–35.

Ritchie SMC, Kissick KE, Bachas LG, Sikdar SK, Parikh C, Bhattacharyya D (2001) Polycysteine and other polyamino acid functionalized microfiltration membranes for heavy metal capture. Environ Sci Technol 35: 3252–3258.

Ritter L, Solomon K, Sibley P, Hall K, Keen P, Mattu G, Linton B (2002) Sources, pathways, and relative risks of contaminants in surface water and groundwater: A perspective prepared for the Walkerton inquiry. J Toxicol Environ Health 65: 1–142.

Rickerby DG, Morrison M (2007) Nanotechnology and the environment: A European perspective. STAM 8: 19–24.

Riu J, Maroto A, Rius FX (2006) Nanosensors in environmental analysis. Talanta 69: 288–301.

Rivas BL, Pereira ED, Moreno-Villoslada I (2003) Water soluble polymer–metal ion interactions. Prog Polym Sci 28: 173–208.

Romero M, Blanco J, Sanchez B, Vidal A, Malato S, Cardona AI, Garcia E (1999) Solar photocatalytic degradation of water and air pollutants: Challenges and perspectives. Solar Energy 66: 169–182.

Romanos Em G, Athanasekou CP, Katsaros FK, Kanellopoulos NK, Dionysiou, DD, Likodimos V, Falaras P (2011) Double-side active TiO_2-modified nanofiltration membranes in continuous flow photocatalytic reactors for effective water purification. J Hazard Mater 211: 304-316

Rozell DJ, Reaven SJ (2011) Water Pollution Risk Associated with Natural Gas Extraction from the Marcellus Shale. Risk Anal 111: 1539-6924.

Rozemeijer JC, Broers HP (2007) The groundwater contribution to surface water contamination in a region with intensive agricultural land use (Noord-Brabant, The Netherlands). Environ Pollut 148: 695-706.

Ryman–Rasmussen, JP, Riviere JE, Monteiro–Riviere NA (2006) Penetration of intact skin by quantum dots with diverse physiochemical properties. Toxicol Sci 91: 159–165.

Sakthivel S, Shankar VM, Palanichamy M, Arabindoo B, Bahnemann DW, Murugesan V (2004) Enhancement of photocatalytic activity by metal deposition: Characterization and photonic efficiency of Pt: Au and Pd deposited on TiO_2 catalyst. Water Res 38: 3001–3008.

Saleh NB, Pfefferle LD, Elimelech M (2008) Aggregation kinetics of multiwalled carbon nanotubes in aquatic systems: measurements and environmental implications. Environ Sci Technol 42: 7963–9.

Salipira KL, Mamba BB, Krause RW, Malefetse TJ, Durbach SH (2007) Carbon nanotubes and cyclodextrin polymers for removing organic pollutants from water. Environ Chem Lett 5: 13–17.

Sánchez A, Recillas S, Font X, Casals E, González E, Puntes V (2011) Ecotoxicity of, and remediation with, engineered inorganic nanoparticles in the environment. Trends in Analy Chem 30: 507-516.

Savage N, Diallo M S (2005) Nanomaterials and water purification: Opportunities and challenges. J Nanopart Res 7: 331– 342.

Sawicki R, Mercier L (2006) Evaluation of mesoporous cyclodextrin-silica nanocomposites for the removal of pesticides from aqueous media. Environ Sci Technol 40: 1978–1983.

Schneiderman E, Stalcup AM (2000) Cyclodextrins: A versatile tool in separation science. J Chromatogr B 745: 83–102.

Schwarzenbach RP, Escher BI, Fenner K, Hofstetter TB, Johnson CA, Von Gunten U, Wehrli B (2006) The challenge of micropollutants in aquatic systems. Science 313: 1072–1077.

Scott R L, Datta S, Gui M, Coker E L, Huggins FE, Daunert S, Bachas L, Bhattacharyya D (2011) Reactive nanostructured membranes for water purification. PNAS 108: 8577–8582.

Sheha RR, El-Zahhar AA (2008) Synthesis of some ferromagnetic composite resins and their metal removal characteristics in aqueous solutions. J Hazard Mater 150: 795–803.

Shi S, Jang J (2007) Thiol containing polymer encapsulated magnetic nanoparticles as reusable and efficiently separable adsorbent for heavy metal ions. Chem Commun10: 4230–4232.

Simate GS, Iyuke SE, Ndlovu S, Heydenrych M, Walubita LF (2012) Human health effects of residual carbon nanotubes and traditional water treatment chemicals in drinking water. Environ Inter 39: 38–49.

Singh R, Pantarotto D, Lacerda L, Pastorin G., Klumpp, C., Prato, M., Bianco, A., Kostarelos, K., 2006. Tissue biodistribution and blood clearance rates of intravenously administered carbon nanotube radiotracers. Proc Natl Acad Sci USA 103: 3357–3362.

Sharifi S, Behzadi S, Laurent S, Forrest ML, Stroevee P, Mahmoudm M (2012) Toxicity of nanomaterials. Chem Soc Rev 41: 2323–2343

Shen YF, Tang J, Nie ZH, Wang YD, Ren Y, Zuo L (2009) Preparation and application of magnetic Fe_3O_4nanoparticles for wastewater purification. Sep Purif Technol 68: 312-319.

Smith A (2006) Nanotech – the way forward for clean water? Filtr Separat 43: 32-33.

Som C, Wick P, Krug H, Nowack B (2011) Environmental and health effects of nanomaterials in nanotextiles and façade coatings. Environ Int 37: 1131–1142.

Son WK, Youk JH, Lee TS, Park WH (2004) Preparation of antimicrobial ultrafine cellulose acetate fibers with silver nanoparticles. Macromol Rapid Commun. 25: 1632–1637.

Sondi I, Salopek-Sondi B (2004) Silver nanoparticles as antimicrobial agent: A case study on E. coli as a model for Gram–negative bacteria. J Colloid Interface Sci 275: 1770–1782.

Song W, Grassian VH, Larsen SC (2005a) High yield method for nanocrystalline zeolite synthesis. Chem Commun 20: 2951–2953.

Song W, Li G, Grassian VH, Larsen SC (2005b) Development of improved materials for environmental applications: Nanocrystalline NaY zeolites. Environ Sci Technol 39: 1214–1220.

Song W, Justice RE, Jones CA, Grassian VH, Larsen SC (2004) Synthesis, characterization, and adsorption properties of nanocrystalline ZSM–5. Langmuir 20: 8301–8306.

Srivastava A, Srivastava ON, Talapatra S, Vajtai R, Ajayan PM (2004) Carbon nanotube filters. Nature Mate 3: 610–614.

Stanton BW, Harris JJ, Miller MD, Bruening ML (2003) Ultrathin, multilayered polyelectrolyte films as nanofiltration membranes. Langmuir 19: 7038–7042.

Stoimenov PK, Klinger RL, Marchin GL, Klabunde KJ (2002) Metal oxide nanoparticles as bactericidal agents. Langmuir 18: 6679–6686.

Sprenger C, Lorenzen G, Hülshoff I, Grützmacher G, Ronghang M, Pekdeger A (2011) Vulnerability of bank filtration systems to climate change. Sci Total Environ 15: 655-663.

Strathmann H (2001) Membrane separation processes: Current relevance and future opportunities. AIChE J 47: 1077–1087.

Sun Y–P, Li X–Q, Cao J, ZhangW–X, Wang HP (2006) Characterization of zero–valent iron nanoparticles. Adv. Colloid Interface Sci 120: 47–56.

Sun D, Meng TT, Loong TH, Hwa TJ (2004) Removal of natural organic matter from water using a nano–structured photocatalyst coupled with filtration membrane. Wat Sci Technol 49: 103–110.

Tavolaro A, Tavolaro P, Drioli E (2007) Zeolite inorganic supports for BSA immobilization: Comparative study of several zeolite crystals and composite membranes. Colloids Surf. B, Biointerfaces 55: 67–76.

Theron J, Walker JA, Cloete TE (2008) Nanotechnology and Water Treatment: Applications and Emerging Opportunities. Critical Reviews in Microbio 34: 43–69.

Tick GR, Lourenso F, Wood AL, Brusseau ML (2003) Pilot–scale demonstration of cyclodextrin as a solubility–enhancement agent for remediation of a tetrachloroethene–contaminated aquifer. Environ Sci Technol 37: 5829–5834.

Tofighy M A, Mohammadi T (2011) Adsorption of divalent heavy metal ions from water using carbon nanotube sheets. J Hazard Mate 185:140-147.

Top A, Ülkü S (2004) Silver, zinc and copper exchange in a Na–clinoptilolite and resulting effect on antibacterial activity. Appl Clay Sci 27: 13–19.

Tully DC, Frechet JMJ (2001) Dendrimers at surfaces and interfaces: Chemistry and applications. J Chem Commun 14: 1229–1239.

Tuutijärvi T, Lu J, Sillanpää M, Chen G (2009) As(V) adsorption on maghemite nanoparticles. J Hazard Mater 66: 1415-1420.

Ullah R, Dutta J (2008) Photocatalytic degradation of organic dyes with manganese-doped ZnO nanoparticles. J Hazard Mater. 156:194–200.

Upadhyayula KKV, Deng S, Mitchell M C, Smith G B (2009) Application of carbon nanotube technology for removal of contaminants in drinking water: A review. Sci Total Environ 408: 1–13.

Urbansky ET, Schock MR (1999) Issues in managing the risks associated with perchlorate in drinking water. J Environ Manage 56: 79–95.

US Environmental Protection Agency. 1998. Microbial and disinfection by-product rules. Federal Register 63: 69389–69476.

US Environmental Protection Agency, 1999. Alternative disinfectants and oxidants guidance manual. EPA Office of Water Report 815-R-99-014.

Uzum C, Shahwan T, Eroglu AE, Hallam KR, Scott TB, Lieberwirth I (2009) Synthesis and characterization of kaolinite-supported zero-valent iron nanoparticles and their application for the removal of aqueous Cu^{2+} and Co^{2+} ions. Appl Clay Sci 43: 172–181.

Van der Bruggen B, Vandecasteele C (2003) Removal of pollutants from surface water and groundwater by nanofiltration: Overview of possible applications in the drinking water industry. Environ Pollut 122: 435–445.

Vaseashta A, Vaclavikova M, Vaseashta S, Gallios G, Roy P, Pummakarnchana O (2007) Nanostructures in environmental pollution detection, monitoring, and remediation. STAM 8: 47–59.

Viessman W, Hammer MJ, Perez E M, Chadik P A (2008) Water Supply and Pollution Control. Menlo Park: Addison-Wesley Longman Publishers. 8th edition.

Vörösmarty CJ, Green P, Salisbury J, Lammers RB (2000) Globalwater resources: Vulnerability from climate change and population growth. Science 289: 284–288.

Vuković GD, Marinković AD, Čolić M, Ristić DM, RadoslavA, Aleksandra A P-G, Uskoković, PS (2010) Removal of cadmium from aqueous solutions by oxidized and ethylenediamine-functionalized multi-walled carbon nanotubes. Chemical Eng J 157: 238–248.

Walha K, Amar BR, Firdaous L, Quéméneur F, Jaouen P (2007) Brackish groundwater treatment by nanofiltration, reverse osmosis and electrodialysis in Tunisia: Performance and cost comparison. Desalination 207: 95–106.

Wang B, Feng WY, Wang TC, Jia G, Wang M, Shi JW, Zhang F, Zhao YL, Chai ZF (2006) Acute toxicity of nano- and microscale zinc powder in healthy adult mice. Toxicol Lett 161: 115–123.

Wang H, Yang L, Yu H, Peng F (2011) A highly efficient and stable visible-light plasmonic photocatalyst Ag-AgCl/CeO_2. WJNSE 1: 129-136.

Warner C L, Addleman R S, Cinson A D, Droubay T C, Engelhard M H, Nash M A, Yantasee W, Warner M G (2010) High-Performance, Superparamagnetic, Nanoparticle- Based Heavy Metal Sorbents for Removal of Contaminants from Natural Waters. ChemSusChem 3: 749-757.

Wegmann M, Michen B, Graule T (2008) Nanostructured surface modification of microporous ceramics for efficient virus filtration. J. European Ceramic Society 28: 1603-1612.

Wiesner MR, Lowry GV, Alvarez P, Dionysiou D, Biswas P (2006) Assessing the risks of manufactured nanomaterials. Environ Sci Technol 40: 4336–4345.

Xu J, Dozier A, Bhattacharyya D (2005a) Synthesis of nanoscale bimetallic particles in polyelectrolyte membrane matrix for reductive transformation of halogenated organic compounds. J Nanopart Res 7: 449–461.

Xu X, Zhou M, He P, Hao Z (2005b) Catalytic reduction of chlorinated and recalcitrant compounds in contaminated water. J Hazard Mater 123: 89–93.

Xu Y, Zhao D (2007) Reductive immobilization of chromate in water and soil using stabilized iron nanoparticles. Water Res 41: 2101–2108.

Yan XM, Shi BY, Lu JJ, Feng CH, Wang DS, Tang HX (2008) Adsorption and desorption of atrazine on carbon nanotubes. J Colloid Interface Sci 321: 30–38.

Yan H, Gong A, He H, Zhou J, Wei Y, Lv L (2006) Adsorption of microcystins by carbon nanotubes. Chemosphere 62: 142–8.

Yang MC, Yang TS, Wong MS (2004) Nitrogen–doped titanium oxide films as visible light photocatalyst by vapor deposition. Thin Solid Films 469: 1–5.

Yang J, Zhang J, Zhu L, Chen S, Zhang Y, Tang Y, Zhua Y, Li Y (2006) Synthesis of nano–titania particles embedded in mesoporous SBA–15: Characterization and photocatalytic activity. J Hazard Mater 137: 952–958.

Yang GCC, Lee H–L (2005) Chemical reduction of nitrate by nano–sized iron, Kinetics and pathways. Water Res 39: 884–894.

Yang GCC, Li CJ (2008) Tubular TiO_2/Al_2O_3 composite membranespreparation, characterization and performance in electrofiltration of oxide-CMP wastewater. Desalination 234: 354-361.

Yang Y, Ren N, Zhang Y, Tang Y (2009) Nanosized cadmium sulfide in polyelectrolyte protected mesoporous sphere: a stable and regeneratable photocatalyst for visible-light-induced removal of organic pollutants, J Photochem Photobiol A: Chem. 201: 111–120.

Yates CR, Hayes W (2004) Synthesis and applications of hyperbranched polymers. Eur. Polym. J. 40: 1257–1281.

Yu JC, Ho W, Yu J, Yip H, Wong PK, Zhao J (2005) Efficient visible light–induced photocatalytic disinfection on sulfur-doped nanocrystalline titania. Environ. Sci. Technol. 39: 1175–1179.

Yu JC, Wu L, Lin J, Li P, Li Q (2003) Microemulsion–mediated solvo–thermal synthesis of nanosized CdS–sensitized TiO_2 crystalline photocatalyst. Chem. Commun. 8: 1552–1553.

Zeman LJ, Zydney AL (1996) Microfiltration and Ultrafiltration. New York: Marcel Dekker principles and applications.

Zhai R, Wan Y, Liu L, Zhang X, Wang W, Liu J, Zhang B (2012) Hierarchical MnO_2 nanostructures: synthesis and their application in water treatment. Water Sci Technol 65: 1054-1059

Zhang LD, Fang M (2010) Nanomaterials in pollution trace detection and environmental improvement. Nano Today 5: 128–142.

Zhang H, Quan X, Chen S, Zhao H, Zhao Y (2006) Fabrication of photocatalyticmembrane and evaluation its efficiency in removal of organic pollutants from water. Separation and Purification Tech. 50: 147-155.

Zhang W-X (2003) Nanoscale iron particles for environmental remediation: An overview. J. Nanopart Res 5: 323–332.

Zhang W-X, Wang CB, Lien HL (1998a) Treatment of chlorinated organic contaminants with nanoscale bimetallic particles. Catal Today 40: 387–395.

Zhang Z, Wang C-C, Zakaria R, Ying JY (1998b) Role of particle size in nanocrystalline TiO_2–based photocatalysts. J Phys Chem B 102: 10871–10878.

Zhang X, Zhang F, Chan KY (2005) Synthesis of titania–silica mixed oxide mesoporous materials, characterization and photocatalytic properties. Appl Catal A 284: 193–198.

Zhan W-X, Elliott DW (2006) Applications of iron nanoparticles for groundwater remediation. Remediation 16: 7–21

Zhao GJ, Stevens SE (1998) Multiple parameters for the comprehensive evaluation of the susceptibility of Escherichia coli to the silver ion. Biometals 11: 27–32.

Zhao X, Wang J, Wu F, Wang T, Cai Y, Shi Y, Jiang G (2010) Removal of fluoride from aqueous media by Fe_3O_4@$Al(OH)_3$ magnetic nanoparticles. J Hazard Matter 173: 102 109.

Zhou Q, Xiao J, Wang W (2006a) Using multi-walled carbon nanotubes as solid phase extraction adsorbents to determine dichlorodiphenyltrichloroethane and its metabolites at trace level in water samples by high performance liquid chromatography with UV detection. J Chromatogr A 1125: 152–158.

Zhou Q, Xiao J, Wang W, Li G, Shi Q, Wang J (2006b) Determination of atrazine and simazine in environmental water samples using multi–walled carbon nanotubes as the adsorbents for preconcentration prior to high performance liquid chromatography with diode array detector. Talanta 68: 1309–1315.

Zhou Q, Xiao J, Wang W (2007) Comparison of multi–walled carbon nanotubes and a conventional absorbent on the enrichment of sulfonylurea herbicides in water samples. Anal Sci 23: 189–192.

Zhu S, Oberdörster E, Haasch ML (2006) Toxicity of an engineered nanoparticle (fullerene, C(60)) in two aquatic species, Daphnia and fathead minnow. Mar Environ Res 62: S5–S9.

Zodrow K, Brunet L, Mahendra S, Li D, Zhang A, Li Q, Alvarez PJ (2009) Polysulfone ultrafiltration membranes impregnated with silver nanoparticles show improved biofouling resistance and virus removal. Water Res 43:715-723.

CHAPTER 3

Remediation of mercury contaminated saltwater with functionalized silica coated magnetite nanoparticles

Abstract

The study aimed to evaluate the efficiency of dithiocarbamate functionalized silica coated magnetite nanoparticles (NPs) for Hg decontamination of saltwater either contaminated with Hg alone or with As and Cd. For this, the residual levels of Hg in seawater were assessed and Hg-contaminated or Hg+As+Cd-contaminated seawater toxicity to aquatic biota, before and after the sorption process, was compared. The results showed that under highly competitive conditions (water salts, Cd and As), the removal of Hg from seawater, by using these magnetic NPs, for the lowest concentration (50 µg/L) was superior to 98% and for the highest concentration (500 µg/L) ranged between 61% to 67%. Despite the great affinity of the magnetic NPs for Hg, they were not effective at removing As and Cd from seawater. In relation to the ecotoxicity endpoints after remediation, the mixture with lower Hg concentration exhibited no toxicity to rotifer *Brachionus plicatilis* and bacteria *Vibrio fischeri;* however, the mixture with higher concentration revealed toxicity. In addition, the toxicity of bacteria *V. fischeri*, rotifer *B. plicatilis* and algae *Phaeodactylum tricornutum*, whose responses where inhibited during its exposure to the non-remediate sample was considerably reduced after treatment with NPs. Furthermore, microalgae *P. tricornutum* appears to be most sensitive species while *Artemia franciscana* showed no toxic effects to the tested solutions. Both chemical and ecotoxicological approaches revealed a high efficiency for the remediation of Hg-contaminated saltwater.

Keywords: *Mercury, Remediation, Ecotoxicological effects, Seawater, Nanoparticles*.

Science of the Total Environment

(2016) 557(558):712-721

3.1. INTRODUCTION

Mercury (Hg) is one of the most hazardous contaminants reported in aquatic environments (Chételat et al., 2015; Lillebø et al., 2011; Pereira et al., 2009), being among the highest priority environmental pollutants in the scope of the European Water Framework Directive (WFD) and on a global scale (Pereira et al., 2009). Most Hg enters aquatic systems in its inorganic form via anthropogenic point discharges, mostly related to chlor-alkali plants, mining activities or through diffuse sources (Lillebø et al., 2011). Despite the existing restrictions on anthropogenic sources of Hg, historically contaminated sediments may still constitute a source of Hg to the aquatic environment and consequently to the biota (Taylor et al., 2012; Covelli et al., 2012; Ma et al., 2013).

Once in the biota, several processes may occur, namely the increase of Hg concentrations through the trophic web (biomagnification), which makes predators and consumers particularly susceptible (Coelho et al., 2008; Pereira et al., 2009; Lillebø et al., 2011; Sandheinrich and Weiner 2011). Mercury toxicity causes behavioral, reproductive, and genotoxic effects in aquatic fauna. Specific symptoms include decreased feeding behavior (Berntssen et al., 2003), decreased feeding efficiency (Fjeld et al., 1998), decreased shoaling behavior (Webber and Haines, 2003), and impaired immune and reproductive system function (Hammerschmidt et al., 2002; Sandheinrich and Miller 2006; Drevnick and Sandheinrich 2003; Drevnick et al., 2006) in aquatic organisms (Sandheinrich and Weiner 2011). A study evaluating the risk posed by trace metals on the culture of seawater bivalves reflected that the Hg is the most toxic among others trace metals for bivalve embryogenesis (Beiras and Albentos, 2004). The high toxicity of Hg, mainly in organic forms, is related to its high affinity to sulphide groups (Guzzi and La Porta, 2008), binding readily to proteins and disturbing the functions where they are involved. Furthermore, its lipophilicity allows it to pass through lipid membranes of cells and facilitates its distribution to all tissues (EPA, 2001).

Keeping in view the previous toxicity aspect, it is equally important to study the complex phenomena controlling the transference of Hg to seawater organisms and develop new techniques for its removal from waters. Various technologies such as ion exchange, reverse osmosis, adsorption, precipitation, membrane filtration and flocculation have been reported for the removal of Hg from water (Lopes et al., 2014a; Lopes et al., 2014b; Zhou

et al., 2013; Urgun et al., 2012; Lopes et al., 2009). Each of these processes present advantages and disadvantages. Although some of these technologies are simple, rapid, quantitative and selective under proper conditions, some require high-energy or large quantities of chemicals that involves high operating and maintenance costs and expensive equipment. Others produce large volumes of solid wastes (*e.g.* precipitation) generating toxic residual sludge, which give rise to another major problem that is the disposal of toxic sludge (Monteagudo et al., 2000; Pacheco et al., 2006), and, finally, others do not achieve the target concentrations after treatment since the Hg removal is incomplete. Chemical precipitation, ion-exchange and adsorption are probably the three processes most used for the removal of Hg from contaminated water (Fu and Wang, 2011).

Recently, nanoparticles (NPs) have emerged as new class of sorbents for recovery, separation and/or pre-concentration of metals. Ngomsik et al., (2005) wrote a mini review on the application of magnetic nano and microparticles in the removal of metals in wastewaters. In particular, magnetic iron oxides such as magnetite (Fe_3O_4) and maghemite (Υ- Fe_3O_4) have been investigated intensively for Hg removal from water (Girginova et al., 2010; Li et al., 2011; Hakami et al., 2012; Figueira et al., 2011; Tavares et al., 2013; Zhang et al., 2013; Rahbar et al., 2014; Shan et al., 2015; Zhang et al 2015; Mehdinia et al., 2015). Recently, Shan et al., (2015) reported the synthesis of Fe_3O_4@SiO_2 magnetic nanoparticles modified by grafting poly(1-vinylimidazole) oligomer as a novel adsorbent to remove Hg(II) from water. This material showed a high adsorption capacity toward the metal that was not inhibited with the increase of ionic strength. Tavares et al., (2013) explored the sorption efficiency of the synthesized magnetite particles coated with siliceous shells and with different degree of dithiocarbamate functionalization in the removal of Hg ions from aqueous solutions by magnetic separation, while Figueira et al., (2011) also took advantage of the high affinity between Hg and sulphur, and used magnetite (Fe_3O_4) NPs functionalized with dithiocarbamate groups as a new type of sorbent to remove Hg(II) from synthetic and natural spiked waters. These studies, like most of the approaches driven in the field of water treatment, aim only the quantification of the residual levels of metals and the amount of the metal effectively sorbed by the material applied (Lopes et al., 2009; Lopes et al., 2011; Girginova et al., 2010; Figueira et al., 2011; Tavares et al., 2013). However, chemical analysis alone is not suitable to test for water good quality status, therefore, it is important to establish a cause-effect relationship

between the concentration of chemicals and consequent environmental damage. Thus, for a proper evaluation of the feasibility of a water treatment, an approach combining both chemical and ecotoxicological assays should be designed, and to the best of our knowledge, the studies following this approach on the subject of reducing or eliminating the toxicity of waters contaminated with metals are scarce (Mishra and Tripathi 2008; Lopes et al., 2014a; Rocha et al., 2014) or inexistent for salt waters.

Moreover, particular attention is also required to understand the efficiency of removal technologies under more realistic conditions for example in the presence of other contaminants like arsenic (As) and cadmium (Cd) since they are non-essential elements and due to their persistent nature and tendency toward bioaccumulation are rated among the most hazardous potentially toxic elements. Cadmium is classified as "priority hazardous substance" by the European Union water framework directive (http://ec.europa.eu/environment/water/water-framework/index_en.html) and As occupies the first position in the Agency for Toxic Substances and Disease Registry (ATSDR), 2011 Substance Priority List (http://www.atsdr.cdc.gov/spl/index.html).

Thus, the main question of this study was to known the real efficiency of dithiocarbamate functionalized silica coated magnetite NPs as a saltwater decontamination material toward Hg, in absence and presence of other hazardous contaminants (As and Cd).

In order to answer to this question, a combined chemical and ecotoxicological approach was designed. This approach included the assessment of the residual levels of Hg in seawater, the modelling of the sorption process, and the evaluation of the seawater toxicity to biota before and after the proposed treatment. The toxicity measurement was carried out through a battery of bioassays, with organisms from different taxonomic groups and exhibiting different key functions at the ecosystem levels, namely the bacterium *Vibrio fisheri* (decomposer), the green algae *Phaeodactylum tricornutum* (producer), the rotifer *Brachionus plicatilis* (primary consumer) and the *Artemia franciscana* (primary consumer). The selection of these species was based on the fact that they are available at low cost, easy to maintain in the laboratory, have been widely used in other ecotoxicological studies as model species, and (ideally) have commercial or ecological importance (Widdows 1993). Additionally, the possible toxic effects caused by the NPs

applied in the decontamination process will also be contemplated. Moreover, the use of a natural seawater instead of a synthetic one allowed us to achieve conditions close to the ones found in aquatic systems and to evaluate the influence posed by this natural matrix (chemically very complex) on the speciation and dynamics of Hg, that can eventually hinder or enhance the sorption process and as well the toxicity to biota.

3.2. MATERIALS AND METHODS

3.2.1. Experimental design

The efficiency of dithiocarbamate functionalized silica coated magnetite NPs (Fe_3O_4@SiO_2/SiDTC) in the remediation of spiked seawater was evaluated in four different scenarios, according with the details in Table 3.1.

Table 3.1 – Information regarding the scenarios of contamination used to test the remediation efficiency of Fe_3O_4@SiO_2/SiDTC nanoparticles.

Solution	Tested concentrations	Remark
I	50 µg/L	Value corresponding to the legal limit for Hg discharge in the environment established in the Directive 84/156/EEC
II	500 µg/L	Value ten times higher than the legal limit for Hg discharge in the environment established in the Directive 84/156/EEC
III	Hg (50µg/L) + As (1000 µg/L) + Cd (200 µg/L)	Mixture where the concentration of all elements corresponds to the legal limits established in the Directives 84/156/EEC and Decreto-Lei nº 236/98, simulating a situation of effluent discharge
IV	Hg (500µg/L) + As (1000 µg/L) + Cd (200µg/L)	Mixture where the concentration of As and Cd corresponds to the legal limits established in the Decreto-Lei nº 236/98, and the concentration of Hg is ten times higher than the legal limit for Hg discharge in the environment established in the Directive 84/156/EEC.

The above mentioned non-remediated solutions (I, II, III and IV) were treated with Fe_3O_4@SiO_2/SiDTC NPs, and the ecotoxicity of the non- and remediated solutions was monitored with and without NPs. In addition, the toxicity of the magnetic NPs alone was also investigated.

3.2.2. Water metals removal studies

3.2.2.1 Chemicals

All chemicals used in this work were of analytical reagent grade and the contaminated solutions were prepared in natural seawater. Arsenic(III) chloride (1000±2

mg/L) and mercury(II) nitrate standard solution (1000±2 mg/L) were purchased from BDH Chemicals Ltd, while the certified standard solution of cadmium(II) nitrate (1001±2 mg/L) was purchased from Merck.

The dithiocarbamate (DTC) functionalized silica coated magnetite nanoparticles (Fe_3O_4@SiO_2/SiDTC NPs) were investigated for metals removal from seawater spiked with single (Hg) or a mixture of (Hg, As and Cd) contaminants. The magnetic NPs were kindly provided by the Associated Laboratory CICECO, University of Aveiro, Portugal, and the details pertaining to their synthesis and characterization can be obtained in Tavares et al., (2013).

Seawater needed for the experiments was collected at Portuguese coast (40.330 N, 8460 W), filtered through 0.45 µm pore size filters and stored in the dark at 4 ºC until further use. A brief characterization of seawater, including pH, salinity, conductivity and multi-elemental analysis was carried out. The pH (8.0), salinity (35) and conductivity (55 mS/cm) were recorded on a WTW meter. Concentrations of major (Ca, K, Mg, Na and Si) and minor elements (Al, As, B, Ba, Be, Cd, Co, Cr, Cu, Fe, Li, Mn, Ni, P, Pb, Sr, V and Zn), obtained by inductively coupled plasma spectroscopy, using a Jobin – Yvon JY70 Plus Spectrometer (data not show), were in line with those reported by Lopes et al., (2014b), which correspond to the natural levels in seawater at Portuguese coast.

3.2.2.2 Batch sorption experiments

The ability of magnetic NPs to decrease the contamination level in seawater samples was evaluated, by carrying out sorption experiments in 1 L batch reactors at room temperature (21±1°C) and under mechanical stirring. Solutions (single or mixtures) were prepared by diluting the corresponding standard solution in seawater to the desired initial concentration. All glassware used in these experiments was acid-washed prior to use with HNO_3 25%, 12 hours, and rinsed with ultra-pure water. Experiments were performed to evaluate the time profile and the effect of the level of contamination on the sorption of Hg, As and Cd onto the functionalized magnetic NPs. Accurately weighed amounts of magnetic NPs (10 mg) were added to the above mentioned solutions (I, II, III and IV), in glass batch reactors, which were immediately placed in an ultrasonic bath for *ca*. 10

seconds, for dispersing the magnetic particles. This time was considered the starting point for each experiment. For every experiment, solutions were continuously stirred, using a glass rod, and samples were withdrawn for analysis at several sampling times. Each sample from solution I and II was analyzed only for Hg quantification and the samples from solution III and IV were analyzed for Hg, As and Cd quantification, after magnetic separation of the NPs from solution using an NdFeB magnet.

Hg analyses were performed by cold vapour atomic fluorescence spectroscopy (CV-AFS), on a flow-injection spectrometer (Hydride/vapour generator PS Analytical Model 10.003, coupled to a PS Analytical Model 10.023 Merlin atomic fluorescence spectrometer; PS Analytical, Orpington, Kent, England) and using $SnCl_2$ as reducing agent. Arsenic and Cd analyses were quantified by Inductively Coupled Plasma Mass Spectrometry (ICP-MS), on a Thermo ICP-MS X Series equipped with a Burgener nebuliser, in the central laboratory of analysis (Laboratório Central de Análises - LCA), University of Aveiro. Control trials were performed in the absence of magnetic NPs with each experiment and under the same experimental conditions.

The amount of contaminant sorbed per unit of NPs, at time t, q_A (mg/g) was estimated from the mass balance between its initial concentration $C_{A,0}$ (μg/L) and concentration at time t in solution C_A (μg/L),

$$q_A = (C_{A,0} - C_A) \times \frac{V}{M}$$

where, V is the volume of solution (L), M is the dry weight of magnetic particles (mg) and the subscript A denotes the contaminant. The results were also compared by removal percentage, which at equilibrium time is defined by:

$$\text{Removal \%} = [(C_{A,0} - C_{A,e})/ C_{A,0}] \times 100$$

where, $C_{A,e}$ (μg/L) is the equilibrium concentration of the contaminant in the solution.

The sorption kinetics of contaminants on NPs was studied using three kinetic models, namely the Lagergren pseudo-first-order model (PFO) (Lagergren 1898), Ho's pseudo-second-order model (PSO) (Ho and McKay 1999) and the Elovich model (Low 1960), expressed respectively by the following equations:

$$q_{A,t} = q_{A,e}(1 - e^{-k_1 t})$$

$$q_{A,t} = \frac{q_{A,e}^2 k_2\ t}{1 + k_2 q_{A,e} t}$$

$$q_{A,t} = \frac{1}{\beta} ln\,(1 + \alpha\beta t)$$

where $q_{A,t}$ and $q_{A,e}$ (both in mg/g) are the amount of contaminant sorbed per gram of NPs, respectively, at time t and at equilibrium; k_1 (h^{-1}) and k_2 (g/ mg h) are, respectively, the kinetic constants of pseudo-first- and pseudo-second-order as well as α (mg/g h) is the initial sorption rate and β (g/mg) is the desorption constant.

After reaching equilibrium the remediated solutions (I, II, III and IV) were divided in two parts. In half volume of the remediated solutions the magnetic NPs were kept in the liquid fraction and this part was marked as solutions containing NPs after remediation (I, II, III and IV), while, in the other half volume the NPs were removed by magnetic separation and this part was marked as remediated solutions (I, II, III and IV) without NPs. Both parts of the solutions were used for ecotoxicity evaluation.

3.2.3. Ecotoxicity assays

To further evaluate the efficiency of NPs in the remediation of Hg-contaminated seawater, the lethal and sublethal effect caused by the NPs and by the non-remediated and remediated (with and without the NPs) solutions was assessed. For this, four model species, belonging to different trophic levels and commonly recommended for use in ecotoxicity assessment, were selected: the bacterium *Vibrio fischeri*, representative of decomposers; the microalgae *Phaeodactylum tricornutum*, representative of producers; the crustacean *Artemia franciscana* and the rotifer *Brachionus plicatilis*, as consumers.

3.2.3.1 V. fisheri bioluminescence inhibition assay

The sublethal ecotoxicity of the above mentioned non-remediated and remediated solutions (with and without NPs) as well as of NPs alone were assessed for the marine bacterium *V. fischeri* through carrying out the bioluminescence inhibition assay, according with the protocol for the Basic Test provided by the supplier (Microtox® Basic Test; AZUR, 1998) and by using a Microtox toxicity analyzer model 500 (Azur Environmental, Carlsbad, CA, USA). The luminescence of the bacteria, exposed to a control and to nine dilutions of the above mentioned solutions (highest dilution 81.9%; a dilution factor of 2× was used) was measured after 5 and 15 minutes exposure periods.

3.2.3.2 72-h growth inhibition assay with P. tricornutum

The assessment of the sublethal toxicity of the NPs and all solutions to the algae *P. tricornutum* was conducted in accordance with OECD Guideline 201 (OECD, 2006; USEPA, 1994; EC, 1992). Individual cultures of this species were maintained in batch cultures, in 5 L flasks, with 4 L of sterilized Woods Hole nutritive culture medium (seawater; Stein, 1973), with continuous aeration and under controlled temperature (20±1ºC) and continuous light. All tests were run, using log phase algal cultures (4 days), at an initial cell concentration of 1×10^4 cells/mL at a final volume of 1 mL in cell culture 24-well plate. The test species was exposed for a 72 hours period to a range of dilutions of the tested solutions and NPs (40.3%, 48.2%, 57.9%, 69.4%, 83.3% and 100.0% for solution I, III and NPs; 8.8%, 13.2%, 19.7%, 29.6%, 44.4%, 66%, 100% for solution II and IV) using the synthetic culture medium of algae – seawater as dilution (Stein, 1973), at 23±1ºC and with a constant luminous intensity (60–120 µE/m^2/s). Three replicate were set up randomly for each treatment and a control (synthetic culture medium) per microplate. The peripheral wells were filled with 1 mL of distilled water, to minimize evaporation in the test wells. During the exposure period, each well was shaken manually twice per day. The cell density of each replicate was measured after 72 hours, under the microscope and using a Neubauer chamber. For each concentration, the average specific growth rate (μ) (for exponentially growing cultures) and the percentage reduction in average growth rate compared to the control value were calculated, after a period of 72 hours, using the following equations: $\mu = (lnC_{72h} - lnC_{0h})/T$ and reduction = $(\mu_{control} - \mu)\times100/\mu_{control}$, where T is the time of exposure expressed in days; C_{72h} and C_{0h} corresponds to the biomass concentration at 72 hours and 0 hours; $\mu_{control}$ is the mean value for μ in the control.

3.2.3.3 24-h mortality assay with B. plicatilis

Twenty-four hours marine rotifer (*Brachionus plicatilis*) mortality assay was conducted by exposing the rotifer to a range of dilutions of non-remediated and remediated solutions with and without NPs and as well to the NPs alone (40.3%, 48.2%, 57.9%, 69.4%, 83.3% and 100.0% for solution I, III and NPs; 8.8%, 13.2%, 19.7%, 29.6%, 44.4%, 66%, 100% for solution II and IV). The cysts were provided by MicroBioTests Inc (Belgium), and were incubated in artificial seawater medium 28-30 hours prior to the start

of the tests at 25°C with continuous illumination. After this period, most cysts were hatched. Approximately 50 larvae were transferred to rinsing well containing test solutions and control (artificial seawater medium). From each rinsing well, 5 larvae were transferred to the six test wells (replicates) containing 1 mL concentration/dilution of the same solution of the rinsing well. The well plate was incubated at 25°C in the dark. After 24 hours alive and dead larvae in the test wells were counted. An organism was considered death when it remained immobile for 15 seconds after gentle prodding.

3.2.3.4 24-h mortality assay with A. fransciscana

Tests were performed according to the MicroBioTest Standard Procedure (MicroBioTests Inc, Belgium). Newly hatched organisms from cysts were exposed for a 24 hour period to a range of dilutions 48.2%, 57.9%, 69.4%, 83.3% and 100.0% of all the non-remediated and remediated solutions (with and without NPs) as well as to NPs alone to evaluate their toxicity plus to a control (artificial seawater medium). *Artemia franciscana* cysts hatching, in petri dish at 25^{o}C, started 30 hours before the beginning of the assay in a standard media. After 30 hours most of the larvae moulted into the instar II-III stage. The bioassay was conducted in a 24-well plate. Each sample and control was tested in 3 replicates of 10 animals with the test solution and media volume of 1 mL per well, respectively. After 24 hours the number of dead and alive organisms was recorded. An organism was considered death when it remained immobile for 15 seconds after gentle prodding.

3.2.4. Data analysis

The MicrotoxOmni software was used to collect the data for the Microtox® toxicity test and it was also used to calculate the EC_{20} and $_{50}$ (concentration provoking 20 and 50% of effect after 5 and 15 minutes of exposure). The Probit Program version 1.63, a parametric statistical method, for the analysis of mortality data (Finney, 1971), was used to calculate the EC_{20} and EC_{50} for *B. plicatilis*, *A. franciscana* and *P. tricornutum*, with the respective 95% confidence limit. One-way analysis of variance (ANOVA) followed by the multi comparison Dunnett test was used to test for statistical differences in the growth of algae exposed to the different dilutions of solutions and the respective control (SigmaPlot

12.0). Assumptions of ANOVA were tested by using the Kolmogorov-Smirnov (for normality) and Bartlett's (homoscedasticity of variance) tests.

The parameters of the kinetic models were obtained by nonlinear regression analysis using GraphPad Prism 6 program (trial version), which uses the least-squares as fitting method and the method of Marquardt and Levenberg for adjusting the variables. The goodness of the fittings to the experimental data was confirmed by the sum of squares (*SS*) and the *R* square (R^2).

3.3. RESULTS

The physicochemical properties of non-remediated and remediated solutions (with and without NPs) showed no clear differences in conductivity, pH and dissolved oxygen values. Whereas, the salinity values were similar among the treatment groups ranging from 32.9 to 34.9 excepting the rotifers media that exhibited 15.1 salinity, as required by the used protocol for their cyst hatching (Table 3.2).

Table 3.2 General physico-chemical characteristics of the tested solutions and the media used as control for the ecotoxicity assays for different species.

Solutions	Salinity (PPT)	Conductivity (mS/cm)	pH	Dissolved oxygen (mg/L)
Algae media	34.9	47.7	7.94	7.2
Rotier media	15.1	24.9	7.99	7.0
Artemia media	33.3	47.6	7.58	7.7
NPs	32.9	48.6	7.77	7.3
Non-remediated sol. I	34.6	49.6	7.98	7.9
Non-remediated sol. II	34.0	48.8	7.88	7.8
Non-remediated sol. III	33.1	47.8	6.95	8.0
Non-remediated sol. IV	34.5	48.6	6.84	7.9
Remediated sol. I with NPs	34,1	48.1	7.36	7.8
Remediated sol. II with NPs	34.4	48.2	7.42	7.1
Remediated sol. III with NPs	33.7	47.0	7.05	7.7
Remediated sol. IV with NPs	33,9	47.2	7.11	7.5
Remediated sol. I without NPs	33,3	47.6	7.34	7.4
Remediated sol. II without NPs	33.4	47.5	7.22	7.0
Remediated sol. III without NPs	33.0	46.9	7.00	7.1
Remediated sol. IV without NPs	33,7	47.1	7.02	7.3

3.3.1. Water metals removal experiments

Figure 3.1 represents the time evolution of the contaminants concentration in the liquid fraction for the different scenarios studied, while Figure 3.3 displays the Hg concentration in the magnetic NPs along with contact time. For all scenarios, the concentration of Hg in solutions decreased over time in the presence of NPs, independently of the presence or absence of other contaminants. The kinetic profiles obtained are characterized by an abrupt decrease on Hg levels in the first hours, representing a rapid uptake of this metal by the functionalized magnetic NPs. When the initial Hg concentration is 50 µg/L (solution I and III) the equilibrium was reached after 48 hours (Figure 3.1A and 3.1C) at $C_{Hg,e}$ values below 1 µg/L (corresponding to more than 98% of Hg removal). Concomitantly, the concentration of Hg in the NPs increased over time reaching a concentration of nearly 5 mg/g (Figure 3.2A). For an initial Hg concentration of 500 µg/L (solutions II and IV), the equilibrium was reached later than the one for the previous initial concentration (ca. 72 hours, Figure 1B and 1D) and the residual Hg concentration in solutions II and IV was, respectively, 192 µg/L (corresponding to 61% of Hg removal) and 164 µg/L (correspond to 67% of Hg removal). In parallel, the concentration of Hg in the NPs increased over time reaching a concentration of nearly 34 mg/g (Figure 3.2B).

Concerning As and Cd concentrations in the liquid fraction no relevant differences were observed between the initial concentration and the concentrations recorded for the increasing contact times (Figure 3.1C and 3.1D).

The sorption kinetic data obtained for the Hg–NPs system were fitted to the non-linear forms of three reaction-based models: pseudo-first order (PFO), pseudo-second order (PSO) reaction and Elovich model. The Elovich model provides the best fit for the sorption kinetics of Hg for all solutions I, II, III and IV (Figure 2), while the fitting obtained with the pseudo-first-order was the least satisfactory of all, for all scenarios. The accuracy of the model is confirmed by the high values of the determination coefficient (R^2) and a low value of sum squares (*SS*) (Table 3.3). The good agreement observed between the kinetic data and the Elovich model, was not dependent on the initial concentration of Hg(II), neither on the presence of other contaminants as can be seen by the R square (R^2)

and the sum squares (*SS*) values. Moreover, for all scenarios, the PFO and PSO models underestimate the experimental q_e values, with relative errors that range from 5.2 to 24.7% for the PFO and from 1.3 to 19.7% for the PSO.

Table 3.3 PFO, PSO and Elovich sorption kinetic constants for the sorption of Hg by magnetic NPs in solutions I, II, III and IV.

				PFO						PSO						Elovich				
Experimental conditions				Best-fit values			Goodness of fit			Best-fit values			Best-fit values			Best-fit values		Best-fit values		
	M	C_0	$q_{A,e}$	k_1	$q_{A,e1}$	E_r	R^2	SS	$S_{x/y}$	K_2	$q_{A,e2}$	E_r	R^2	SS	$S_{x/y}$	α	β	R^2	SS	$S_{x/y}$
	mg/L	μg/L	mg/g	1/h	mg/g	%				g/mg h	mg/g	%				mg/g h	g/mg			
I	10.9	50	4.6	1,51	3.89	14.9	0.82	3,33	0.58	0.46	4.16	9.2	0.92	1.47	0.38	227.8	2.37	0.99	0.12	0.11
II	10.1	500	34.7	0.12	31.97	7.5	0.81	357	5.24	0.001	34.21	6.4	0.87	253	4,42	38.34	0.21	0.95	102.6	2.809
III	10.1	50	4.9	5.90	3.74	24.7	0.67	6.08	0.78	1.71	4.00	19.7	0.80	3.99	0.63	743.6	2.52	0.98	0.344	0.19
IV	10.8	500	33.6	0.09	31.76	5.23	0.91	193.3	3.86	0.004	34.44	1.3	0.94	133	3.20	15.62	0.18	0.96	84.38	2.55

For comparison, the experimental $q_{A,e}$ is shown together with that obtained from the fitting corresponding to first- and second-order kinetics, as well as the relative error (E_r) and the goodness of the fittings.

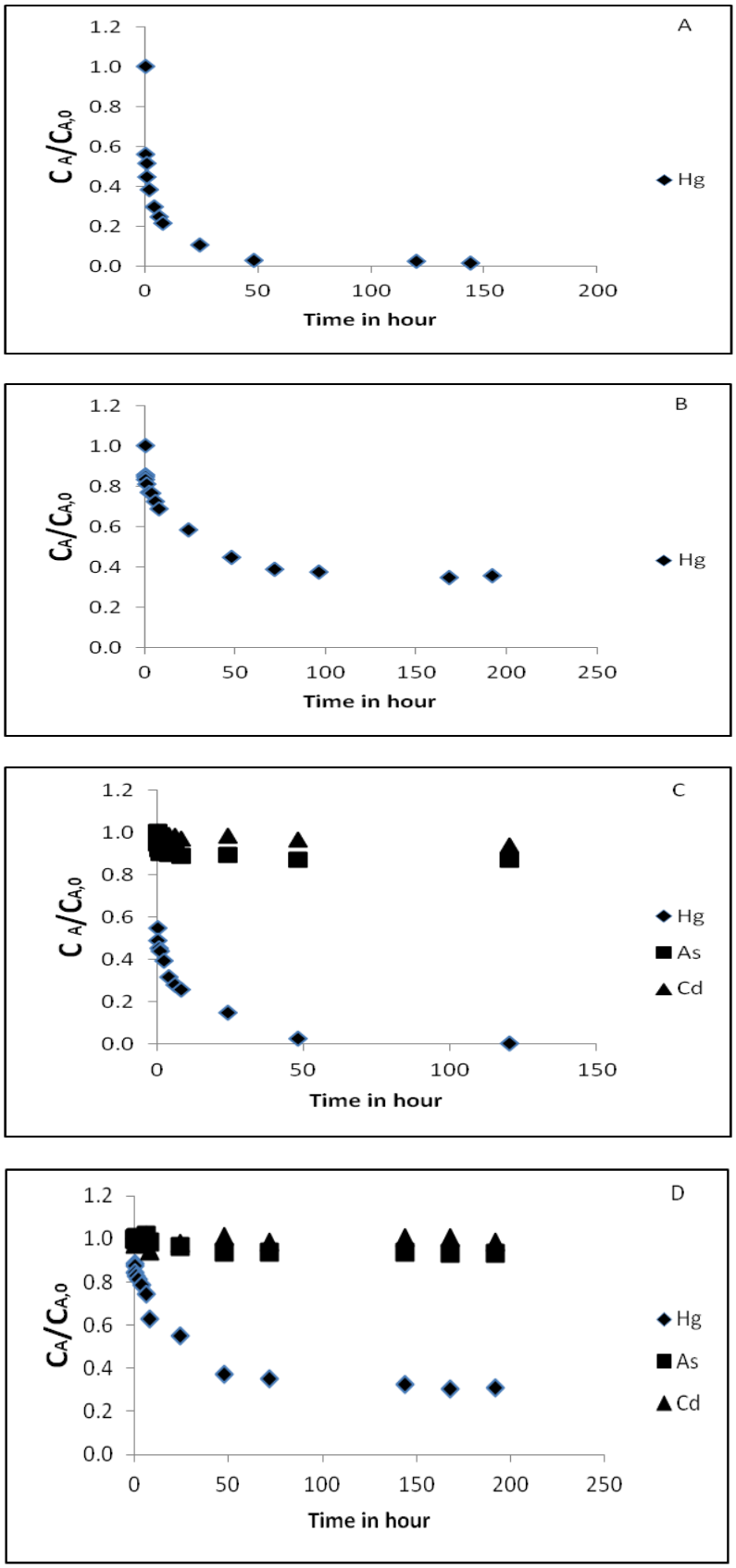

Figure 3.1 Normalized concentrations ($C_A/ C_{A,0}$) of contaminants with time. A – Solution I: Hg 50µg/L; B – Solution II: Hg 500µg/L; C – Solution III: Hg 50µg/L, As 1000µg/L, Cd 200µg/L and D – Solution IV: Hg 500µg/L, As 1000µg/L, Cd 200µg/L.

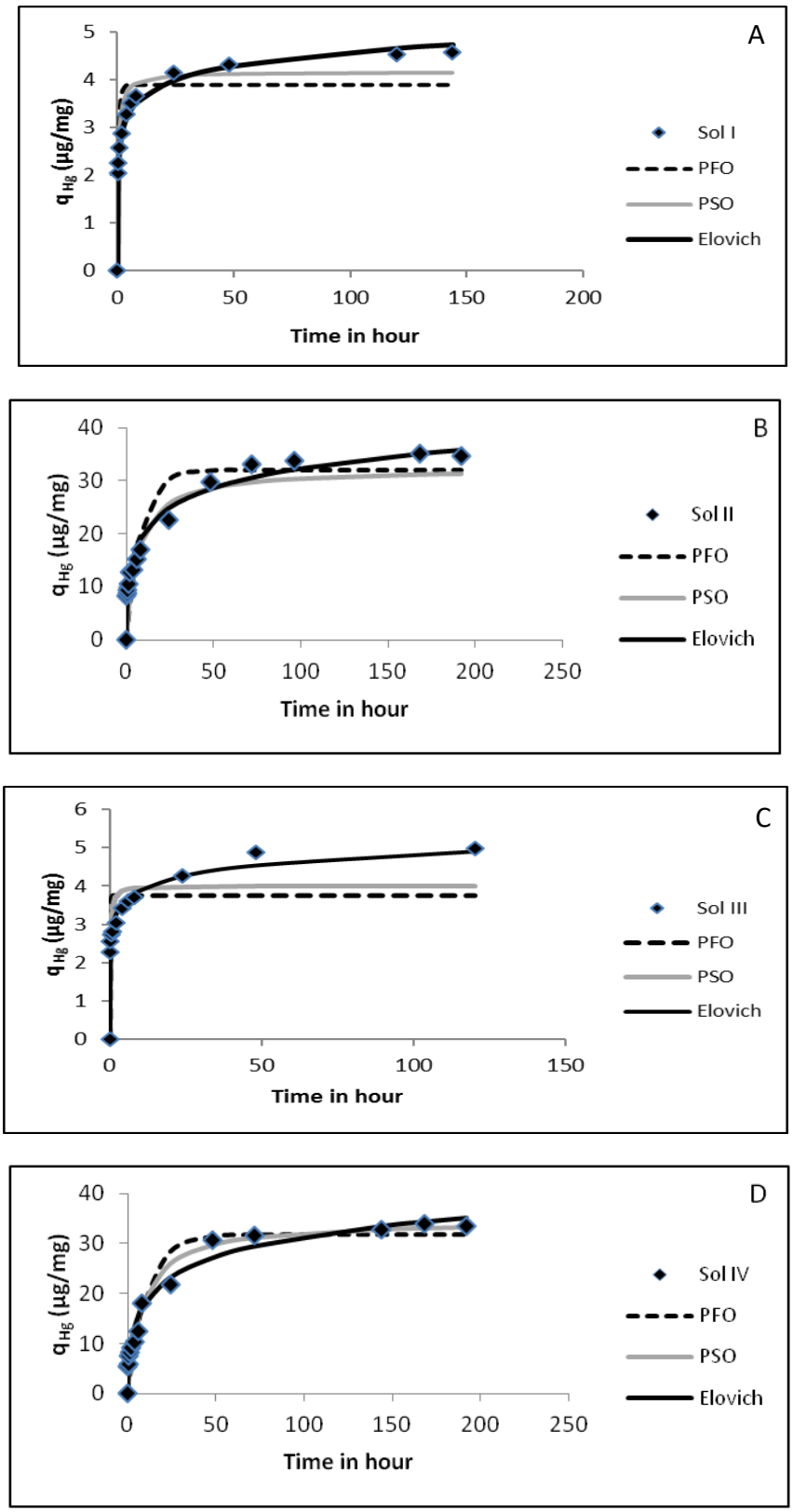

Figure 3.2 Kinetic modeling of the experimental data obtained from the sorption process of Hg onto magnetic NPs along with contact time for initial Hg concentrations of 50 µg/L (A and C) and 500 µg/L (B and D). The following reaction based models were used: pseudo-first order (PFO), pseudo-second order (PSO), and Elovich.

3.3.2. Ecotoxicity assays

The magnetic NPs used for the remediation experiment exhibited no toxicity to the different species, except for *P. tricornutum*, where some effects were observed in growth (EC_{50}=95.3%; Table 3.4). Non-remediated solutions I and III caused significant lethal effects to *B. plicatilis* (EC_{50} of solution I and III could not be computed, but, a highest mortality of 20% and 38.4% was registered at 100% of solution I and III, respectively) and *P. tricornutum* (solution I EC_{50}=37.4%; solution III EC_{50}=52.8%). Though, a decrease in lethal toxicity of solution I and III occurred when comparing toxicity of non-remediated and remediated solutions for *B. plicatilis*. The mortality decreased from 20.0% to 4.50% (with NP) and 0% (without NP) for solution I, and from 38.4% to 6.8% (with NP) and 3.8% (without NP) for solution III (Table 3). These two remediated solutions (I and III), both with and without NPs, caused significant effects in the growth of *P. tricornutum*, which occurred at a lower intensity than in the non-remediated solutions. The growth inhibition decreased from non-remediated to remediated: 95.0% to 47.0% (with NPs) and 50% (without NPs) for solution I and 95.0% to 37.0% (with NPs) and 47.0% (without NPs) for solution III (Table 3). Moreover, a significant ($p<0.05$) increase was observed in the average growth rate of *P. tricornutum* at different dilutions after 72 hours in remediated solution I and III (with and without NPs) when compared to non-remediated solutions (Figure 3.3).

The non-remediated solution II and IV caused significant adverse effects to all the tested species except to *A. franciscana* (Table 3.4). The EC_{50} for solution II (non-remediated) was similar among bacteria *V. fisheri* (EC_{50}=6.80% at 5minutes), *B. plicatilis* (EC_{50}=6.48%) and *P. tricornutum* (EC_{50}=6.50%). Additionally, the toxicity of the remediated solution II (with and without NPs after remediation) is much lower than the non-remediated to *V. fisheri*, *B. plicatilis* and *P. tricornutum* (Table 3.4). The non-remediated solution IV induced the highest toxic effects to *P. tricornutum* followed by *V. fisheri* and *B. plicatilis* (Table 3.4). Whereas, remediated solution IV (with and without NPs) caused lower toxic effects to *V. fisheri* and *P. tricornutum* in comparison to non-remediated solution IV (Table 3.4). A significant increase ($p<0.05$) was observed in algal growth at different dilutions of remediated solutions of II and IV (with and without NPs) when compared to non-remediated solutions (Figure3.3).

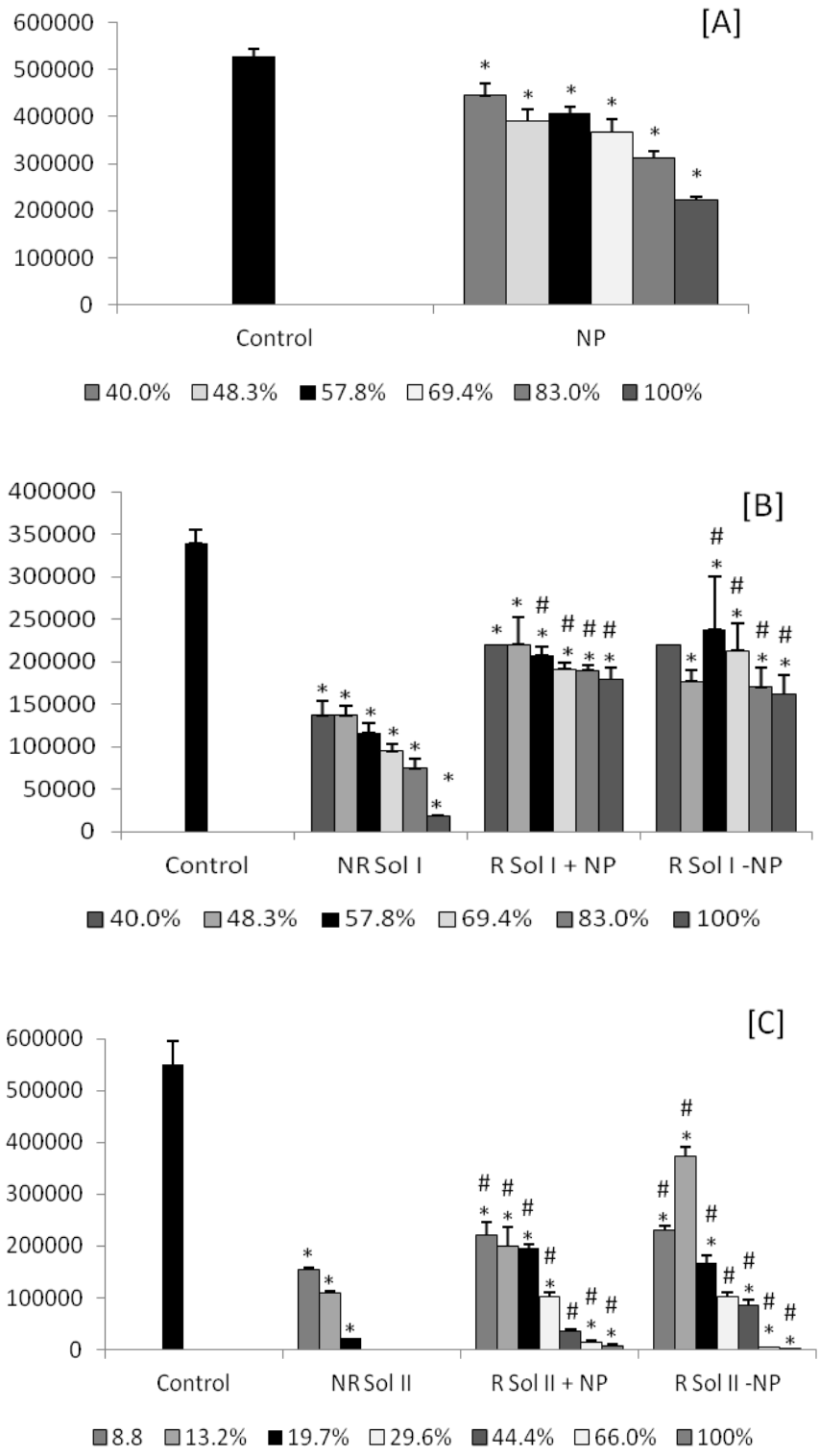

Figure 3.3 Average specific growth rate of *P. tricornutum* exposed [A] with NPs, [B] with solution I, [C] with solution II, [D] with solution III and [E] with solution IV, after 72 hours. The values are expressed as means + standard error. Statistically significant differences ($p < 0.05$) are marked by symbols: * (vs. control), # (vs. NR Sol to the same corresponding dilutions).

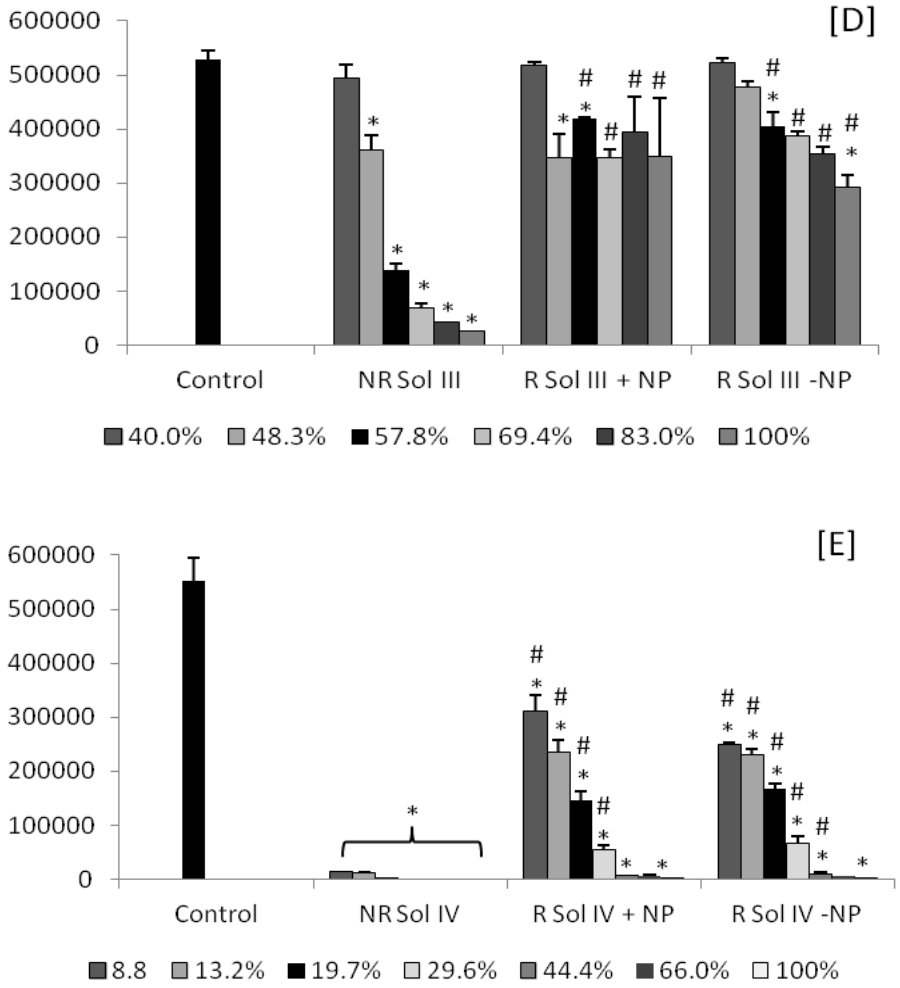

Figure 3.3. continued. Average specific growth rate of *P. tricornutum* exposed [A] with NPs, [B] with solution I, [C] with solution II, [D] with solution III and [E] with solution IV, after 72 hours. The values are expressed as means + standard error. Statistically significant differences ($p < 0.05$) are marked by symbols: * (vs. control), # (vs. NR Sol to the same corresponding dilutions).

Table 3.4 Percentage of dilutions of NP, non-remediated (NR) and remediated (R) solutions I, II, III and IV (with and without NPs) (95% confidence limits), provoking 20% or 50% (EC_{20} and EC_{50}, respectively) in the measured endpoints at the four tested aquatic species. For cases where ECx could not be computed, the highest percentage of effect (%) observed at the highest tested concentration is provided.

Tested solutions	Test	*Vibrio fischeri*		*Artemia franciscana*	*Brachionus plicatilis*	*Phaeodactylum tricornutum*
	Endpoint	Luminescence inhibition		Mortality	Mortality	Growth Inhibition
	Duration	5 min	15 min	24 h	24 h	72 h
NP	EC_{50} (%)	NT	NT	NT	NT	95.3 (84.7-115)
	EC_{20} (%)	NT	NT	NT	NT	47.0 (39.5 – 52.5)
	Effect (%)	10.7	10.7	6.40	4.00	58.0
NR sol. I	EC50 (%)	NT	NT	NT	NC	37.4 (29.4-43.1)
	EC20 (%)	NT	NT	NT	95.2 (0.08-97.0)	18.2 (10.5-24.5)
	Effect (%)	13.2	14.3	0	20.0	95.0
R sol. I with NPs	EC50 (%)	NT	NT	NT	NT	NC
	EC20 (%)	NT	NT	NT	NT	12.2 (1.80-27.0)
	Effect (%)	0	0	0	4.50	47.0
R sol. I without NPs	EC50 (%)	NT	NT	NT	NT	NC
	EC20 (%)	NT	NT	NT	NT	NC
	Effect (%)	0	0	0	0	50.0
NR sol. II	EC50 (%)	6.80 (0.70- 69.9)	4.30 (2.95- 6.20)	NT	6.48 (3.28-78.4)	6.5 (4.9-7.8)
	EC20 (%)	NC	3.40 (0.22-52.1)	NT	1.35 (0.13-98.5)	3.8 (2.3-5.1)
	Effect (%)	99.6	99.93	10.0	100	100
R sol. II with NPs	EC50 (%)	16.7 (2.3-19.4)	NC	NT	NC	8.3 (6.2-10.2)
	EC20 (%)	NC	NC	NT	48.3 (6.7-88.0)	2.90 (1.7-4.1)
	Effect (%)	71.5	47.6	3.10	28.0	99.0
R sol. II without NPs	EC50 (%)	30.3 (5.6-98.5)	30.7 (6.7-138.5)	NT	NC	11.6 (4.4-17.5)
	EC20 (%)	NC	NC	NT	77.9 (0.98-121)	4.7 (0.59-8.9)
	Effect (%)	50.9	58.8	3.20	21.7	99.0
NR sol. III	EC50 (%)	NT	NT	NT	NC	52.8 (46.2-58.7)
	EC20 (%)	NT	NT	NT	98.1 (0.32-120)	41.5 (32.1-47.3)
	Effect (%)	19.5	18.8	6.40	38.4	95.0
R sol. III with NPs	EC50 (%)	NT	NT	NT	NT	NT

	EC20 (%)	NT	NT	NT	NT	43.5 (55-134)
	Effect (%)	12.5	13.1	0	6.80	37.0
R sol. III without NPs	EC50 (%)	NT	NT	NT	NT	NT
	EC20 (%)	NT	NT	NT	NT	57.4 (51.7-62.2)
	Effect (%)	0	0	3.10	3.80	47.0
NR sol. IV	EC50 (%)	8.25 (2.10-31.8)	9.25 (1.8-69.3)	NT	10.6 (23-89.1)	1.23 (0.032-3.7)
	EC20 (%)	3.90 (1.10-57.7)	NC	NT	6.6 (12.6-97.0)	0.49 (0.005-2.3)
	Effect (%)	74.9	78.3	9.60	100	100
R sol. IV with NPs	EC50 (%)	38.3 (1.9-78.8)	40.5 (4.7-84.8)	NT	NC	11.2 (9.8-12.5)
	EC20 (%)	14.9 (2.4-87.7)	NC	NT	NC	5.5 (4.5-7.0)
	Effect (%)	33.1	37.4	6.4	13.7	100
R sol. IV without NPs	EC50 (%)	44.6 (1.50-70.13)	46.7 (3.7-98.7)	NT	NC	11.08 (8.4-11.5)
	EC20 (%)	NC	NC	NT	NC	5.7 (3.4-5.9)
	Effect (%)	25.1	26.2	6.60	10.7	99.0

NT- no toxicity. NC- Could not be computed

3.4. DISCUSSION

Several studies have shown the removal of priority environmental contaminants (As, Cd and Hg) by using different sorbents (Otero et al., 2009; El-Said et al., 2010; Figueira et al., 2011; Tavares et al 2013; Rocha et al., 2014). Recently, few studies showed the competitive removal of Hg and Cd in a binary system from water using titanosilicate (Cardoso et al., 2013), rice husk (El-said et al., 2010) and cork (Lopes et al., 2014b). However, the study on their removal from multi-component tertiary-systems is lacking.

Magnetic nanoparticles functionalized with dithiocarbamate groups, which have the great advantage to be used as sorbent for water due to the water separation facility, were tested to remove hazardous elements from spiked seawater, in single and tertiary conditions. The results obtained clearly indicate us that under the experimental conditions tested, the dithiocarbamate functionalization of the NPs is only effective for Hg and their effectiveness toward Hg is independently of the presence of contaminants such as Cd or As. Indeed, the effect of ionic interaction on the sorption process can be evaluated by the ratio of the amount of Hg sorbed in the presence of the other contaminants, $q_e^{tertiary}$; to the amount of Hg sorbed when it is present alone in the solution, q_e^{Hg}. The $q_e^{tertiary}/q_e^{Hg}$ values for both contamination scenarios was around 1 (1.08 for $C_{Hg,0}$ of 50 μg/L and 0.96 for $C_{Hg,0}$ of 500 μg/L), indicating that the sorption capacity of NPs towards Hg is not greatly affected by the presence of As and Cd. In fact, the process seems to be limited by the number of the sorption sites for Hg than by the strong ionic competition. This hypothesis is supported by the fact that when using 10 mg/L of magnetic NPs, the removal efficiency was the same for the same initial Hg concentration, independently of the presence or absence of the other contaminants and decrease from ca. 98 to ca. 61-67% due to an increase of 10 times on the initial Hg concentration, suggesting that all sorption sites of the material were full. In this context, a study done by El-Said (2010) deals with the competitive adsorption of Cd and Hg ions onto rice husk ash from single component and binary systems, revealed that the combined effect of the binary mixture of Cd and Hg seems to be antagonistic (the effect of the mixture is less than that of each of the components in the mixture).

It is expected that the main mechanism involved on the sorption of Hg by the magnetic particles functionalized with the dithiocarbamate, involve the binding of Hg species to the dithiocarbamate groups present at the surface of the particles (Lopes et al., 2013), as a result of the high values of the stability constants reported for Hg dithiocarbamate complex (Ks 10^{38})

(Venkatesan et al., 2002). According to Lopes et al (2013) it is possible that the sorption mechanism involves a set of equilibria that depend on the Hg(II) species present in solution and, on the type of coordination environment involving the Hg species and the surface ligands.

The good agreement observed between the experimental results and the fittings accomplished by the Elovich model (R^2=0.95–0.99) for all scenarios tested suggest the existence of a heterogeneous sorption mechanism. Actually, the results of the kinetic modelling assume a chemical sorption or chemisorption, i.e. suggest that the rate- limiting step in the Hg sorption is a chemical interaction between Hg ions and superficial functional groups of the sorbent, which may involves valence forces through sharing or exchange of electrons, coordination, chelation, and/or complexation rather than physisorption (Ho and McKay, 1999).

Additionally, comparing the efficiency of the magnetic NPs in terms of Hg removal percentages obtained in spiked seawater with the ones obtained in spiked Milli-Q water, for the same initial Hg concentration (50 µg/L), and for others sorbents, in the current experiment, the used NPs performed better (Hg removal=98%) than some biosorbents like rice husk (Hg removal=81%) or cork powder from used stoppers (Hg removal=62%) and ETS-4 microporous titanosilicate (Hg removal=58%) (Rocha et al., 2014; Lopes et al., 2013; Lopes et al., 2014a). Moreover, the percentage of Hg removed by magnetic separation using NPs in the current work is even higher (98% after 48 hours) than that reported previously (Girginova et al., 2010; Figueira et al., 2011) for the same type of NPs, but that have been functionalized after their synthesis and used only for single contaminant removal of Hg in the absence of hazardous contaminants. Indeed, Girginova et al., (2010) reported only 74% of Hg removal under the same initial Hg concentration (50 µg/L) after 48 hours in spiked ultra-pure water. However, Figueira et al., (2011) have reported complete Hg removal (99.8%) from spiked ultra-pure water after 96 hours, for similar initial Hg concentration by the same magnetic nanoparticles. Recently, a study done by Tavares et al., (2013) is aligned with the current results, where the capacity of magnetite coated with siliceous hybrid shells to Hg uptake under ionic and no ionic competition was evaluated using natural seawater and ultra-pure water spiked only with Hg. The results depicted that the natural seawater is a complex matrix due to the presence of several cations and anions e.g. sodium ions (Na^+), chloride (Cl^-) and magnesium (Mg^{2+}) and organic matter that could compete with or for the Hg ions. Nevertheless, reports are also available on the efficiency of thiol functionalized, poly(1-vinylimidazole)-grafted and chitosan-coated magnetic NPs for the removal of Hg however not in particular to the context of seawater (Li et al., 2011; Hakami et al., 2012; Rahbar et al., 2014; Shan et al., 2015; Zhang et al., 2015).

According to Tavares et al., (2013), the initial slopes of the removal curves for spiked ultra-pure water and seawater are different indicating that by increasing the complexity of the matrix from ultra-pure water to seawater, the Hg uptake using the magnetic sorbent occurs at distinct initial rate but reaches almost the same final removal percentage, 99.9% for ultra-pure water and 98.6% for seawater. These results suggested that the used magnetic sorbent is capable in their Hg uptake efficiency under ionic competitive conditions (Hg/seawater system), reinforcing the potential of this type of material to remediate Hg contaminated seawaters.

The results obtained from the bioassays clearly show a differential sensitivity of the four species to the tested contaminants. Among all the tested species, the microalgae *P. tricornutum* was found to be the most sensitive species while *A. franciscana* showed no toxic effects to the tested solutions. Functionalized silica coated magnetite magnetic NPs was found to be an innocuous material to the selected test organisms except for *P. tricornutum* with a higher EC_{50} values (95.3%). To the best of author's knowledge, no study has previously reported the use of NPs to evaluate the effectiveness of the clean-up technologies of Hg-contaminated sites. However, some studies are available using a battery of bioassays to check the efficiency of rice husk biowaste and microporous material to remove the Hg from water (such as tap and river water) (Lopes et al., 2014; Rocha et al., 2014). In this context, Lopes et al., (2014) revealed that the removal was inefficient in terms of toxicity reduction to *D. magna*; however, it was effective in the complete reduction of toxicity for the green alga, *Pseudokirchneriella subcapitata.* Whereas, Rocha et al., (2014) reported that the remediation process with rice husk biowaste was extremely efficient in river waters spiked with lower levels of Hg (50 μg/L). In addition, this process of remediation was also able to eliminate the toxicity to *P. subcapitata* and rotifer *Brachionus calyciflorus* and ensure the total survival of *Daphnia magna* species. Moreover, for higher Hg concentration (500 μg/L), the remediation process was not as efficient in removing ecotoxicity. On the other hand, by using single microtox test Mishra and Tripathi (2008) revealed a 75% reduction in the toxicity of wastewater after treatment with fly ash. The results from the ecotoxicity tests indicate that the remediation process with these NPs, for seawater spiked with lower Hg concentration (50 μg/L) as well as As and Cd concentrations were in their legal limits, was able to eliminate the toxicity to the exposed organism's rotifer *B. plictilis* and bacteria *V. fischeri,* but unable to eliminate the toxicity to *P. tricornutum.* Increasing ten times the concentrations of Hg (500 μg/L) but with As and Cd concentrations remaining the same in seawater, the results from the remediation with NPs were not suitable in the detoxification process. However, the toxicity of bacteria *V. fischeri,* rotifer *B. plicatilis* and

algae *P. tricornutum*, whose responses where inhibited during its exposure to the non-remediate sample was considerably reduced after treatment with NPs. These organisms were highly sensitive towards contaminants, which allowed for recognition of the fact that waters containing NPs after treatment were less efficient in the detoxification process than waters without NPs still present. This fact may be due to some of the Hg ions associated with NPs may be exchangeable with Ca and/or other ions present in seawater, thereby releasing Hg again back into the remediated seawater (Lopes et al., 2014a).

Toxicity assessment performed in our study is not usually carried out in parallel with the study of water remediation. However, our main findings clearly highlight its importance since even with the occurrence of chemical remediation the contaminated seawater still exerted toxic effects to the studied species. Rather, a multidisciplinary approach combining both chemical and ecotoxicological tools affords more reliable conclusions about the real effectiveness of the clean-up technologies proposed for contaminated waters. For the first time, the current work highlights the importance of using a battery of bioassays with organisms from different trophic levels, to obtain an accurate ecotoxicological hazard assessment of the detoxification process using functionalized silica coated magnetite NPs.

3.5. CONCLUSIONS

The magnetic nanoparticles used in the current study were efficient for the removal of Hg from single- and multi-contaminated (Hg+Cd+As) seawater. The presence of other contaminants displayed no interference or effects on the rate of removal of Hg by the NPs. The removal of Hg by the NPs was faster for lower concentrations (Hg 50 µg/L). Concerning ecotoxicological profile, difference in toxicities was observed for remediated and non-remediated solutions. The non-remediated solutions caused higher toxicity than the remediated one highlighting the effectiveness of the magnetic NPs on the remediation and detoxification processes. Moreover, the ecotoxicological analyses allow to conclude that after the remediation process, the mixture with lower hazardous substances did not exhibit toxicity to the exposed organisms viz. rotifer *B. plictilis* and bacteria *V. fischeri*, while the mixture with higher levels of contaminants, still showed toxicity, indicating that the remediation was not totally effective in the detoxification processes. Yet, the toxicity of bacteria *V. fischeri*, rotifer *B. plicatilis* and algae *P. tricornutum*, whose responses where inhibited during its exposure to the non-remediated sample was considerably reduced after treatment with NPs. Microalgae *P. tricornutum* appears to be the most sensitive one while *A. franciscana* showed no toxic effects

to the tested solutions. In general, the presence of NPs in the seawater did not show toxicity to the selected species. Thus, the efficiency of the magnetic nanoparticles (high removal percentage and decrease of water toxicity) combined with its magnetic property proved this material a very promissory adsorbent and can be applied for both in-situ and/or ex-situ treatment applications, in systems like coastal lagoons, harbours, estuaries, or even aquacultures. One possible practical way to treat these systems is to pump the contaminated water to treatment tanks containing the magnetic nanoparticles that can be easily replaced by new ones after their saturation, or the direct deposition of the NPs in the water followed by magnetic recovery.

Overall, both chemical and ecotoxicological approaches revealed a high efficiency for the remediation of Hg-contaminated saltwater.

3.6. REFERENCES

ATSDR (2011) Agency for Toxic Substances and Disease Registry. Substance Priority List (http://www.atsdr.cdc.gov/spl/index.html).

Azur Environmental. (1998) Microtox-Acute Toxicity Basic Procedures. Carsbad, California. 1998.

Beiras R., Albentos M (2004) Inhibition of embryo development of the commercial bivalves Ruditapes decussatus and Mytilus galloprovincialis by trace metals; implications for the implementation of seawater quality criteria. Aquaculture 230: 205–213

Berntssen MHG, Aatland A, Handy RD (2003) Chronic dietary mercury exposure causes oxidative stress, brain lesions, and altered behavior in Atlantic salmon (Salmo salar) parr. Aquat Toxicol 65:55–72

Covelli S, Protopsalti I, Acquavita A, Sperle M, Bonardi m, Emili A (2012)Spatial variation, speciation and sedimentary records of mercury in the Guanabara Bay (Rio de Janeiro, Brazil). Continental Shelf Research 35:29-42

Chételat J, Amyot M, Arp P, Blais JM, Depew D, Emmerton CA, Evans M, Gamberg M, Gantner N, Girard C, Graydon J, Kirk J, Lean D, Lehnherr I, Muir D, Nasr M, J Poulain A, Power M, Roach P, Stern G, Swanson H, van der Velden S (2015) Mercury in freshwater ecosystems of the Canadian Arctic: Recent advances on its cycling and fate. Sci Total Environ. 509:41–66.

Coelho JP, Nunes M, Dolbeth M, Pereira ME, Duarte AC, Pardal MA (2008)The role of two sediment dwelling invertebrates on the mercury transfer from sediments to the estuarine trophic web. Estuar Coast Shelf Sci 78:516–523.

Cardoso SP, Lopes CB, Pereira E, Duarte AC, Silva CM (2013) Competitive Removal of Cd^{2+} and Hg^{2+} Ions from Water Using Titanosilicate ETS-4: Kinetic Behaviour and Selectivity. Water Air Soil Pollut 224:1535.

Decreto-Lei nº 236/98, Ministério do Ambiente. vol. 176. Diário da Republica—I Série A, 1998.

Directive 84/156/EEC, Council Directive 84/156/EEC of 8 March 1984 on limit values and quality objectives for mercury discharges by sectors other than the chlor-alkali electrolysis industry, Off. J. Eur. Commun. (1984) 74:29.

Drevnick PE, Sandheinrich MB (2003) Effects of dietary methylmercury on reproductive endocrinology of fathead minnows. Environ Sci Technol 37:4390–4396

Drevnick PE, Sandheinrich MB, Oris JT (2006) Increased ovarian follicular apoptosis in fathead minnows (Pimephales promelas) exposed to dietary methylmercury. Aquat Toxicol 79:49–54

EC, (1992) Environment Canada, Biological Test Method: Growth Inhibition Test Using the Freshwater Alga Selenastrum capricornutum. Report EPS 1/RM/25, Environment Canada, Ottawa, ON, Canada.1992.

El-Said AG, Badawy NA, Garamon SE (2010) Adsorption of cadmium (II) and mercury (II) onto natural adsorbent rice husk ash (RHA) from aqueous solutions: study in single and binary system. J Am Sci 12:400–409.

EPA (2001) Environmental Protection Agency. Mercury Update: Impact on Fish Advisories. EPA-823-F-01-011 June

EU, European Union water frame work directive (http://ec.europa.eu/environment/water/water-framework/index_en.html) Cadmium is classified as "priority hazardous substance"

Figueira P, Lopes CB, Daniel-da-Silva AL, Pereira E, Duarte AC, Trindade T (2011) Removal of mercury (II) by dithiocarbamate surface functionalized magnetite particles: Application to synthetic and natural spiked waters. Water Res 45: 5773-5784.

Finney DJ (1971) Probit analysis, 3rd edn. Cambridge University Press, Cambridge.

Fjeld E, Haugen TO, Vøllestad LA (1998) Permanent impairment inthe feeding behavior of grayling (Thymallus thymallus) exposed to methylmercury during embryogenesis. Sci Total Environ 213:247–254

Fu F, Wang Q (2011) Removal of heavy metal ions from wastewaters: A review. Journal of Environmental Management 92: 407-418

Geis S, Fleming K, Korthals E et al, (2000) Modifications to the algal growth inhibition test for use as a regulatory assay. Environ Toxicol Chem 19:36–41.

Girginova PI, Daniel-Da-Silva AL, Lopes CB, Figueira P, Otero M, Amaral VS, Pereira E, Trindade T (2010) Silica coated magnetite particles for magnetic removal of Hg(II) from water. J Colloid Interface Sci 2010; 345:234–240

Guzzi G, La Porta C (2008) Molecular mechanisms triggered by mercury. Toxicology 244:1–12.

Hammerschmidt CR, Sandheinrich MB, Weiner JG, Rada RG (2002) Effects of dietary methylmercury on reproduction of fathead minnows. Environ Sci Technol 36:877–883.

Hakami O, Zhang Y, Banks CJ (2012) Thiol-functionalised mesoporous silica-coated magnetite nanoparticles for high efficiency removal and recovery of Hg from water. Water Res 46(12): 3913-3922.

Ho YS, G. McKay G. (1999) Pseudo-second order model for sorption processes. Process Biochem 34:451–465

Lagergren S. (1898) Zur theorie der sogenannten adsorption gelo¨ ter stoffe. Kungliga Svenska Vetenskapsakademiens. Handlingar 24; (4)1-39.

Li G, Zhao Z, Liu J (2011) Effective heavy metal removal from aqueous systems by thiol functionalized magnetic mesoporous silica. J Hazard Mater 192(1):277-283.

Lillebø AI, Coelho JP, Pato P, Válega M, Margalho R, Reis M, Raposo J, Pereira E, Duarte AC, Pardal MA (2011)Assessment of mercury in water, sediments and biota of a Southern European Estuary (Sado Estuary, Portugal). Water Air Soil Pollut 214:667–680.

Lopes CB, Otero M, Lin Z, Silva CM, Rocha J, Pereira E, Duarte AC (2009) Removal of Hg^{2+} ions from aqueous solution by ETS-4 microporous titanosilicate--Kinetic and equilibrium studies. Chem Eng J 151:247-254.

Lopes CB, Pereira E, Lin Z, Pato P, Otero M, Silva CM, Duarte AC, Rocha J (2011) Fixed-bed removal of Hg^{2+} from contaminated water by microporous titanosilicate ETS-4: experimental and theoretical breakthrough curves. Micropor Mesopor Mat 145: 32-40

Lopes CB, Figueira P, Tavares DS, Lin Z, Daniel-da-Silva AL, Duarte AC, Rocha J, Trindade T, Pereira E (2013)Core-shell magnetite-silica dithiocarbamate-derivatised particles achieve the Water Framework Directive quality criteria for mercury in surface waters. Environ Sci Pollut R 9:5963-5974.

Lopes CB, Lopes I, Duarte AC, Soares AMVM Rocha J, Pereira E (2014a) A Multidisciplinary Approach to Evaluate the Efficiency of a Clean-Up Technology to Remove Mercury from Water. Bull Environ Contam Toxicol 93(2):138-43.

Lopes CB, Oliveira JR Rocha LS, Tavares DS, Silva CM, Silva SP, Hartog N, Duarte AC, Pereira E. (2014a) Cork stoppers as an effective sorbent for water treatment: the removal of mercury at environmentally relevant concentrations and conditions. Environ Sci Pollut Res 21:2108–2121 DOI 10.1007/s11356-013-2104-0

Low MJD. (1960) Kinetics of chemisorption of gases on solids. Chemical Reviews 60(3):267–312.

Ma J, Hintelmann H, Kirk JL, Muir DCG (2013) Mercury concentrations and mercury isotope composition in lake sediment cores from the vicinity of a metal smelting facility in Flin Flon, Manitoba. Chemical Geology 336:96-102

Mehdinia A, Akbari M, Kayyal TB, Azad M (2014) High-efficient mercury removal from environmental water samples using di-thio grafted on magnetic mesoporous silica nanoparticles. Environ Sci Pollut Res 22(3):2155-2165.

Mishra A, Tripathi BD (2008) Utilization of fly ash in adsorption of heavy metals from wastewater. Toxicol Environ Chem 90(6):1091– 1097

Monteagudo JM., Ortiz M.J(2000) Removal of inorganic mercury from mine waste water by ion exchange. J. Chem. Technol. Biotechnol. 75: 767–772.

Ngomsik AF, Bee A, Draye M, Cote G, Cabuil V (2005)Magnetic nano-and microparticles for metal removal and environmental applications: A review. Comptes Rendus Chimie 8:963–970.

OECD 2006 (Organization for Economic Co-Operation and Development). Freshwater Alga and Cyanobacteria Growth Inhibition Test. OECD Guideline for Testing of Chemicals 201, Paris, France,.

Otero M, Lopes CB, Coimbra J, Ferreira TR, Silva CM, Lin Z, Rocha J, Pereira E, Duarte AC (2009) Priority pollutants (Hg^{2+} and Cd^{2+}) removal from water by ETS-4 titanosilicate. Desalination 249(2):742–747

Pacheco S. Medina M, Valencia F, Tapia J (2006) Removal of inorganic mercury from polluted water using structured nanoparticles. J. Environ. Eng. ASCE 342–349.

Pereira ME, Lillebø AI, Pato P, Válega M, Coelho JP, Lopes CB, Rodrigues S, Cachada A, Otero M, Pardal, MA, Duarte AC (2009) Mercury pollution in Ria de Aveiro (Portugal): a review of the system assessment. Environ Monit Assess 155:39–49.

Rahbar N, Jahangiri A, Boumi S, Khodayar MJ(2014)Mercury Removal From Aqueous Solutions With Chitosan-Coated Magnetite Nanoparticles Optimized Using the Box-Behnken Design. Jundishapur J Nat Pharm Prod. 9(2)

Rocha L, Lopes CB, Borges JA, Duarte AC, Pereira E (2014) Valuation of unmodified rice husk waste as an eco-friendly sorbent to remove mercury: a study using environmental realistic concentrations. Water Air Soil Pollut 224(7): 1–18. doi:10.1007/ s11270-013-1599-9

Sandheinrich MB, Miller KM (2006) Effects of dietary methylmercury on reproductive behavior of fathead minnows (Pimephales promelas). Environ Toxicol Chem 2006; 25: 3053–3057.

Sandheinrich MB, Weiner JG (2011) Methylmercury in freshwater fish: recent advances in accessing toxicity of environmentally relevant exposures. In: Beyer WN, Meador JP (eds) Environmental contaminants in biota: interpreting tissue concentrations. Taylor and Francis, CRC Press, Boca Raton 169–190

Shan C, Ma Z, Tong M, Ni J (2015) Removal of Hg(II) by poly(1-vinylimidazole)-grafted Fe3O4@SiO2 magnetic nanoparticles. Water Res 2015; 69:256-260.

Tavares DS, Daniel-da-Silva AL, Lopes CB, Silva NJO, Amaral VS, Rocha J, Pereira E, Trindade T. (2013) Efficient sorbents based on magnetite coated with siliceous hybrid shells for removal of mercury ions. J Mater Chem 1: 8134-8143.

Taylor DL, Linehan JC, Murray DW, Prell WL (2012) Indicators of sediment and biotic mercury contamination in a southern New England estuary. Marine Pollution Bulletin 64:807-819.

Urgun-Demirtas M, Benda PL, Gillenwater PS, Negri MC, Xiong H, Snyder SW(2012) Achieving very low mercury levels in refinery wastewater by membrane filtration. J Hazard Mater 15;215-216.

USEPA 1994 (United States Environmental Protection Agency). Short-Term Methods for Estimating the Chronic Toxicity of Effluents and Receiving Waters to Freshwater Organisms. EPA 600/7-91-002. Washington, DC, EUA.

Venkatesan KA, Srinivasan TG, Vasudeva Rao PR(2002) Removal of complexed mercury from aqueous solutions using dithiocarbamate grafted on silica gel. Separ Sci Technol 6:1417-1429.

Webber HM, Haines TA(2003) Mercury effects on predator avoidance behavior of a forage fish, golden shiner (Notemigonus crysoleucas). Environ Toxicol Chem 22:1556–1561

Wang M, Wang Y, Zhang L, Wang J, Hong H, Wang D (2013) Quantitative proteomic analysis reveals the mode-of-action for chronic mercury hepatotoxicity to marine medaka (Oryzias melastigma). Aquat Toxicol 15: 130-131.

Widdows J. (1993) Marine and estuarine invertebrate toxicity tests. In Handbook of ecotoxicology, Vol 1, ed P Calow, Blackwell Science Ltd, Oxford:145–166.

Zhang S, Zhang Y, Liu J, Xu Q, Xiao H, Wang X, Xu H, Zhou J (2013) Thiol modified Fe3O4@SiO2 as a robust, high effective, and recycling magnetic sorbent for mercury removal. Chem Eng J 226:30-38.

Zhou X, Zhang JZ, Qiu XK, Wang DY (2013) Removal of Hg in wastewater by zero-valent iron. Huan Jing Ke Xue. 34(11):4304-10.

CHAPTER 4

Influence of temperature on nanoparticles remediated seawater-induced biochemical stress responses in Anguilla anguilla L.: Part I. Evaluation of lipid peroxidation, protein carbonyl oxidation and oxidative DNA lesions

Abstract

This study aimed to evaluate the influence of temperature on the toxicity of Hg-contaminated saltwater before and after its remediation using dithiocarbamate functionalized silica coated magnetite nanoparticles (NPs) in the presence of hazardous contaminants. For this, the sublethal toxicity of saltwater contaminated with mercury (Hg) and with a mixture of Hg, arsenic (As) and cadmium (Cd) was assessed before and after remediation with the NPs. To attain this objective, *Anguilla anguilla* gills were exposed, under three different temperatures, to saltwater contaminated with Hg solely and to saltwater contaminated with a mixture of Hg, Cd and As, before and after remediation with the NPs. Gills were also exposed to a negative control and to the NPs concentration used for saltwater remediation. The following endpoints were monitored for all tested treatments: DNA damage by measuring 8-hydroxy-2′-deoxyguanosine (8-OHdG) formation, lipid peroxidation (LPO) and protein carbonyls oxidation (PCs). In non-remediated solutions, Hg induced LPO, 8-OHdG formation and protein oxidation at both Hg concentrations (50 µg/L and 500 µg/L), either alone or in mixture, at all the exposed temperature (20 ºC, 24 ºC and 28 ºC). In remediated solution (with and without NPs), the damage was lower than in the non-remediated solutions suggesting the ability of functionalized NPs for Hg decontamination. Nevertheless, the remediated solutions with NPs displayed higher toxicity than the remediated solutions without NPs. Concerning the influence of temperature, in non-remediated solutions, gill exposure revealed a significant LPO, PC and 8-OHdG increase at all treatments with increasing temperature. In remediated solution, the influence of temperature was more prominent at the highest temperature as a significant modulations in LPO, PC contents and 8-OHdG in different solution was observed at 28C. In remediated solution without NPs, the similar pattern of responses was not recorded as in remediate solutions with NPs among studied parameters since the biochemical effects were limited to Hg concentrations alone. Paradoxically, it was pointed out that remediation technologies efficient in decreasing the toxicity of contaminants at normal temperature can be at the risk of increased temperature and should be remodelled under the climate change scenario in future. Finally, *A. anguilla* gill proved to be a good *ex vivo* model for Hg plus hazardous contaminants toxicity assessment under the climate change scenario.

Key words: *Climate change, Temperature, Mercury,Damage endpoints, Ex-vivo, Anguilla anguilla, Gill*

Article to be submitted to Environmental Science and Pollution Research

4.1. INTRODUCTION

Mercury (Hg) is one of the priority environmental contaminants according to European water framework directive (Directive 2008/105/EC, European Parliament 2008). Because of its high toxicity and known carcinogenic potential (Yabanli and Alparslan 2015) there is a constant need to develop more efficient techniques for its removal from waters. A successful example is the use of dithiocarbamate functionalized with silica coated magnetite magnetic nanoparticles (NPs) as a nano-remediation material to remove Hg either when alone or in a mixture with other contaminants from saltwater (Mohmood et al., 2016). Besides, have studied the efficiency of these NPs in the remediation of Hg- contaminated saltwaters, both Hg alone and in mixture with Cd and As, Mohmood et al. (2016) also studied the toxicity of NPs and water before and after the remediation process, the using several marine species (such as rotifer, bacteria and algae). The results obtained from the study showed that under highly competitive conditions (high ionic strength, Cd and As), the efficiency of magnetic NPs in the removal of Hg from seawater, was above 98% for low Hg concentrations (50 µg/L) and between 61% to 67% for higher Hg concentrations (500 µg/L). Furthermore, Mohmood et al. (2016) also found that such Hg removal was associated with a reduction in the ecotoxicity of the Hg-contaminated saltwater (both solely and in the presence of Cd and As). However, despite the great affinity of the magnetic NPs for Hg, they were not effective at removing As and Cd from seawater (≈ 0% removal). This work was developed under lab-control conditions at 20 °C. Therefore, it is important to understand if the removal efficiency is sufficient enough to remove the toxicity at different temperatures since, higher temperatures may lead to higher metabolic rates, higher uptake of chemicals and increase toxicity (Sokolova et al., 2008; Khan et al., 2006; MacLeod and Pessah 1973). So even, the low levels of Hg that remain in the remediated solutions could be toxic at temperatures higher than 20 ºC. Recent models predict that the mean global temperature increase by the end of the 21st century is likely to exceed 1.5 °C in all scenarios (IPCC, 2013). The U.N. Intergovernmental Panel on Climate Change (IPCC) has completed five assessments covering the evidence, impacts, and mitigation of climate change (IPCC, 2013). They report unequivocal global warming with evidence of increases in global mean air and ocean temperatures, widespread snow and ice melt, and rising global sea level. It is also expected that a rise in global temperature will be accompanied by increased temperature fluctuations and frequency of extreme temperatures (Trenberth et al., 2007). Available studies in this perspective reflect that the toxicity and absorption of Hg is highly dependent on temperature as well as biological factors and the warmer water is expected to affect Hg

accumulation in aquatic organisms (Welfinger-Smith et al., 2011). Moreover, various studies investigated how absorption of metals (such as mercury, lead, cadmium, and copper) by various species is affected by changes in water temperature (Cember et al., 1978; Tessier et al., 1994; Khan et al., 2006; Guinot et al., 2012; Dijkstra et al., 2013; Pack et al., 2014).

Hence, a clear lacuna is perceptible in the literature on the effect of increased temperature on the toxicity of the Hg after its nano-remediation in biota. Moreover, Hg's toxicity effect before and after the nano-remediation process in fish, represent a major drive area of research that has not yet been well covered. Fishes are poikilotherms and changes in water temperature have a great impact on their physiology (Clark et al., 2008; Perez-Casanova e al., 2008; Hattori et al., 2009; Said Ali et al., 2010; Pack et al., 2014). A gradual change in water temperature can be physiologically compensated for, but a rapid temperature change may disturb organisms' homeostasis and thus becomes a stress.

Fishes as test organisms fulfils every requirements as bioindicator species (Sedeño-Díaz and López-López 2012; Belpaire and Goemans 2007) and can exhibit a cumulative response to interactive effects of stressors (Hegyi et al., 2006). When stressors, singularly or in combination, are severe enough to challenge the homeostatic mechanisms beyond the compensatory limits of fish or permanently alter them, biochemical processes generally adapt to compensate for the stress (Schreck et al., 2002). In this perspective, several decades of research focused on studying the connection between oxidative stress and health parameters have resulted in identification of important oxidative stress biomarkers such as the products of oxidation of biological molecules: lipids, proteins and DNA (Ercegovac et al., 2010). Moreover, the above mentioned biomarkers have also shown their utility as good representative of pro-oxidant state (Ercegovac et al., 2010). The increase of ROS-induced lipid peroxidation was correlated in fish with environmental oxygen concentration, metals and organic contaminants (Lackner 1998). However, data related to the interactive effect of temperature on the Hg's behaviour is missing. Proteins are considered to be important targets of free radical attack in cells (Almroth et al., 2008; Lushchak, 2011) and thus compromise antioxidant defence, cellular function, and survival (Padmini, 2010). Studies on dynamics showed that proteins can be oxidized before lipids or DNA in ROS exposed cells (Du & Gebicki, 2004). Regarding DNA oxidative damage, the formed free radicals attack not only DNA bases but also the deoxyribose backbone of DNA, reacting five times faster with nucleobases (Valavanidis et al., 2009). The oxidation of guanine in the C8 position results in the formation of 8-hydroxy-2′-deoxyguanosine (8-OHdG), a predominant and one of the most studied oxidative DNA lesions due to its easy formation and mutagenicity (Valko et al., 2004).

The absence of base damage repair may lead to strand misreading, mutations, altered gene expression, strand breaks, microsatellite instability and loss of heterozygosity, chromosomal aberrations, cytostasis, cytotoxicity or neoplastic growth (Croteau and Bohr 1997; Evans et al., 2004).

Keeping in view the previously described lacunae in knowledge, the current study aimed to assess the influence of temperature on the toxicity of nano-remediated Hg-contaminated saltwater in the presence and absence of arsenic (As) and cadmium(Cd). In order to accomplish the objective, *Anguilla anguilla* gills were chosen as a biological model to assess adverse effects, as these are the main organs which remain contiguously in contact with water and thus a slight change in temperature would predispose gill towards an early change in biomarker responses. In addition, the study involves assessment of effects at the mitochondria level (namely effects on DNA damage by measurement using antibody based assays (8-OHdG), lipid peroxidation and protein carbonyl oxidation) since oxidative stress responses tend to be higher in metabolically active tissues such as gill *versus* other organs in fish (Lemaire et al., 1993; Ansaldo et al., 2000). When mitochondria become dysfunctional, for example, through long-term exposure to environmental toxicants, they produce less cell energy and more ROS having its consequences at supra-cellular level (Ahmad et al., 2013). The *ex vivo* approach was adopted, which allowed us to directly assess the temperature effects on the gills as a more likely scenario under natural environmental conditions (Britto et al 2012).

4.2. MATERIALS AND METHODS

4.2.1. Chemicals

All chemicals used in this work were of analytical reagent grade. Bovine serum albumin (BSA), bradford reagent, butylated hydroxytoluene (BHT), diethylenetriaminepentaacetic acid (DTPA), methanol, phosphate buffered saline (PBS), potassium hydroxide (KOH), RPMI-1640 medium tricloroacetic acid (TCA), trizma hydrochloride reagent grade (Tris-HCl), 2-thiobarbituric acid (TBA), 2,4-dinitrophenylhydrazine (DNPH), ethylenediaminetetraacetic acid (EDTA), guanidine hydrochloride, triton X-100, acetonitrile and calcium chloride used for this study were purchased from Sigma. Arsenic (III) chloride (1000 ± 2 mg/L) and mercury (II) nitrate standard solution (1000 ± 2 mg/L) were purchased from BDH Chemicals Ltd, while the

certified standard solution of Cadmium (II) nitrate (1001 ± 2 mg/L) was purchased from Merck.

Regarding the NPs, dithiocarbamate (DTC) functionalized silica coated magnetite materials were previously investigated for remediation of seawater spiked with single (Hg) or a mixture of (Hg, As and Cd) contaminants. The magnetic NPs were kindly provided by the Associated Laboratory CICECO, University of Aveiro, Portugal. The details pertaining to the synthesis and characterization of these magnetic NPs (Fe_3O_4@SiO_2/SiDTC) can be obtained in Tavares et al., (2013).

4.2.2. Fish

European eel *A. anguilla* with an average weight of 50 ± 5 g were collected in 2013 from an unpolluted area of Aveiro Lagoon - Murtosa (40.7370° N, 8.6399° W), Portugal, as adopted by Guilherme et al. (2010). The eels were transported in anoxia (or in recipient without water), which is a most satisfactory way for the transportation of this species as seen by Santos and Pacheco (1996) on *A. anguilla* stress biomarkers recovery study. The fish were acclimated to laboratory conditions in aerated, filtered, and dechlorinated tap water in a 50-L aquarium for 1 week, at room temperature (20 °C) under natural photoperiod. Fish were not fed during the acclimatization period. After acclimation, fish were sacrificed by cervical transection according with the method adopted by Mieiro et al. (2011) in order to minimize the influence of this technique on the measurements on the endpoints studied.

4.2.3. Preparation of test solutions before and after remediation

For the current study, the test solutions used to assess the remediation efficiency of NPs were the same as described in chapter 3 (Table 3.1). Concerning physicochemical properties, non-remediated and remediated solutions (with or without NPs) showed no clear differences in conductivity, pH and dissolved oxygen values. In addition, the salinity values were similar among the treatment groups ranging from 32.9 to 34.9.

4.2.4. Experimental design

4.2.4.1. Gill processing and test solutions exposure

The gill exposure methodology was based on the method described by Maciel et al., (2010), with some modifications. Initially, fish were sacrificed, and the gills were dissected. Afterwards, the gills were isolated and gill arches were separated. During separation, the gill arches were divided randomly into different treatment groups (three replicates in each group and three gill arches per replica) according to the following manner: 1) control – seawater only; 2) NPs – 10 mg/L (concentration used for remediation); 3) non-remediated solutions I, II, III and IV (solution I where Hg concentration is in legal limits discharge 50 µg/L; solution II where Hg concentration is 10 times higher to its legal limit; solution III where mixture of Hg, As and Cd in legal limits discharge; IV where the concentration of As and Cd corresponds to their legal limit and the concentration of Hg is ten times higher than its legal limit discharge); 4) remediated solutions with NPs I, II, III and IV; 5) remediated solutions without NPs I, II, III and IV. The gills arches were submerged in 1 mL of the test suspensions in eppendorfs under constant agitation for 1 h at three different temperatures (20 ºC, 24 ºC and 28 ºC). These temperatures were chosen as per the defined value given by the IPCC (2007) stating a 0.2 °C increase in the mean global temperature per decade in the next 2 decades and a 1.8 to 4 °C increase by the year 2100 (IPCC, 2007). However, the more recent models predict that the mean global temperature increase by the end of the 21st century is likely to exceed 1.5 °C in all scenarios (IPCC, 2013). At the end of the exposure, the gill arches were removed, blotted, weighed and stored intact at -80 ºC for later Hg analysis as well as homogenization and the determination of biochemical markers.

4.2.4.2. Mercury analysis in gill

For total mercury (T-Hg) analysis, *A. anguilla* gill samples were freeze-dried, homogenized and weighed for fresh-weight determination. The gill tissue samples were analysed for T–Hg by atomic absorption spectrometry (AAS) with thermal decomposition and gold amalgamation, using an Advanced Mercury Analyser (AMA) LECO 254.21. The accuracy and precision of the analytical methodology for T-Hg determinations were assessed by replicate analysis of certified reference materials (CRM) IAEA (tuna fish) for biological samples. The precision of the method was always better than 9% ($n > 3$), with a recovery efficiency between 92–103%.

4.2.4.3. Gill mitochondrial isolation

Gill mitochondria were isolated adopting the procedure of Sayeed et al. (2006) with slight modifications. All procedures were carried out on ice. Briefly, the gill samples were thawed and kept into ice-cold isolation medium (0.25 M sucrose containing 0.002 M EDTA and 0.002 mM Tris HCl, pH 7.6). Gill tissue was minced in fresh isolation medium and gently homogenized in isolation medium using a hand-held homogenizer with a loose fitting pestle. The resulting 5% (w/v) homogenate was centrifuged at 500 times gravity (× *g*) for 10 minutes. The supernatant fraction was retained, whereas the pellet was washed with fresh isolation medium and recovered by centrifugation at 500 × *g* for 10 minutes. The supernatant fractions were combined and again centrifuged at 500 × *g* for 10 minutes. The resulting supernatant fraction was centrifuged at 1000 × *g* for 15 minutes to obtain the mitochondrial pellet. The pellet was first washed with isolation medium and then with respiration reaction buffer (70 mM sucrose, 220 mM mannitol, 2 mM HEPES, 0.5 mM EDTA, 2.5 mM $MgCl_2$, 0.5 mM KH_2PO_4, and 2 mM K_2HPO_4, pH 7.4). The purified mitochondria were sedimented by centrifugation at 12,000 × *g* for 10 minutes. The final mitochondrial pellet was resuspended in respiration reaction buffer (300 µL) to produce a suspension containing 25 – 40 mg of mitochondrial protein/mL and stored. Protein was measured by the Bradford method (Bradford 1976), using BSA as standard.

4.2.4.4. Isolation of chromatin extracts for analysis of 8-hydroxyguanine

Isolation of chromatin was carried out according to the procedure of Avery et al., (1996) with slight modifications. A portion of each gill tissue (50 mg) was placed in a falcon tube and homogenized in 1.1 mL of cold sucrose buffer (0.25 M sucrose, 3 mM $CaCI_2$, 50 mM tris-HCl) containing 1% Triton X- 100 and allowed to stand in an ice bath for 10 minutes. Following this, the mixture was centrifuged at 1000 × *g* for 15 minutes at 4 °C. The pellet was resuspended in 1.2 mL cold sucrose buffer for 10 minutes and recentrifuge at the same conditions. Nuclei were suspended in 1.2 mL 50 mM tris-HCl, placed in an ice bath for 10 minutes and centrifuged for 15 minutes. This was repeated with 10 mM and 5 mM tris-HCl buffers. Chromatin was transferred to an eppendorf and further processed for 8-OHdG assay measurements using kit.

4.2.5. Measurements of biochemical stress responses

4.2.5.1. Lipid peroxidation measurement

Lipid peroxidation was determined in the previously prepared isolated mitochondria adopting the procedure of Ohkawa et al. (1979) and Bird and Draper (1984) with some modifications. Briefly, to a 50 µL mitochondrial preparation, 500 µL of 12% TCA in aqueous solution, 450 µL of Tris-HCl buffer (60 mM, pH 7.4 and 0.1 mM DTPA), and 500 µL 0.73 % TBA was added with a final volume of 1.5 mL. The mixture was heated for 15 minutes in a water bath set at boiling temperature. The Eppendorfs were then removed and cooled to room temperature. The contents from each Eppendorf (1.5 mL) were centrifuged at 12,000 rpm for 3 minutes. The absorbance of the supernatant was measured at 535 nm. The rate of LPO was expressed as nmol of thiobarbituric acid reactive substances (TBARS) formed per milligram of protein ($\varepsilon = 1.56\times10^5$ 1/M cm, ε represents molar extinction coefficient).

4.2.5.2. Protein oxidation

Protein oxidation in gill mitochondria was measured as the concentration of protein carbonyls (PCs) by using DNPH assay (Sohal et al., 2006). The mitochondrial preparation was divided into two portions, each containing 2 to 4 mg of protein. To one portion, 4 mL of 2 N HCl was added and then incubated for 1 h at room temperature with intermittent shaking. The other portion was treated with 4 mL of 10 mM DNPH in 2 N HCl and then incubated for 1 h at room temperature with intermittent shaking. After incubation, the mixture was precipitated with 10% TCA and centrifuged at 500 × g for 5 minutes to precipitate proteins. The precipitate was washed thrice with 4 mL of ethanol/ethyl acetate (1:1). The final protein precipitate was dissolved in 6 M guanidine hydrochloride and the absorption was measured at 370 nm. Carbonyl content was calculated using the molar extinction coefficient of 22.1 /mmol cm and the results were expressed as nmol carbonyls/mg mitochondrial protein.

4.2.5.3. 8-hydroxy-2'-deoxyguanosine (8-OHdG) assessment

The amount of 8-OHdG was assessed by means of a competitive *in vitro* enzyme-linked immunosorbent assay (ELISA) using an IBL International GmbH (Germany) kit. Results were expressed as ng/mL.

4.2.5.4 Protein concentration measurement

Total protein was determined according to the Bradford method (1976) using bovine serum albumin (BSA) as standard. The assay mixture contained 990 µL of Bradford reagent,

10 µL of diluted BSA (2.5 mg/mL) and 10 µL milli-Q water. The absorbance of plate was measured at 595 nm after incubate during 10 minutes in dark.

4.2.6. Statistical Analysis

The software SigmaPlot 12.0 was used for statistical analysis of data. Data were tested for Normality (Shapiro-Wilk) and Equal Variance. A two-way ANOVA was carried out in order to ascertain differences in between three exposed temperature and treatments groups and followed by Holm-Sidak method. Spearman rank correlation factor (r) was used to test significant relations between T-Hg in gill tissue and biochemical parameters (LPO, 8-OHdG and PC). A significance level of 0.05 was ascertained in all test procedures.

4.3. RESULTS

4.3.1. Mercury levels in tissue

In all non-remediated solutions, *A. anguilla* gill exposure revealed a significant ($P<0.05$) increase in T-Hg concentration at all the three temperatures (20, 24 and 28 °C) when compared to control (Figure 4.1). In remediated solutions (with and without NPs), the gill analyses showed a significant increase in T-Hg only after exposure to those solutions initially containing 10 times higher Hg concentration either alone (solution II) or in mixture of As and Cd (solution IV) at all temperatures. However, a significant decrease was perceptible in gill T-Hg contents when the remediated solutions (with and without NPs) were compared with the non-remediated solutions at all three temperatures only at higher concentrations of Hg either alone (Solution II) or in mixture (solution IV). Moreover, no significant difference was observed in gill T-Hg content when exposures of single solutions of Hg at both lower and higher concentrations (I and II) were compared with their corresponding concentration in mixtures (III and IV).

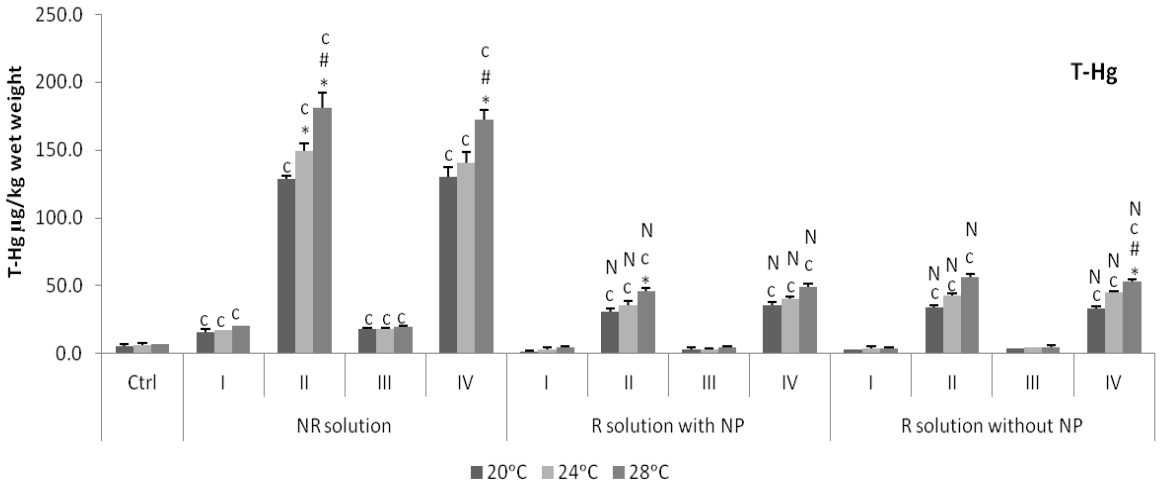

Figure 4.1. Average of total mercury (T-Hg) concentration in *A. anguilla* gills after 1h-exposure to non-remediated (NR), remediated (R) with and without NPs, solutions (**I** = Hg 50 µg/L, **II** = Hg 500 µg/L, **III** = Hg 50 µg/L, As 1000 µg/L, Cd 200 µg/L and **IV** = Hg 500 µg/L, As 1000 µg/L, Cd 200 µg/L). Inter-group significant differences (P<0.05) have been denoted by letters: c (vs. control), N (vs. non-remediated), and inter-temperature significant differences have been marked by symbols: * (vs. 20 °C), # (vs. 24 °C). Error bars represent the standard error.

Inter-temperature comparison revealed no statistically significant changes in gill T-Hg contents among controls. However, in non-remediated solutions at higher Hg concentration either alone (solution II) at 24 °C (vs. 20 °C) and 28 °C (vs. 20 °C and 24 °C) or in mixture (solution IV) only at 28 °C (vs. 20 °C and 24 °C) a significant increase in T-Hg content was observed. Moreover, in remediated solution with NPs only at higher concentration of Hg alone whereas, in remediated solution without NPs at higher concentration of Hg in mixture (solution IV) a significant difference was observed at 28 °C (vs. 20 °C).

4.3.2. Biochemical responses

Evaluation of lipid peroxidation, protein carbonyl oxidation and oxidative DNA lesions

Within the same temperature, comparison between control and NPs revealed a significant increase in PC and 8-OHdG content ($P < 0.05$: Figure 4.2) at the highest temperature (28 °C).

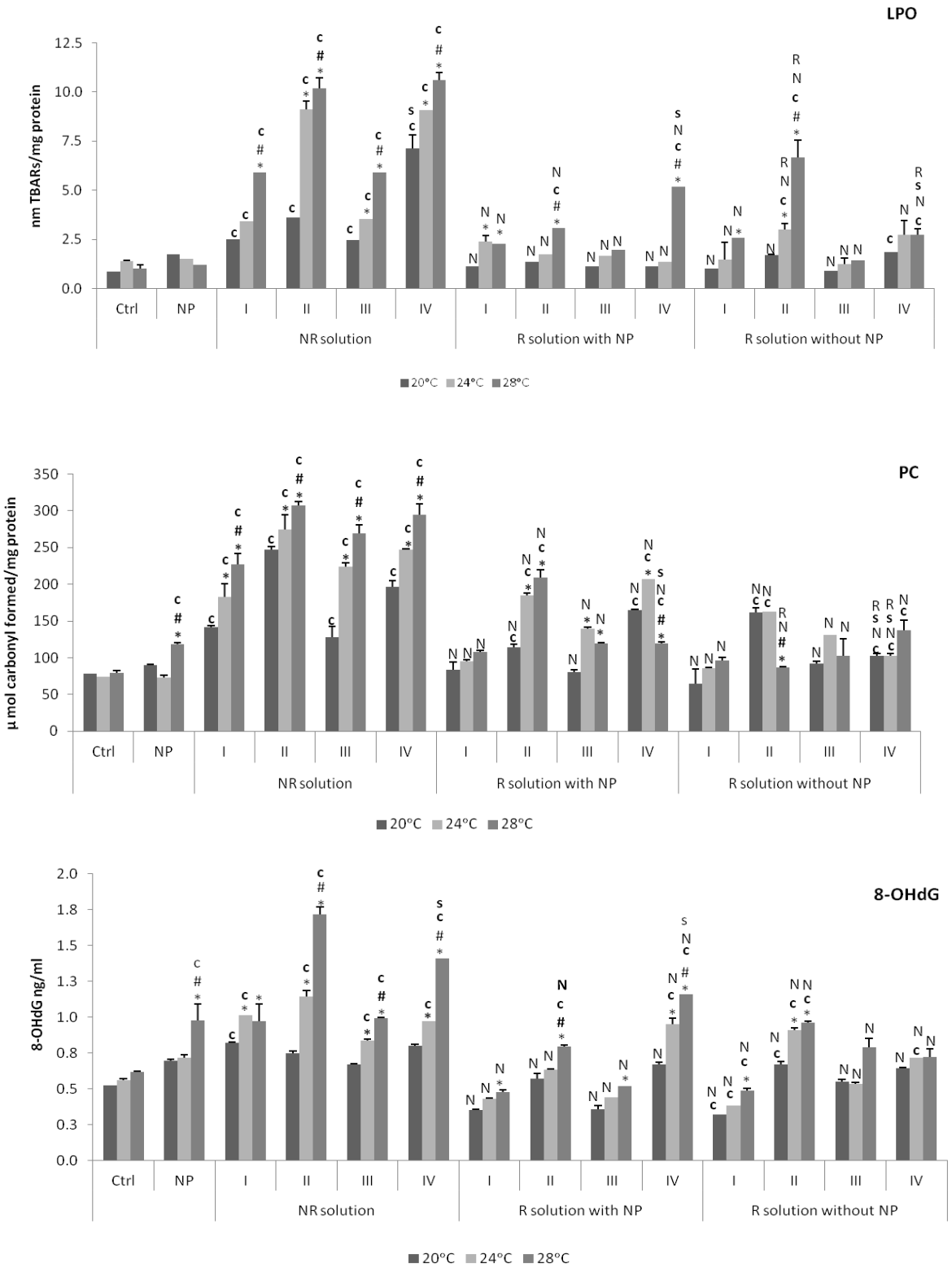

Figure 4.2. *Anguilla anguilla* gill lipid peroxidation, LPO; protein carbonyl, PC oxidation; and 8-hydroxy-2′-deoxyguanosine, 8-OHdG formation in response to the exposure of non-remediated (NR), remediated (R) with NPs and without NPs solutions (Solution I = Hg 50 µg/L, II = Hg 500 µg/L, III = Hg 50 µg/L, As 1000 µg/L, Cd 200 µg/L and IV= Hg 500 µg/L, As 1000 µg/L, Cd 200 µg/L). Inter-group significant differences have been denoted by letters: c (*vs.* respective control), N (*vs.* respective non-remediated), R (*vs.* respective remediated with NP), s (*vs.* Hg alone solutions) and inter-

temperature significant differences (P<0.05) have been marked by symbols: * (vs. 20 °C), # (vs. 24 °C). Error bars represent the standard error.

In general, gills in non-remediated solutions with Hg either alone or in mixture reflected an increase in LPO, PC content and 8-OHdG levels when compare to control. Similar increase in LPO, PC content and 8-OHdG was observed in the remediated solutions with or without NPs; however, only at higher concentration of Hg either alone or in mixture at different temperature. Nevertheless, a significant decrease was observed in 8-OHdG level at lower Hg concentration alone in remediated solutions without NP when compared to control. Interestingly, comparison between remediated and non-remediated solutions with and without NPs at all temperatures displayed a significant decrease in LPO, PC contents and 8-OHdG levels. Moreover, the comparison between remediated solutions with or without NPs revealed a significant increase in LPO at higher Hg concentration alone (solution III, 24 °C and 28 °C) in remediated solutions without NP. Regarding the comparison of the effects of Hg either single or in mixture, in non-remediated solutions, a significant increase in LPO (20 °C) whereas, a decrease in 8-OHdG (28 °C) levels were observed at higher Hg concentration in mixture when compared to Hg alone. In the remediated solution with NPs, in LPO and 8-OHdG levels a significant increase was observed at higher Hg concentration in the mixture at 28 °C, however a decrease was observed in PC content in comparison to their related Hg concentration alone. In the case of remediated solutions without NPs, a significant decrease in LPO was observed at higher concentration of Hg in the mixture at 28 °C whereas, in PC contents at 20 °C and 24 °C a decrease was observed in comparison to the corresponding concentration of Hg alone.

As per the influence of temperature, no significant changes in *A. anguilla* gill LPO, PC and 8-OHdG were found among controls exposed at the different temperatures. In NPs exposed group, among the three measured endpoints, PC and 8-OHdG showed a significant increase at 28 °C comparatively to 20 °C and 24 °C. In non-remediated solutions, at 24 °C (*vs.* 20 °C) a significant increase in LPO, PC contents and 8-OHdG levels was also observed in all the solutions except in LPO at lower concentration of Hg alone. The similar increase in LPO, PC contents and 8-OHdG levels was observed in all the solutions in comparison to 20°C and/or 24 °C. In context of remediated solution with NPs, at 24 °C (vs. 20 °C), a significant increase was observed in LPO (solution I), PC (solution II, III and IV) and 8-OHdG level (solution IV), whereas 28 °C (*vs.* 20 °C and/or 24 °C), gill exposure revealed a significant increase in LPO (solution I, II and IV), PC contents (solution II) and 8-OHdG (at all the solutions). A decrease

at highest temperature was also perceptible in PC content at higher concentration of Hg alone. In the perspective of remediated solution without NPs, At the difference of 4 °C temperature *i.e.* 24 °C (*vs.* 20 °C) a significant increase was observed in LPO and 8-OHdG level only at the highest concentration of Hg alone (solution II). gill exposure at highest temperature (28 °C *vs*. 20 °C and/or 24 °C) confirmed a significant increase only in LPO and 8-OHdG level at lower concentration of Hg either alone and in mixture however, a decrease was observed in PC content (at solution II).

Regarding the relationships between the measured parameters (*i.e*., T-Hg in gill *v*s. LPO, PC and 8-OHdG), the Spearman's rank tests revealed no significant correlations ($P>0.05$; $R^2< 0.5$).

4.4. DISCUSSION

Concerning Hg accumulation in non-remediated solutions, the increase of T-Hg in gill at legal limit and 10 times higher concentration either alone or in mixture (As, Cd) seems obvious since gills have already been referred as important organ for Hg uptake from water compartment under both *in vivo* and *in vitro* condition (Dijkstra et al., 2013, Mieiro et al., 2011; Guilherme et al., 2008; Nolan et al., 1984). An increase of T-Hg in gill is in disagreement with the study done by Laporte et al. (2002). These authors showed a slight decrease in inorganic Hg uptake in gill of *Callinectes sapidus* suspecting that the interaction of the other metals (Cd, Zn and Pb) and metalloid (As) somehow modified the behaviour of inorganic Hg. Moreover, the exposure of the gills in the presence of a suite of metals and metalloids showed that the inorganic Hg uptake was largely by different mechanisms to that of the other elements, as there was little interaction in terms of uptake rate (Laporte et al., 2012). However, in the current study, it is evident that As and Cd did not influence Hg uptake. In the present work, in remediated solution, the increase in T-Hg at higher concentration (single or in the mixture) was observed that seems obvious taking into account the more availability of Hg since the removal of Hg was only 61% to 67% after nano-remediation process (see chapter 3). In remediated solutions, both with and without NPs, the Hg uptake was significantly lower than in non-remediated solutions, which is a clear evidence of the effectiveness of NPs in Hg removal from contaminated solution strengthening the previous studies reported by Mohmood et al. (2016) and Lopes et al. (2013) taking into account the spiked Hg water. Moreover, the presence of other elements did not influence the efficiency of NPs-remediation, since a similar

Hg-uptake was observed in treatments with Hg alone and in mixture both for non-remediated and remediated solutions. Thus, suggesting that the presence of As and Cd were not the critical determinant for Hg accumulation.

Regarding the influence of temperature on Hg uptake, in general, it was observed that an increase in temperature to 28 ºC was associated with a significant increase in Hg uptake in tested solutions. These findings are in the agreement of the findings of Pack et al. (2014) who showed T-Hg and methyl Hg contents increase with the increase in temperature in both metal-exposed loaches. Moreover, the T-Hg and methyl Hg content in the 0.1 mg/L MeHg-treated groups of loaches maintained at 28 ºC showed 4.7- and 4-fold more absorbed than those maintained at 18 ºC and 1.6- and 1.7-fold greater absorbed than those maintained at 23 ºC (Pack et al., 2014). The increase in uptake of Hg with increasing temperatures was also observed at higher concentration of Hg alone and with mixture in the remediated solutions with NPs (solution II) and without NPs (solution IV), respectively. Thus the interactive role of temperature on the Hg uptake should be considered in the current study.

Concerning the biochemical responses, comparison between control and NPs revealed a significant increase in PC and 8-OHdG content at 28 °C and thus pointing clearly the NP's toxicity inducing potential which was not perceptible in the previous study considering different trophic levels of marine species at the same NPs concentrations (Mohmood et al., 2016). However, no response to the LPO increase can suggest an array of ROS unable to induce LPO since it is evident in the literature that alkoxyl radicals apparently have a greater importance in protein oxidation chains than they do in lipid peroxidation, in which peroxyl radicals are key chain propagating species (Stohs 1995). In this perspective, only available study in aquatic organisms revealed that the 10 mg/L iron oxide NPs exposed mussels were able to cause an increase in PC, DNA damage and LPO, in relation to unexposed groups of mussels as a result of oxidative stress (Taze et al., 2016).

In non-remediated solutions, Hg induced oxidative stress, either alone or in mixture, at both lower and higher Hg concentration and at all temperatures as signalled by increase in PC content, LPO and 8-OHdG (except DNA at 28 °C in solution I and at 20 °C in solution II, III and IV). Moreover, the current finding clearly evidence that the legal limit of Hg is able to induce significant toxic effects in fish. Increase in LPO, PC and 8-OHdG looks obvious since several studies regarding Hg toxicity revealed an increase in oxidative damage to fish tissues under both *in vivo* and *in vitro* conditions (Mohmood et al., 2014; Mieiro et al., 2011;

Sevcikova et al., 2011; Monteiro et al., 2010; Huang et al., 2010; Valavanidis et al., 2009; Berntssen et al., 2003). The nonalignment of 8-OHdG induction with temperature and metals concentration may be directed towards DNA repair process effective at highest temperature in lower Hg concentration alone and lowest temperature in mixture. Moreover, though not significant statistically, incremental pattern should also be considered for the current result interpretation of 8-OHdG induction.

In remediated solutions with NPs, ROS scavenging activity was seen hampered partially since increase in LPO (solution II and IV at 28 °C), PC (in solution II and IV at all temperatures) and 8-OHdG (in solution II at 28 °C and in solution IV at 24 °C and 28 °C) were observed only in solutions containing higher Hg concentration. These changes may correspond to the effectiveness of NPs in Hg remediation taking into account the fact that the remediated solution contains less concentration of Hg in comparison to the non-remediated solutions in the previous study (Mohmood et al., 2016). These results are similar to the ones obtained with exposure to the remediated solutions without NPs; only at higher concentration of Hg (alone or mixture) an increase in LPO (in solution II at 24 °C and 28 °C as well as in solution IV at 20 °C and 28 °C), PC (in solution II at 20 °C and 24 °C as well as in solution IV at all temperatures) and 8-OHdG (in solution II at all temperatures as well as in solution IV at 24 °C) occurred in comparison to control. In agreement, several studies regarding Hg toxicity and the change in temperature revealed an increase in LPO in fish tissues (Huang et al., 2010; Verlecar et al., 2007). Moreover, a decrease in 8-OHdG at lower Hg concentration corroborates the efficiency of NPs in Hg remediation. Interestingly, a significant decrease was also observed in LPO, PC contents and 8-OHdG levels at all remediated solutions with and without NPs at all temperatures when compared with non-remediated solutions. However, persistence of significant LPO increase at Hg higher concentration alone in solution without NPs (solution II at 24 °C and 28 °C) indicate the incomplete removal of Hg at higher concentration as observed in our previous study.

Influence of temperature on NPs is clearly evident on PC and 8-OHdG levels in the current study as significant induction in these two parameters was observed. To the author's knowledge this study was the first of its kind to look into the information about the toxicity of NPs used for Hg nano-remediation under the influence of temperature in fish gill. The findings may suggest that the change in temperature affect the affinity and cellular uptake of NPs and thus cause effects at highest temperature as proposed by Mahmoudi et al. (2013) in mammals

exposed to protein coated NPs where it was seen that a slight temperature changes are able to affect protein affinity and cellular uptake/toxicity of NPs.

On the perspective of non-remediated solutions, gill exposure revealed a significant LPO, PC and 8-OHdG increase at all treatments with increasing temperature. According to Sekine et al., (1996) modulation of temperature can influence toxicity of contaminants. For example, the overall interactive effects of water temperature and contaminants have already been seen in fish (Sokolova et al., 2008; Kaur et al., 2005). Thus, an acute change in ambient temperature may results in a change in membrane fluidity and local transitions of the lipid bilayer, which can affect membrane integrity and permeability, as well as the mobility and function of membrane-associated receptors, transport and channel proteins (Sokolova et al., 2008; Hochachka and Somero 2002;Hazel 1995). In remediated solution with NPs, the irregular influence of temperature was seen at both the temperature *i.e.* 24°C and 28 °C on gills biochemical parameters. Though, the effect of temperature on LPO, PC and 8-OHdG was more prominent at the highest temperature and at the higher Hg concentration either alone or in mixture, a decrease was also observed at the highest temperature in PC contents at higher Hg concentration in mixture. In this perspective, the explanation based on metal–temperature effects on fish gills may vary depending on the biochemical endpoints can be suggested here as proposed by (Otomo et al., 2012). Nevertheless, the interactive effect of temperature with the residual Hg levels left after remediation cannot be overlooked since 61-67% Hg was remediated from the higher concentration previously. In remediated solution without NPs, the similar pattern of responses was not recorded as in remediate solutions with NPs among studied parameters since the biochemical effects were limited to Hg concentrations alone. Thus, increase in temperature by 8°C revealed an increase in LPO and 8-OHdG (in solution I and II) and a decrease in PC content (in solution II), whereas increase of 4°C temperature depicted increase in LPO and 8-OHdG in solution II confirming that the oxidative stress inducing potential of Hg remediated solutions further increases with increase in temperature. The results clearly indicated that the elevated temperature is responsible to increase toxicity even after the removal of NPs from the remediated solutions. No observed effects in mixture of Hg at elevated temperature should not be considered the absence of effects since the modulation in antioxidants induction has been observed at the corresponding treatments scenarios as dealt in the next chapter (Chapter5). Paradoxically, it was pointed out that remediation technologies efficient in decreasing the toxicity of contaminants at normal temperature can be at the risk of increased temperature and should be remodelled considering the consequences of climate change scenario in future.

Whilst comparing single versus mixture solutions, all the significant changes in the studied parameters were observed only at higher Hg concentration in the mixture and at the highest temperature, except LPO (non-remediated solution at 20 °C). Thus, LPO increase at 20 °C in non-remediated solutions clearly reflected the interactive effect of Hg with As and Cd. However, in case of 8-OHdG the effect of temperature should also be considered due to its appearance at elevated temperature and besides having a difference from the lower temperature (20 °C and 24 °C). The current study is in agreement with the previous study done by Senthamilselvan et al., (2012) proving that the combined metal toxicity (Hg plus Cd) induced DNA damage of fish *Lates calcarifer* more than individual metal toxicity. In remediated solution with NPs, at the highest temperature, a significant LPO and 8-OHdG increase was observed at higher Hg concentration in the mixture; moreover, a decrease was also perceptible in PC content when compared to single solutions of Hg. Individual effects of contaminants were potentiated by the presence of NPs; thus, an increase was observed by the interaction of NPs with mixture at higher temperature. Moreover, in this context the effects of NPs on PC oxidation at the highest temperature should also be considered as a clear indication of NPs on the role in ROS production. In addition, Mohmood et al (2014) already reported that the interference of the co-exposure of Hg with silica coated iron oxide NPs can modulate toxicity induced by their individual exposures as depicted in *A. anguilla* under *in vitro* conditions. In case of remediated solutions without NPs, a significant decrease in LPO was observed at higher concentration of Hg in the mixture (solution IV) at 28 °C whereas, in PC contents at 20 °C and 24 °C a decrease was observed when comparing the solution of Hg with mixture to the Hg alone, may be due to the absence of NPs from the remediated solutions. Moreover, our results also showed a significant decrease in the remediated solution without NPs when compared to the remediated solutions with NPs in the similar conditions where the decrease in mixtures was observed when compared Hg concentration alone. Taking into account the previous scenario (*i.e.* remediated solution with NPs) the role of NPs in oxidative stress induction cannot be overlooked.

4.5. CONCLUSION

In non-remediated solutions, Hg induced oxidative damage (LPO increase, 8-OHdG formation and PC oxidation) at all concentrations, either alone or in mixture in *A. anguilla* gill. In remediated solution (with and without NPs), the damage was lower than the non-remediated

solutions suggesting to that the ability of functionallized NPs for Hg decontamination. Nevertheless, the remediated solutions with NPs displayed higher toxicity than the remediated solutions without NPs. Concerning NPs alone, no change in biochemical responses were observed in fish exposed to NPs at 20°C.

Influence of temperature on NPs was clearly evident on PC and 8-OHdG levels as significant induction in these two parameters at highest temperature was observed in fish. In non-remediated solutions, gill exposure revealed a significant LPO, PC and 8-OHdG increase at all treatments with increasing temperature. In remediated solution with NPs, the influence of temperature was more prominent at the highest temperature as a significant increase in LPO (solution I, II and IV), PC contents (solution II) and 8-OHdG (at all the solutions) as well as a decrease in PC content (solution IV) was observed at 28C. In remediated solution without NPs, the similar pattern of responses was not recorded as in remediate solutions with NPs among studied parameters since the biochemical effects were limited to Hg concentrations alone. Thus, increase in temperature by 8°C revealed an increase in LPO and 8-OHdG (in solution I and II) and a decrease in PC content (in solution II), whereas increase of 4°C temperature depicted increase in LPO and 8-OHdG in solution II confirming that the oxidative stress inducing potential of Hg remediated solutions further increases with increase in temperature. Paradoxically, it was pointed out that remediation technologies efficient in decreasing the toxicity of contaminants at normal temperature can be at the risk of increased temperature and should be remodelled under the climate change scenario in future.

In the current study, based on the results of T-Hg accumulation and macromolecular damage responses viz. increased LPO, PC oxidation and 8-OHdG formation at three temperatures, *Anguilla anguilla* gill appears to be a very promising organ to be processed *ex vivo* for the assessment of the climate change stress in future studies.

4.6. REFERENCES

Ahmad I, Singh M K, Pereira ML, Pacheco M, Santos M A, Duarte AC, Pereira E, Grácio J. (2013) Morphological, compositional and ultrastructural changes in the Scrobicularia plana shell in response to environmental mercury – An indelible fingerprint of metal exposure? Chemosphere 90:2697–2704

Almrot BC, Sturve J, Stephensen E, Holth TF, Förlin L (2008) Protein Carbonyls and Antioxidant Defences in Corkwing Wrasse (Symphodus melops) from a Heavy Metal Polluted and a PAH Polluted Site. Marine Environmental Research. 66:271–277.

Ali SK, Ferencz A, Nemcsok J, Hermesz E (2010) Expressions of heat shock and metallothionein genes in the heart of common carp (Cyprinus carpio): effects of temperature shock and heavy metal exposure, Acta Biol. Hung. 61:10– 23

Ansaldo M, Luquet CM, Evelson PA, Polo JM, Llesuy S (2000) Antioxidant levels from different Antarctic fish caught around South Georgia and Shag Rocks. Polar Biol. 23: 160–165

Avery EL, Dunstan RH, Nell A (1996) The Detection of Pollutant Impact in Marine Environments: Condition Index, Oxidative DNA Damage, and Their Associations with Metal Bioaccumulation in the Sydney Rock Oyster Saccostrea commercialis 1996. Arch. Environ. Contam. Toxicol. 31, 192-198

Bradford MM (1976) A rapid and sensitive method for the quantitation of microgram quantities of protein utilizing the principle of protein-dye binding. Anal Biochem 7:248-254.

Belpaire C, Goemans G (2007) Eels: contaminant cocktails pinpointing environmental contamination ICES Journal of Marine Science 64: 1423-1436

Berntssen MHG, Aatland A, Handy RD (2003) Chronic dietary mercury exposure causes oxidative stress, brain lesions, and altered behaviour in Atlantic salmon (Salmo salar) parr. Aquat Toxicol 65(1):55–72.

Bird RP, Draper AH (1984) Comparative studies 568 on different methods of malondyhaldehyde determination, Methods in Enzymology, Academic Press 299–305

Britto RS, Garcia ML, Rocha AM, Flores JA, Pinheirc MVB, Monserrat JM, Ferreira JLR (2012) Effects of carbon nanomaterials fullerene C60 and fullerol C60(OH)18–22 on gills of fish Cyprinus carpio (Cyprinidae) exposed to ultraviolet radiation. Aquatic Toxicology; 114–115, 15:80–87

Brown CA, Sharp D, T. Collura CM. (2016) Effect of climate change on water temperature and attainment of water temperature criteria in the Yaquina Estuary, Oregon (USA). Estuarine, Coastal and Shelf Science; 169:136–146

Cember H, Curtis E H, Gordon Blaylock B (1978) Mercury bioconcentration in fish: temperature and concentration effects. Environ. Pollut. 17: 311–319

Clark TD, Sandblom E, Cox GK, Hinch SG, Farrell AP (2008) Circulatory limits to oxygen supply during an acute temperature increase in the Chinook salmon (Oncorhynchus tshawytscha), Am. J. Physiol. Regul. Integr. Comp. Physiol. 295:1631–R1639.

Costa LC, Mohmood I, Trindade T, Saleem M, Duarte AC, Pereira E, Ahmad I (2015) Rescheduling the process of nanoparticle removal used for water mercury remediation can increase the risk to aquatic organism: evidence of innate immune functions modulation in European eel (Anguilla anguilla L.) Environ Sci Pollut Res Int. 22(23):18574-89.

Croteau DL, Bohr VA (1997) Repair of oxidative damage to nuclear and mitochondrial DNA in mammalian cells. J Biol Chem 272:25409–25412.

Dijkstra JA, Buckman KL, Ward D, Evans DW, Dionne M, Chen CY (2013) Experimental and Natural Warming Elevates Mercury Concentrations in Estuarine Fish. PLoS One. 8(3): e58401.

Du J, Gebicki MJ (2004) Proteins are major initial cell targets of hydroxyl free radicals. Int. J. Biochem. Cell Biol. 36:2334-2343

Ercegovac M, Jovic N, Simic T, Beslac-Bumbasirevic L, Sokic D, Djukic T, Savic-Radojevic A, Matic M, Mimic-Oka J, Pljesa-Ercegovac M (2010) Byproducts of protein, lipid and DNA oxidative damage and antioxidant enzyme activities in seizure. Seizure 19: 205–210

European Parliament, C., 2008. Directive 2008/105/EC of the European Parliament and of the Council of 16 December 2008 on environmental quality standards in the field of water policy, amending and subsequently repealing Council Directives 82/176/EEC, 83/513/EEC, 84/156/EEC, 84/491/EEC, 86/280/EEC and amending Directive 2000/60/EC of the European Parliament and of the Council. Official Journal of the European Union.

Evans MD, Dizdaroglu M, Cooke MS (2004) Oxidative DNA damage and disease: induction, repair and significance. Mutat Res/Rev Mutat Res 567:1–61.

Guilherme S, Válega M, Pereira ME, Santos MA, Pacheco M (2008) Erythrocytic nuclear abnormalities in wild and caged fish (Liza aurata) along an environmental mercury contamination gradient. Ecotoxicol Environ Saf 70:411–421.

Guilherme S, Gaivao I, Pereira ME, Santos MA, Pacheco M (2010) European eel (Anguilla anguilla) genotoxic and pro-oxidant responses following short-term exposure to Roundup—a glyphosate-based herbicide. Mutagenesis 5;523–530.

Guinot D, Ureña R, Pastor A, Varó I, Del Ramo J, Torreblanca A (2012) Longterm effect of temperature on bioaccumulation of dietary metals and metallothionein induction in Sparus aurata. Chemosphere 87: 1215–1221.

Hattori RS, Fernandino JI, Kishii A, Kimura H, Kinno T, Oura M, Somoza GM, Yokota M, Strussmann CA, Watanabe S (2009) Cortisol-induced masculinization: does thermal stress affect gonadal fate in pejerrey, a teleost fish with temperature-dependent sex determination? PLoS One 4 (2009) e6548.

Hazel JR (1995) Thermal adaptation in biological membranes: Is homeoviscous adaptation the explanation? Annu Rev Physiol 57:19–42

Hegyi A, Beres T, Varadi L, Lefler KK, Toth B, Urbanyi B (2006) Investigation of long-term stress induced by several stressors by determination of the concentration of different blood plasma components in a model of Prussian carp (Carassius auratus gibelio BLOCH, and Common carp (Cyprinus carpio L., 1758), Acta Biol. Hung. 57: 301–313.

Hochachka PW, Somero GN (2002) Biochemical adaptation: mechanism and process in physiological evolution. Oxford University Press, Oxford

Huang W, Cao L, Ye Z, Yin X, Dou S (2010) Antioxidative responses and bioaccumulation in Japanese flounder larvae and juvenile esunder chronic mercury exposure. Comp. Biochem. Physiol. C152(1),99–106.

Hylander LD, Meili M (2005) The rise and fall of mercury: converting a resource to refuse after 500 years of mining and pollution. Crit. Rev. Environ. Sci. Technol. 35:1-36.

Khan MAQ, Ahmed SA, Bogdon C, Khodadoust A, Ajayi O, Vaugh M. Effect of Temperature on Heavy Metal Toxicity to Juvenile crayfish, Orconectes immunis (Hagen). Environ. Toxicol. 2006;5: 513-520

Lackner R (1998) ‘‘Oxidative stress’’ in fish by environmental pollutants. In: Braunbeck, T., Hinton, D.E., Streit, B. (Eds.), Fish Ecotoxicology. Birkhauser Verlag, Basel, pp. 203–224.

Laporte J-M, Andres S, Mason RP (2002) Effect of ligands and other metals on the uptake of mercury and methylmercury across the gills and the intestine of the blue crab (Callinectes sapidus) 2001 Comparative Biochemistry and Physiology Part C 131 185–196

Lemaire P, Viarengo A, Canesi L, Livingstone DR (1993) Pro-oxidant and antioxidant processes in gas gland and other tissues of cod (Gadus morhua). J. Comp. Physiol. 163: 477–486

Lopes CB, Figueira P, Tavares DS, Lin Z, Daniel-da-Silva AL, Duarte AC, Rocha J, Trindade T, Pereira E (2013) Core-shell magnetite-silica dithiocarbamate-derivatised particles achieve the Water Framework Directive quality criteria for mercury in surface waters. Environ Sci Pollut R; 9:5963-5974.

Lushchak VI (2011) Adaptive response to oxidative stress: Bacteria, fungi, plants and animals. Comparative Biochemistry and Physiology. Toxicology & harmacology: CBP, 153: 175-190.

Maciel FE, Ramos BP, Geihs MA, Vargas MA, Cruz BP, Meyer-Rochow VB, Vakkuri O, Allodi S, Monserrat JM, Nery LEM (2010) Effects of melatonin in connection with the antioxidant defense system in the gills of the estuarine crab Neohelice granulate Gen. Comp. Endocrinol., 165: 229–236

MacLeod J C, Pessah E. (1972) Temperature Effects on Mercury Accumulation, Toxicity, and Metabolic Rate in Rainbow Trout (Salmo gairdneri). Journal of the Fisheries Research Board of Canada 30(4): 485-492

Mahmoudi M, Shokrgozar A, Behzadia S (2013) Slight temperature changes affect protein affinity and cellular uptake/toxicity of nanoparticles. Nanoscale 5:3240-3244

Mieiro CL, Bervoets L, Joosen R, Blust R, Duarte AC, Pereira ME, Pacheco M (2011) Metallothioneins failed to reflect mercury external levels of exposure and bioaccumulation in marine fish – Considerations on tissue and species specific responses. Chemosphere 85, 114–121

Mohmood I, Lopes CB, Lopes I, Tavares DS, Soares AM, Duarte AC, Trindade T, Ahmad I, Pereira E (2016) Remediation of mercury contaminated saltwater with functionalized silica coated magnetite nanoparticles. Science of the Total Environment 557:712-721

Mohmood I, Ahmad I, Asim M, Costa L, Lopes CB, Trindade T, Duarte AC, Pereira E (2014) Interference of the co-exposure of mercury with silica coated iron oxide nanoparticles can modulate genotoxicity induced by their individual exposures - A paradox depicted in fish under in vitro conditions. Environ Sci Pollut Res Int. 22(5):3687-96.

Monteiro DA, Rantin FT, Kalinin AL (2010) Inorganic mercury exposure: toxicological effects, oxidative stress biomarkers and bioaccumulation in the tropical freshwater fish matrinxa˜, Brycon amazonicus (Spix and Agassiz, 1829) Ecotoxicology 19:105–123.

Nishizaki MT, Carrington E (2014)The effect of water temperature and flow on respiration in barnacles: patterns of mass transfer versus kinetic limitation. Journal of Experimental Biology 217: 2101-2109

Nolan RJ, Rick DL, Freshour NL. (1984) Chlorpyrifos: Pharmacokinetic in human volunteers. Toxicol Appl Pharmacol 73(1):8–15.

Ohkawa H, Ohishi N, Yagi K (1979). Assay for lipid peroxides in animal tissues by thiobarbituric acid reaction. Anal. Biochem. 95, 351-358.

Otomo PV, Reinecke SA, Reinecke AJ (2012) Combined effects of metal contamination and temperature on the potworm Enchytraeus doerjesi (Oligochaeta). Journal of Applied Toxicology 33;1520–1524

Padmini, E. (2010). Physiological Adaptations of Stressed Fish to Polluted Environments: Role of Heat Shock Proteins. Reviews of Environmental Contamination and Toxicology, Vol. 206, pp. 1–27, ISSN 0179-5953

Pack EC, Kim CH, Lee SH, Lim CH, Sung DG, Kim MH, Park KH, Hong SS, Lim KM, Choi DW, Kim SW (2014) Effects Of Environmental Temperature Change On Mercury Absorption In Aquatic Organisms With Respect To Climate Warming Journal of Toxicology and Environmental Health, Part A, 77:1477–1490.

Pacyna EG, Pacyna JM, Steenhuisen F, Wilson SJ (2006) Global anthropogenic mercury emission inventory for 2000. Atmospheric Environment, 40:4048-4063.

Perez-Casanova JC, Rise ML, Dixon B, Afonso LO, Hall JR, Johnson SC, Gamperl AK (2008) The immune and stress responses of Atlantic cod to long-term increases in water temperature, Fish Shellfish Immunol. 24:600–609.

Peuranen S, Keinanen M, Tigerstedt C, Vuorinen PJ (2003) Effects of temperature on the recovery of juvenile grayling (Thymallus thymallus) from exposure to Al + Fe, Aquat. Toxicol. 65:73–84.

Russell BD,Connell SD, Findlay HS, Tait K, Widdicombe S, Mieszkowska N (2013) Ocean acidification and rising temperatures may increase biofilm primary productivity but decrease grazer consumption. Philos Trans R Soc Lond B Biol Sci. 368(1627): 20120438.

Sayeed I, Parvez S, Winkler-Stuck K, Seitz G, Trieu I, Wallesch CW, Schonfeld P, Siemen D (2006) Patch clamp reveals powerful blockade of the mitochondrial permeability transition pore by the D2-receptor agonist pramipexole. FASEB J 20(3):556–558.

Santos M A, Pacheco M (1996) Anguilla anguilla L. Stress Biomarkers Recovery in Clean Water and Secondary Treated Pulp Mill Effluent. Ecotox Environ Saf 35:96-100.

Schreck CB (2002) Accumulation and long-term effects of stress in fish, in: G.P. Moberg, J.A. Mench (Eds.), The Biology of Animal Stress, CABI Publishing, Wallingford, UK, 147–158

Senthamilselvan D, Chezhian A, Suresh E, Ezhilmathy R (2012) Toxic effects of heavy metals (cadmium plus mercury) on haematological parameters and DNA damage in Lates calcarifer. Journal of Toxicology and Environmental Health Sciences Vol. 4:156-161,

Sekine M, Nakanishi H, Ukita M (1996) Study on fish mortality caused by the combined effects of pesticides and changes in environmental conditions, Ecol. Model. 86: 259–264.

Sevcikova M, Modrá H, Slaninova A, Svobodova Z (2011) Metals as a cause of oxidative stress in fish: A review Veterinární Medicína 56:537-546

Sohal RS, Kamzalov S, Sumien N, Ferguson M, Rebrin I, Heinrich KR, Forster MJ (2006) Effect of coenzyme Q10 intake on endogenous coenzyme Q content, mitochondrial electron transport chain, antioxidative defenses, and life span ofmice. Free Radic Biol Med 40(3):480–487.

Sokolova IM, Lannig G (2008) Interactive effects of metal pollution and temperature on metabolism in aquatic ectotherms: implications of global climate change. Climate Research 37: 181–201

Stohs SJ (1995) The role of free radicals in toxicity and disease - J Basic Clin Physiol Pharmacol 6(3-4): 205-228

Tarja N, Kirsti E, Marja L, Kari E (2003) Thermal and metabolic factors affecting bioaccumulation of triazine herbicides by rainbow trout (Oncorhynchus mykiss), Environ. Toxicol. 18: 219–226.

Tavares DS, Daniel-da-Silva AL, Lopes CB, Silva NJO, Amaral VS, Rocha J, Pereira E, Trindade T (2013) Efficient sorbents based on magnetite coated with siliceous hybrid shells for removal of mercury ions. J Mater Chem 1: 8134-8143..

Taze C, Panetas I, Kalogiannis S, Feidantsis K, Gallios GP, Kastrinaki G, Konstandopoulos AG, Václavíková M, Ivanicova L, Kaloyianni M (2016). Toxicity assessment and comparison between two types of iron oxide nanoparticles in Mytilus galloprovincialis. Aquat Toxicol. 172:9-20.

Tessier L, Vaillancourt G, Pazdernik L (1994) Comparative study of the cadmium and mercury kinetics between the short-lived gastropod Viviparus georgianus(Lea) and pelecypod Elliptio complanata(Lightfoot), under laboratory conditions. Environ. Pollut. 85: 271–282.

Valavanidis A, Vlachogianni T, Fiotakis C (2009) 8-Hydroxy-2'-deoxyguanosine (8-OHdG): a critical biomarker of oxidative stress and carcinogenesis. J Environ Sci Health Part C: Environ Carcinog Ecotoxicol 27:120–139.

Welfinger-Smith G, Minholz JL, Byrne S, Waghiyi V, Gologergen J, Kava J, Apatiki M, Ungott E, Miller PK, Arnason JG, Carpenter DO (2011) Organochlorine and metal contaminants in traditional foods from St. Lawrence Island, Alaska. J. Toxicol. Environ. Health A 74: 1195–1214

Valko M, Izakovic M, Mazur M, Rhodes CJ, Telser J (2004) Role of oxygen radicals in DNA damage and cancer incidence. Mol Cell Biochem 266:37–56.

Verlecar XN, Jena KB, Chainy GNB (2007) Biochemical markers of oxidative stress in Perna viridis exposed to mercury and temperature. Chemico-Biological Interactions 167:219–226

Xiu M, Pan L, Jin Q (2014). Bioaccumulation and oxidative damage in juvenile scallop Chlamys farreri exposed to benzo[a]pyrene, benzo[b]fluoranthene and chrysene. Ecotoxicol Environ Saf. 107:103-10

Xiong DW, Fang T, Yu LP, Sima XF, Zhu WT (2011) Effects of nano-scale TiO2, ZnO and their bulk counter parts on zebra fish: acute toxicity, oxidative stress and oxidative damage Sci. Total Environ., 409: 1444–1452

Yabanli M, Alparslan Y (2015) Potential Health Hazard Assessment in Terms of Some Heavy Metals Determined in Demersal Fishes Caught in Eastern Aegean Sea. Bull Environ Contam Toxicol 95:494-498

CHAPTER 5

Influence of temperature on nanoparticles remediated seawater-induced biochemical stress responses in Anguilla anguilla L.: Part II. Evaluation of enzymatic and non-enzymatic antioxidants

Abstract

The study aimed to assess the influence of temperature on the toxicity of Hg-contaminated saltwater before and after its remediation using dithiocarbamate functionalized silica coated magnetite nanoparticles (NPs), in the absence and presence of other hazardous contaminants (Cd and As), by evaluating fish antioxidants defence modulation responses using *ex vivo* approach. The enzymatic (catalase, glutathione peroxidase, glutathione reductase and glutathione S-transferase, GST) and non-enzymatic (non-protein thiol and total glutathione, GSH) antioxidants responses were monitored under the conditions of non-remediated solutions (before Hg remediation), remediated solutions (after Hg remediation) with and without NPs. An overall antioxidants induction was observed in all exposure scenarios (non-remediated and remediated solutions with and without NPs), except GR (in remediated solutions with NPs), GST, GPx and thiols (the later 3 in remediated solutions without NPs). Moreover, the antioxidants induction remains unaffected in presence of other contaminants. Comparing the different scenarios, a less pronounced antioxidants induction in remediated solutions (*vs.* non-remediated) was observed suggesting that the antioxidants modulatory response is due to the incomplete remediation of the Hg from the remediated solutions. Regarding the influence of temperature, in non-remediated, all antioxidants showed a differential response at increased temperatures depending on the Hg being alone or in a mixture, *i.e.* Hg individual exposure to gill revealed a significant antioxidants increase at increased temperature, whereas a decrease was perceptible under the scenario of Hg in mixture. In remediated solutions with NPs, antioxidants induction was discernible at 24 ºC in GPx, GR and thiols at lower concentration of Hg in mixture, whereas at 28 ºC all the antioxidants (except GPx) showed a significant increase suggesting that in predicted scenarios of increasing temperature the remediated water that caused almost no oxidative effects at 20 ºC, can exhibit oxidative effects with future increasing temperature. In remediated solution without NPs, the modulatory effect of temperature on antioxidants induction was perceptible even after the removal of NPs since at 24 ºC only CAT (solution I, II, IV) and GSH (solution III), whereas at 28 ºC all the antioxidants (CAT) showed a significant increase. Moreover, the antioxidant induction was less pronounced when compared to the non-remediated solutions at increased temperature suggesting that the benefits of the NPs decontamination further decrease with the increase of temperature. Overall, the antioxidant defences were likely overwhelmed in the fish gill, leading to increased Hg accumulation and exaggerated Hg toxicity when the temperature was increased. These observations have important implications for the survival of fish in polluted environments during seasonal warming and/or global climate change

Key words: *Climate change, Temperature, Mercury, Antioxidants responses, Ex-vivo, Anguilla anguilla, Gill*

Article to be submitted to Environmental Science and Pollution Research

5.1. INTRODUCTION

Mercury (Hg) is considered as one of the priority environmental contaminants (Sousa et al., 2013) due to its high toxicity to biota and global scale occurrence. Currently we know that its presence in aquatic systems cannot be exclusively attributed to individual emissions of Hg, but instead are mainly due to widespread air pollution. So, even in remote areas without anthropogenic pressures it is possible to detect the presence of Hg. Therefore, given this worldwide distribution and the fact that Hg undergoes bioaccumulation and biomagnification, its presence in aquatic systems, even at very low concentrations, represents a serious risk to biota. Moreover, its well-known toxicity is highly dependent on both abiotic (e.g. temperature) and biotic factors (Dijkstra et al., 2013). For instance, Pack et al. (2014) concluded that several factors, associated to climate change, stimulate the methylation of Hg, converting less toxic Hg species into one of the most toxic species (methymercury, MeHg). This is particularly worrying, since latest models proposed by the U.N. intergovernmental Panel on Climate Change (IPCC 2013) predict that the mean global temperature increase by the end of the 21st century is likely to exceed 1.5 °C in all scenarios. It has also been simulated that ocean warming rates of 0.4 °C and 1 °C may predict increases in the mean MeHg concentration of 1.7% (range, 1.6 – 1.8%) and 4.4% (range, 4.1 – 4.7%), respectively, resulting in elevated MeHg concentrations in fish (Booth and Zeller, 2005). Therefore, warmer waters are expected to affect Hg accumulation in aquatic organisms, including fish (Welfinger-Smith et al., 2011).

Additionally, the assessment of Hg-toxicity profile can become even more challenging and complex since Hg is not the only hazardous contaminant in the environment and, commonly, aquatic organisms are subjected to a multi-contamination scenario. Therefore, there is a constant need to take necessary steps towards its removal from the environment. In this direction, a credible number of research papers have revealed the evaluation of potential use of silica coated iron oxide nanoparticles functionalized with dithiocarbamate groups (Fe_3O_4@SiO_2/SiDTC, hereafter called NPs) for the removal of Hg and other potential toxic elements from contaminated waters (Tavares et al., 2013, 2014, Mohmood et al., 2016). Recent research revealed the efficiency of this nano-remediation process in the reduction of Hg toxicity from Hg remediated seawater by assessing the lethal effect on different marine organisms (Mohmood et al., 2016). The study was carried out at two levels of contamination, and the results showed that after nano-remediation, the mixture with lower Hg concentration (50 µg/L) exhibited no toxicity to rotifer *Brachionus plicatilis* and bacteria *Vibrio fischeri*; however, the mixture with higher concentration (500 µg/L) revealed toxicity. This work was

developed under laboratory controlled temperature (20 °C), and therefore, it is important to understand if the efficiency of the nano-remediation process is sufficient enough to mitigate the water toxicity, when affected by abiotic factors like the increase of water temperature. Such increase in water temperature may lead to higher metabolic rates, higher uptake of chemicals and consequently to the increase of water toxicity (Sokolova et al., 2008; Khan et al., 2006; MacLeod and Pessah 1973). Thus, the low levels of Hg remaining in solutions after the nano-remediation could became more toxic at temperatures higher than 20 ºC. In this perspective, the influence of increased temperature on toxicity reduction of Hg remediated seawater was also evaluated taking into account the sub-lethal effects on fish, by assessing the oxidative stress induced macromolecular damages such as lipids peroxidation (LPO), proteins carbonyls (PC) and 8-hydroxy-2′-deoxyguanosine (8-OHdG) formations (Chapter 4). The obtained results (Chapter 4) pointed out that the nano-remediation efficiency (confirmed by decrease in toxicity at 20 ºC) may be compromised under future scenarios of temperature increase (Chapter 4). Therefore, it is important to address the role of antioxidants defence mechanism in response to Hg remediated seawater induced damage under more realistic conditions. Interestingly, despite the successful employment of various enzymatic and non-enzymatic antioxidants responses in assessing contaminates status under both field and simulated laboratory conditions (Ahmad et al., 2004, 2006, 2011, 2012), no study in the literature has been reported in this context.

Fishes as test organisms fulfils every requirements as bioindicator species (Sedeño-Díaz and López-López 2012; Belpaire and Goemans 2007) and can exhibit a cumulative response to interactive effects of stressors (Hegyi et al., 2006). Under normal physiological condition, fish maintain a balance between generation and neutralization of reactive oxygen species (ROS) by modulating antioxidants induction. Mercury in particular, challenges ROS scavenging capacity by reacting not only with proteins' sulfhydryl groups (Patnaik et al., 2010), but also by modulating enzymatic (CAT-catalase; GST-glutathione S-transferase, GPx-glutathione peroxidase and GR-glutathione reductase) and non-enzymatic (non-protein thiol and glutathione-GSH) antioxidants (Ahmad et al., 2008; Mieiro et al., 2011; Sevcikova et al., 2011). Thus, the current study aimed to assess the influence of increased temperature on the role of antioxidants responses against toxicity of nano-remediated Hg-contaminated saltwater in the presence and absence of arsenic (As) and cadmium (Cd). In order to accomplish the objectives, the same approach was considered as describe in Chapter 4, in addition to considering the assessment of various enzymatic (CAT, GST, GPx, GR) and non-enzymatic (non-protein thiols, GSH) antioxidants status.

5.2. MATERIALS AND METHODS

5.2.1. Chemicals

All chemicals used in this work were of analytical reagent grade. Bovine serum albumin (BSA), bradford reagent, butylated hydroxytoluene (BHT), diethylenetriaminepentaacetic acid (DTPA), methanol, phosphate buffered saline (PBS), potassium hydroxide (KOH), RPMI-1640 medium tricloroacetic acid (TCA), trizma hydrochloride reagent grade (Tris-HCl), 2-thiobarbituric acid (TBA), 1-Chloro-2,4-dinitrobenzene (CDNB), 5,5′-Dithiobis(2-nitrobenzoic acid) (DTNB), ethylenediaminetetraacetic acid (EDTA), guanidine hydrochloride used for this study were purchased from Sigma. arsenic(III) chloride (1000 ± 2 mg/L) and mercury(II) nitrate standard solution (1000 ± 2 mg/L) were purchased from BDH Chemicals Ltd, while the certified standard solution of cadmium(II) nitrate (1001 ± 2 mg/L) was purchased from Merck.

Regarding the NPs, dithiocarbamate (functionalized silica coated magnetite materials) were investigated for remediation of seawater spiked with single (Hg) or a mixture of (Hg, As and Cd) contaminants. The magnetic NPs were kindly provided by the Associated Laboratory CICECO, University of Aveiro, Portugal. The details pertaining to the synthesis and characterization of these magnetic NPs can be obtained in Tavares et al. (2013).

5.2.2. Fish and experimental design

Fish gill obtained previously were processed for the current study. The information regarding the fish and experimental design can be seen in the Materials and Methods section of Chapter 4.

5.2.3. Measurements of Antioxidants defence responses

5.2.3.1. Enzymatic antioxidants

Catalase (CAT) activity measurement

Catalase activity was assayed according to the methods adopted by Ahmad et al., (2011) with little modifications. Reaction mixture consisted of 100 µL phosphate buffer (0.05 M, pH 7.0), 50 µL H_2O_2 (50 mM) and 10 µL of mitochondrial preparations in a final volume of 160 µL. The absorbance of each plate was measured at 240 nm, on SpectraMax 384 Plus

Microplate Reader, during 3 minutes. Catalase activity was calculated in terms of μmol H_2O_2 consumed/min/mg protein (ε = 43.5 /M cm).

Glutathione peroxidase (GPX) activity measurement

Glutathione peroxidase activity was assayed according to the methods adopted by Ahmad et al. (2011) with little modifications. Briefly, reaction mixture consisted of 60 μL of phosphate buffer (0.1 M, pH 7.0), 20 μL of mitochondrial preparations, 20 μL of GR (2.40 U/mL), 20 μL of GSH (10 mM), 20 μL sodium azide (1 mM), 20 μL EDTA/Na_2 (10 mM), 20 μL of NADPH, 20 μL of H_2O_2 (1.5 mM) in total volume of 200 μL. Oxidation of NADPH was recorded spectrophotometrically at 340 nm during 3 minutes with 30 seconds time interval, at room temperature on SpectraMax 384 Plus Microplate Reader. The enzyme activity was calculated as nmol NADPH oxidized/min/mg protein ($\varepsilon = 6.22\times10^3$ /M cm).

Glutathione reductase (GR) activity measurement

Glutathione reductase activity was assayed in sample according to the method described by Mohandas et al. (1984) with some modifications. Briefly, the assay mixture contained 0.0086 g of NADPH, 0.0327 g of GSSG (oxidized glutathione), 0.0098 g DTPA and then dissolved in 25 mL of distilled water. The final volume was made 50 mL by adding 25 mL of phosphate buffer (0.05 M). Then 150 μL of reaction mixture and 10 μL of mitochondrial preparations were mixed during some minutes. The absorbance of each plate was measured at 340 nm during 3 minutes with 30 seconds time interval on SpectraMax 384 Plus Microplate Reader. The enzyme activity was calculated as nmol NADPH oxidized/min/mg protein ($\varepsilon = 6.22\times10^3$ /M cm).

Glutathione S-transferase (GST) activity measurement

Glutathione S-transferase activity was assayed in sample using the method of Habig et al. (1974) with some modifications. The reaction mixture consisting 125 μL buffer (before adding the buffer was kept in the hot water bath at 30 °C), 10 μL mitochondrial preparations, 8 μL reduced glutathione (20 mM) and 8 μL CDNB (20 mM) in total volume of 151 μL was assayed. The change in absorbance was recorded on SpectraMax 384 Plus Microplate Reader at 340 nm and the enzyme activity calculated as mmol CDNB conjugate formed/min/mg protein (ε = 9.6 /mM cm).

5.2.3.2. Non-enzymatic antioxidants

Total non-protein thiols (NP-SH)

Non-protein thiols were measured as described by methods adopted by Ahmad et al. (2008) with few modifications. Briefly, the mitochondrial preparations 25 µL was precipitated with a solution of 25 µL (1:1) of sulphosalicydic acid (5%) in eppendorf, vortexed for few seconds and were left in the ice for 45 minutes to precipitate. Afterward, all the eppendorfs were centrifuged at 2500 × g during 5 minutes. The assay mixture contained 30 µL of filtered aliquot, 150 µL of phosphate buffer (0.1 M, pH 7.4) and 15 µL DTNB (10 mM) in a total volume of 195 µL. The optical density of reaction product was read immediately at 412 nm on a spectrophotometer SpectraMax 384 Plus Microplate Reader and the results were expressed as µmol TNB formed/mg protein ($\varepsilon = 136 \times 10^3$ /mM cm).

Total glutathione (GSH)

Total glutathione contents were measured as described by the methods adopted by Ahmad et al. (2008) with a little modification. Briefly, the mitochondrial preparations of 25 µL was precipitated with a solution of 25 µL (1:1) of sulphosalicydic acid (5%) in eppendorfs, vortexed for few seconds and were left in the ice for 45 minutes to precipitate. Afterward, eppendorfs were centrifuged at 2500 × g during 5 minutes. TGHT content was determined in the resulting supernatant adopting the enzymatic recycling method using GR excess, whereby the sulfhydryl group of GSH reacts with DTNB producing a yellow coloured TNB. The rate of TNB production is directly proportional to this recycling reaction, which is in turn directly proportional to the concentration of GSH in the sample. The formation of TNB was measured at 412 nm on SpectraMax 384 Plus Microplate Reader and the results were expressed as nmol TNB formed/min/mg protein ($\varepsilon = 14.1 \times 10^3$ /M cm).

5.2.4. Protein concentration measurement

Total protein was determined according to the Bradford method (1976) using bovine serum albumin (BSA) as standard. The assay mixture contained 990 µL of Bradford reagent, 10 µL of diluted BSA (2.5 mg/mL) and 10 µL miliQ-water. The absorbance of plate was measured at 595 nm after incubate during 10 min in dark on SpectraMax 384 Plus Microplate Reader.

5.2.5. Statistical Analysis

The software SigmaPlot 12.0 was used for statistical analysis of data. Data were tested for Normality (Shapiro-Wilk) and homoscedasticity of Variance. A two-way ANOVA was carried out in order to ascertain differences between three exposed temperature and treatments groups and was followed by the Holm-Sidak test. Spearman rank correlation factor (r) was used to test significant relations between T-Hg in gill tissue antioxidants responses. A significance level of 0.05 was ascertained in all test procedures.

5.3. RESULTS

The results presented below describe the observations based on the antioxidants responses during different exposure conditions at changing temperature. The details pertaining to Hg levels in tissue can be seen in the results section of Chapter 4.

Within the same temperature, comparison between control and NPs revealed no significant changes except for CAT and GPx, which exhibited an increased activity when exposed to the NP at the highest temperature (28 °C) (Figure 5.1). In non-remediated solutions, significant increase in enzymatic (CAT, GPx, GR, GST) and non-enzymatic (thiols and T-GSH) antioxidants was observed at all three temperatures, except in GPx at 24 ℃ and 28 ℃ in the solution III when compared to respective controls. On the perspective of remediated solutions with NPs, no defined pattern of antioxidants induction was observed as an increase was observed in CAT (solutions I, III at 24 ℃ and II, IV at all temperatures), GPx (solution III at 24 ℃), GR (solutions III, IV at 24 ℃ and 28 ℃), GST (solutions II and IV at 28 ℃), thiols (solution I–IV at 24℃ and/or 28 ℃), GSH (solution I–IV at 24 ℃, 28 ℃) and decrease was perceptible in GPx (solutions I, II, III at 28 ℃) and GST (solutions I and III at 20 ℃) when compared to respective controls. In remediated solution without NPs, comparison with control revealed an incremental trend of enzymatic antioxidants induction in fish; however, at different temperature and treatments. Thus, a significant increase was observed in CAT (solution I–IV at 24 ℃), GPx (solution II at 20 ℃), GR (solution I –IV at 20 ℃ and 28 ℃), GST (solutions II, IV at 28 ℃), thiols (solution IV at 28 ℃) and GSH (solution I at 28 ℃; III at 24 ℃, 28℃; solution II, IV at all temperatures)

Comparison of remediated solutions with non-remediated solutions reflected a significant decrease in enzymatic (CAT, GPx, GR, and GST) and non-enzymatic (thiols and

GSH) antioxidants in all remediated solutions, with and without NPs, at different temperatures, except in GPx activity at solution III, in remediated solution without NPs.

Looking at the influence of As and Cd on the effects of Hg in non-remediated solutions, a significant decrease was observed in gill mitochondrial CAT activity only at higher Hg concentration in the mixture (solution IV at 28°C) in comparison to corresponding single Hg concentration. In addition, a significant decrease was observed in GPx and GR at lower and higher Hg concentrations in mixture solutions (solutions III and IV at 28 °C) when compared to corresponding single Hg concentrations. Moreover, in non-enzymatic antioxidants a significant decrease was observed in both lower and higher Hg concentrations in mixture solutions (solutions III and IV at 28 °C) when compared to corresponding Hg concentrations alone. In remediated solution with NPs, among enzymatic antioxidants, a significant increase was observed in CAT (solution III at 24 °C) and GST (solution III at 28 °C) activity in comparison to lower Hg concentration alone, whereas in GR activity a significant increase was observed at both lower and higher Hg concentrations in mixture solutions (solutions III and IV at 28 °C) when compared to their corresponding single Hg concentrations.

Inter-temperature comparison revealed no statically significant changes in *A. anguilla* gill enzymatic and non-enzymatic antioxidants among controls at different temperatures. In NPs exposed group, a significant increase was observed at the highest temperature (28 °C) in CAT and GPx among all the studied enzymatic and non-enzymatic parameters when compared to 20 °C. In non-remediated solutions, comparing 24 °C *vs*. 20 °C, gill exposure revealed a significant increase in GPx (solution I) and GR (solutions I and II), as well as a decrease in CAT, GPx and GR activity at higher concentration of Hg in mixture. At 28 °C, a significant increase in CAT (solutions I and II), GPx (solution I), GR (solutions I, II and III), GST (all solutions), thiols (solutions I and II) and GSH (solutions II and IV), whereas a decrease in CAT (solutions III and IV), GPx (solutions III and IV), GR (solution IV), thiols (solutions III and IV) was observed when compared to 20°C and/or 24 °C. In remediated solutions with NPs, at the difference of 4 °C (24 °C *vs* 20 °C), a significant increase in CAT (solutions III and IV), GPx (solutions III and IV), GR (solutions I and III), GST (solutions II, III and IV), thiols (solution III) and GSH (solutions III and IV) was observed when compared to 20 °C. At highest temperature (28°C *vs*. 20°C and/or 24 °C) a significant increase in CAT (solution II), GR (solutions I, III and IV), GST (solutions II, III and IV), thiols (solutions II, III and IV) and GSH (solutions III and IV) whereas a decrease in CAT (solutions III and IV), GPx (all

solutions) and GSH (solution II) activity was observed. In remediated solutions without NPs, between all the studied parameters, at 24 °C, a significant increase in CAT (solutions I, II and IV), GST (solution IV) and GSH (solution III) activity was observed when compared to 20 °C. At 28 °C (*vs*. 20°C and/or 24 °C), a significant increase in CAT (solution IV), GR (all solutions), GST (solutions III and IV), thiols (solution IV) and GSH (solutions I and III) activity was observed whereas a decrease was observed in CAT (solutions I and II) and GPx (solutions I, II and III) activity.

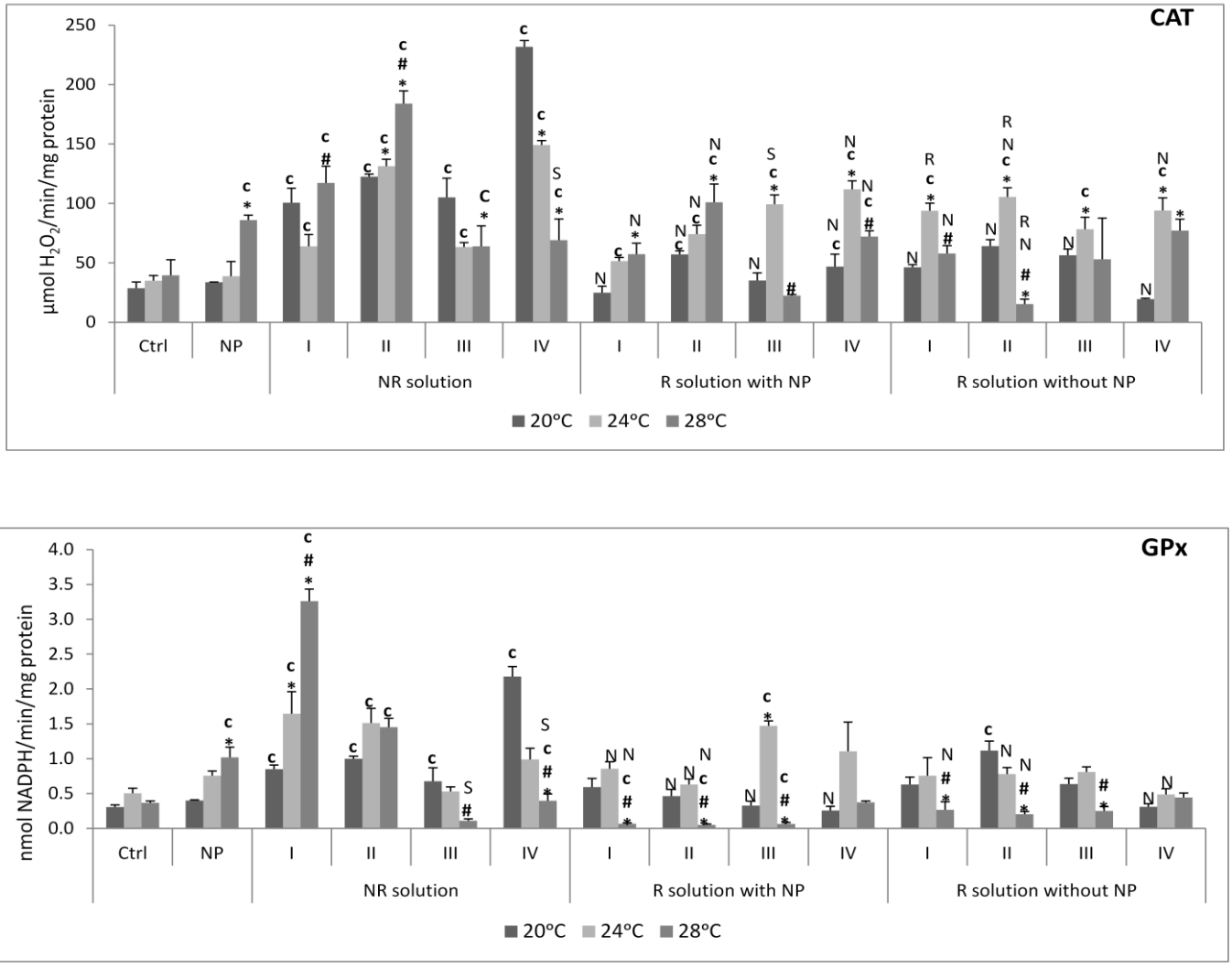

Figure 5.1. *A. anguilla* gill antioxidant (catalase, CAT; glutathione peroxidase, GPx; glutathione reductase, GR; glutathione S-transferase, GST; thiols and total glutathione, GSH) modulation in response to the exposures of non-remediated (NR), remediated (R) with NPs and without NPs solutions (Solution **I** = Hg 50 µg/L, **II** = Hg 500 µg/L, **III** = Hg 50 µg/L, As 1000 µg/L, Cd 200 µg/L and **IV=** Hg 500 µg/L, As 1000 µg/L, Cd 200 µg/L). Inter-group significant differences ($p<0.05$) have been denoted by letters: c (*vs*. control), N (*vs*. non-remediated), R (*vs*. remediated with NP), s (*vs*. Hg alone solutions) and inter-temperature significant differences have been marked by symbols * (*vs*. 20 °C), # (*vs*. 24 °C). Error bars show the standard error.

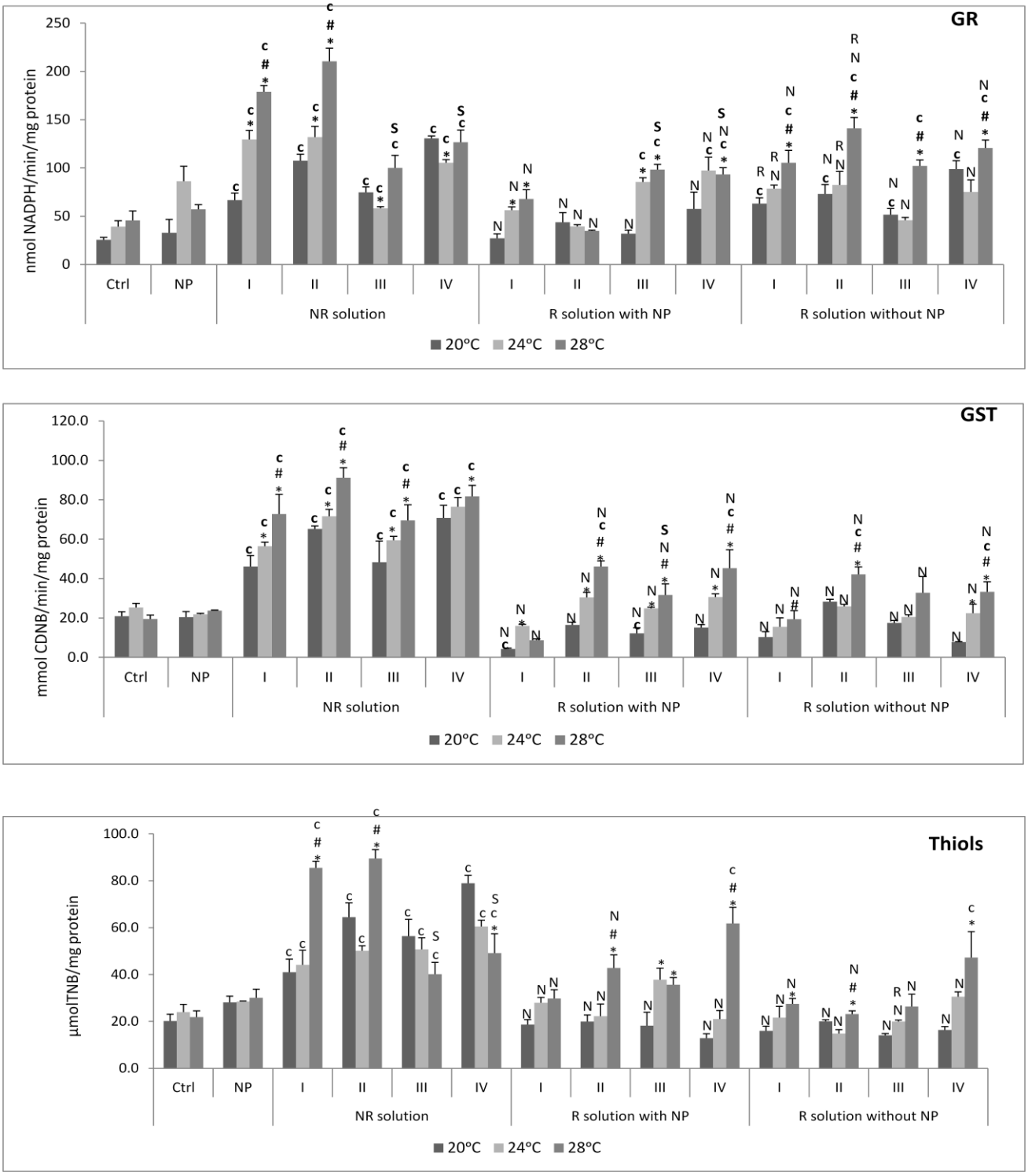

Figure 5.1. continued *A. anguilla* gill antioxidant (catalase, CAT; glutathione peroxidase, GPx; glutathione reductase, GR; glutathione S-transferase, GST; thiols and total glutathione, GSH) modulation in response to the exposures of non-remediated (NR), remediated (R) with NPs and without NPs solutions (Solution **I** = Hg 50 µg/L, **II** = Hg 500 µg/L, **III** = Hg 50 µg/L, As 1000 µg/L, Cd 200 µg/L and **IV=** Hg 500 µg/L, As 1000 µg/L, Cd 200 µg/L). Inter-group significant differences ($p<0.05$) have been denoted by letters: c (*vs*. control), N (*vs*. non-remediated), R (*vs*. remediated with NP), s (*vs*. Hg alone solutions) and inter-temperature significant differences have been marked by symbols * (*vs*. 20 °C), # (*vs*. 24 °C). Error bars show the standard error.

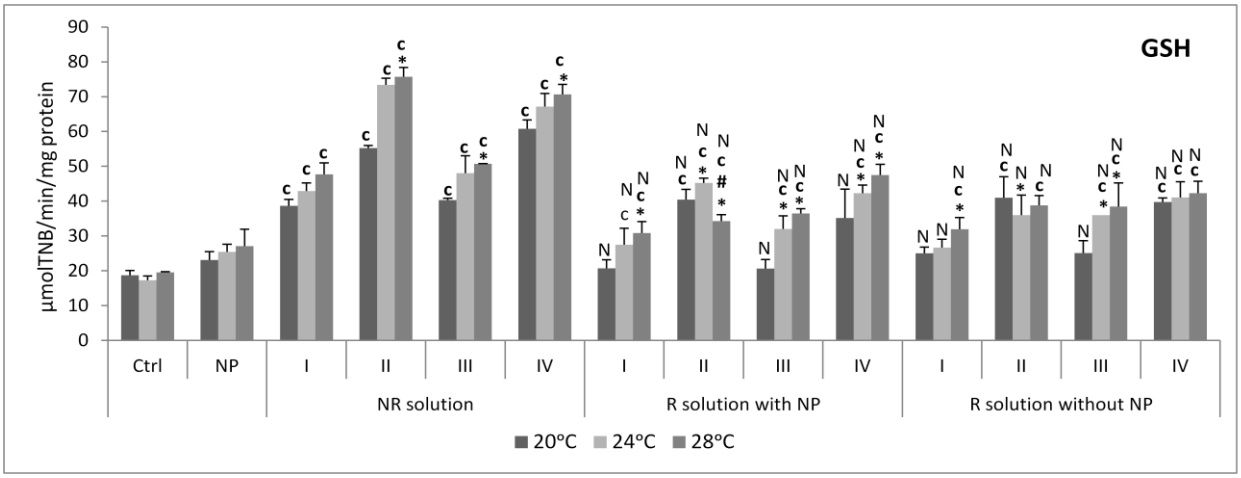

Figure 5.1. continued *A. anguilla* gill antioxidant (catalase, CAT; glutathione peroxidase, GPx; glutathione reductase, GR; glutathione S-transferase, GST; thiols and total glutathione, GSH) modulation in response to the exposures of non-remediated (NR), remediated (R) with NPs and without NPs solutions (Solution **I** = Hg 50 µg/L, **II** = Hg 500 µg/L, **III** = Hg 50 µg/L, As 1000 µg/L, Cd 200 µg/L and **IV=** Hg 500 µg/L, As 1000 µg/L, Cd 200 µg/L). Inter-group significant differences ($p<0.05$) have been denoted by letters: c (*vs*. control), N (*vs*. non-remediated), R (*vs*. remediated with NP), s (*vs*. Hg alone solutions) and inter-temperature significant differences have been marked by symbols * (*vs*. 20 °C), # (*vs*. 24 °C). Error bars show the standard error.

5.4. DISCUSSION

Following the results obtained in Chapter 4, the current study constitutes a further step in order to achieve the understanding of antioxidants protection responses against Hg before and after their nano-remediation, in absence and presence of other hazardous contaminants such as As and Cd, as well as exposure at increased temperature. It was observed that NPs alone showed no induction of antioxidants in fish in comparison to control kept at the reference temperature (20 °C). To the authors, it is the first study of its kind and the finding under *ex vivo* condition marks a clear difference with the only *in vitro* studies using the same NPs done by Srikanth et al (2015) and Anjum et al (2014), showing the modulation of antioxidants by the NPs exposure suggesting that the role of NPs may be different under more natural environmental conditions. While studying the role of antioxidants under different contaminants scenarios, an overall antioxidants inducing trend was perceptible in the gill responses under non-remediated solutions. Thus, CAT and GPX induction that provides an indication of the higher H_2O_2 amount production in solutions of Hg alone or in mixture was observed in the current study. Interestingly, the antioxidants induction was not sufficient to prevent pre-

oxidative damage, such as the induction in LPO, PC and 8-OHdG that was observed and reported in the previous chapter. Detoxification enzymes, such as GST, which helps in eliminating reactive compounds by forming conjugates with glutathione and subsequently eliminating them as mercapturic acid, thereby protecting cells against ROS damage (Rodriguez-Ariza et al., 1991), was also induced. According to Ahmad et al. (2008), GST induction in the presence of Hg suggests its antioxidant action against metals, rather than its role at phase II detoxification, since metals have not been reported as substrate to GSTs. The GR induction suggests its important role in maintaining the thiol status of the cell. As GR is involved in regenerating reduced glutathione from oxidized glutathione, its induction becomes highly essential under all stress conditions, which has been seen in the present study. In this perspective, the generation of new GSH and thiol cannot be overlooked. The GSH rise detected cannot be explained by the increased regeneration of oxidized glutathione carried out by this enzyme, but represents a GSH new synthesis as an adaptive response towards its increased use (Ahmad et al., 2008). As per the thiols contents increase it can be suggested that other thiols (e.g. N-acetyle-L-cysteine) are also playing an important role in Hg toxicity adaptations.

In remediated solutions with NPs, no defined pattern of antioxidants responses was observed in comparison to control suggesting an adaptation to increase the detoxification activity generated due to the incomplete removal of the Hg from the solutions after remediation. However, a significant reduction in the levels of all the antioxidants was observed in comparison to non-remediated solutions suggesting the NPs' efficiency in reducing the potential of Hg induced antioxidants increase, in parallel to decreased Hg accumulation. Therefore, all the studied antioxidants came to levels near their normal/basal level except increase in CAT (solutions I and III at 24 ℃ and solutions II and IV at all temperatures), GPX (solution III at 24 °C), GR (solutions III and IV at 24 ℃ and 28 °C), GST (solutions II and IV at 28 ℃), thiols (solutions I toIV at 24℃ and/or 28 °C), GSH (solutions I to IV at 24 °C, 28 °C) and decrease in GPx (solutions I, II and III at 28 °C) and GST (solutions I and III at 20 °C) strengthening the observation that the incomplete removal of Hg was most probably the cause of antioxidants modulations in different exposure conditions providing protection against oxidants.

In remediated solution without NPs, a significant increase in CAT (solution I–IV at 24 °C), GPx (solution II at 20 °C), GR (solutions I–IV at 20 ℃ and 28 ℃), GST (solutions II and IV at 28 °C), thiols (solution IV at 28 °C) and GSH (solution I at 28 °C; solutions III at 24 °C and 28°C; solutions II, IV at all temperatures), was still persistent suggesting that the

continuity of the role of GSH and its restoring enzymes to cope with the oxidative stress induced by Hg left after remediation. The results observed with increasing temperatures may be due the combine effect of contaminants with elevated temperatures. The details of these results are been given below.

Coming to the aspect of increased temperature impacts on various conditions, no significant effect of increased temperatures on antioxidants responses were observed when comparison was made among controls kept at three temperatures. However, the influence of temperature in the effects of NPs and of Hg either alone or combined with other contaminants is clearly evident in the current study since, increased CAT and GPX activities were observed at the highest temperature in NPs exposed gill showing the rise in effects due to NPs and temperature interaction. Moreover, this indicates that the NPs antioxidants inducing potential did not corroborate with macromolecular damage observed earlier (Chapter 4), as a significant PC and 8-OHdG increase to the same exposure conditions was perceptible. This difference in responses highlights the advantages of using protein carbonyls as a complementary tool of oxidative stress due to the rapid formation (Almroth et al., 2008; Dalle-Donne et al 2003) and relative stability of accumulated carbonylated proteins in tissues (Melzner et al., 2009). However, not all the antioxidants were induced since other antioxidants reflected no response to NPs exposure. The high activities of the H_2O_2 scavenging enzymes such as CAT and GPx, showed in fish gill (Figure 5.1), suggest excess of H_2O_2 production as a result of elevated temperature affecting the metabolism and therefore influence the uptake/ excretion of NPs. Effective induction of these enzymes in cells and tissues would help to clear the peroxides accumulated under stress however, not fully applicable as PC induction was there in our previous study.

In non-remediated solutions, all antioxidants at different temperatures showed a differential response depending on the Hg being alone or in mixture; *i.e.* Hg individual exposure to gill revealed a significant antioxidants increase, whereas a decrease was perceptible under the scenario of Hg in mixtures. The increase in antioxidants is a clear reflection of the oxidative stress inducing potential of Hg. To neutralize the impact of reactive oxygen species (ROS), both enzymatic and non-enzymatic antioxidants are activated (Lopez-Torres et al., 1993). In addition, the decrease in the activities of antioxidant enzymes may result when the stress, (in this case temperature and the mixture of contaminants), is overwhelmed and cannot be compensated anymore (Kaur et al 2005). These data may be

interpreted as possible protection by antioxidant and detoxifying enzymes, which could be sensitive to ROS generated during thermal stress however, not able to abolish the damage.

In remediated solutions with NPs, all antioxidants showed a significant increase in gill at temperature of 24 ºC when exposed to Hg concentration either alone or in mixtures suggesting that the interactive effect of temperature on Hg left after its removal from the seawater solutions by using NPs. Nevertheless, a decrease in antioxidants activities was also perceptible in comparison to non-remediated solutions clearly indicating the NPs effective role in Hg remediation, making Hg less available for oxidative stress induction. In contrary, at the highest temperature CAT and GPx showed a significant decrease in addition to general antioxidants induction. The antioxidants decrease should be considered as the stress is overwhelmed and cannot be compensated anymore (Kaur et al 2005) as suggested previously. In this particular situation the role of NPs, at this particular temperature in antioxidants induction cannot be overlooked since NPs alone at the highest temperature showed a significant increase of some enzymes (CAT and GPx).

In the remediated solution without NPs, the modulatory effect of temperature is perceptible even after the removal of NPs from the remediated solution with NPs. Moreover, the antioxidant induction was less pronounced as compared to the non-remediated solutions. Hence, at 24 ℃ a significant increase in CAT (at all solutions), GST (at higher Hg concentration in the mixture) and GSH (at lower Hg concentration in the mixture) activity was observed. Whereas, at the highest temperature (28 ℃) a significant decrease in CAT and GPx activity as well as an increase in GR, GST, thiols and GSH was observed. This incremental trend of antioxidants induction is clearly reflecting that the Hg that remained in solution after the remediation or the presence of other contaminations was augmented by increasing temperature.

While comparing single *vs.* mixture solutions, in non-remediated solutions, only at the highest temperature (28 °C) a significant decrease in CAT at higher Hg concentration, as well as in GPx, GR and thiols at both (lower and higher) concentrations of Hg in mixture solutions was observed. The decrease in antioxidant (CAT, GPx, GR and Thiols) at the highest temperature in mixture clearly indicates the antioxidant protection failure due to interaction of contaminants with temperature. In remediated solutions with NPs, the overall effect of temperature and contaminants was perceptible at both the temperature; however, specific to CAT, GR and GST only. Thus, CAT increase was observed at 24 °C, whereas GR and GST

increase was observed at 28 °C. The results suggest that in predicted scenarios of increasing temperature the remediated water that caused almost no oxidative effects at 20 ºC, can exhibit oxidative effects in mixture with future increasing temperature.

5.5. CONCLUSION

An overall antioxidants induction was observed in all exposure scenarios (non-remediated and remediated solutions with and without NPs), except for GR (in remediated solutions with NPs), GST, GPx and thiols (the later 3 in remediated solutions without NPs). In addition, the antioxidants induction remains unaffected in presence of As and Cd. Comparing the different scenarios, a less pronounced antioxidants induction in remediated solutions (*vs.* non-remediated) was observed, suggesting that the antioxidants modulatory response is due to the incomplete nano-remediation of the Hg. Regarding the influence of temperature, in non-remediated solutions, all antioxidants showed a differential response at elevated temperatures depending on the Hg being alone or in a mixture. In remediated solutions with NPs, antioxidants induction was discernible at 24 ºC in GPx, GR and thiols at lower concentration of Hg in mixture, whereas at 28 ºC all the antioxidants (except GPx) showed a significant increase suggesting that in predicted scenarios of increasing temperature the remediated water, can exhibit oxidative effects with future increasing temperature. In remediated solution without NPs, the modulatory effect of temperature on antioxidants induction was perceptible even after the removal of NPs. Moreover, the antioxidant induction was less pronounced when compared to the non-remediated solutions at increased temperature suggesting that the benefits of the NPs decontamination further decrease with the increase of temperature. Overall, the antioxidant defences were likely overwhelmed in the fish gill, leading to exaggerated Hg toxicity when the temperature was increased. These observations have important implications for the survival of fish in polluted environments during seasonal warming and/or predicted global climate change scenarios.

Anguilla anguilla gill proved to be a good *ex viv*o model for Hg and other hazardous contaminants toxicity assessment under the climate change scenario. The data presented here emphasizes the importance of need for more research to understand the extent of the ability or lack of that in aquatic organisms to tolerate metals and other biocidal chemical insults during the current climate change.

5.6. REFERENCES

Ahmad I, Pacheco M, Santos MA (2004) Enzymatic and non-enzymatic antioxidants as an adaptation to phagocyte-induced damage in Anguilla anguilla L. following in situ harbor water exposure. . Ecotoxicology And Environmental Safety 3, 57, 290-302.

Ahmad I, Maria VL, Oliveira M, Pacheco M, Santos MA (2006) Oxidative stress and genotoxic effects in gill and kidney of Anguilla anguilla L. exposed to chromium with or without pre-exposure to β-naphthoflavone. Mutation Research 1, 608, 16-28.

Ahmad I, Maria VL, Oliveira M, Serafim A, Bebianno MJ, Pacheco M, Santos MA (2008) DNA damage and lipid peroxidation vs. protection responses in the gill of Dicentrarchus labrax L. from a contaminated coastal lagoon (Ria de Aveiro, Portugal). Science Of The Total Environment 406, 1-2, 298-307.

Ahmad, I., Mohmood, I., Mieiro, C. L., Coelho, J. P., Pacheco, M., Santos, M. A., Duarte, A. C., Pereira, E (2011) Lipid peroxidation versus antioxidant modulation in the bivalve Scrobicularia plana in response to environmental mercury–organ. Aquatic Toxicology. 103, 3-4, 150-158.

Ahmad I, Mohmood I, Coelho JP, Pacheco M, Santos MA, Duarte AC, Pereira E (2012) Role of non-enzymatic antioxidants on the bivalves' adaptation to environmental mercury: Organ-specicities and age effect in Scrobicularia plana inhabiting a contaminated lagoon. Environmental Pollution 163, 218 – 225

Ahmad I, Singh M K, Pereira ML, Pacheco M, Santos M A, Duarte AC, Pereira E, Grácio J. (2013) Morphological, compositional and ultrastructural changes in the Scrobicularia plana shell in response to environmental mercury – An indelible fingerprint of metal exposure? Chemosphere 90:2697–2704

Anjum NA, Srikanth K, Mohmood I, Sayeed I, Trindade T, Duarte AC, Pereira E, Ahmad I (2014) Brain glutathione redox system significance for the control of silica-coated magnetite nanoparticles with or without mercury co-exposures mediated oxidative stress in European eel (Anguilla anguilla L.). Environmental Science and Pollution Research. 21: 7746-7756

Ansaldo M, Luquet CM, Evelson PA, Polo JM, Llesuy S (2000) Antioxidant levels from different Antarctic fish caught around South Georgia and Shag Rocks. Polar Biol. 23: 160–165

Almroth BC, Sturve J, Stephensen E, Holt TF, Förlin L (2008) Protein carbonyls and antioxidant defenses in corkwing wrasse Symphodus melops from a heavy metal polluted and a PAH polluted site. Mar Environ Res 66:271-277.

Booth S, Zeller D (2005) Mercury, foodbwebs, and marine mammals: Implications of diet and climate change for human health. Environ. Health Perspect. 113: 521–526.

Bradford MM (1976) A rapid and sensitive method for the quantitation of microgram quantities of protein utilizing the principle of protein-dye binding. Anal Biochem 7:248-254.

Britto RS, Garcia ML, Rocha AM, Flores JA, Pinheirc MVB, Monserrat JM, Ferreira JLR (2012) Effects of carbon nanomaterials fullerene C60 and fullerol C60(OH)18–22 on gills of fish Cyprinus carpio (Cyprinidae) exposed to ultraviolet radiation. Aquatic Toxicology; 114–115, 15:80–87.

Dalle-Donne I, Rossi R, Giustarini D, Milzani A, Colombo R (2003) Protein carbonyl groups as biomarkers of oxidative stress. Clinica Chim Acta 329:23-38.

Habig WH, Pabst MJ, Jakoby WB (1974) Glutathione-S-transferases, the first enzymatic step in mercapturic acid formation. The Journal of Biological Chemistry 249: 7130-7139.

Halliwell B, Gutteridge JMC (1999) Free Radicals in Biology and Medicine, Clarendon Press, Oxford.

Kaur M, Atif F, Ali M, Rehman H, Raisuddin S (2005) Heat stress-induced alterations of antioxidants in the freshwater fish Channa punctata Bloch, J. Fish Biol. 67: 1653–1665.

Khessiba A, Romeo M, Aissa P (2005) Effect of some environmental parameters on catalase activity measured in mussels (Mytilus galloprovincialis) exposed to lindane. Environ Pollut 133: 275–281.

Lemaire P, Viarengo A, Canesi L, Livingstone DR (1993) Pro-oxidant and antioxidant processes in gas gland and other tissues of cod (Gadus morhua). J. Comp. Physiol. 163: 477–486.

Lopez-Torres M, Perez-Campo R, Cadenas S, Rojas C, Barja G (1993) A comparative study of free radicals in vertebrates – II. Non-enzymatic antioxidants and oxidative stress, Comp. Biochem. Physiol. B 105: 757–763.

Melzner F, Gutowska MA, Langenbuch M, Dupont S, Lucassen M, Thorndyke MC, et al., (2009) Physiological basis for high CO2 tolerance in marine ectothermic animals: pre-adaptation through lifestyle and ontogeny? Biogeosciences 6: 2313-31.

Mieiro CL, Duarte AC, Pereira ME, Pacheco M (2011): Mercury accumulation patterns and biochemical endpoints in wildfish (Liza aurata): A multi-organ approach. Ecotoxicol Environ Saf 74:2225-32.

Mohandas J, Marshall JJ., Duggins G G, Horvath J S, Tiller D (1984) Low activities of glutathione-related enzymes as factors in the genesis of urinary bladder cancer. Cancer Research 44: 5086-5091.

Mohmood I, Lopes CB, Lopes I, Tavares DS, Soares AM, Duarte AC, Trindade T, Ahmad I, Pereira E (2016) Remediation of mercury contaminated saltwater with functionalized silica coated magnetite nanoparticles. Science of the Total Environment 557: 712-721

Pack EC, Kim CH, Lee SH, Lim CH, Sung DG, Kim MH, Park KH, Hong SS, Lim KM, Choi DW, Kim SW (2014) Effects of Environmental Temperature Change On Mercury Absorption in Aquatic Organisms with Respect to Climate Warming Journal of Toxicology and Environmental Health, Part A, 77: 1477–1490.

Parihar MS, Javeri T, Hemnani T, Dubey AK, Prakash P (1997) Response of superoxide dismutase, glutathione peroxidase and reduce glutathione antioxidant defense in gills of freshwater catfish (Heteropneustes fossilis) to short term elevated temperature. J Therm Biol 22: 151–156.

Patnaik BB, Roy A, Agarwal S, Bhattachar S (2010) Induction of oxidative stress by non-lethal dose of mercury in rat liver: Possible relationships between apoptosis and necrosis. Journal of Environmental Biology 31: 413-416.

Rodriguez-Ariza A, Dorado G, Peinado J, Pueyo C, Lopez-Barea J (1991) Biochemical effects of environmental pollution in fishes from Spanish South-Atlantic littoral. Biochem. Soc. Trans., 19, 301S.

Srikanth K, Anjum NA, Trindade T, Duarte AC, Pereira E, Ahmad I (2015) Lipid peroxidation and its control in Anguilla anguilla hepatocytes under silica-coated iron oxide nanoparticles (with or without mercury) exposure. Environmental Science and Pollution Research. 22: 9617-9625.

Sevcikova M, Modrá H, Slaninova A, Svobodova Z (2011) Metals as a cause of oxidative stress in fish: A review Veterinární Medicína 56: 537-546

Sousa ACA, Teixeira I, Marques B, Vilhena H, Vieira L, Soares AMVM, Nogueira AJA, Lillebø AI (2013) Mercury, pets and hair: baseline survey of a priority environmental pollutant using a noninvasive matrix in man best friend. Ecotoxicology. 22: 1435-1442.

Tavares DS, Daniel-da-Silva AL, Lopes CB, Silva NJO, Amaral VS, Rocha J, Pereira E, Trindade T (2013) Efficient sorbents based on magnetite coated with siliceous hybrid shells for removal of mercury ions. J Mater Chem 1: 8134-8143.

Verlecar XN, Jena KB, Chainy GNB (2007) Biochemical markers of oxidative stress in Perna viridis exposed to mercury and temperature. Chemico-Biological Interactions 167: 219–226

Welfinger-Smith G, Minholz JL, Byrne S, Waghiyi V, Gologergen J, Kava J, Apatiki M, Ungott E, Miller PK, Arnason JG, Carpenter DO (2011) Organochlorine and metal contaminants in traditional foods from St. Lawrence Island, Alaska. J. Toxicol. Environ. Health A 74: 1195–1214.

CHAPTER 6

Interference of the co-exposure of mercury with silica coated iron oxide nanoparticles can modulate genotoxicity induced by their individual exposures - A paradox depicted in fish under in vitro conditions

Abstract

The study aimed to assess the genotoxic potential of silica coated iron oxide nanoparticle functionalized with dithiocarbamate groups (NPs, 100 nm) *in vitro* exposure alone or its interference with mercury (Hg) co-exposure in the blood of European eel (*Anguilla anguilla*) by evaluating 8-hydroxy-2´-deoxyguanosine (8-OHdG), lipid peroxidation (LPO) and erythrocytic nuclear abnormalities (ENA). Four groups were made: i) 2×10^6 erythrocytes+RPMI-1640 (control); ii) 2×10^6 erythrocytes+NPs (2.5 mg/L); iii) 2×10^6 erythrocytes+Hg (50 µg/L); iv) 2×10^6 erythrocytes+NPs+Hg. Blood plasma was also processed following the previous exposure conditions. Samplings were performed at 0, 2, 4, 8, 16, 24, 48 and 72 hour of exposure. The results revealed significant ENA increases at both early (2, 4, 8) and late (16, 24, 48, 72) hour of exposure to NPs alone. However, NPs exposure combined with Hg co-exposure revealed no ENA increase at 2 hour, suggesting that NPs-Hg complex formation is efficient to eliminate the DNA damage-induced by individual exposure to NPs or Hg at early hour. Hence, the initial occurrence of antagonism between NPs and Hg was perceptible; however, at late hour of exposure, NPs was unable to mitigate the mercury-accrued negative impacts. Plasma exposure to NPs alone displayed a significant increase in 8-OHdG levels at 2 and 48 hour exposure. However, NPs in combination with Hg co-exposure revealed an increase in 8-OHdG levels at all the exposure length (except 16 hour), suggesting that both NPs and Hg independently oxidized DNA. In addition, an additive effect on 8-OHdG levels at both early and late hours, and on LPO only at late hour (except 24 hour), suggested that DNA is more susceptible to per-oxidative damage than lipid.

Keywords: *In vitro genotoxicity; Anguilla anguilla L.; Iron oxide nanoparticles; Mercury; co-exposure*

Environmental Science Pollution Research

(2014)22(5):3687-96

6.1. INTRODUCTION

The increasing production and use of magnetic iron oxide nanohybrid particles have inevitably raised concerns about their genotoxic potential assessment in aquatic organisms. This possible hazard is closely related to the fact that aquatic ecosystems act as the ultimate repository for all the classes of contaminants of which, one-third were shown to be carcinogenic in animals (Claxton et al., 1998). In addition, there is no available report reflecting interaction of iron oxide nanoparticles with other aquatic contaminants that have still not disappeared from the aquatic environment (*e.g*. mercury: Hg), where the resultant toxic effects may appear synergistic, or antagonistic due to contaminants interaction. Moreover, the literature also revealed that there is a need to focus on the evaluation of iron oxide nanoparticle genotoxicity in fish because of their virtual presence everywhere in the aquatic environment and playing a major ecological role in the aquatic food-webs. Until recently, most studies on iron oxide nanoparticle genotoxicity inducing potential have focused on mammals and/or on different types of cell lines (Auffman et al., 2006; Hong et al., 2011; Singh et al., 2013), leaving a complete knowledge gap on its genotoxicity investigation in aquatic organisms including fish.

The iron oxide nanoparticles exposure in the aquatic ecosystem is extremely primitive and is not sufficient for making accurate predictions (Zhu et al., 2012), hence need more attention to understand the full mechanism involved in its toxicity assessment in fish. The most intracellular and *in vivo* nanotoxicities from iron oxide nanoparticles arise from the production of excess reactive oxygen species (ROS) (Kim et al., 2011). When cells are exposed to iron oxide nanoparticles at high doses, it results in the production of ROS with high chemical reactivity leading to DNA damage. ROS not only attack DNA bases but also the deoxyribose backbone of DNA, reacting five times faster with nucleobases (Cadet et al., 1997). The oxidation of guanine in the C8 position results in the formation of 8-hydroxy-2´-deoxyguanosine (8-OHdG), a predominant and one of the most studied oxidative DNA lesions due to its easy formation and mutagenicity (Valko et al., 2004). The absence of base-damage repair may lead to strand misreading, mutations, altered gene expression, strand breaks, microsatellite instability and loss of heterozygosity, chromosomal aberrations, cytostasis, cytotoxicity or neoplastic growth (Croteau and Bohr 1997; Evans et al., 2004).

8-OHdG is an easily repairable genetic alteration unlike chromosomal breakages, which represent a more serious and irreversible lesion. The detection of micronuclei, together with

other nuclear abnormalities in fish erythrocytes (erythrocytic nuclear abnormalities (ENA) provide an index of accumulated genetic damage during the life span of the cells. Micronuclei, small cellular chromatin bodies that appear when a whole chromosome or a fragment fails to migrate with one of the two daughter nuclei formed during mitosis, may be induced by oxidative stress, exposure to clastogens or aneugens, or by genetic defects in cell-cycle checkpoints and/or DNA repair genes (Bonassi et al., 2007). The ENA assay has been successfully applied to detect exposure to genotoxic xenobiotics in a large number of species (Oliveira et al., 2008; Guilherme et al., 2008; Mohmood et al., 2012). However, at the molecular level, mechanisms by which iron oxide nanoparticles induce genotoxicity in fish is largely unknown. Moreover, a particular attention is also required towards the magnitude of iron oxide nanoparticles genotoxicity-inducing potential whether it is repairable or irreparable.

Keeping in view the above description and the knowledge gap of iron oxide nanoparticles genotoxicity as well as its interaction with Hg, a pervasive environmental pollutant, the following hypotheses have been tested in this study: Is the exposure of iron oxide nanoparticles alone or its interference with Hg co-exposure able to induce or modulate genotoxicity in fish? Moreover, what is the role of ROS in iron oxide nanoparticles-induced DNA-damaging risk assessment? To test this hypothesis, genetic lesions both reparable (8-OHdG) and irreparable (ENA measurement) were assessed in the blood of *A. anguilla in vitro*. In addition, lipid peroxidation (LPO) was performed to assess the role of ROS production in DNA-damaging risk as well as relative susceptibilities of DNA and plasma lipid towards peroxidative damage. *In vitro* model system was adopted due to their rapidity, effectiveness, relevance and importance to assess nanoparticles for a number of toxicological endpoints in the absence of clear regulatory guideline(s) on the NPs testing/evaluation in fish (Arora et al., 2012). According to Santos et al., (2000) *in vitro A. Anguilla* organ cultures are good ecotoxicological models for toxicity studies since organ cultures involve “the maintenance or growth of tissues, organ primordia or the whole or parts of an organ *in vitro* for a period of 24 hours or longer, in a way, which may allow differentiation and/or preservation of architecture and/or function”. These *in vitro* systems, used for toxicological research, have advantages such as the utilization of a small number of animals, controlled experimental conditions, genetic heterogeneity removal, small quantities of test chemicals and amount of toxic wastes (Santos et al., 2000).

In the current study, silica-coated Fe_3O_4 nanoparticle functionalized with dithiocarbamate group (hereafter called the NPs) was considered because of its wide application with no reports on its potential toxicity in *A. anguilla*. In addition, a complete Hg removal (ca. 99.8%) has also been observed using 2.5 mg /L NPs for an initial Hg concentration of 50 µg /L, (Tavares et al., 2013), displaying its utility in Hg contaminated sites cleanup.

6.2. MATERIALS AND METHODS

6.2.1. Silica coated Fe_3O_4 nanoparticle functionalized with dithiocarbamate groups (NP)

The NPs, considered for this experiment, were kindly provided by CICECO, University of Aveiro, Portugal where the magnetic removal of the NPs is an additional step in water treatment processes and thus generates a need to assess the importance of its removal as a necessary step and whether it should be as expeditious as metal removal from water. The details pertaining to characterization of Fe_3O_4 and surface modified Fe_3O_4 (Fe_3O_4@SiO_2/SiDTC) can be obtained elsewhere (Tavares et al., 2013). After ultra-sonication dispersal, NPs-agglomeration state in the RPMI-1640 (Roswell Park Memorial Institute-1640) medium was performed as well as the distribution of NPs particle diameters was also observed using the Dynamic Light Scattering method (Zen 3500, Malvern ZS Nano S analyzer). The size of the NPs used in the current study was 100 nm and the specific surface area and average zeta potential of NPs were 20.2 m^2 g^{-1} and -10.45 mV, respectively. Based on the study performed by Tavares et al., (2013) where the authors evidenced a high efficiency of Fe_3O_4@SiO_2/SiDTC concentration (2.5 mg /L) for the removal of Hg up to concentration of 50 µg /L, in the current bio-experiment, 2.5 mg /L and 50 µg /L were chosen as test concentrations respectively for NPs and Hg. In the current bio-experiment, a stock solution (10 mg /L) of previously prepared NPs was made and sub-diluted to the final concentration of 2.5 mg /L in RPMI-1640 medium. In order to prevent the NPs agglomeration, the /L5 dispersed NPs were mixed using vortex for 20 s and sonicated for 2× 20s with a 20 s pause in between the sonication. In parallel, the stock solution of Hg (10 mg /L) was made and diluted in order to get the required concentration of Hg 50 µg /L in different exposure groups.

6.2.2. Experimental protocols

European eel *A. anguilla* (n=3) with an average weight of 50 ± 5 g were collected from the Aveiro Lagoon, Murtosa (Portugal). The eels were transported in anoxia and acclimated to laboratory conditions in aerated, filtered, and dechlorinated tap water in 50-L aquarium for 1 week, at 20 °C according to the methods adopted by Santos and Pacheco (1996). Fish were not fed during acclimatization period. After acclimation, fish were sacrificed by decapitation; their blood was collected from the posterior cardinal vein with a heparinised Pasteur pipette and immediately centrifuged (13,400 × g, 5min) to isolate erythrocytes and plasma for ENA assessment and plasma 8-hydroxy-2-deoxyguanosine (8-OHdG) determination respectively. Four groups were made according to the following manner for both erythrocytes and plasma.

6.2.2.1 Erythrocytes processing and contaminants exposure

The isolated erythrocytes after centrifugation were used for the ongoing experiment. The erythrocytes were dissolved and maintained in RPMI medium at a density of 1×10^6 cells/mL. Using four aliquots of 2 mL, the erythrocytes were divided into four exposure groups: i) 2×10^6 erythrocytes + 2 mL RPMI served as control; ii) 2×10^6 erythrocytes + 2 mL of NPs (2.5 mg /L) in RPMI referred as NPs; iii) 2×10^6 erythrocytes + 1 mL RPMI + I mL Hg (100 µg/L); and iv) 2×10^6 erythrocytes + 1 mL of NPs (5 mg/L) in RPMI + I mL Hg (100 µg/L). The cells were maintained for 24 hours and the medium was exchanged with fresh medium every 24 hours by centrifugation at 3000 rpm. The pellet obtained in each group was re-suspended in fresh RPMI medium and the Hg concentrations were maintained up to 50 µg/L. Blood smears were prepared immediately after incubation at 0, 2, 4, 8, 16, 24, 48 and 72 hours from each group, air dried, fixed with methanol during 10 min and stored at room temperature until stained with Giemsa stain.

6.2.2.2 Plasma processing contaminants exposure

A. Anguilla blood plasma protein was precipitated by the addition of an equal volume of salicylic acid, and precipitated protein was separated by centrifugation at 3,000 × g for 15 min at 4 °C. Supernatant was transferred to a new tube and mixed with 10 volumes of HBSS (to reduce deviation). Using four aliquots of 2 mL, the diluted plasma was divided into four exposure groups: i) 750 µl of diluted plasma + 0 µl of HBSS + 0 µl of NPs served as control; ii) 250 µl of diluted plasma + 250 µl of HBSS + 250 µl of NPs (7.5 mg/L), denominated as NPs group; iii) 250 µl of diluted plasma + 250 µl of HBSS + 250 µl of Hg (150 µg/L), referred as Hg group; and iv) 250 µl of diluted plasma + 250 µl of NPs (7.5 mg/L) + 250 µl of Hg (150

µg/L), referred as NPs + Hg group. Samples were collected immediately after incubation at 0, 2, 4, 8, 16, 24, 48 and 72 hours from each group and stored at -80 ^{o}C for the 8-OHdG determinations and lipid peroxidation estimation.

6.2.3. Genotoxic response

6.2.3.1. Erythrocytic nuclear abnormalities (ENA) assay

Previously stored blood smears fixed with methanol during 10 min were stained with Giemsa (5%) during 30 min. ENA were scored in 1000 mature erythrocytes samples/fish to determine the frequency of the following categories: MN, lobed nuclei (L), binucleates or segmented nuclei (S), and kidney-shaped nuclei (K). In addition, notched nuclei (N) were also scored as suggested by Ayllón and Garcia-Vazquez (2001). The final result was expressed as the mean value (‰) of the sum for all of the individual lesions observed (MN + L + S + K + N).

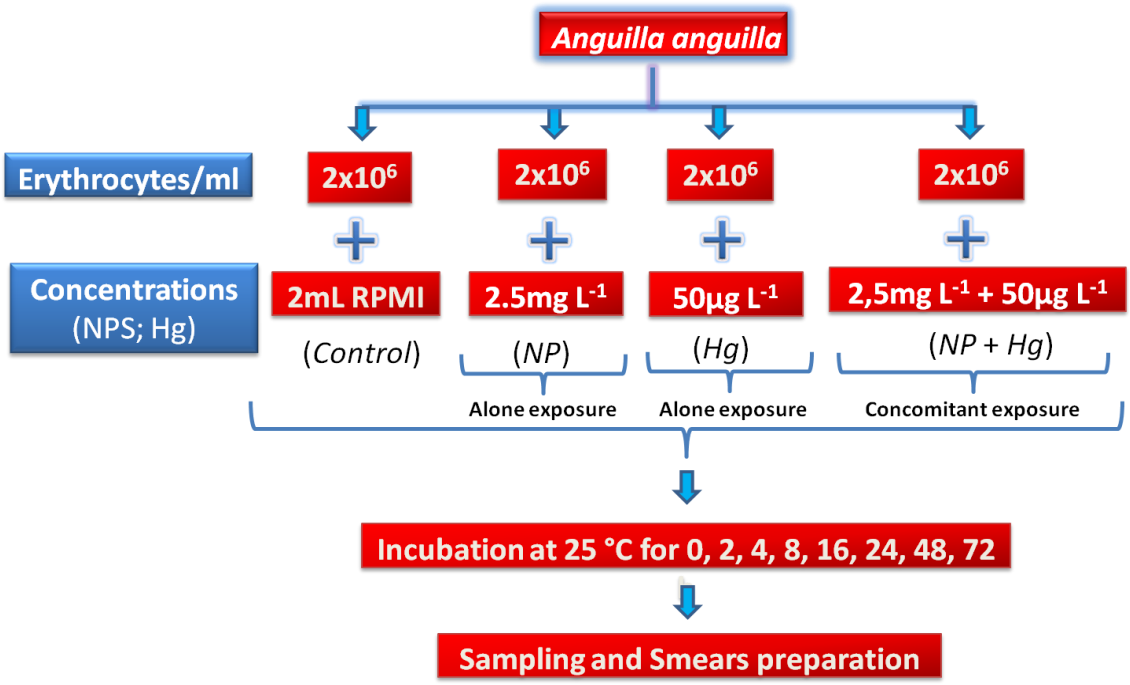

Schematic representation of the experimental protocol followed in the present study. (NPs: silica-coated iron oxide nanoparticles; Hg: mercury).

6.2.3.2. 8-Hydroxy-2´-deoxyguanosine (8-OHdG) assessment

The amount of 8-OHdG was assessed by means of a competitive *in vitro* enzyme-linked immunosorbent assay (ELISA) using an IBL International GmbH (Germany) kit. Results were expressed as ng/mL.

6.2.4. Lipid peroxidation (LPO) estimation

LPO was determined in the previously prepared cells suspension. Briefly, to a 50 µL cell suspension, 500 µL of 12% TCA in aqueous solution, 450 µL of Tris-HCl buffer (60 mM, pH 7.4 and 0.1 mM DTPA) and 500 µL 0.73% TBA was added with a final volume 1.5 mL. The mixture was heated for 15 min in water bath set at boiling temperature. The eppendorfs were then removed and cooled to room temperature. The contents from each eppendorf (1.5 mL) were centrifuged at 12000 rpm for 3 minutes. To the absorbance of the supernatant was measured at 535 nm. The rate of LPO was expressed as nmol of thiobarbituric acid reactive substances (TBARS) formed per milligram of protein using a molar extinction coefficient of 1.56×10^5 $M^{-1}.cm^{-1}$.

6.2.5. Protein concentration measurement

Total protein was determined according to the Bradford method (1976) using bovine serum albumin (BSA) as standard. The assay mixture contained 990 µL of Bradford reagent, 10 µL of diluted BSA (2.5 mg/mL) and 10 µL miliQ-water. The absorbance of plate was measured at 595 nm after incubate during 10 min in dark.

6.2.5. Statistical Analysis

SPSS (PASW statistics 18) for Windows was used for statistical analysis of data. All of the data were first tested for normality and homogeneity of variance to meet statistical demands. ANOVA was performed in order to assess significant effects between the group. This analysis was followed by a post-hoc Tukey test to signal significant differences between groups. Spearman rank correlation factor (r) was used to test significant relations between ENA and 8-OHdG. A significance level of 0.05 was ascertained in all test procedures.

6.3. RESULTS

Results depiction ‘given below’ has been considered describing first genotoxic responses inter-group variations within the same hours of exposure followed by inter-hours comparisons within the same group.

6.3.1. 8-OHdG Assessment

A anguilla plasma *in vitro* exposure to NPs alone resulted a significant increase in 8-OHdG level at 2 and 48 hours of exposure, when compared to control (Figure 6.1). *In vitro* exposure to Hg alone also caused a significant increase in 8-OHdG level at 8, 24, 48 and 72 hours. Significant increases in 8-OHdG levels from 2 to 72 hours (except 16 hours) were also

perceptible in plasma concomitantly exposed to NPs and Hg. Moreover, a significant increase in 8-OHdG level was also observed when concomitant NPs+Hg group was compared to NPs alone.

Inter-hour comparison revealed no statistically significant 8-OHdG changes in any of the group (NPs, Hg, NPs+Hg) studied.

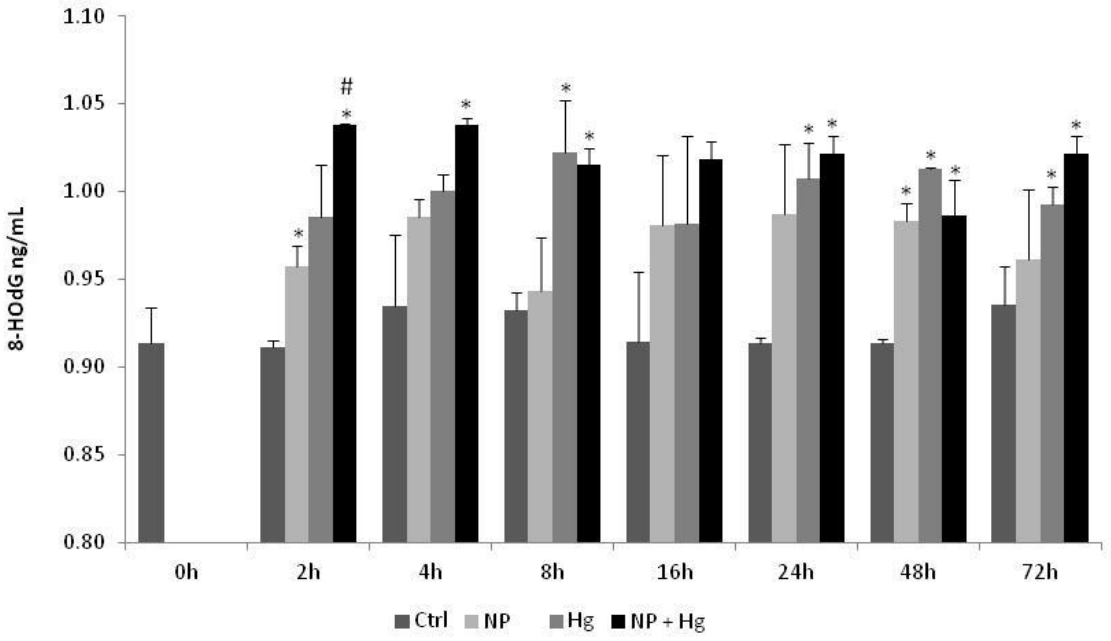

Figure 6.1. 8-hydroxy-2-deoxyguanosine (8-OHdG) levels modulation in *A. anguilla* blood plasma under *in vitro* exposure to silica coated ironoxide nanoparticle functionalized with dithiocarbamate (NPs), mercury (Hg) and NPs+Hg for 72 hours. The values are expressed as means ± S.E. Inter-group significant differences have been denoted by symbols (* *vs*. control; # *vs*. NPs) where h represents hours.

6.3.2. Lipid Peroxidation

The effects of NPs alone *in vitro* exposure to *A. Anguilla* plasma for 72 hours caused a significant increase in LPO at 8, 16 and 48 hours in comparison to control (Figure 6.2). In addition, a significant increase was also observed in LPO from 8 to 72 hours when exposed to Hg alone. However, when the two individual groups *viz*. NPs and Hg were compared, significant increase in LPO was demonstrated at 24 and 72 hours when plasma exposed to Hg. The plasma parallel exposed to NPs and Hg revealed the increase in LPO at 16, 24, 48 and 72 hours when compared to control. Moreover, a significant LPO increase was perceptible in this

group when compared to NPs at 16, 24 and 72 hours. However, a decrease in LPO was observed in this group at 24 hours when compared to Hg alone.

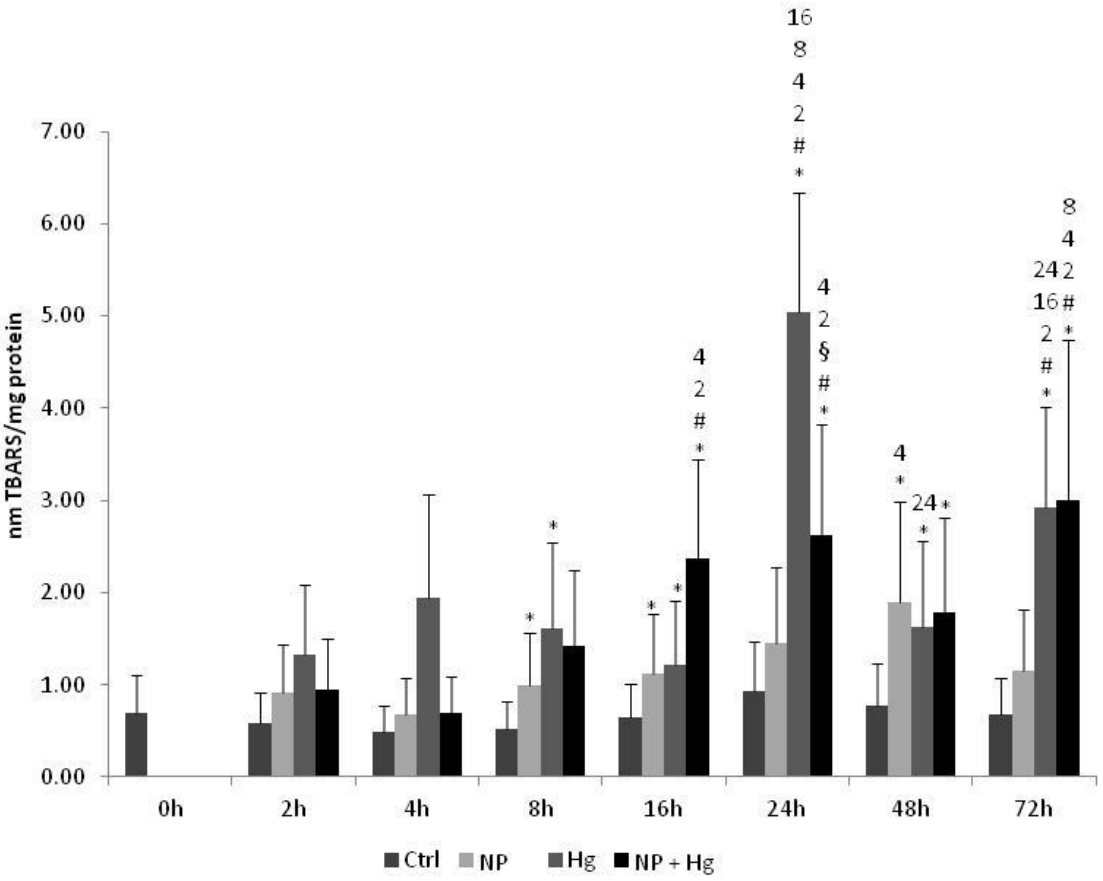

Figure 6.2. Lipid peroxidation (nm TBARS/mg protein) in *A. anguilla* blood plasma under *in vitro* exposure to silica coated ironoxide nanoparticle functionalized with dithiocarbamate (NP), mercury (Hg) and NP + Hg for 72 hours. The values are expressed as means ± S.E. Inter-group significant differences have been denoted by symbols (* vs. control; # vs. NP; § vs. Hg) and inter hour significant differences have been marked by numbers (2 vs. 2 h; 4 vs. 4 h; 8 vs. 8 h; 16 vs. 16 h; 24 vs. 24 h; 48 vs. 48; 72 vs. 72 h) where h represents hours.

Inter-hour comparison revealed no statically significant change among controls of each exposure time. Effects of NPs *in vitro* exposure alone on plasma revealed an increase in LPO only at 48 hours (*vs*. 4 hours). Moreover, the Hg exposed plasma reflected increase in LPO after 24 hours (*vs*. 2, 4, 8, 16 hours) and 72 hours (2, 16 hours), whereas a decrease was displayed in LPO at 48 hours and 72 hours (*vs*. 24 hours). Plasma concomitantly exposed to NPs and Hg revealed a significant increase in LPO at 16 (*vs*. 2, 4 hours), 24 (*vs*. 2, 4 hours), and 72 hours (*vs*. 2, 4, 8 hours).

6.3.3. ENA Frequency

In vitro effects of NPs exposure alone on *A. anguilla* erythrocytes revealed a significant ENA frequency increase at all the exposure length (except 16 hour) when compared to control (Figure 6.3). Moreover, a significant ENA frequency increase was also observed in erythrocytes exposed to Hg alone. In addition, when the two individual groups *viz.* NPs and Hg were compared, significant ENA increase was perceptible in erythrocytes exposed to Hg for 2, 8, 16 and 24 hours. On the perspective of the effects of NPs+Hg concomitant exposure on erythrocytes, a significant increase in ENA frequency was observed at all the exposure time intervals (except 2 hour) when compared to control. Effects of NPs+Hg concomitant exposure on ENA frequency was also significantly pronounced when compared to NPs and Hg alone exposure.

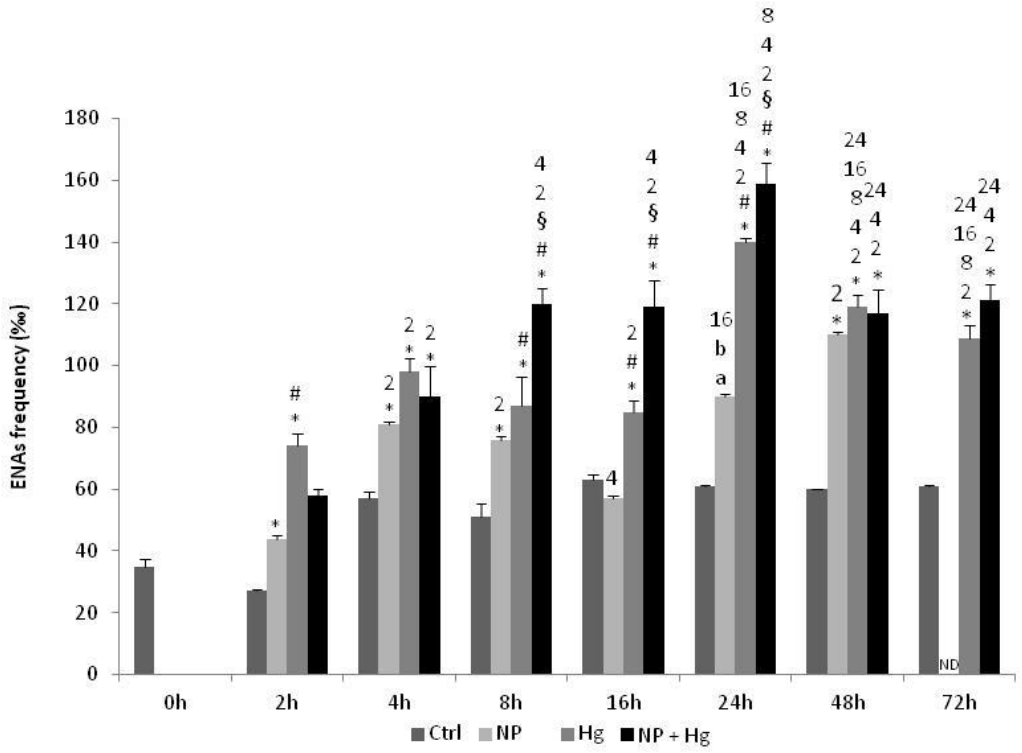

Figure 6.3. Erythrocytic nuclear abnormalities frequency in *A. anguilla* under *in vitro* exposure to silica coated iron oxide nanoparticles functionalized with dithiocarbamate (NPs), mercury (Hg) and NPs+Hg for 72 hours. The values are expressed as means ± S.E. Inter-group significant differences are marked by symbols (* *vs.* control; # *vs*. NPs; § *vs.* Hg) and inter hour significant differences have been marked by numbers (2 *vs*. 2 h; 4 *vs*. 4 h; 8 *vs*. 8 h; 16 *vs*. 16 h; 24 *vs*. 24 h; 48 *vs*. 48; 72 *vs*. 72 h) where h represents hours.

Inter-hour comparison revealed no statistically significant difference among the controls during the 72 hours exposure period. However, effects of NPs *in vitro* exposure alone revealed a significantly higher ENA frequency at 4 (*vs*. 2 hours), 8 (*vs*. 2 hours), 24 (*vs*. 2, 16 hours) and 48 hours (*vs*. 2 hours), whereas Hg exposed erythrocytes reflected ENA frequency increase after 4 (*vs*. 2 hours), 16 (*vs*. 2 hours), 24 (*vs*. 2, 4, 8 hours), 48 (*vs*. 2, 4, 8, 16 hours) and 72 hours (*vs*. 2, 8, 16 hours). The erythrocytes concomitantly exposed to NPs+Hg reflected increased ENA frequency after 2 (*vs*. 2 hours), 8 (*vs*. 2, 4 hours), 16 (*vs*. 2, 4 hours), 24 (*vs*. 2, 4, 8 hours), 48 (*vs*. 2, 4, 24 hours) and 72 hours (vs. 2, 4, 24 hours).

6.4. DISCUSSION

6.4.1. *Anguilla anguilla* plasma 8-OHdG levels under NPs, Hg alone or concomitant exposure

A significant increase in plasma 8-OHdG of *A. anguilla* clearly reflects increased ROS production and its concomitant association to DNA damage by NPs at 2 and 48 hours of exposure. In the current study, a key mechanism underlying the NPs genotoxicity can be directed towards its ability to induce oxidative stress since the interaction of HO• radical with the nucleobases of the DNA strand, such as guanine, leads to the formation of C8-hydroxyguanine (8-OHGua) or its nucleoside form deoxyguanosine (8-hydroxy-2-deoxyguanosine). Initially, the reaction of the HO• addition leads to the generation of radical adducts, and then by one electron abstraction, the 8-OHdG is formed. The 8-OHdG undergoes keto-enol tautomerism, which favors the oxidized product 8-oxo-7,8-dihydro-2-deoxyguanosine (8-oxodG) (Valavanidis et al., 2009). Thus, the significant increase in 8-OHdG levels at 2 and 48 hours clearly revealed the discontinuity of NPs-induced oxidative stress for 72 hours once it is generated. The current 8-OHdG induction should be attributed to the overall effects of different classes of compounds constituting NPs rather than any individual since the reports are already available reflecting that each constituent of the current NPs in the cell may be a source of the toxicity (Mu et al., 2012; Lin et al., 2006; Soloneski et al., 2003). On the perspective of *in vitro* Hg exposure to plasma, a significant 8-OHdG increase at early (8 hours) and late (24, 48, 72 hours) hour of exposure was revealed suggesting that the Hg, though it is a known genotoxicants to fish under both *in vivo* and *in vitro* condition (Mohmood et al., 2012; Pereira et al., 2010; Guilherme et al., 2008; Al-Sabti, 1994; Babich et al., 1990), is not as effective as NPs since NPs generated the genotoxic response at very early hour (2 hours) of exposure in comparison to LPO induction (8 hours). Moreover, this study is

the first of its kind and represents the association of ROS generation with DNA damage in fish by forming 8-OHdG.

NPs in combination with Hg co-exposure revealed an increase in 8-OHdG levels at all the exposure length (except 16 hours). This observation suggests that NPs' oxidative stress inducing potential in the presence of Hg once initiated may persist for a long time. Moreover, upon two hour-exposure, it is clear that concomitant exposure of NPs and Hg have additive effects on 8-OHdG levels since NPs alone increased 8-OHdG levels significantly. However, at a later time point (48 hours), the effects of NPs and Hg on the 8-OHdG levels became antagonistic since no significant change was observed on 8-OHdG levels after co-exposure to NPs and Hg in comparison to either NPs or Hg alone. It is important to highlight here that during early hour of exposure the NPs and Hg independently oxidize DNA through Fenton-type reaction and the production of ROS, respectively. However, during late hour of exposure (72 hours), the concomitant exposure was able to mitigate the Hg accrued negative impact, however not at the control level. Hence, the occurrence of antagonism during late hour may be further seen as a principle of NPs-mediated Hg-NPs complex formation (Girginova et al., 2010; Tavares et al., 2013).

6.4.1 *Anguilla anguilla* plasma LPO under NPs, Hg alone or concomitant exposure

Polyunsaturated fatty acids of plasma lipids are likely to be the most abundant and susceptible targets of free radical attack. In the current study, a significant LPO increase was observed at the end of the 8 hour exposure implying that NPs may lead to an acute oxidative stress in terms of higher levels of LPO; whereas, NPs lead to a chronic oxidative stress during late hour (16 and 48 hour) of exposure periods.

It seems that early hour of exposure to NPs in combination with Hg is able to abolish LPO completely; whereas, at late hour of exposure, this combination was unable to minimize the negative effects since LPO induced by NPs was further induced when come in contact with Hg (16 hours) exposure. Though the extent of LPO was significantly high at 8 hour of NPs exposure (compared to control) but damage extent increased with increase in the period of exposure to NPs (48 hours).

It can be implied from this observation that NPs lead to an acute oxidative stress in terms of higher levels of 8-OHdG during 2 hour of exposure; whereas, NPs lead to a chronic oxidative stress in terms of LPO during the rest of exposure periods.

It seems that during early hour more capacity of damage reversal is there in comparison to late hour as reflected by additive or incomplete antagonistic effects. The induction of oxidative stress is due to the inherent abilities of NPs to produce ROS, especially owing to their chemical composition and interactions with the cellular components (Nel et al., 2006). The current study revealed a higher sensitivity of cellular DNA to nanoparticle-accrued oxidation, when compared to plasma lipids under similar conditions. Earlier, the production of radical through Fenton- and HaberWeiss-type reactions has been considered as the cause of bare NPs - mediated cytotoxicity (Brunner et al., 2006). To the other, as it is also true with the current results during early hour of exposure on LPO, coating of NPs with SiO2 was evidenced to substantially reduce their potential toxic effects by preventing particle aggregation and increasing their stability in solution (Corr et al., 2008). However, long-term exposure disrupts the cell damage.

6.4.2. *Anguilla anguilla* ENA frequency under NPs, Hg alone or concomitant exposure

Effects of NPs exposure alone on ENA frequency revealed that there is significant ENA frequencies increase at all the exposure length (except 16 hours) in fish *A. anguilla*. Moreover, the maximum rate of ENA induction was observed at 48 hour of exposure. NPs, which is a complex mixture of silica-coated iron oxide nanoparticle functionalized with dithiocarbamate group showed this genotoxic/clastogenic effects for the first time in fish *A. anguilla*. To the author's knowledge, no study previously reported ENA frequency induction in fish under NPs *in vitro* conditions, which is one of the parameters recommended by OECD to evaluate the nanomaterial toxicity in a very short period of time (Arora et al., 2012). In addition, the maximum rate of ENA induction observed at 48 hour of exposure in the current *in vitro* study aligns with the *in vivo* study done by Song et al., (2011), showing the maximum induction of micro-nucleated reticulocytes formation after 48 hours in mice. Previously a joint approach of micronuclei with other erythrocytic nucear abnormalities has been reported in evaluating the genotoxicity of various classes of pollutants, including metal to different fish species (Ayllón and Garcia-Vazquez 2001; Guilherme et al., 2008; Mohmood et al., 2012). Thus, the current results support the proposition that ENA may originate from lesions induced for short period of time after the administration of nanoparticles and may remain persistent upto 48 hours. The

lack of increased ENA at 16 hours can be considered unexpected or reparable since 8-OHdG induction is perceptible to the same exposure length, though, statistically insignificant.

On the perspective of Hg individual exposure, a significant increase from 2 to 72 hours was observed. Moreover, the increase was even more than nanoparticles alone in first 24 hours (except 4 hours). The current observation aligns with earlier studies revealing that Hg is well known genotoxicant to fish under both *in vivo* (Mohmood et al., 2012; Pereira et al., 2010; Guilherme et al., 2008) and *in vitro* conditions (Al-Sabti 1995; Babich et al., 1990). Exposure time variation in these observations *i.e.* more ENA in Hg exposed group after 2, 8, 16 and 24 hours in comparison to NPs and no difference after 48 and 72 hours when these two groups were compared can be conditioned either through fish blood cells' DNA repairing capacity and/or the balance between erythrocytic prooxidants versus antioxidants. Out of these two explanations, the prooxidants/antioxidants imbalance seems to be more applicable since equal 8-OHdG level formations is perceptible in the current study, which is the resultant effect of the ROS production.

NPs combined with Hg co-exposure revealed no ENA increase upon 2 hour exposure, suggesting that NPs-Hg complex formation is efficient to eliminate the DNA damage induced by NPs and Hg individual exposure. Hence, the occurrence of antagonism between NPs and Hg is further strengthened here as a principle of NPs-mediated Hg-NPs complex formation as stated above by Girginova et al.,(2010) and Tavares et al., (2013). However, it was clearly observed that at late hour exposure, NPs is unable to mitigate the mercury-accrued negative impacts. Moreover, an additive effect was perceptible at 8, 16 and 24 hour of exposure. Thus, the hypothesis that NPs interaction with Hg may diminish their toxicity inducing potential seems to be applicable only at acute exposure of 2 hours. Moreover, though ENA frequency was not significantly high at 2 hour of exposure (compared to control), its extent significantly increased until 24 hours following a decrease at 48 and 72 hours (not until the control level). The previous observations clearly indicated that decreased NPs potential of removing Hg-accrued negative impacts over time resulted in increased ENA frequencies.

6.4.3. Relationship between *A. anguilla* plasma 8-OHdG levels, LPO and ENA frequency under NPs and Hg alone and/or concomitant exposure

Effects of NPs alone on fish blood revealed a non-time dependent relationship between 8-OHdG levels, LPO and ENA frequency. At both, early (2, 4, 8 hours) and late (16, 24, 48, 72 hours) hour of exposure, despite ENA frequency increase, no concomitant increase in 8-OHdG

levels and LPO was observed. 8-OHdG formation appeared at the end of the 2 hour of exposure and LPO was observed at the end of 8 hour of exposure, suggesting that DNA is first to respond to NP induced ROS production than lipid. LPO induced at 8 hours remained persisted until 72 hours with the significant increase at 16 and 48 hours. The research findings seem obvious since 8-OHdG represents an early sign of damage, which might be a subject of repair process. The ENA assay, based on the detection of micronuclei and other nuclear anomalies (Pacheco and Santos 1997) signals *in vivo* chromosome breakage (clastogenicity) or loss and mitotic spindle apparatus dysfunction (aneugenicity) (Fenech 2000; Stoiber et al., 2004) Hence, ENAs are irreparable lesions, representing later and less transient alterations when compared to 8-OHdG formations. Moreover, the similar results related to the relative sensitivities of the 8-OHdG levels and micronucleus measurements have been compared in mouse splenocytes *in vitro* (Kobus et al., 1993).

On the other hand, NPs combined with Hg co-exposure displayed an additive effect on 8-OHdG levels at both early (2,4,8 hours) and late hour (24,48,72 hours) of exposure, and on LPO only at late hour of exposure indication that ROS scavenging activity of NPs combined with Hg exposure occurs only at early hour (2-8 hours). At late hour of exposure, except the antagonistic effect at 24 hours, LPO was increased in an additive manner, suggesting the failure of ROS scavenging capacity with the increase of exposure time. Interestingly, Hg exposure alone revealed the presence of ROS signals only at late hour of exposure since both 8-OHdG and LPO were significantly increased probably explaining the reason why the formation of 8-OHdG or LPO was more pronounced at late hour of exposure.

Interaction between emerging contaminants and other conventional anthropogenic ones including iron has been shown to induce the formation of ROS through a Fenton-like reaction and to induce intracellular oxidative stress (Diabaté et al., 2002; Voelkel et al., 2003). This is what we observed in the current study since a positive correlation was found between ENA and 8-OHdG at 2 ($r = 0{,}637$; $p = 0{,}0260$), 24 ($r = 0{,}578$; $p = 0{,}0492$) and 72 hour of exposure ($r = 0{,}827$; $p = 0{,}00593$). The concomitant increase in these two parameters was perceptible at NPs, Hg and NPs+Hg exposure, strengthening the explanation that generation of ROS was unsuppressed. Moreover, plasma LPO increase exposed either to NPs, Hg or NPs+Hg at the end of different exposure period in parallel or unparallel to 8-OHdG and ENA increase seems to be aggravating the degenerative processes. In this perspective, malonaldehyde, one of the products of LPO has been shown to be highly reactive and an important mediator of DNA damage as a result of oxidative stress (Wang and Liehr 1995). Moreover, studies have also demonstrated that un-

functionalized iron oxide nanoparticles and Hg are capable to increase LPO in fish (Rajkumar and Tennyson 2013; Li et al., 2009) and mammals (Ahamed et al., 2013; Faix et al., 2005; Salonen et al., 1995). Thus the mechanisms based on oxidative DNA damage, mediated by redox cycling and free radical generation may be responsible for the formation of DNA adducts by aldehyde decomposition products of lipid peroxides. However, there have been no studies on the effects of these contaminants on the 8-OHdG levels in fish. The relative sensitivities of the 8-OHdG levels and micronucleus measurements have been compared in mouse splenocytes *in vitro* (Kobus et al., 1993).

6.5. CONCLUSIONS

NPs exposure alone is able to induce genotoxicity in *A. anguilla* blood cells at both early (2, 4, 8 hours) and late (16, 24, 48, 72 hours) hour of exposure as revealed by significant increase in irreparable genetic lesions *i.e.* ENA. However, NPs combined with Hg co-exposure revealed no ENA increase at the end of 2 hour exposure suggesting that NPs-Hg complex formation is efficient to eliminate the DNA damage induced by either NPs or Hg individual exposure. Hence, the occurrence of antagonism between NPs and Hg was perceptible; however, at late hour exposure, NPs was unable to mitigate the mercury-accrued negative impacts.

Significant increase in reparable genetic lesions *viz*. 8-OHdG at 2 (early) and 48 (late) hours clearly suggested the discontinuity of the NPs induced $HO^{\cdot}$ radical production for 72 hours. However, NPs in combination with Hg co-exposure revealed an increase in 8-OHdG levels at all the exposure length (except 16 hours) suggesting that both NPs and Hg independently oxidized DNA through the ROS production. In addition, positive correlations between ENA and 8-OHdG confirmed that NPs' oxidative stress inducing potential was increased with Hg co-exposure and remains persisted until 72 hours.

NPs exposure combined with Hg co-exposure also revealed an additive effect on 8-OHdG levels at both early and late hour of exposure, and on LPO only at late hour (except 24 hours) of exposure suggesting that DNA is more susceptible to per-oxidative damage than lipid. In addition, LPO increase in an additive manner may suggest the failure of ROS scavenging activity of NPs overtime since Hg exposure alone induced 8-OHdG or LPO to late hour of exposure only.

On the perspective of *in vitro* Hg exposure to plasma, a significant 8-OHdG increase at

early (8 hours) and late (24, 48, 72 hours) hour of exposure was revealed indicating that Hg is not as capable as NPs to induce genotoxicity since NPs generated the genotoxic response at very early hour (2 hours) of exposure.

A. anguilla proved to be a good *in vitro* model for NPs toxicity assessment.

Finally, results confirmed that the consideration of other contaminants is equally important while interpreting the fish genotoxic responses to NPs in a multi-contamination state. In addition, the current results suggested that the step of NPs-Hg complex removal must not be underrated and should be processed without any more ado.

6.5. REFERENCES

Ahamed M, Alhadlaq HA, Alam J, Khan MA, Ali D, Alarafi S (2013) Iron oxide nanoparticle-induced oxidative stress and genotoxicity in human skin epithelial and lung epithelial cell lines. Curr Pharm Des 19:6681-90.

Al-Sabti K (1995) in vitro binucleated blocked hepatic cell technique for genotoxicity testing in fish. Mutat. Res. 335: 109-120.

Arora S, Rajwade JM, Paknikar KM (2012) Nanotoxicology and *in vitro* studies: The need of the hour. Toxicol. Appl. Pharmacol 258:151–165.

Auffan M, Decome L, Rose J, Orsiere T, De MM, Briois V (2006) *In vitro* interactions between DMSA-coated maghemite nanoparticles and human fibroblasts: a physicochemical and cyto-genotoxical study. Environ Sci Technol 40:4367–4373.

Ayllon F, Garcia-Vazquez E (2001) Induction of micronuclei and other nuclear abnormalities in European minnow Phoxinus phoxinus and mollie Poecilia latipinna: an assessment of the fish micronucleus test. Mutat Res/Genet Toxicol Environ Mutagen 2000: 467:77–186.

Babich H, Goldstein SH, Borenfreund E (1990) *In vitro* cyto- and genotoxicity of organomercurials to cells in culture. Toxicol Lett 50:3–9.

Bonassi S, Znaor A, Ceppi M, Lando C, Chang WP, Holland N, Kirsch-Volders M, Zeiger E, Ban S, Barale R, Bigatti MP, Bolognesi C, Cebulska-Wasilewska A, Fabianova E, Fucic A, Hagmar L, Joksic G, Martelli A, Migliore L, Mirkova E, Scarfi MR, Zijno A, Norppa H, Fenech M (2007) An increased micronucleus frequency in peripheral blood lymphocytes predicts the risk of cancer in humans. Carcinogenesis 28:625–631.

Bradford MM (1976) A rapid and sensitive method for the quantitation of microgram quantities of protein utilizing the principle of protein-dye binding. Anal Biochem 7:248-254.

Brunner TJ, Wick P, Manser P, Spohn P, Grass R N, Limbach L K, Bruinink A, Stark W J (2006) In vitro cytotoxicity of oxide nanoparticles: Comparison to Asbestos, Silica, and the Effect of Particle Solubility. Environ Sci and Tech 40: 4374-4381.

Cadet J, Berger M, Douki T, Ravanat J (1997) Oxidative damage to DNA: formation, measurement, and biological significance. Rev Physiol Biochem Pharmacol 131:1–87.

Claxton WT, Wilson AB, Mackie GL, Boulding EG (1998) A genetic and morphological comparison of shallow- and deep-water populations of the introduced dreissenid bivalve Dreissena bugensis. Can J Zool 76:1269-1276.

Corr SA, Rakovich YP, Gun'ko YK (2008) Multifunctional magnetic-fluorescent nanocomposites for biomedical applications. Nanoscale Res Lett 3:87-104.

Croteau DL, Bohr VA (1997) Repair of oxidative damage to nuclear and mitochondrial DNA in mammalian cells. J Biol Chem 272:25409–25412.

Diabaté S, Muelhopt S, Paur H-R, Krug HF (2002) Proinflammatory effects in lung cells after exposure to fly ash aerosol via the atmosphere or the liquid phas. Ann Occup Hyg 46:382–385.

Evans MD, Dizdaroglu M, Cooke MS (2004) Oxidative DNA damage and disease: induction, repair and significance. Mutat Res/Rev Mutat Res 567:1–61.

Faix S, Faixova Z, Boldizarova K, Javorsky P (2005) The effect of long-term high heavy metal intake on lipid peroxidation of gastrointestinal tissue in sheep. Vet. Med. – Czech 50: 401–405.

Fenech M (2000) The in vitro micronucleus technique. Mutat. Res 455:81–95.

Girginova P I, Daniel-da-Silva A L, Lopes C B, Figueira P, Otero M, Amaral V S, Pereira E, Trindade T (2010) Silica coated magnetite particles for magnetic removal of Hg2+ from water. Journal of Colloid and Interface Science 345:234-240.

Guilherme S, Válega M, Pereira ME, Santos MA, Pacheco M (2008) Erythrocytic nuclear abnormalities in wild and caged fish (Liza aurata) along an environmental mercury contamination gradient. Ecotoxicol Environ Saf 70:411–421.

Hong SC, Lee JH, Lee J, Kim HY, Park JY, Cho J, Han DW (2011) Subtle cytotoxicity and genotoxicity differences in superparamagnetic iron oxide nanoparticles coated with various functional groups. Int J Nanomedicine 6:3219-3231.

Hwang ES, Bowen PE (2007) DNA damage, a biomarker of carcinogenesis: Its measurement and modulation by diet and environment. Crit Rev Food Sci Nutr 47:27–50.

Kim JE, Shin JY, Cho MH (2011) Magnetic nanoparticles: an update of application for drug delivery and possible toxic effects. Arch Toxicol 86:685-700.

Kobus K, Turner J, Priestley B, Dreosti I (1993) A comparison of the 8-hydroxydeoxyguanosine and micronucleus techniques for the assessment of x-ray and UV induced genotoxicity, Res Commun Chem Pathol Pharmacol 80: 249-252.

Li H, Zhou Q, Wu Y, Fu J, Wang T, Jiang G (2009) Effects of waterborne nano-iron on medaka (Oryzias latipes): antioxidant enzymatic activity, lipid peroxidation and histopathology. Ecotox Environ Safe 72: 684–692.

Lin W, Huang Y, Zhou X-D, Ma Y (2006) *In vitro* toxicity of silica nanoparticles in human lung cancer cells. Toxicol Appl Pharmacol 217:252–259.

Mohmood I, Mieiro CL, Coelho JP, Anjum NA, Ahmad I, Pereira E, Duarte AC, Pacheco M. (2012) Mercury-Induced Chromosomal Damage in Wild Fish (*Dicentrarchus labrax* L.) Reflecting Aquatic Contamination in Contrasting Seasons. Arch Environ Contam Toxicol 63:554–562.

Mu Q, Hondow NS, Krzemiński L, Brown AP, Jeuken LJC, Routledge MN (2012) Mechanism of cellular uptake of genotoxic silica nanoparticles. Particle and Fibre Toxicol 9:29-31.

Nel A, Xia T, Madler L, Li N (2006) Toxic potential of materials at the nanolevel. Science, 311: 622-627.

Oliveira M, Serafim A, Bebianno MJ, Pacheco M. Santos MA (2008) European eel (Anguilla anguilla L.) metallothionein, endocrine, metabolic and genotoxic responses to copper exposure. Ecotoxicol. Environ Saf 70:20–26.

Pacheco M, Santos M A (1997) Induction of EROD activity and genotoxic effects by polycyclic aromatic hydrocarbons and resin acids on juvenile eel Anguilla anguilla L. Ecotoxicol Environ Saf 38: 252–259.

Pereira C, Guilherme S, Barroso C, Verschaeve L, Pacheco M, Mendo S (2010) Evaluation of DNA damage induced by environmental exposure to mercury in Liza aurata using the comet assay. Arch Environ Contam Toxicol 58:112–122.

Rajkumar JSI, Tennyson S (2013) Mercury induced biochemical alterations as oxidative stress in Mugil cephalus in short term toxicity test. Curr World Environ 8: 55-59.

Salonen JT, Seppänen K, Nyyssönen K, Korpela H, Kauhanen J, Kantola M, Tuomilehto J, Esterbauer H, Tatzber F, Salonen R (1995) Intake of mercury from fish, lipid peroxidation, and the risk of myocardial infarction and coronary, cardiovascular, and any death in eastern Finnish men. Circulation. 91(3):645-55.

Santos M A, Pacheco M (1996) *Anguilla anguilla* L. Stress Biomarkers Recovery in Clean Water and Secondary Treated Pulp Mill Effluent. Ecotox Environ Saf 35:96-100.

Santos MA, Pacheco M, Magalhães I (2000) Anguilla anguilla L. Liver Organ Culture as a Toxicological Model: In and *In Vitro* Liver EROD Induction by beta-Naphthoflavone. Fresenius Environ Bull 9:527 - 534.

Singh SP, Rahman MF, Murty USN, Mahboob M, Grover P (2013) Comparative study of genotoxicity and tissue distribution of nano and micron sized iron oxide in rats after acute oral treatment. Toxicol Appl Pharmacol 266:56–66.

Soloneski L, Reigosa MA, Larramendy ML (2003) Effect of the dithiocarbamate pesticide zineb and its commercial formulation, the azzurro. V. Abnormalities induced in the spindle apparatus of transformed and non-transformed mammalian cell lines. Mutat Res 536:121-129.

Song M-F, Li Y-S, Kasai H, Kawai K (2012) Metal nanoparticles-induced micronuclei and oxidative DNA damage in mice. J Clin Biochem Nutr 50:211–216.

Stoiber T, Bonacke D, Bohm K, Bolt H, Thier R, Degen G, Unger E (2004) Disturbed microtubule function and induction of micronuclei by chelate complexes of mercury (II). Mutat.Res 563:97–106.

Tavares DS, Daniel-da-Silva AL, Lopes CB, Silva NJO, Amaral VS, Rocha J, Pereira E, Trindade T (2013) Efficient sorbents based on magnetite coated with siliceous hybrid shells for removal of mercury ions. J Mater Chem 1: 8134-8143.

Valavanidis A, Vlachogianni T, Fiotakis C (2009) 8-Hydroxy-2'-deoxyguanosine (8-OHdG): a critical biomarker of oxidative stress and carcinogenesis. J Environ Sci Health Part C: Environ Carcinog Ecotoxicol 27:120–139.

Valko M, Izakovic M, Mazur M, Rhodes CJ, Telser J (2004) Role of oxygen radicals in DNA damage and cancer incidence. Mol Cell Biochem 266:37–56.

Voelkel K, Krug H F, Diabaté S (2003) Formation of reactive oxygen species in rat epithelial cells upon stimulation with fly ash. J Biosci 28:51–55.

Wang M Y, Liehr J G (1995) Lipid hydroperoxide induced endogenous DNA adducts in hamsters: possible mechanism of lipid hydroperoxide mediated carcinogenesis. Arch Biochem Biophys 16:1941–1945.

Zhu X, Tian S, Cai Z (2012) Toxicity Assessment of Iron Oxide Nanoparticles in Zebrafish (Danio rerio) Early Life Stages. PLoS ONE 2012; e46286. doi: 10.1371/journal.pone.0046286. Epub 27

CHAPTER 7

Rescheduling the process of nanoparticle removal used for water mercury remediation can increase the risk to aquatic organism: evidence of innate immune functions modulation in European eel (Anguilla anguilla L.)

Abstract

The study aimed to assess the mechanisms of innate immune function responses to silica coated iron oxide nanoparticles functionalized with dithiocarbamate groups (NPs) exposure alone and its associated mercury (Hg) in European eel (*Anguilla anguilla* L.) phagocytes isolated from peritoneum (P-phagocytes), gill (G-phagocytes), head-kidney (HK-phagocytes) and spleen (S-phagocytes). The study evaluated viability, phagocytosis, oxidative burst activity (OBA) and lipid peroxidation (LPO). Four groups were made: i) 2×10^6 phagocytes+RPMI-1640 (control); ii) 2×10^6 phagocytes+NPs (2.5 mg /L); iii) 2×10^6 phagocytes+Hg (50 µg /L); iv) 2×10^6 phagocytes+NPs+Hg. Samplings were performed at 0, 2, 4, 8, 16, 24, 48 and 72 hours of exposure. *A. anguilla* P-, G-, HK- and S-phagocytes *in vitro* exposure to NPs alone revealed either increased (except HK-phagocytes at 16 hours) or no change in viability suggesting that the cells are metabolically active and resistant to NPs exposure alone. In terms of phagocytes overactivation and reactive oxygen species (ROS) production as an indirect mechanism of immunotoxicity, the phagocytes responded in the following manner: P- > S- > HK- = G-phagocytes for NPs exposure alone; S- > HK- > P- = G-phagocytes for Hg exposure alone; and HK- > G- = S- > P-phagocytes for concomitant exposure. Overall, considering Hg as a surrogate for metals and its association with NPs, as well as the likelihood that it could pose a serious threat to aquatic organisms by modulating their immune defense mechanisms if accidentally discharged into the aquatic environment, current results suggest that the step of NPs-Hg complex removal must not be underrated and should be processed without any more ado.

Keywords: *In vitro immunotoxicity; Anguilla Anguilla* L.*; Iron oxide nanoparticles; Mercury; Metal removal*

Environmental Science Pollution Research (2015)22(23):18574-89.

7.1. INTRODUCTION

A credible number of research papers have revealed the evaluation of potential use of silica coated iron oxide nanoparticles functionalized with dithiocarbamate groups (Fe_3O_4@SiO_2/SiDTC, hereafter called NPs) in removal of mercury (Hg) and other potential toxic elements from contaminated waters (Tavares et al., 2013, 2014). Moreover, the research in this direction also claimed the advantages of using NPs in such a way that they can be removed from water using a magnetic field taking the toxic elements associated and leaving the water with better quality (Ambashta et al., 2010; Kim et al., 2011). However, the magnetic removal of the NPs is an additional step in water treatment processes and thus generates a need to assess the importance of its removal as a necessary step and whether it should be as expeditious as metal removal from water. What may be the probable risk to aquatic biota if there is a delay in the process of NPs removal from water? Nevertheless, accidental discharge of NPs and its associated Hg in the environment should be considered as a pre-requisite for its safe and efficient multidisciplinary applications.

Immune function alterations have shown their utility in the pollution monitoring programmes (Matranga and Corsi, 2012). Any undesirable immunomodulation of fish in response to NPs and its associated Hg can provide information not only about the health status of the affected organisms but also on the sustainable preparation of NPs and their applications. The great potential of NPs engineering is that particles may be manipulated to reduce/eliminate immunosupression while retaining their environmental friendly potential. The immune system has a specialized subset of cells, names professional phagocytes, equipped for rapidly and efficiently ingesting invading microorganisms at sites of inflammation (Krpetic et al., 2010; Jovanovic and Palic, 2012). Phagocytosis plays an essential role on host defence mechanisms through the uptake and destruction of pathogens, and contributes to the inflammation and the immune response (Isani et al., 2013). Phagocytosis has shown its utility in detecting interference with the development and functioning of immune response after exposure to metals and non-metals (Shaw and Handy, 2011; Paul and Sengupta, 2013). Pollutants not only induce damage but also activate the phagocytes, which further contribute to the increased burden of reactive oxygen species in fish (Rousselet et al., 2013). Therefore, the enhanced rates of dithiocarbamate oxygenation associated with NPs or Hg redox cycling may be a likely mechanism of toxicity through oxidative stress. However, few available reports reflect its utility in nanoparticle risk assessment in general and no report on NPs in particular for fish in the aquatic environment (Handy et al., 2008 a, Handy et al., 2008 b, Handy et al., 2008 c,

Klaine et al., 2008; Moore 2006; Jovanovic and Palic, 2012). Thus, keeping in view the previously described lacunae, the current study has been hypothesized as: can NPs activates or suppresses fish phagocytes response inappropriately? Moreover, is NPs able to regulate the magnitude and specificity of a competent immune response related to the presence of Hg? The expected mechanism of toxicity of NPs-Hg interaction may involve increased oxidative stress as a consequence of enhanced NP's oxygenation rates rendering fish immune defenses less effective to a concomitant Hg exposure. To test these hypotheses, the following immonotoxicity endpoints *viz.*, phagocytes viability, phagocytosis, oxidative burst activity (OBA) and peroxidative damage were evaluated in phagocytes isolated from peritoneum, gill, head kidney and spleen of *Anguilla. anguilla* taking into account their ability to mirror the pollutant's potential biological impacts (Ahmad et al., 2003; 2004). *A. anguilla* was considered for the current study since it is being widely used as a model animal system to characterize varied environmental pollutants due to its high sensitivity (Geeraerts and Belpaire, 2010).

7.2. MATERIALS AND METHODS

7.2.1. Chemicals

Bovine serum albumin (BSA), bradford reagent, butylated hydroxytoluene (BHT), diethylenetriaminepentaacetic acid (DTPA), dimethyl sulfoxide (DMSO), Giemsa solution, hank's balanced salt solution (HBSS), /L5 medium, methanol, nitroblue tetrazolium (NBT), phosphate buffered saline (PBS), potassium phosphate mono- and dibasic (KH_2PO_4, K_2HPO_4), potassium hydroxide (KOH), Roswell Park Memorial Institute-1640 medium (RPMI-1640 medium), 2-thiobarbituric acid (TBA), tricloroacetic acid (TCA), trizma hydrochloride reagent grade (Tris-HCl), trypan blue solution, zymosan used for this study were of analytical grade and were purchased from Sigma.

7.2.1.1. *Silica coated Fe_3O_4 nanoparticle functionalized with dithiocarbamate (Dtc) groups (NPs)*

The NPs, considered for this experiment, were kindly provided by CICECO Research Unit, University of Aveiro, Portugal. The details pertaining to characterization of Fe_3O_4 and surface modified Fe_3O_4 (Fe_3O_4@SiO_2/SiDTC) can be obtained elsewhere (Tavares et al., 2013). After ultra-sonication dispersal, NPs-agglomeration state in the RPMI-1640 medium was performed as well as the distribution of NPs diameters was also observed using the Dynamic Light Scattering method (Zen 3500, Malvern ZS Nano S analyzer). The size of the NPs used in the

current study was 100 nm and the specific surface area and average zeta potential of NPs were 20.2 m^2 g^{-1} and -10.45 mV, respectively. Based on the study performed by Tavares et al., (2013) where the authors evidenced a high efficiency of Fe_3O_4@SiO_2/SiDTC (2.5 mg /L) for the removal of Hg up to concentration of 50 µg /L, the current bio-experiment included 2.5 mg /L and 50 µg /L were chosen as test concentrations, respectively, for NPs and Hg. In the current bio-experiment, a stock solution (10 mg /L) of previously prepared NPs was made and sub-diluted to the final concentration of 2.5 mg /L in RPMI-1640 medium with 10% FBS, Penicillin 100 IU. In order to prevent the NPs agglomeration, the /L5 dispersed NPs were mixed using vortex for 20 seconds and sonicated for 2×20 seconds with a 20 seconds pause in between the sonication. In parallel, the stock solution of Hg (10 mg /L) was made and diluted in order to get the required concentration of Hg 50 µg /L in different exposure groups**.**

7.2.2. Experimental protocols

European eel *A. anguilla* (n=3+3) with an average weight of 50 ± 5 g were collected from the Aveiro Lagoon, Murtosa (Portugal). In the experiment, total 6 fish were used in two sets. The first set of 3 fish was used for all measurements and the second set of 3 fish was used to repeat the experiment of first set. Fish sizes, for this *in vitro* study, were adopted following the study of Mohmood et al., (2014) taking into account the balance between the statistical requirements and the lowest number of animal sacrifice to achieve our goals. At the time of fish capture, the water characteristics of fishing area were as follows: salinity 6.5%, temperature 18ºC, pH 7.4 and dissolved oxygen 7.47 mg /L. The eels were maintained in 50 L aquarium with submerged water filters for one week with the following physiochemical conditions: temperature - 20 ºC, pH - 7.4, and dissolved oxygen - 8.67 mg /L. Fish were not fed during holding and acclimatization period mainly to avoid the water quality depletion as adopted by Santos and Pacheco (1996) and Mohmood et al., (2014). After acclimation, peritoneum and gill-adhered phagocytes were isolated using method previously described by Ahmad et al., (2003). Briefly, the fish blood was drained by severing the caudal vein to avoid the contamination of red blood cell with peritoneal and gill exudates. An abdominal incision was made and peritoneal cavity and gill were thoroughly rinsed into siliconized test tubes, transferred to separate unsiliconized petri-dishes with cold HBSS and kept incubated during 1 hour for adherence. These unsiliconized petri-dishes supernatant was decanted and the cells detached with the help of a cell scraper in fresh cold HBSS medium (pH 7.2). Detached cells were centrifuged in siliconized tubes at 2500 rpm for 10 minutes (3×) and the final cell pellet was re-suspended in 1 mL of medium RPMI-1640 with 10% FBS, Penicillin 100 IU. Cells

were counted using a Neubauer hemocytometer. Differential counts were performed to assess the phagocytes population in the cell suspension to avoid red blood cells contamination.

7.2.3. Isolation of phagocytes from head kidney and spleen

Head kidney (pronephros) and spleen in fish were dissected out and cells were isolated according to the method described by Fatima et al., (2000) and Tellez- Bañuelos et al., (2009). Briefly, it was minced using a cell dissociation sieve tissue grinder kit (Sigma) and the cells were separated from tissue in RPMI-1640. The suspension was layered onto Histopaque-1077 and centrifuged at 1800 rpm for 30 minutes. The cell layer was collected, washed twice with RPMI-1640 with 10% FBS, Penicillin 100 IU and used for experiments.

Phagocytes isolated from the peritoneum, gill and head-kidney reflected similarity in their morphology as confirmed by their light microscopic images of 0, 24, 48 and 72 hours of exposure (Figure 7.2-7.4). Due to lack of samples, the spleen phagocytes could not processed for microscopic images.

7.2.4. Phagocytes processing and contaminants exposure

Phagocytes isolated from peritoneum, gill, head-kidney and spleen in RPMI medium with 10% FBS, Penicillin 100 IU were centrifuged and the phagocytes were maintained at a density of 1×10^6 cells/mL. Using four aliquots of 2 mL, the phagocytes were divided into four exposure groups: (i) 2×10^6 phagocytes + 2 mL RPMI served as control, (ii) 2×10^6 phagocytes + 2 mL of NPs (2.5 mg L^{-1}) in RPMI referred as NPs, (iii) 2×10^6 phagocytes + 1 mL RPMI + 1 mL Hg (100 µg L^{-1}), and (iv) 2×10^6 phagocytes + 1 mL of NP (5 mg L^{-1}) in RPMI + 1 mL Hg (100 µg L^{-1}) for each fish following the protocol given in figure 7.1. After 24 and 48 hours, the medium of mentioned four groups were renewed by centrifugation at 3000 rpm. The pellet obtained in each group was re-suspended in fresh RPMI medium and the Hg concentrations were maintained up to 50 µg /L. Samples were collected immediately after incubation at 0, 2, 4, 8, 16, 24, 48 and 72 hours from each group and stored at -80 °C for various biochemical estimations. A little sample (10 µL) was immediately processed for the gross estimation of phagocytes viability and slides preparation for phagocytosis as well as oxidative burst activity from each group. In order to estimate the optimum time enabling NPs to target immune cells, the study period was extended up to 72 hours.

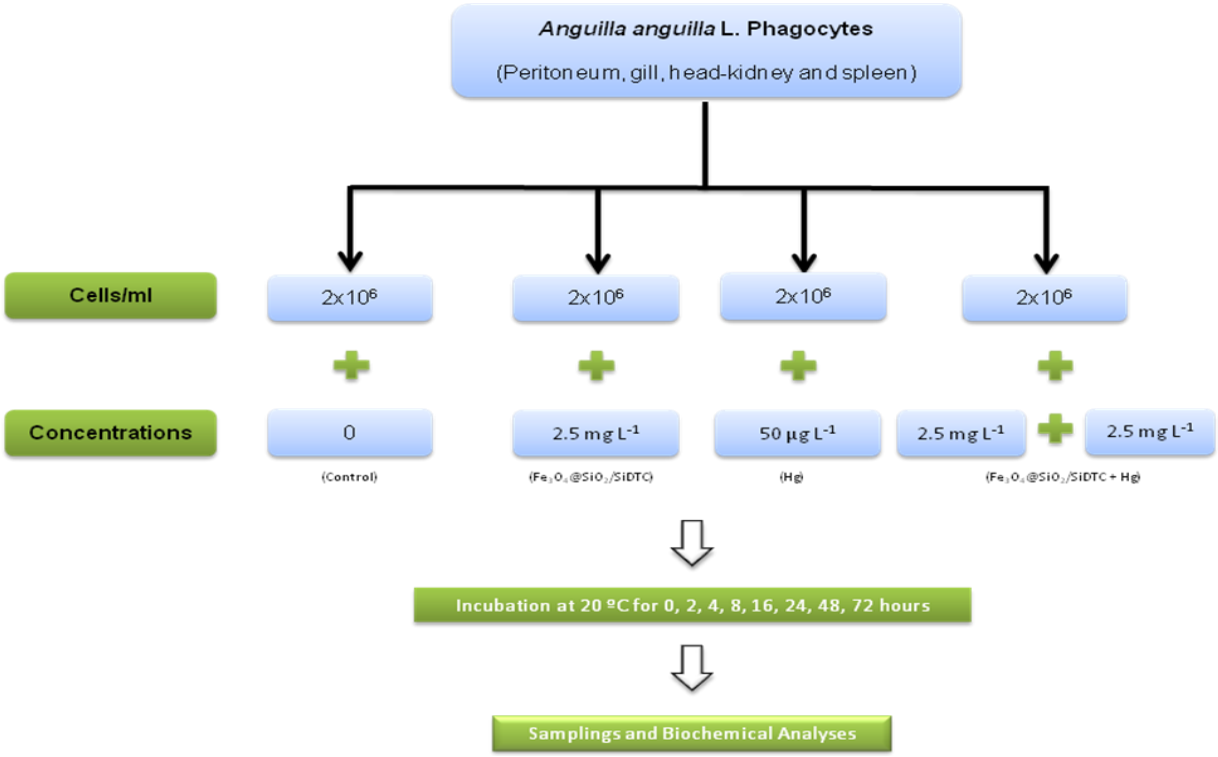

Figure 7.1. Schematic representation of the experimental protocol followed in the present study (Fe_3O_4@SiO_2/SiDTC - silicacoated iron oxide nanoparticles (NPs); Hg - mercury).

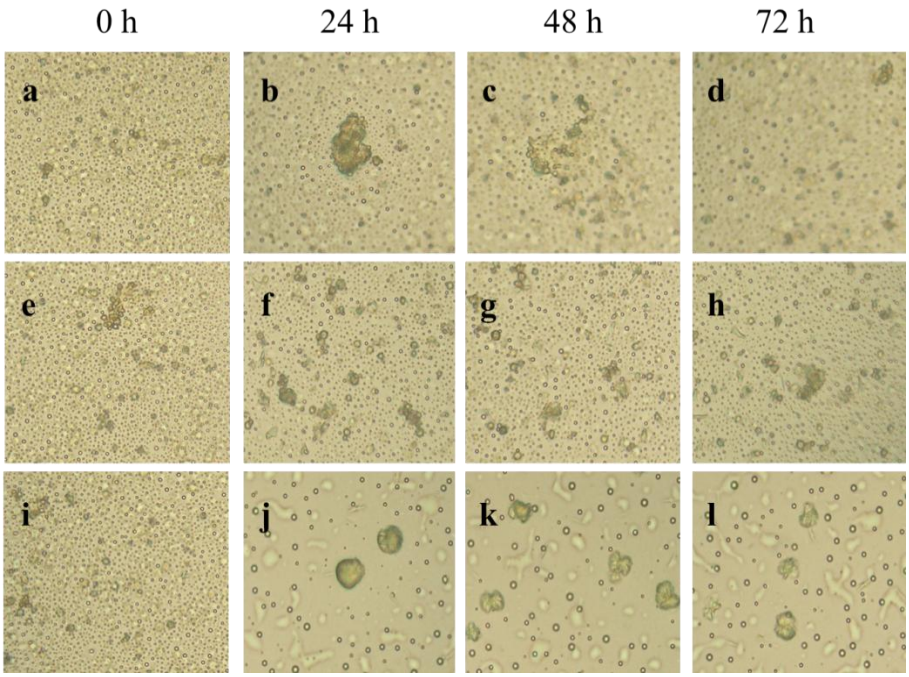

Figure 7.2. *A. Anguilla* peritoneum exudates phagocytes morphology showing lamellopedia in response to silica coated Fe_3O_4 nanomaterial functionalized with dithiocarbamate groups (NP) and mercury (Hg) alone (a-d for NP; e-h for Hg) and concomitant exposure (i-l for NP+Hg) for 24, 48 and 72 hours in comparison to control (0 hour).

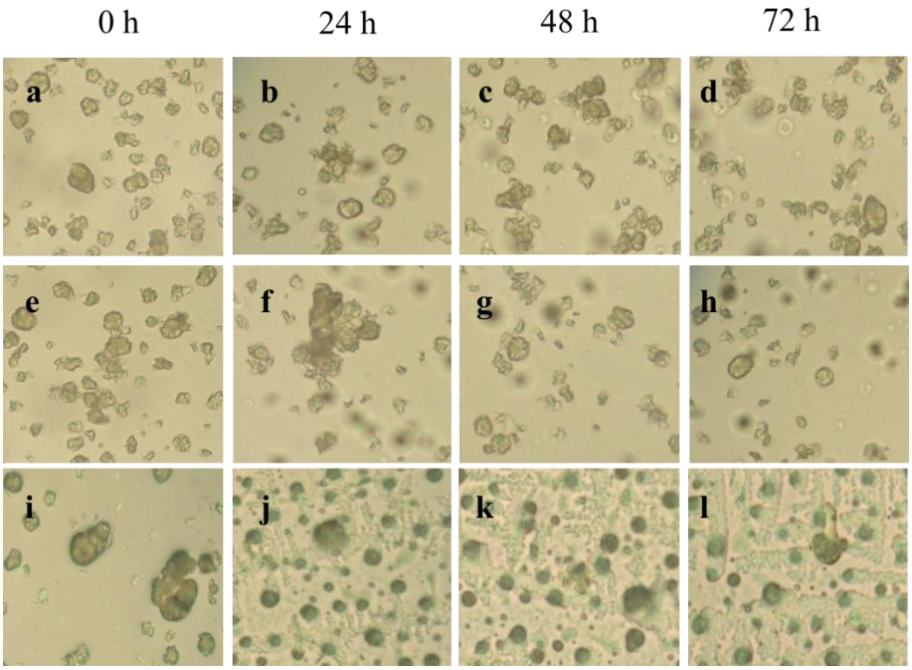

Figure 7.3. *A. Anguilla* gill adhered phagocytes morphology showing lamellopedia in response to silica coated Fe_3O_4 nanoparticle functionalized with dithiocarbamate groups (NPs) and mercury (Hg) alone (a-d for NPs; e-h for Hg) and concomitant exposure (i-l for NPs+Hg) for 24, 48 and 72 h in comparison to control (0 h).

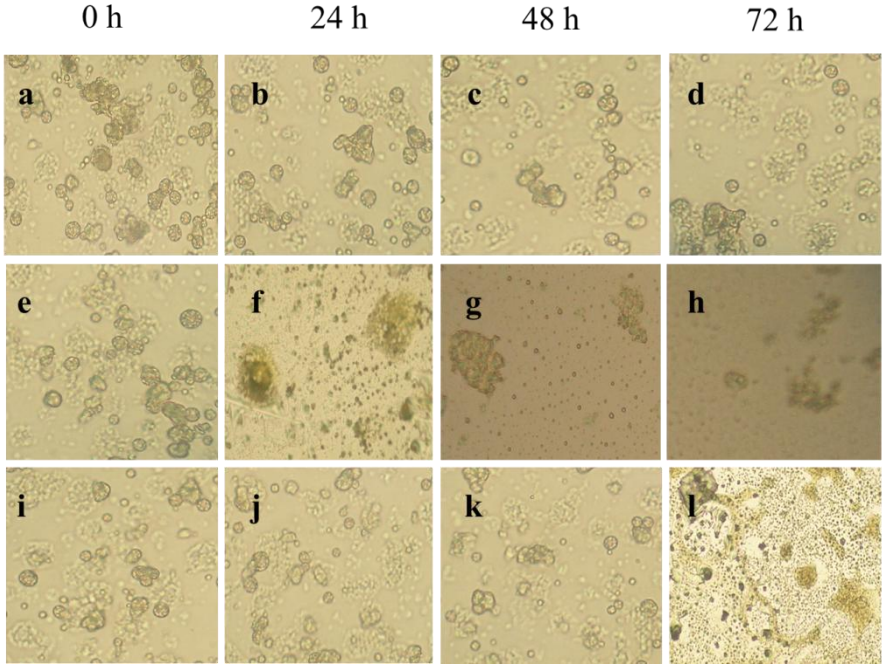

Figure 7.4. *A. Anguilla* . Head kidney resident phagocytes morphology showing lamellopedia in response to silica coated Fe_3O_4 nanoparticle functionalized with dithiocarbamate groups (NPs) and mercury (Hg) alone (a-d for NPs; e-h for Hg) and concomitant exposure (i-l for NPs+Hg) for 24, 48 and 72 h in comparison to control (0 h).

7.2.5. Phagocytes innate immune responses

7.2.5.1. Phagocytes viability

The viability of phagocytes was determined by trypan blue dye exclusion method of Raisuddin et al., (1993). Briefly, the assay consisted of 25 µL of trypan blue solution, 15 µL of PBS, 10 µL cell suspensions and 10 µL of zymossan. The mixture was allowed to stand for 15 minutes. Then, a little amount of the suspension was transferred onto cover slide and counted in duplicate under the light microscope (Olympus BX40) at a magnification of 400× and 300 cells were analysed per animal. Cell viability was expressed as percentage by applying the following equation: Cell viability (%) = number of viable cells/number of viable cells + number of dead cells × 100.

Phagocytic activity of phagocytes was evaluated using the suspension assay as described by Ahmad et al. (1998) with some modification. Briefly, 10µL aliquot, was mixed with 15 µL of medium containing 10% FBS and 10 µL zymossan. The mixture was incubated at 25 °C for one hour with occasional shaking. After incubation, 10µL volume of this mixture was smeared on glass slide, air-dried and stained with Giemsa stain. The slides were observed under a light microscope (Olympus BX40) using oil immersion. At least 400 cells were counted. Phagocytosis was expressed as phagocytic index by applying the following equation: Phagocytic Index (%) = Percentage of phagocytes containing at least five zymossan × Average number of zymossan particles engulfed by phagocytes.

7.2.5.2. Oxidative burst activity (OBA) assay

The previously collected samples were processed for oxidative burst activity in peritoneal, gill, head kidney and spleen phagocytes according to the method of Fujiki and Yano. (1997) with some modifications as adopted by Ahmad et al., (2004). Briefly, an aliquot (20 µL) of phagocyte suspension was mixed with 100 µL PBS containing 0.1% NBT and zymosan suspension (1 mg/mL). The mixture was incubated at 25 ºC for 2 hours with continuously shaking. After the incubation, the suspension was centrifuged at 3000 rpm for 10 minutes. The cell pallet was washed two times, first with 200 µL of PBS and then centrifuge at 3000 rpm during 10 minutes and the second with 70% methanol, air dried at 60 ºC for 15 minutes and suspended with 100 µL of 2M KOH and 10 µL of DMSO. The mixture was well suspended using the vortex for 30 seconds. After centrifugation at 3000 rpm for 3 minutes, the absorbance of supernatant was measured at 630 nm, which denotes the NBT reduction potential of phagocytes. The OBA was expressed as A_{630} nm 10^{-6} cells.

7.2.5.3. Estimation of lipid peroxidation (LPO)

LPO was determined in the previously prepared cells suspension. Briefly, to a 50 µL cell suspension, 500 µL of 12% TCA in aqueous solution, 450 µL of Tris-HCl buffer (60 mM, pH 7.4 and 0.1 mM DTPA) and 500 µL 0.73% TBA was added with a final volume 1.5 mL. The mixture was heated for 15 minutes in water bath set at boiling temperature. The eppendorfs were then removed and cooled to room temperature. The contents from each eppendorf (1.5 mL) were decanted into 2 mL microtubes and centrifuged at 12000 rpm for 3 minutes. The absorbance of the plate was measured at 535 nm. The rate of LPO was expressed as nmol of thiobarbituric acid reactive substances (TBARS) formed per milligram of protein ($\varepsilon = 1.56 \times 10^5$ /M cm).

7.2.6. Protein concentration measurement

Total protein was determined according to the Bradford method (1976) using bovine serum albumin (BSA) as standard. The assay mixture contained 990 µL of Bradford reagent, 10 µL of diluted BSA (2.5 mg/mL) and 10 µL miliQ-water. The absorbance of plate was measured at 595 nm after incubate during 10 minutes in dark.

7.2.7. Statistical analysis

Microsoft excel software and SPSS (PASW statistics 18) for Windows was used for statistical analysis of data. All of the data were first tested for normality and homogeneity of variance to meet statistical demands. The t-test was applied for significant differences in order to compare results within and between the groups (control, NPs, Hg and NPs+Hg). A significance level of 0.05 was ascertained in all test procedures.

7.3. RESULTS

7.3.1. Peritoneal exudates phagocytes (P-phagocytes) responses

7.3.1.1. Inter-group comparisons

A. anguilla P-phagocytes *in vitro* exposure to NPs alone in comparison to control revealed a significant increase in viability at 2, 8 and 16 hours, phagocytic index at 4, 8, 16 and 48 hours, and OBA at 8 hours; whereas, a decrease in phagocytosis at 24 hours and LPO at 2 and 72 hours was also perceptible when compared to control (Figure 7.5).

Effects of Hg exposure alone (versus control) revealed a significant increase in viability at 8 and 16 hours, phagocytic index at 16 hours, and OBA at 8 hours; whereas a decrease in phagocytic index at 8 hours, OBA at 24 hours, and LPO at 16 hours.

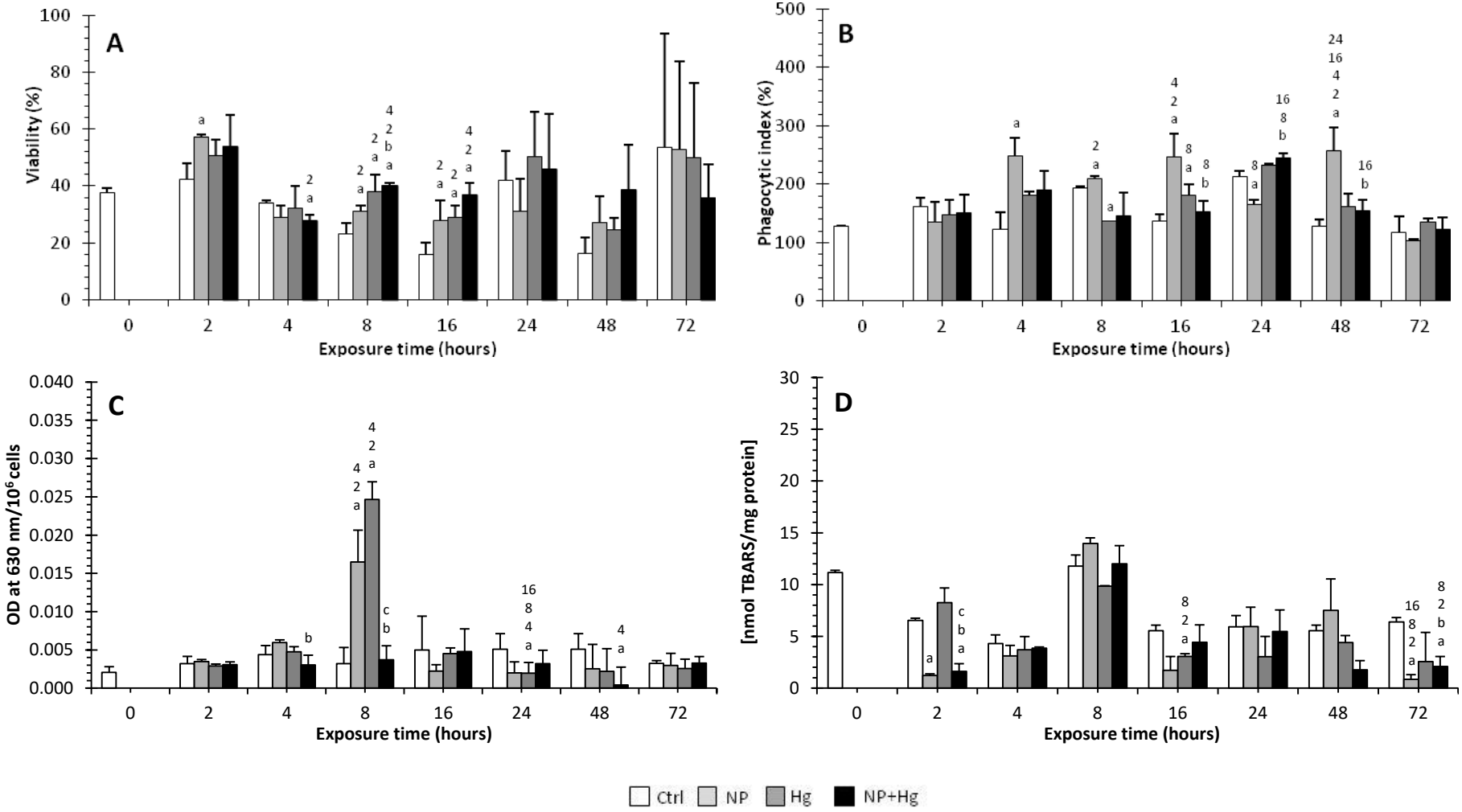

Figure 7.5. *A. anguilla*. *in vitro* peritoneum exudates phagocytes: viability (%) (A), phagocytic index (%) (B), oxidative burst activity (%) (C) and lipid peroxidation (D) under exposure to silica coated Fe_3O_4 nanomaterial functionalized with dithiocarbamate groups (NPs) and mercury (Hg) alone or concomitantly for a period of 72 hours. The values are expressed as means ± S.D. Inter-group significant differences have been denoted by letters: a (*vs*. control), b (*vs*. NP), c ($_{vs}$. Hg) and inter-hours significant differences have been marked by numbers: 2 (*vs*. 2 hours), 4 (*vs*. 4 hours), 8 (*vs*. 8 hours), 16 (*vs*. 16 hours), 24 (*vs*. 24 hours) and 48 (*vs*. 48 hours).

Effects of NPs and Hg concomitant exposure displayed a significant increase only in viability at 8 and 16 hours when compared to control; whereas, a decrease was perceptible in viability at 4 hours, OBA at 48 hours, and LPO at 2 and 72 hours in comparison to control. Upon comparison of NPs+Hg exposure with NPs alone, a significant increase in viability at 8 hours, phagocytic index at 24 hours, and LPO at 2 and 72 hours was observed; whereas, a decrease was perceptible in phagocytic index at 16 and 48 hours, and OBA at 4 and 8 hours. A decrease was also observed in OBA at 8 hours and LPO at 2 hours when the concomitant NP+Hg group was compared with Hg group alone.

7.3.1.2. Inter- hours comparisons

Inter-hours comparisons revealed no statistically significant difference among the controls during the 72 hour exposure period in all the studies parameters. However, NPs exposure alone lead to significantly increase in phagocytosis at 8 hours (*vs. 2 hours*), 16 hours (*vs. 2 and 4 hours*), and 48 hours (*vs. 2, 4, 16 and 24 hours*), OBA at 8 hours (*vs. 2 and 4 hours*); whereas a decrease in viability at 8 and 16 hours (*vs. 2 hours*), phagocytosis at 24 hours (*vs. 8 hours*) and LPO at 72 hours (*vs. 2, 8 and 16 hours*).

Concerning Hg exposed P-phagocytes, a significant increase in phagocytosis at 16 hours (*vs. 8 hours*), OBA at 8 hours (*vs. 2 and 4 hours*); whereas a decrease in viability at 8 and 16 hours (*vs. 2 hours*), OBA at 24 hours (*vs. 2, 8 and 16 hours*) and LPO at 16 hours (*vs. 2 and 8 hours*) was observed.

P-phagocytes concomitantly exposed to NPs and Hg revealed a significant increase in viability at 8 and 16 hours (*vs. 4 hours*), phagocytosis at 16 hours (*vs. 8 hours*); whereas a decrease was observed in viability at 4, 8 and 16 hours (*vs. 2 hours*), OBA at 24 and 48 hours (*vs. 4 hours*), and LPO at 72 hours (*vs. 2 and 8 hours*) respectively.

7.3.2. Gill-adhered phagocytes (G-phagocytes) responses (Figure 7.6.)

7.3.2.1. Inter-group comparisons

A. anguilla G-phagocytes *in vitro* exposure to NPs alone in comparison to control revealed a significant increase in phagocytic index at 8 hours, LPO at 2, 4 and 72 hours; whereas, a decrease in viability at 48 hours and phagocytosis at 16 hours was perceptible in the current study.

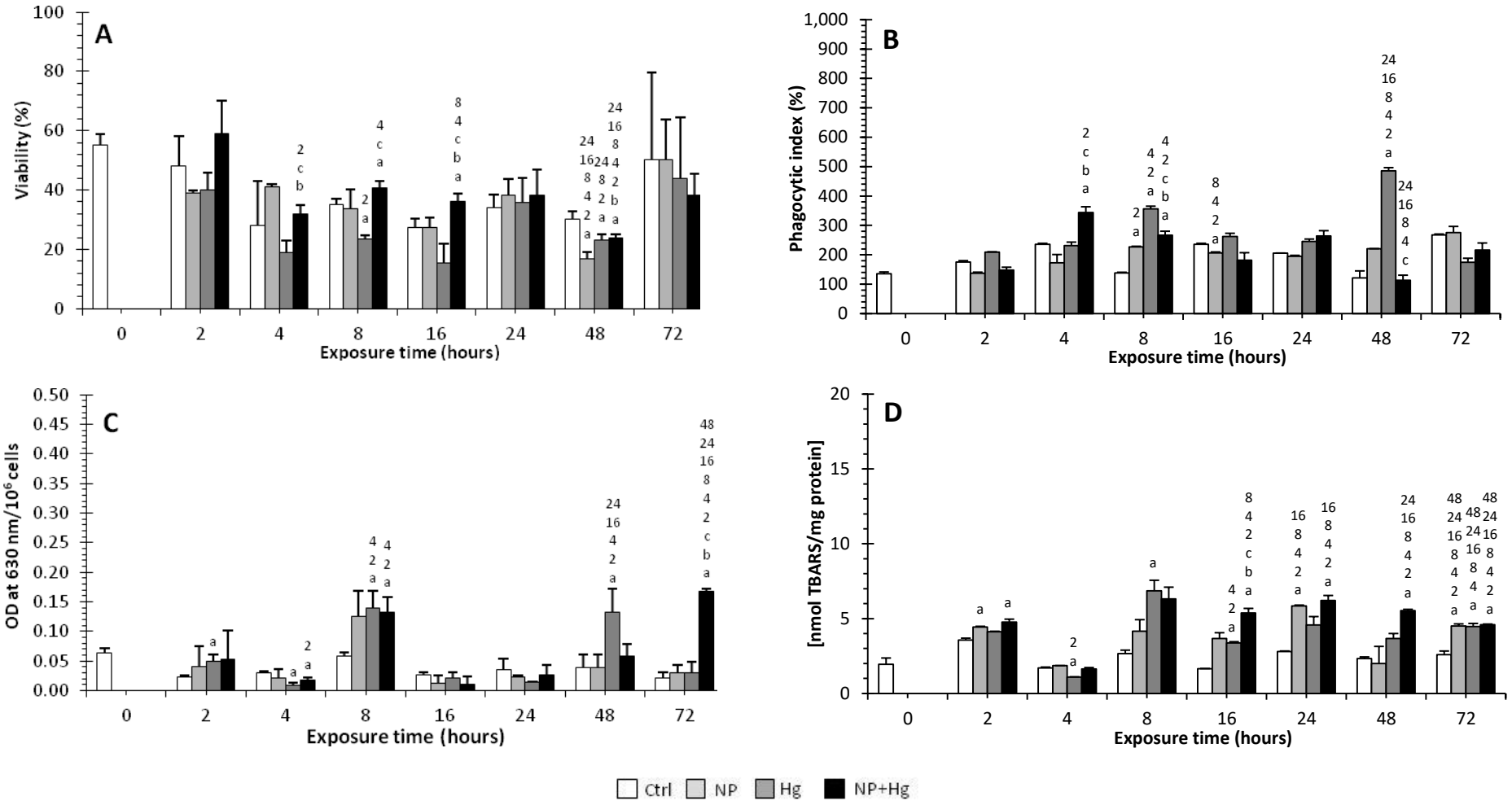

Figure 7.6. *A. anguilla in vitro* gill-adhered phagocytes: viability (%) (A), phagocytic index (%) (B), oxidative burst activity (%) (C) and lipid peroxidation (D) under exposure to silica coated Fe_3O_4 nanomaterial functionalized with dithiocarbamate groups (NPs) and mercury (Hg) alone or concomitantly for a period of 72 hours. The values are expressed as means ± S.D. Inter-group significant differences have been denoted by letters: a (*vs*. control), b (*vs*. NP), c (*vs*. Hg) and inter-hours significant differences have been marked by numbers: 2 (*vs*. 2 hour), 4 (*vs*. 4 hour), 8 (*vs*. 8 hour), 16 (*vs*. 16 hour), 24 (*vs*. 24 hour) and 48 (*vs*. 48 hour).

Effects of Hg exposure alone (*versus* control) revealed a significant increase in phagocytic index at 8 and 48 hours, OBA at 2, 8 and 48 hours, and LPO at 8, 16 and 72 hours; whereas a decrease in viability at 8 and 48 hours, OBA at 4 hours, and LPO at 4 hours.

Effects of NPs and Hg concomitant exposure displayed a significant increase in viability at 8 and 16 hours, phagocytosis at 4 and 8 hours, OBA at 8 and 72 hours, and LPO at 2, 16, 24, 48 and 72 hours in comparison to control group; whereas a decrease was perceptible in viability at 48 hours, phagocytosis at 48 hours and OBA at 4 hours. However, in comparison to NPs alone exposure, a significant increase in viability at 16 and 48 hours, phagocytic index at 4 and 8 hours, OBA at 72 hours and LPO at 16 hours was observed. On the other, a decrease was perceptible in viability at 4 hours in comparison to NPs. Upon comparison of NPs+Hg with Hg alone, an increase was observed in viability at 4, 8 and 16 hours, phagocytic index at 4 hours, OBA at 72 hour and LPO at 16 hours. A decrease was also observed in phagocytosis at 8 and 48 hours when the concomitant NPs+Hg group was compared with Hg group alone.

7.3.2.2. Inter- hours comparisons

Inter-hours comparisons revealed no statistically significant difference among the controls during the 72 hour exposure period in all the studies parameters. However, NPs exposure alone lead to significantly increase in phagocytosis at 8 hours (*vs. 2 hours*) and 16 hours (*vs. 2 and 4 hours*), LPO at 24 hours (*vs. 2, 4, 8 and 16 hours*) and 72 hours (*vs. 2, 4, 8, 16 and 48 hours*); whereas a decrease in viability at 48 hours (*vs. 2, 4, 8, 16 and 24 hours*), phagocytosis at 16 hours (*vs. 8 hours*) and LPO at 72 hours (*vs. 24 hours*).

Concerning Hg exposed G-phagocytes, a significant increase in phagocytosis at 8 hours (*vs. 2 and 4 hours*) and 48 hours (*vs. 2, 4, 8, 16 and 24 hours*), OBA at 8 hours (*2 and 4 hours*) and 48 hours (*vs. 2, 4, 16 and 24 hours*), LPO at 16 hours (*vs. 4 hours*) and 72 hours (*vs. 4, 16 and 48 hours*); whereas a decrease in viability at 8 hours (*vs. 2 hours*) and 48 hours (*vs. 2, 8 and 24 hours*), and LPO at 4 and 16 hours (*vs. 2 hours*) and 72 hours (*vs. 8 and 24 hours*).

G-phagocytes concomitantly exposed to NPs and Hg revealed a significant increase in viability at 8 and 16 hours (*vs. 4 hours*), phagocytosis at 4 and 8 hours (*vs. 2 hours*), OBA at 8 hour (*vs. 2 and 4 hours*) and 72 hours (*vs. all exposure period*), LPO at 72 hours (*vs. 4 hours*); whereas a decrease was observed in viability at 4 hours (*vs. 2 hours*), 16 hours (*vs. 8 hours*) and 48 hours (*vs. 2, 4, 8, 16 and 24 hours*), phagocytosis at 8 hours (*vs. 4 hours*) and 48 hours

(*vs. 4, 8, 16 and 24 hours*), OBA at 4 hours (*vs. 2 hours*) and LPO at 72 hours (*vs. 2, 8, 16, 24 and 48 hours*).

7.3.3. Head kidney phagocytes (HK-phagocytes) responses

7.3.3.1. Inter-group comparisons

A. anguilla HK-phagocytes *in vitro* exposure to NPs alone in comparison to control revealed a significant increase in viability at 8 hours; whereas, a decrease in viability at 16 hours, phagocytosis at 16 and 24 hours, OBA at 4 hours and LPO at 4 and 16 hours was perceptible in the current study (Figure 7.7).

Effects of Hg exposure alone (*versus* control) revealed a significant increase in LPO at 8 hours; whereas a decrease in viability at 8 and 16 hours, phagocytosis at 2, 4 and 8 hours, and LPO at 48 hours in comparison to control.

Effects of NPs and Hg concomitant exposure displayed a significant increase in phagocytosis at 2 hours, in OBA at 4 and 8 hours, and in LPO at 8 hours in comparison to control group; whereas a decrease was perceptible in viability at 48 hours, in phagocytosis at 4 and 16 hours and in LPO at 4 hours. However, in comparison to NPs alone exposure, a significant increase in phagocytic index at 48 hours, and OBA at 4 and 8 hours was observed. On the other, a decrease was perceptible in viability at 8 hours and phagocytosis at 4 and 16 hours in comparison to NPs. Upon comparison of NPs+Hg with Hg alone, an increase was observed in viability at 2 hours, phagocytic index at 4 hours, OBA at 4 and 8 hours. A decrease was also observed in viability at 8 hours when the concomitant NPs+Hg group was compared with Hg group alone.

7.3.3.2. Inter-hours comparisons

Inter-hours comparisons revealed no statistically significant difference among the controls during the 72 hour exposure period in all the studies parameters. However, NPs exposure alone lead to significantly increase in LPO at 16 hours (*vs. 2, 4 and 8 hours*); whereas a decrease in viability at 8 hours (*vs. 2 hours*) and 16 hours (*vs. 2, 4 and 8* hours), phagocytosis at 16 hours (*vs. 2 and 4 hours*) and 24 hours (*vs. 4 hour*), and OBA at 4 hours (*vs. 2 hours*).

Concerning Hg exposed HK-phagocytes, a significant increase in viability at 16 hours (*vs. 8 hours*), phagocytosis at 4 and 8 hours (*vs. 2 hours*), LPO at 8 hours (*vs. 2 and 4 hours*) and 48 hours (*vs. 4 and 8 hours*); whereas a decrease in phagocytosis at 8 hours (*vs. 4 hours*).

HK-phagocytes concomitantly exposed to NPs and Hg revealed a significant increase in OBA at 4 hours (*vs. 2 hours*) and 8 hours (*vs. 2 and 4 hours*), LPO at 8 hours (*vs. 2 and 4 hours*); whereas a decrease was observed in viability at 16 hours (*vs. 2 and 8 hours*), phagocytosis at 4 hours (*vs. 2 hour*), 16 hours (*vs. 2, 4 and 8 hours*) and 48 housr (*vs. 4, 8, 16 and 24 hours*).

7.3.4. Spleen phagocytes (S-phagocytes) responses

7.3.4.1. Inter-group comparisons

A. anguilla S-phagocytes *in vitro* exposure to NPs alone in comparison to control revealed a significant increase in phagocytosis at 4 hours and LPO at 8 hours; whereas, a decrease in phagocytosis at 2, 8 and 72 hours, OBA at 2, 4 and 72 hours was perceptible in the current study (Figure 7.8). No significant increase or decrease was observed in viability in comparison to control.

Effects of Hg exposure alone (*versus* control) revealed a significant increase in viability at 16 hours, and phagocytosis at 2 and 24 hours; whereas a decrease phagocytosis at 72 hours, and LPO at 4, 24 and 72 hours when compared to control.

Effects of NPs and Hg concomitant exposure resulted in a significant increase in viability at 2 hours, phagocytosis at 4 and 24 hours, and LPO at 8 hours in comparison to control group; whereas a decrease was perceptible in viability at 2 hours, phagocytosis at 4 and 16 hours, OBA at 2, 4, 16 and 24 hours, and in LPO at 4 and 72 hours. However, in comparison to NPs alone exposure, a significant increase in phagocytic index at 8 hours, OBA at 4 hours, and LPO at 8 hours was perceptible. On the other hand, a decrease was perceptible in phagocytosis and OBA at 4 and 16 hours in comparison to control. Upon comparison of NPs+Hg with Hg alone, an increase was observed in LPO at 72 hours. A decrease was also observed in phagocytosis at 16 and 24 hours when the concomitant NPs+Hg group was compared with Hg group alone.

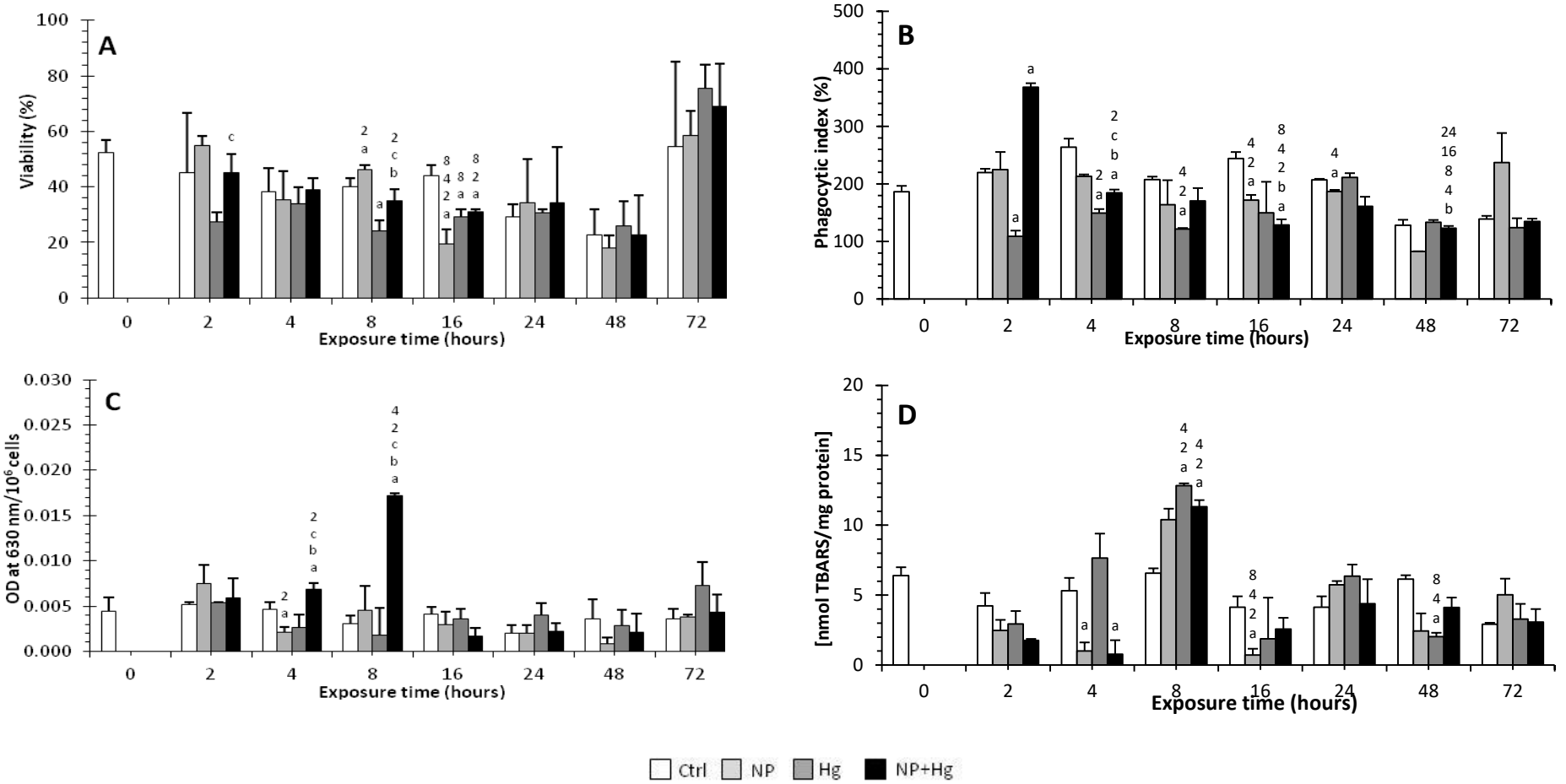

Figure 7.7. *A. anguilla* . *in vitro* head kidney resident phagocytes: viability (%) (A), phagocytic index (%) (B), oxidative burst activity (%) (C) and lipid peroxidation (D) under exposure to silica coated Fe_3O_4 nanomaterial functionalized with dithiocarbamate groups (NPs) and mercury (Hg) alone or concomitantly for a period of 72 hours. The values are expressed as means ± S.D. Inter-group significant differences have been denoted by letters: a (*vs*. control), b (*vs*. NPs), c (*vs*. Hg) and inter-hours significant differences have been marked by numbers: 2 (*vs*. 2 hours), 4 (*vs*. 4 hours), 8 (*vs*. 8 hours), 16 (*vs*. 16 hours), 24 (*vs*. 24 hours) and 48 (*vs*. 48 hours).

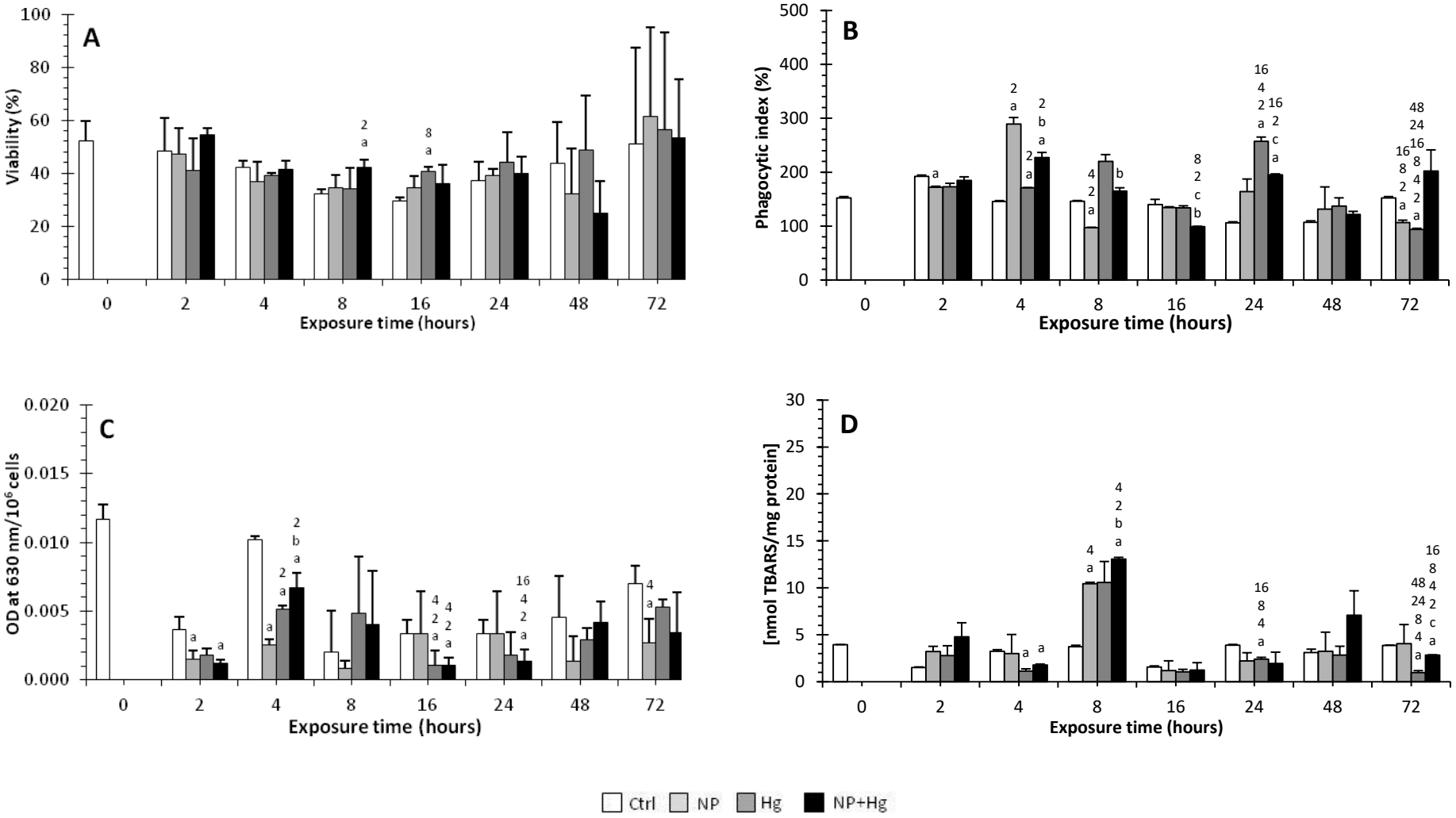

Figure 7.8. *A. anguilla in vitro* spleen resident phagocytes: viability (%) (A), phagocytic index (%) (B), oxidative burst activity (%) (C) and lipid peroxidation (D) under exposure to silica coated Fe_3O_4 nanomaterial functionalized with dithiocarbamate groups (NPs) and mercury (Hg) alone or concomitantly for a period of 72 hours. The values are expressed as means ± S.D. Inter-group significant differences have been denoted by letters: a (*vs.*

control), b (*vs*. NPs), c (*vs*. Hg) and inter-hours significant differences have been marked by numbers: 2 (*vs*. 2 hour), 4 (*vs*. 4 hour), 8 (*vs*. 8 hour), 16 (*vs*. 16 hour), 24 (*vs*. 24 hour) and 48 (*vs*. 48 hour).

7.3.4.2. Inter-hours comparisons

Inter-hours comparisons revealed no statistically significant difference among the controls during the 72 hour exposure period in all the studies parameters. However, NPs exposure alone lead to significantly increase in phagocytosis at 4 hours (*vs. 2 hours*) and 72 hours (*vs. 8 hours*), OBA at 72 hours (*vs. 2 hours*) and LPO at 8 hours (*vs. 4 hours*); whereas a decrease in phagocytosis at 8 hours (*vs. 2 and 4 hours*) and 72 hours (*vs. 2 and 16 hours*).

Concerning Hg exposed S-phagocytes, a significant increase in viability at 16 hours (*vs. 8 hours*), phagocytosis at 24 hours (*vs. 2, 4 and 16 hours*), OBA at 4 hours (*vs. 2 hours*), LPO at 24 hours (*vs. 8 hours*); whereas a decrease in phagocytosis at 4 hours (*vs. 2 hours*) and 72 hours (*vs. all exposure period*), OBA at 16 hours (*vs. 2 and 4 hours*) and LPO at 24 hours (*vs. 8 hour*) and 72 hours (*vs. 4, 8, 24 and 48 hours*).

S-phagocytes concomitantly exposed to NPs and Hg revealed a significant increase in phagocytosis at 4 hours (*vs. 2 hours*) and 24 hours (*vs. 2 and 16 hours*), OBA at 4 hours (*vs. 2 hours*) and 24 hours (*vs. 2 and 16 hours*), LPO at 8 hours (*vs. 2 and 4 hours*) and 72 hours (*vs. 4 and 16 hours*); whereas a decrease was observed in viability at 8 hours (*vs. 2 hours*), OBA at 16 hours (*vs. 2 and 4 hours*) and 24 hours (*vs. 4 hour*), and LPO at 72 hours (*vs. 2 and 8 hours*).

7.4. DISCUSSION

7.4.1. P-phagocytes responses

A. anguilla P-phagocytes i*n vitro* exposure to NPs alone revealed either increase (2, 8 and 16 hours) or no change in viability suggesting that the cells are metabolically active and resilient to NPs exposure alone. This result is consistent with other reports that nanoparticles do not show obvious acute lethal toxicity to cells within 24 hours of incubation (Lima et al., 2011; Semete et al., 2010). However, no change after 24, 48 and 72 hours may suggest that cell viability was uncompromised after 24 hour exposure to NPs and the nature of change in viability following initial exposures were transient. NPs can either bind to the external cell membrane or can be internalized into the cytoplasm. NPs that are bound externally do not affect cell viability, although, they may interfere with cell-surface interactions or may simply

detach from the cell membrane (Bulte et al., 2004 a). However, since the current study includes phagocytes having inherent property of engulfing and attacking particles that have been signalled for removal by various mechanisms in the host, the current viability increase may strengthens the explanation given by Bulte et al., (2004 b) that NPs may be internalized within the cells with no effects on their viabilities. Phagocytosis process with nanoparticles has been very well document and is capable of internalizing particles up to 100 nm in size (Bartneck et al., 2010; Dobrovolskaia and McNeil, 2007).

On the perspective of NPs induced inappropriate fish phagocytes responses, a significant increase P-phagocytes activation (4, 8, 16 and 48 hours) was observed in the current study indicating that the NPs has the potential to induce innate immune response similar to that of the lower concentration of conventional metals, non-metals and industrial effluents in fish (Ahmad et al., 1998, 2003, 2004; Santos et al., 2006). Since NPs are characterized by both metals and organic compounds having known toxic potential, the stimulation of phagocytes may be attributed to the organic components of NPs because of their molecular size acting as elicitor of phagocytes. At the initial (2 hour) and end (72 hour) of the exposure, no response was observed; however, the decrease was observed at 24 hours. Since the decrease did not arise from a drop in the cells viability induction, phagocytic activity may be emerged or induced on the following exposure as is the case of the current study, supposedly as a consequence of the limited ingestion capacity arising from the interaction along the time. Moeller et al., (2012) described this phenomenon in humans with incubation of macrophages (100 nM SRL (rapamycin) nanoparticle (≈91 μg /L)), which caused a reduction of phagocytosis by 10–20%.

A significant increase in OBA was observed at 8 hour of exposure. Moreover, increase in P-phagocytosis at 8 hours was concomitantly associated to the excess production of ROS (as measured by OBA) to the same exposure time (8 hours). The results are in accordance of Zhu et al., (2012) who observed that the adherence and/or adsorption of iron oxides nanoparticles aggregates may cause excessive production of ROS. In addition, it is also evident from the current observation that besides the direct action of NPs in ROS production, activation of phagocytes cannot be overlooked to be a part of an indirect mechanism of immunotoxicity since fish phagocytes engulf invading foreign agents and normally kill them by the release of cytotoxic ROS. Activated phagocytes undergo oxidative burst phenomenon and release toxic oxygen products such as superoxide ($O2^{\bullet}$-), hydrogen peroxide (H_2O_2), singlet oxygen ($^1O_2$) and hydroxyl radicals ($OH^{\bullet}$) (Ahmad et al., 2003, 2004, 2011 a, b; Fatima et al., 2000; Santos

et al., 2006). This approach of over ROS production has also been met with the differences in antioxidants status successfully (Ahmad et al., 2000, 2004, 2011 a, b; 2012). No association of phagocytic induction with ROS production at the rest points of the exposure may be directed to the change in oxidation state of iron oxides nanoparticles and protein-iron oxides nanoparticles interaction as suggested by Berry et al., (2003, 2004) and Mahmoudi et al., (2009, 2010). With the increase in exposure time, the modulation of phagocytes induction is perceptible reaching the value of control at the end of exposure time, which also corroborate with the observation of no ROS production and no LPO increase (except 8 hours), suggesting that the innate immune modulation is well tuned with the phagocytes function responses in maintaining the overall cells tolerance. Iron oxides nanoparticles (Magnetite (Fe_3O_4) and maghemite (γ-Fe_2O_3)) can reveal different cellular responses because of their ability to experience oxidation/reduction reactions. For example, Fe_3O_4 has been shown to cause higher levels of oxidative damage in A549 human lung epithelial cell line in the absence of decreased cell viability as compared to γ-Fe_2O_3 remaining to its potential to undergo oxidation (Karlsson et al., 2008, 2009). Moreover, Singh et al., (2010) hypothesised that the toxicity of iron oxides nanoparticles may be decreased by coating magnetite particles resulting in fewer oxidative sites that are less reactive and thereby produce less macromolecule damage over time (Mahmoudi et al., 2009).

Similar modulation in viability and phagocytosis was observed for Hg exposure alone; however, at different point of exposure time. Thus, a decrease in phagocytosis was observed at 8 hours, whereas an increase in viability at 8 and 16 hours, and phagocytosis at 16 hours was observed. According to Sauvé et al., (2002), *in vitro* toxicity of Hg may exhibit: i) lack of cell cytotoxicity and stimulation of the phagocytosis; ii) lack of cell cytotoxicity and normal phagocytosis; iii) relatively low metal-related cytotoxicity and dramatic inhibition of phagocytosis; and iv) relatively high cytotoxicity accompanied by a drastic inhibition of the phagocytosis in aquatic animals. However, the previous explanation seems to not be applicable in the current *in vitro* study on fish and suggest an alternate explanation of the viability induction and decrease or increase in phagocytosis may also exist. Moreover, the role of phagocytes in free radicals production cannot be suggested here since no activation was observed and thus ROS production at 8 hours is the result of direct Hg interaction with phagocytes causing excessive production of ROS. A decrease in phagocytosis is well documented in the literature following either *in vivo* or *in vitro* Hg exposure (Fournier et al., 2001). Moreover, a decrease in phagocytic index may strengthen the explanation of the

limited ingestion capacity arising from the interaction of Hg with phagocytes along the time since the decrease did not arise from a drop in the cells viability induction as described above for NP. Similar to the response of NPs, Hg exposed phagocytes reflected increased OBA (at 8 hours) and no LPO suggesting the same kind of phagocytes response towards Hg maintaining the cells viability. The occurrence of no OBA induction and either LPO decrease or no LPO along the time can suggest that in the presence of lower ROS levels, adaptive mechanisms might have been activated, providing a better protection to Hg exposed phagocytes.

A clear interference of NPs exposure with Hg co-exposure can be seen in the current study since viability increased upon 2 hour of NPs exposure went to normal with Hg co-exposure; at 4 hours it decreased as well as at 8 hour it increased further. Moreover, activation of phagocytes as observed by increase in phagocytosis (4, 8, 16 and 48 hours) and OBA (8 hours) after NPs exposure alone went to normal with Hg co-exposure. In addition, association between phagocytes overactivation and ROS production (OBA increase at 8 hour) at both NPs and Hg individual exposure went to normal in concomitant NPs+Hg exposure. The only decrease in viability at early hour (4 hours) indicated that the interaction of NPs with Hg can influence bioavailability/bioaccessibility as well as toxicity potential of either NPs and/or Hg. This can be in agreement with the hypothesis that NPs-metal interaction may result in increased toxicity via oxidative stress as a consequence of enhanced NPs oxygenation rates rendering fish immune defenses less effective to a concomitant metal exposure. Moreover, it is also evident that NPs exposure with its increased exposure time provides immuno-protection against Hg accrued negative effects (phagocytosis decrease at 8 hours; OBA increase at 8 hours). Hence, the occurrence of antagonism between NPs and Hg cannot be ignored, which is further evidenced as a principle of NPs-mediated Hg-NPs complex formation (Girginova et al., 2010; Tavares et al., 2013) in P-phagocytes.

7.4.2. G-phagocytes responses

G-phagocytes *in vitro* exposure to NPs alone reflected a decrease in the cell viability at late (48 hours) hour of exposure confirming the report of Lima et al., (2011) that nanoparticle do not show acute lethal toxicity to cells within 24 hours of incubation. Moreover, viability decrease (48 hours) followed by an increase (72 hours) clearly indicated that cell viability was uncompromised at the exposures to NPs. On the perspective of phagocytosis, at the initial (2 hours) and end (72 hours) of the exposure, no response was observed; however, a significant increase at 8 hour and decrease at 16 hours was observed. Since the decrease did not arise from a drop in the cells viability induction, phagocytic activity emerged at the rest

of the exposure times (24, 48 and 72 hours) is plausible, supposedly as a consequence of the limited ingestion capacity arising from the interaction along the time as suggested above. No OBA induction was observed in the phagocytes after exposure to NPs alone; however, LPO increase once generated remained persistent until 72 hours with a punctual increase at 2, 24 and 72 hours. Moreover, it was also clear that there is no association between viability and LPO since LPO increase (2 hours) was preceded by viability decrease (48 hours), which is in accordance with the study done by Perreault et al., (2012). The primary mechanism proposed to explain NPs immunotoxicity is via Fe-initiated free radical formation (Fraga et al., 2002; Valko et al., 2005). In this direction, damage to lipid by NPs may be enhanced by the involvement of H_2O_2, hydroxyl, and superoxide radicals, respectively (Jain et al., 2007; Lloyd et al., 1997; Manibusan et al., 2007). However, the finding that lipid damage is not corroborated by ROS as measured by OBA make it unlikely that the mechanisms involved are based simply on ROS production (Roesslein et al., 2013). Therefore, NPs can directly interact with lipid, constituting an alternative mechanism for NPs immunotoxicity (Planque et al., 2011). Moreover, the LPO increase was not corroborated either with phagocytic induction (except 8 hour) or ROS production in the current study further validating that NPs toxicity mechanism is not depending on free radicals production.

It is clear that Hg exposure alone is toxic at both early (8 hours) and late (48 hours). In addition, a clear correlation among viability decrease, phagocytosis increase, OBA increase and LPO increase is perceptible to the same exposure time in the current study suggesting the involvement of ROS in addition to the direct damage of Hg to G-phagocytes. It was also evident that G-phagocytes showed no failure to maintain the phagocytes activities at the end of the exposure period (72 hours) after exposure to NPs alone.

A clear immune functions modulation was perceptible in the current study from co-exposure to NPs with Hg. At 4 hour of exposure, normal response of phagocytosis after NPs exposure alone was increased in co-exposure to Hg. Increased phagocytosis at 8 hours was further increased significantly as well as decrease in phagocytosis at 16 hours came to normal after Hg co-exposure. Moreover, Hg co-exposure to NPs also generated ROS at 8 and 72 hours. In addition, previously induced LPO at 2, 24 and 72 hours remained persistent after Hg co-exposure. Thus, a synergistic effect of NPs against Hg induced viability decrease (8 hours) and antagonistic effect of NPs against increased phagocytosis (8 and 48 hours), OBA (48 hours) and LPO (8 hours) was observed for concomitant exposure. Taking into account the above presented mechanisms for Hg toxicity, the NPs anti-immunotoxic action may be

related to the inhibition or less activation of phagocytes contributing to the less ROS production abolishing associated damage as proved by the current findings. It seems that at early hour, Hg exposure induced ROS (2 and 8 hours) was abolished completely by NPs co-exposure at 2 hours due to normal phagocytosis, and an incomplete ROS elimination was observed at 8 hours corroborating the less phagocytic activation when compared to Hg exposure alone. However, at the end of the exposure (72 hours), both NPs and Hg are equally immunotoxic since their interaction seems to generate ROS individually, and the damage remains same at both the cases when compared to their individual exposure. Thus, it is possible to predict that the likelihood of ROS involvement in damage is more in Hg exposure (48 hours), whereas NPs has direct lipid damage in the current study. Moreover, long term exposure resulting in bioaccumulation of NPs and Hg seems to overwhelm the activated state of phagocytes. In addition, it is also clear that despite the viability decrease (48 hours), there is a fine-tuning between phagocytosis, OBA and LPO resulting a confrontation of overall viability decrease at the end of the exposure time.

7.4.3. HK-phagocytes responses

HK-phagocytes *in vitro* exposure to NPs displayed viability decrease at 16 hours corroborating the decrease in phagocytosis with no signals of ROS and peroxidative damage to the same exposure time. The results suggest the same mechanisms of direct action for NPs with no ROS involvement as described above for the G-phagocytes. However, the magnitude of the viability and phagocytosis decrease was not stable and remained modulated reaching to normal at the end of exposure. Hg exposure alone depicted a viability decrease at 8 and 16 hours suggesting that Hg alone is immunotoxic. Moreover, the decrease at 8 hours was corroborating to the decrease in phagocytosis. Thus, the mechanisms proposed by Sauvé et al., (2002) that *in vitro* toxicity of Hg may exhibit relatively low metal-related cytotoxicity and dramatic inhibition of phagocytosis (Sauvé et al., 2002) can be suggested here for the same observation. However, the role of phagocytes in free radicals production cannot be suggested here since no activation was observed and thus LPO induction at 8 hours is the result of direct Hg interaction with phagocytes causing damage to lipid. A decrease in phagocytosis is well documented in the literature following either *in vivo* or *in vitro* Hg exposure (Fournier et al., 2001). Moreover, a decrease in phagocytic index may strengthen the explanation of the limited ingestion capacity arising from the interaction of Hg with phagocytes along the time.

NPs in the presence of Hg co-exposure either increased the responses (phagocytosis at 2 hours, OBA at 4 and 8 hours, and LPO at 8 hours) or brought the responses to the normal level (viability at 8 hours and phagocytosis at 24 hours) at the end of the different exposure periods indicating a clear immunotoxic interference of NPs with Hg. It was also clear that between these two immunotoxic agents, only Hg is responsible to induce oxidative stress because of its ability to induce LPO directly (8 hours) as depicted in the current study. However, ROS involvement in peroxidative damage cannot be overlooked since NPs and Hg interaction generated a significant OBA increase at 8 hours. Moreover, viability at 8 hours was preserved, whereas at 16 hours, it increased but not reached up to the control level. Phagocytosis decreased at 16 hours was further decreased ROS were significantly increased at early hour (4 and 8 hours); whereas, the damage remained the same at both, Hg and NPs+Hg. It is important to highlight here that interaction produced synergistic (8 hours) and antagonistic (16 hours) effects on viability. Phagocytes responses once decreased at 16 hours remained feebler with the co-exposure clarifying the direct additive action of NPs and Hg on phagocytic activity. Overall, no or increased NPs effect were prevalent at early hour of exposure; whereas, at late hour of exposure the decrease was prevalent reaching to normal. In parallel, Hg induced negative effects observed at early hours remained persistent at late hour of exposure reaching to normal at the end of the exposure length (72 hours). Thus the tuning of immune defence and oxidative stress resulted in a way that the mitigation of immunotoxic affects was perceptible at the end of the NPs and Hg co-exposures.

7.4.4. S-phagocytes responses

No effect of NPs exposure alone on the viability of S-phagocytes was observed; however, their functional activity (phagocytic activity) was modulated and remains suppressed at the end of exposure time (72 hours). Moreover, since phagocytic decrease was not at the drop of viability, their modulation along the time seems plausible. NPs were also able to damage the phagocytes (8 hours); however, the ROS were not involved as depicted by no OBA difference to the same exposure length. The same explanation of NP's direct effect on damage instead of ROS involvement can be suggested here as described above for gill.

Hg exposure alone reflected an increase in viability at 16 hours and phagocytosis at 4 and 24 hours; moreover, a decrease in phagocytosis was also perceptible at 72 hours among all the studied parameters. Moreover, since phagocytic modulatory responses were not at the drop of viability, their modulation to the normal levels can be suggested here as described above.

A positive interaction of NPs and Hg can be seen in the S-phagocytes since viability was increased or preserved or remained same, phagocytosis as suppressed previously was recovered to normal. However, no ROS or LPO (except 8 hours) was observed in concomitant exposure.

7.4.5. General comparisons

Phagocytes have heterogeneous phenotypes and complex functions within both innate and adaptive immune responses (Gordon, 1998). To date, most experimental studies have been performed on P-, G-, HK- and S-phagocytes (Wang et al., 2013). However, differences among phagocytes from these particular sources remain unclear. In the current study, it seems that the contaminants' recognizing power of different phagocytes isolated from different sources was different for NPs and anthropogenic conventional metal such as Hg. More immunotoxic effects were observed in NPs than Hg in P-, S-, and HK-phagocytes, which indicated that NPs play an important role in immunotoxicity of these phagocytes. However, G-phagocytes showed equal magnitude of immunotoxicity regarding phagocytosis assay showing their susceptibilities towards damage more than others. It was also evident that S-phagocytes failed to maintain the phagocytosis at the end of the exposure period (72 hours) after exposure to NPs alone.

The overall capabilities of the phagocytes towards the maintenance of phagocytosis were in the order of S- < P- < G- and < HK-phagocytes. On the other hand, in case of Hg the sequence was following the order of S- < HK- < P = G-phagocytes. However, in concomitant exposure, P-phagocytes were normal from the beginning to the end of the exposure and thus reflecting its robustness in regards to NPs and their modulatory role in Hg induced immunotoxicity until control level. The overall decreasing sequence of phagocytes maintenance was P- > S- = G- > HK-phagocytes. It was also proved by another endpoint of OBA and LPO. These differences could be related to the differences in lineages of the phagocytes as suggested by Jovanovic et al., (2014); however, the same lineages of the phagocytes observed in the current study (Figure 7.6-7.8) agrees with the opinion of Feng et al., (2011) and Parra et al., (2012) who demonstrated in mammals that more robustness of the P- phagocytes may be related to their more mature nature in comparison to the other phagocytes isolated from the different organs. Moreover, the different responses of the phagocytes may be based on differences in their natural antioxidant concentrations, which are

the first line of defence against the toxic pathway (Mukherjee et al., 2010). Enzymatic and non-enzymatic differences between different fish phagocytes were previously detected in other studies as causes of phagocytes innate immune functions modulation (Ahmad et al., 2000, 2004, 2012; Santos et al., 2004), which might clarify discrepancies found in the literature on the aquatic toxicity of NPs.

7.5. CONCLUSIONS

A. anguilla P-, G-, HK- and S-phagocytes *in vitro* exposure to NPs alone revealed either increase (except HK-phagocytes at 16 hours) or no change in viability suggesting that the cells are metabolically active and resilient to NPs exposure alone. Moreover, maintenance of the phagocytosis was perceptible in the current study since phagocytosis decrease was not at the drop of viability decrease in P-, G- and S-phagocytes.

Phagocytes differential immune response after NPs and Hg exposure alone and in combination was perceptible. In terms of phagocytosis modulation and ROS production the phagocytes responded in the following manner: P- > S- > HK- = G-phagocytes for NPs exposure alone; S- > HK- > P- = G-phagocytes for Hg exposure alone, and HK- > G- = S- > P-phagocytes for concomitant exposure. Thus, P-, S- and HK-phagocytes were more vulnerable towards NPs induced immunotoxicity, whereas G-phagocytes showed equal magnitude of immunotoxicity to both NPs and Hg. It was also evident that S-phagocytes failed to maintain the phagocytosis at the end of the exposure period (72 hours) after exposure to NP and Hg alone.

On the perspective of NP´s regulatory role in relation to Hg induced immunotoxicity, it was revealed that P-phagocytes were normal from the beginning to the end of the exposure and thus reflecting its robustness in regards to NPs and their modulatory role in Hg induced immunotoxicity until control level. The overall decreasing sequence of phagocytes maintenance was P- > S- = G- > HK-phagocytes. It was also proved by another endpoint of OBA and LPO.

Overall, considering Hg as a surrogate for metals and its association with NPs, as well as the likelihood that it could pose a serious threat to aquatic organisms by modulating their immune defense mechanisms if accidentally discharged into the aquatic environment, current

results suggest that the step of NPs-Hg complex removal must not be underrated and should be processed without any more ado.

7.6. REFERENCES

Ahmad I, Coelho J, Mohmood I, Anjum NA, Pacheco M., Santos MA, Duarte AC, Pereira E (2012) Mercury contaminated systems under recovery can represent an increased risk to seafood human consumers – a paradox depicted in bivalves' body burdens. Food Chemistry **133**: 665–670

Ahmad I, Coelho JP, Mohmood I, Pacheco M, Santos MA, Duarte AC, Pereira E (2011 a) Immunosuppression in the infaunal bivalve *Scrobicularia plana* environmentally exposed to mercury and association with its accumulation. Chemosphere **82**: 1541 – 1546

Ahmad I, Mohmood I, Mieiro CL, Coelho JP, Pacheco M, Santos MA, Duarte AC, Pereira E (2011 b) Lipid peroxidation versus antioxidant modulation in the bivalve *Scrobicularia plana* in response to environmental mercury–organ specificities and age effect Original Research Article. Aquatic Toxicology. **103**: 150 – 158

Ahmad I, Pacheco M, Santos MA (2004) Enzymatic and nonenzymatic antioxidants as an adaptation to phagocyte-induced damage in *Anguilla anguilla* L. following in situ harbor water exposure. Ecotoxicology and Environmental Safety **57**: 290–302

Ahmad I, Pacheco M, Santos MA (2003) Naphthalene-induced differential tissue damage association with circulating fish phagocyte induction. Ecotoxicology and environmental safety **54**: 7–15

Ahmad I, Hamid T, Fatima M, Chand HS, Jain SK, Athar M, Raisuddin S (2000) Induction of hepatic antioxidants in freshwater catfish (*Channa punctatus* Bloch) is a biomarker of paper mill effluent exposure. Biochimica et Biophysica Acta (BBA) **1523**: 37–48

Ahmad I, Fatima M, Athar M, Khan NZ, Raisuddin S (1998) Responses of Circulating Fish Phagocytes to Paper Mill Effluent Exposure. Bulletin of Environmental Contamination and Toxicology **61**: 746–753

Ambashta RD, Sillanpaa M (2010) Water purification using magnetic assistance: a review. Journal Hazard Mater **180**: 38–49

Bartneck M, Keul HA, Singh S, Czaja K, Bornemann J, Bockstaller M., Moeller M, Zwadlo-Klarwasser G, Groll J (2010) Rapid uptake of gold nanorods by primary human blood phagocytes and immunomodulatory effects of surface chemistry. ACS Nano **4**: 3073–3086

Berry CC, Wells S, Charles S, Aitchison G, Curtis AS (2004) Cell response to dextran-derivatised iron oxide nanoparticles post internalisation. Biomaterials **25**: 5405–13

Berry CC, Wells S, Charles S, Curtis AS (2003) Dextran and albumin derivatised iron oxide nanoparticles: influence on fibroblasts *in vitro*. Biomaterials **24**: 4551–7

Bradford MM (1976) Rapid and sensitive method for the quantitation of microgram quantities of protein utilizing the principle of protein-dye binding. Analytical Biochemistry **72:** 248–25

Bulte JM, Kraitchman DL (2004 a) Monitoring cell therapy using iron oxide MR contrast agents. Current Pharmaceutical Biotechnology **5**: 567–584

Bulte JW, Kraitchman DL (2004 b) Iron oxide MR contrast agents for molecular and cellular imaging. NMR in Biomedicine **17**: 484–499

Dobrovolskaia MA, McNeil SE (2007) Immunological properties of engineered nanomaterials. Nature Nanotecnology **2**: 469–478

Fatima M, Ahmad I, Sayeed I, Athar M, Raisuddin S (2000) Pollutant-induced over-activation of phagocytes is concomitantly associated with peroxidative damage in fish tissues. Aquatic Toxicology **49**: 243–250

Feng X, Deng T, Zhang Y, Su S, Wei C, Han D (2011) Lipopolysaccharide inhibits macrophage phagocytosis of apoptotic neutrophils by regulating the production of tumour necrosis factor alpha and growth arrest-specific gene 6. Immunology **132**: 287–295

Fraga CG, Oteiza PI (2002) Iron toxicity and antioxidant nutrients. Toxicology **180**: 23–32

Fournier M, Pellerin J, Clermont Y, Morin Y, Brousseau P (2001) Effects of *in vivo* exposure of *Mya arenaria* to organic and inorganic mercury on phagocytic activity of hemocytes. Toxicology **161**: 201–211

Fujiki K, Yano T (1997) Effects of sodium alginate on the non-specific defence system of the common carp (*Cyprinus carpio* L.). Fish and Shellfish Immunology **7**: 417–427

Geeraerts C, Belpaire C (2010) The effects of contaminants in European eel: a review. Ecotoxicology **19**: 239–266

Girginova PI, Daniel-da-Silva AL, Lopes CB, Figueira P, Otero M, Amaral VS, Pereira E, Trindade T (2010) Silica coated magnetite particles for magnetic removal of Hg^{2+} from water. Journal of Colloid and Interface Science **345**: 234–240

Gordon S (1998) The role of the macrophage in immune regulation. Immunologic Research **149**: 685–688

Handy R, Henry T, Scown T, Johnston B, Tyler C (2008 a) Manufactured nanoparticles: their uptake and effects on fish - a mechanistic analysis. Ecotoxicology **17**: 396–409

Handy R, Owen R, Valsami-Jones E (2008 b) The ecotoxicology of nanoparticles and nanomaterials: current status, knowledge gaps, challenges, and future needs. Ecotoxicology **17**: 315–325

Handy R, von der Kammer F, Lead J, Hassellöv M, Owen R, Crane M (2008 c) The ecotoxicology and chemistry of manufactured nanoparticles. Ecotoxicology **17**: 287–314

Isani G, Falcioni ML, Barucca G, Sekar D, Andreani G, Carpenè E, Falcioni G (2013) Comparative toxicity of CuO nanoparticles and $CuSO_4$ in rainbow trout. Ecotoxicology and Environmental Safety **97**: 40–46

Jain TK, Reddy MK, Morales MA, Leslie-Pelecky DL, Labhasetwar V (2007) Biodistribution, Clearance and Biocompatibility of Iron Oxide Magnetic Nanoparticles in Rats. Molecular Pharmaceutics **5**: 316–327

Jovanovic B, Whitley EM, Palic D (2014) Histopathology of fathead minnow (*Pimephales promelas*) exposed to hydroxylated fullerenes. Nanotoxicology **8**: 755-763

Jovanović B, Palić D (2012) Immunotoxicology of non-functionalized engineered nanoparticles in aquatic organisms with special emphasis on fish - Review of current knowledge, gap identification, and call for further research. Aquatic Toxicology **118–119**:141–151

Karlsson HL, Gustafsson J, Cronholm P, Moller L (2009) Size dependent toxicity of metal oxide particles - a comparison between nano- and micrometer size. Toxicology Letters **188**: 112–8

Karlsson HL, Holgersson A, Moller L (2008) Mechanisms related to the genotoxicity of particles in the subway and from other sources. Chemical Research in Toxicology **21**: 726–31

Kim BC, Lee J, Um W, Kim J, Joo J, Lee JH, Kwak JH, Kim JH, Lee C, Lee H, Addleman RS, Hyeon T, Gu MB, Kim J (2011) Magnetic mesoporous materials for removal of environmental wastes. Journal Hazard Mater **192**: 1140–1147

Klaine SJ, Alvarez PJ, Batley GE, Fernandes TF, Handy RD, Lyon DY, Mahendra S, McLaughlin MJ, Lead JR (2008) Nanomaterials in the environment: Behavior, fate, bioavailability, and effects. Environmental Toxicology and Chemistry **27**: 1825–1851

Krpetic Z, Porta F, Caneva E, Dal Santo V, Scari G (2010) Phagocytosis of biocompatible gold nanoparticles. Langmuir **26**: 14799–14805

Lima R, Espirito AP, Porto R, Fraceto L (2011) Evaluation of cyto- and genotoxicity of poly(lactide-co-glycolide) nanoparticles. Journal of Polymers and the Environment **19**: 196–202

Lloyd RV, Hanna PM, Mason RP (1997) The origin of the hydroxyl radical oxygen in the Fenton reaction. Free Radical Biology & Medicine **22**: 885–888

Mahmoudi M, Simchi A, Imani M, Shokrgozar MA, Milani AS, Hafeli UO, Stroeve P (2010) A new approach for the *in vitro* identification of the cytotoxicity of superparamagnetic iron oxide nanoparticles. Colloids and Surfaces B: Biointerfaces **75**: 300–309

Mahmoudi M, Simchi A, Imani M, Milani AS, Stroeve P (2009) An *in vitro* study of bare and poly(ethylene glycol)-co-fumarate coated superparamagnetic iron oxide nanoparticles: a new toxicity identification procedure. Nanotechnology **20**: 225104–22512

Manibusan MK, Odin M, Eastmond DA (2007) Postulated Carbon Tetrachloride Mode of Action: A Review. Journal of Environmental Science and Health, Part C **25**: 185–209

Matranga V, Corsi I (2012) Toxic effects of engineered nanoparticles in the marine environment: Model organisms and molecular approaches. Marine Environmental Research **76**: 32–40

Moeller S, Kegler R, Sternberg K, Mundkowski RG (2012) Influence of sirolimus-loaded nanoparticles on physiological functions of native human polymorphonuclear neutrophils. Nanomedicine: Nanotechnology, Biology and Medicine **8**: 1293–1300

Mohmood I, Ahmad I, Asim M, Costa L, Lopes CB, Trindade T, Duarte AC, Pereira E (2014) Interference of the co-exposure of mercury with silica-coated iron oxide nanoparticles can modulate genotoxicity induced by their individual exposures—a paradox depicted in fish under in vitro conditions. Environmental Science and Pollution Research **22**: 3687–3696

Moore MN (2006) Do nanoparticles present ecotoxicological risks for the health of the aquatic environment? Environment Internacional **32:** 967–976.

Mukherjee SP, Lyng FM, Garcia A, Davoren M, Byrne HJ (2010) Mechanistic studies of *in vitro* cytotoxicity of poly(amidoamine) dendrimers in mammalian cells. Toxicology and Applied Pharmacology **248**: 259–68

Nagelkerke LA, Pannevis MC, Houlihan DF, Secombes CJ (1990) Oxygen uptake of rainbow trout (*Oncorhynchus mykiss*) phagocytes following stimulation of the respiratory burst. Journal of Experimental Biology **154**: 339–353

Parra D, Rieger A, Li J, Zhang YA, Randall LM, Hunter CA, Barreda DR, Sunyer JO, (2012) Pivotal advance: peritoneal cavity B-1 B cells have phagocytic and microbicidal capacities and present phagocytosed antigen to $CD4^+$ T cells. Journal of Leukocyte Biology **91**: 525–536

Paul N, Sengupta M (2013) Lead induced overactivation of phagocytes and variation in enzymatic and non-enzymatic antioxidant defenses in intestinal macrophages of *Channa punctatus*. Modern Research in Inflammation **2**: 28–35

Perreault F, Melegari SP, Costa CH, Oliveira AL, Popovic R, Matias WG (2012) Genotoxic effects of copper oxide nanoparticles in Neuro 2A cell cultures. Science of the Total Environment **441**: 117–124

Planque MR, Aghdaei S, Roose T, Morgan H (2011) Electrophysiological Characterization of Membrane Disruption by Nanoparticles. ACS Nano **5**: 3599–3606

Raisuddin S, Singh KP, Zaidi SI, Paul BN, Ray PK (1993) Immunosuppressive effects of aflatoxin in growing rats. Mycopathologia **124**: 189–194

Roesslein M, Hirsch C, Kaiser JP, Krug HF, Wick P (2013) Comparability of *in vitro* tests for bioactive nanoparticles: a common assay to detect reactive oxygen species as an example. International Journal of Molecular Sciences **14**: 24320–24337

Rousselet E, Levin M, Gebhard E, Higgins BM, DeGuise S, Godard-Codding CJ (2013) Evaluation of immune functions in captive immature loggerhead sea turtles (*Caretta caretta*). Veterinary Immunology and Immunopathology **156**: 43–53

Santos MA, Pacheco M, Ahmad I (2006) Responses of European eel (*Anguilla anguilla* L.) circulating phagocytes to an in situ closed pulp mill effluent exposure and its association with organ-specific peroxidative damage. Chemosphere **63**: 794–801

Santos MA, Pacheco M, Ahmad I (2004) *Anguilla anguilla* L. antioxidants responses to *in situ* bleached kraft pulp mill effluent outlet exposure. Environment International **30**: 301–308

Santos MA, Pacheco M (1996) *Anguilla anguilla* L. Stress Biomarkers Recovery in Clean Water and Secondary-Treated Pulp Mill Effluent. Ecotoxicology and environmental safety **35**: 96–100

Sauvé S, Brousseau P, Pellerin J, Morin Y, Senecal L, Goudreau P, Fournier M (2002) Phagocytic activity of marine and freshwater bivalves: *in vitro* exposure of hemocytes to metals (Ag, Cd, Hg and Zn). Aquatic toxicology **58**: 189–200

Semete B, Booysen L, Lemmer Y, Kalombo L, Katata L, Verschoor J, Swai HS (2010) *In vivo* evaluation of the biodistribution and safety of PLGA nanoparticles as drug delivery systems. Nanomedicine: Nanotechnology, Biology and Medicine **6**: 662–671

Shaw BJ, Handy RD (2011) Physiological effects of nanoparticles on fish: a comparison of nanometals versus metal ions. Environment International **37**: 1083–1097

Singh N, Gareth JS, Asadi R, Doak S (2010) Potential toxicity of superparamagnetic iron oxide nanoparticles (SPION). Nano Reviews **1**. 10.3402/nano.v1i0.5358

Tavares DS, Lopes CB, Daniel-da-Silva AL, Duarte AC, Trindade T, Pereira E (2014) The role of operational parameters on the uptake of mercury by dithiocarbamate functionalized particles. Chemical Engineering Journal **254**: 559–570

Tavares DS, Daniel-da-Silva AL, Lopes CB, Silva NJ, Amaral VS, Rocha J, Pereira E, Trindade T (2013) Efficient sorbents based on magnetite coated with siliceous hybrid shells for removal of mercury ions. Journal of Materials Chemistry A **1**: 8134–8143

Tellez-Bañuelos MC, Santerre A, Casas-Solis J, Bravo-Cuellar A, Zaitseva G (2009) Oxidative stress in macrophages from spleen of Nile tilapia (*Oreochromis niloticus*) exposed to sublethal concentration of endosulfan. Fish & Shellfish Immunology **27**: 105–111

Valko M, Morris H, Cronin M TD (2005) Metals, Toxicity and Oxidative Stress. Current Medicinal Chemistry **12**: 1161–1208

Wang C, Yu X, Cao Q, Wang Y, Zheng G, Tan TK, Zhao H, Zhao Y, Wang Y, Harris D (2013) Characterization of murine macrophages from bone marrow, spleen and peritoneum. BMC Immunology **14**: 1–10

Zhu X, Tian S, Cai Z (2012) Toxicity assessment of iron oxide nanoparticles in zebrafish (*Danio rerio*) early life stages. PLoS One **7**: 1–6

CHAPTER 8

Overview

8. OVERVIEW

This chapter has been conceived with the intention to overview the various topics dealt within chapter 2 to 7 by integrating i) the discussions of the main outcomes of each chapter, ii) their link to the objectives of the thesis, and iii) their contribution to the scientific knowledge in order to investigate mercury (Hg) toxicity, its nano-remediation and the influence of increased temperature in the toxicity of Hg, either alone or in the presence of arsenic (As) and cadmium (Cd) to seawater organisms.

It is important to point out that the present research has contributed to understand the efficacy of newly synthesised functionalized silica coated nanoparticles (NPs) for Hg decontamination in single and multi-contaminated spiked seawater, by using, both chemical and ecotoxicological lines of evidence. The research also enlightens the effect of increased temperature, within the context of climate change, on fish (*A. anguilla*) gill and its effect on the efficiency of NPs in the toxicity reduction of Hg alone or in the presence of other elements like As and Cd. To study the problem related with temperature increase the *ex vivo* approach was adopted, which allowed us to directly assess the temperature effects on the gills as a more likely scenario under natural environmental conditions and reducing interfering variables (Britto et al., 2012). Nevertheless, *in vitro* studies were also considered to check the intrinsic behaviour of the NPs and their eco-friendly nature keeping in view hour to day experiments, by using health parameters related to immune and genetic responses. In accordance, this study was performed at the following three interdisciplinary interface of biology chemistry: 1) chemical efficacy of the nano-remediation process and ecotoxicity evaluation; 2) the toxicity reducing potential of the nano-remediation process under the climate change scenario, by evaluating the interactive effect of increased temperature on NPs remediated seawater-induced biochemical stress responses (damage *vs.* protection) in fish under *ex vivo* conditions; 3) the toxicity of Hg and NPs to a seawater organism, by evaluating the toxicity of Hg and the NPs used for Hg-removal, mainly focusing on the geno- and immunotoxicity.

After the extensive literature search and revision on the existing knowledge related to the use of nanotechnology in water contaminants removal (Chapter 2), the Chapter 3 came into existence in order to observe the efficacy of NPs to remove Hg from seawater spiked with single (Hg) or with a mixture of contaminants (Hg, As and Cd), where the evaluation of the ecotoxicity of Hg in presence of As and Cd using seawater organisms in nano-remediated and

non nano-remediated seawater was a key question. The results reflected that the NPs are very efficient and selective for the removal of Hg from single- and multi-contaminated (Hg + Cd + Pb) spiked seawater; the magnetic NPs with dithiocarbamate functionalization are unable to remove As and Cd, and their co-existence with Hg has no interference or effect on the rate of Hg removal by the NPs. Nevertheless, the removal of Hg by the NPs is faster for lower concentrations (Hg 50 µg/L). Concerning the ecotoxicological profile, difference in toxicities was observed for remediated and non-remediated solutions. As expected, the non-remediated solutions caused higher toxicity than the remediated ones, highlighting the effectiveness of the magnetic NPs on the toxicity removal. Moreover, the ecotoxicological results allow to conclude that after the remediation process, the mixture with lower concentrations of the three elements did not exhibit toxicity to the exposed organisms *viz*. rotifer *B. plicatilis* and bacteria *V. fischeri,* while the mixture with higher levels of contaminants, still showed toxicity, indicating that the remediation was not totally effective. Yet, the toxicity to bacteria *V. fischeri*, rotifer *B. plicatilis* and algae *P. tricornutum*, whose responses where inhibited during its exposure to the non-remediated sample, was considerably reduced after treatment with NPs. The microalgae *P. tricornutum* appears to be the most sensitive tested species, while *A. franciscana* showed no adevres effects after being exposed to the tested solutions. In general, the presence of NPs in the seawater did not show toxicity to the selected species. Thus, the combination of high efficiency toward Hg-removal, decrease of water toxicity and magnetic property of the NPs, make this nanomaterial a very promissory and selective adsorbent for application in both *in-situ* and/or *ex-situ* treatment applications, in systems like coastal lagoons, harbours, estuaries, or even aquacultures. However, an optimization of the operational conditions (e.g amount of NPs) should be investigated in order to achieve complete removal efficiency.

In pursuance of the influence of increased temperature, which may considerably effect the efficiency magnetite NPs in the toxicity removal of Hg-contaminated seawater in the absence and presence of As and Cd, Chapter 4 (damage responses such as protein oxidation, LPO and 8-OHdG formation) and Chapter 5 (antioxidants protection) were planned. *Ex viv*o approach was adopted, which allowed us to assess the influence of temperature in the toxicity of the studied elements on the gills as a more likely scenario under natural environmental conditions (Britto et al., 2012) considering biochemical stress responses in *A. anguilla*. In addition, the effect of temperature on Hg accumulation was also observed in remediated and non-

remediated solutions. Concerning the effect of temperature on the uptake of Hg, all the studied groups (non-remediated and remediated with and without NPs) displayed a significant increase in Hg uptake in higher Hg concentration alone and in mixture at the highest temperature. Moreover, the effect of temperature on Hg uptake was more pronounced at higher Hg concentration alone in non-remediated solution or in mixture in remediated solution without NPs.

In Chapter 4, where the damage response (protein oxidation, LPO and 8-OHdG) was studied, Hg induced oxidative damage (LPO increase, 8-OHdG formation and protein oxidation), either alone or in mixture at all exposed temperatures (20 ºC, 24 ºC and 28 ºC) in non-remediated solutions. After remediation (both in solutions with and without NPs), the damage was lower than before remediation confirming the ability of functionalized NPs for Hg toxicity removal. Nevertheless, the remediated solutions with NPs displayed higher toxicity than the remediated solutions without NPs. Concerning NPs alone, no change in biochemical responses were observed in fish exposed to NPs at 20°C. The influence of temperature on NPs toxicity was clearly evident in the levels of PC and 8-OHdG as significant induction in these two parameters, at the highest temperature, was observed in fish gill. In non-remediated solutions, a significant increase was observed for LPO, PC and 8-OHdG at all treatments with increasing temperature. In remediated solution with NPs, the influence of temperature was more prominent at the highest temperature as a significant increase in LPO (solution I, II and IV), PC contents (solution II) and 8-OHdG (at all solutions) and a decrease in PC content (solution IV) were observed at 28 °C. In remediated solution without NPs, a different pattern of responses was observed, since effects at the studied biochemical markers were limited to Hg concentrations alone. Thus, increase in temperature by 8 °C revealed an increase in LPO and 8-OHdG (in solution I and II) and a decrease in PC content (in solution II), whereas increase of 4 °C temperature depicted increase in LPO and 8-OHdG in solution II confirming that the oxidative stress inducing potential of Hg remediated solutions further increases with an increase in temperature. This study allows foresee that under future climate change scenarios, a rise in water temperature will promote the absorption of Hg and consequently will increase damage to lipid, protein and DNA, in *A. anguilla* gill (Chapter 4). It was pointed out that the adopted remediation technology is highly efficient in decreasing the toxicity of Hg at an average temperature of 20 ºC; however, its efficiency may be reduced under scenarios of increased temperature, and, thus, should be remodelled under the climate change scenario in future.

Chapter 5 constituted a further step in order to achieve the understanding of antioxidants protection responses against nano-remediated Hg in the presence and absence of As and Cd, as well as to an exposure within the increasing temperature scenario. The main observation of this study is that an overall antioxidants induction was observed in all exposure scenarios (non-remediated and remediated solutions with and without NPs), except GR (in remediated solutions with NPs) and GST, GPx and thiols (in remediated solutions without NPs). Moreover, the antioxidants induction remains unaffected in the presence of As and Cd. Comparing the different scenarios, a less pronounced antioxidants induction in remediated solutions (*vs.* non-remediated) was observed, suggesting that the antioxidants modulatory response is due to the incomplete nano-remediation of the Hg. Regarding the influence of temperature, in non-remediated solutions, all antioxidants showed a differential response at increased temperatures, depending on the Hg being alone or in a mixture: gills exposed to Hg alone revealed a significant antioxidants increase at high temperature, whereas a decrease was perceptible under the scenario of Hg in mixture. In remediated solutions with NPs, antioxidants induction was discernible at 24 ºC in GPx, GR and thiols at lower concentration of Hg in mixture, whereas at 28 ºC all the antioxidants (except GPx) showed a significant increase suggesting that in predicted scenarios of increasing temperature the remediated water that caused almost no oxidative effects at 20 ºC, can exhibit oxidative effects. In remediated solution without NPs, the modulatory effect of temperature on antioxidants induction was perceptible even after the removal of NPs since at 24 ºC only CAT (solution I, II, IV) and GSH (solution III), whereas at 28 ºC all the antioxidants (CAT) showed a significant increase. Moreover, the antioxidant induction was less pronounced when compared to the non-remediated solutions at increased temperature suggesting that the efficiency of the NPs remediation decreases with the increase of temperature. Overall, the antioxidant defences were likely overwhelmed in the fish gill, leading to increased Hg accumulation and exaggerated Hg toxicity when the temperature was increased. These observations have important implications for the survival of fish in polluted environments during seasonal warming and/or predicted global climate change scenarios.

In order to get the information on Hg contaminants and/or by the NPs used in the nano-remediation process, Chapter 6 and Chapter 7 were planned focusing on genotoxicity and immunotoxicity. In these chapters an *in vitro* model system was adopted due to its rapidity, effectiveness, relevance and importance to assess NPs toxicity for a number of endpoints in the absence of clear regulatory guideline(s) on the NPs testing/evaluation in fish (Arora et al. 2012).

The results in Chapter 6 revealed that the NPs exposure alone is able to induce genotoxicity (significant increase in irreparable genetic lesions *i.e.* ENA) in *A. anguilla* blood cells at both early (2, 4, 8 hours) and late (16, 24, 48, 72 hours) hour of exposure. However, NPs combined with Hg revealed no ENA increase at the end of 2 hour exposure suggesting that NPs-Hg complex formation is efficient to eliminate the DNA damage induced by either NPs or Hg individual exposure. Hence, the occurrence of antagonism between NPs and Hg was perceptible; however, at late hour exposure, NPs were unable to mitigate the mercury-accrued negative impacts. The significant increase in reparable genetic lesions *viz.* 8-OHdG at 2 (early) and 48 (late) hours clearly suggested the discontinuity of the NPs induced $HO^{\cdot}$ radical production for 72 hours. However, NPs in combination with Hg revealed an increase in 8-OHdG levels at all the exposure length (except 16 hours) suggesting that both NPs and Hg independently oxidized DNA through the ROS production. In addition, positive correlations between ENA and 8-OHdG confirmed that NPs' oxidative stress inducing potential was increased with Hg co-exposure and persisted until 72 hours. In addition, NPs exposure combined with Hg co-exposure also revealed an additive effect on 8-OHdG levels at both early and late hour of exposure, and on LPO only at late hour (except 24 hours) of exposure suggesting that DNA is more susceptible to per-oxidative damage than lipid. In addition, LPO increase in an additive manner may suggest the failure of ROS scavenging activity of NPs overtime since Hg exposure alone induced 8-OHdG or LPO to late hour of exposure only. On the perspective of *in vitro* Hg exposure to plasma, a significant 8-OHdG increase at early (8 hours) and late (24, 48, 72 hours) hour of exposure was revealed indicating that Hg is not as capable as NPs to induce genotoxicity since NPs generated the genotoxic response at very early hour (2 hours) of exposure. Finally, results confirmed that the consideration of other contaminants is equally important while interpreting the fish genotoxic responses to NPs in a multi-contamination state. In addition, the current results suggested that the step of NPs-Hg complex removal must not be underrated and should be processed without any more ado.

In Chapter 7, the results elucidated that the *A. anguilla* peritoneum (P-phagocytes), gill (G-phagocytes), head-kidney (HK-phagocytes) and spleen (S-phagocytes) *in vitro* exposure to NPs alone revealed either increase (except HK-phagocytes at 16 hours) or no change in viability suggesting that the cells are metabolically active and resilient to NPs exposure alone. Moreover, maintenance of the phagocytosis was perceptible in the current study since phagocytosis decrease was not at the drop of viability decrease in P-, G- and S-phagocytes.

Phagocytes differential immune response after NPs and Hg exposure alone and in combination was perceptible. In terms of phagocytosis modulation and ROS production the phagocytes responded in the following manner: P- > S- > HK- = G-phagocytes for NPs exposure alone; S- > HK- > P- = G-phagocytes for Hg exposure alone, and HK- > G- = S- > P-phagocytes for exposure to both chemicals. Thus, P-, S- and HK-phagocytes were more vulnerable towards NPs induced immunotoxicity, whereas G-phagocytes showed equal magnitude of immunotoxicity to both NPs and Hg. It was also evident that S-phagocytes failed to maintain the phagocytosis at the end of the exposure period (72 hours) after exposure to NPs and Hg alone. On the perspective of NP´s regulatory role in relation to Hg induced immunotoxicity, it was revealed that P-phagocytes were normal from the beginning to the end of the exposure and thus reflecting its robustness in regards to NPs and its modulatory role in Hg induced immunotoxicity until control level. The overall decreasing sequence of phagocytes maintenance was P- > S- = G- > HK-phagocytes. It was also proved by another endpoint of OBA and LPO. Overall, considering Hg and its association with NPs, as well as the likelihood that it could pose a serious threat to aquatic organisms by modulating their genetic responses and immune defence mechanisms if accidentally discharged into the aquatic environment, current results suggest that the step of NPs-Hg complex removal must not be underrated and should be processed without any more ado.

The work presented herein provided a new knowledge on the understanding of the efficiency of newly synthesised functionalized silica coated NPs for Hg decontamination in presence or absence of hazardous contaminants (As and Cd) in seawater as checked by using ecotoxicological line of evidence within scenarios of increasing temperature. In addition, this study also enlightens a better understanding of the effect of temperature, after detoxification process of Hg by using NPs from seawater in presence and absence of other hazardous contaminants.

As major outcomes, the NPs were efficient for Hg decontamination from single- and multi-contaminated seawater. Moreover, NP's efficiency in decreasing toxicity of seawater contaminated with Hg at 20 ºC can be at the risk under scenarios of increased temperature as a consequence of climate change. In addition, the step of NPs-Hg complex removal must not be underrated and should be processed without any more ado since the interference of the co-exposure of Hg with NPs can modulate health parameters (genotoxicity, immunotoxicity) induced by their individual exposures. Eventually, this work also strengthened the opinion that the combined use of chemical and ecotoxicological measurements is a practical and

suitable approach, which revealed a high efficiency for the remediation of Hg-contaminated seawater. Nevertheless, *A. anguilla* gill proved to be a good *ex vivo* model for Hg and other hazardous contaminants toxicity assessment under the climate change scenario. These results may be used as basic data to predict the potential adverse effects of Hg with water temperature changes resulting from climate warming and hazardous contaminants pollution. Moreover, the data presented here emphasizes the importance of need for more research to understand the extent of the ability or lack of that in poikilotherms to tolerate metals contamination under predicted scenarios of climate change.

The observations of this study open up new insights on the efficiency of newly synthesised NPs to remove Hg as well as the interactive effects of temperature on Hg before and after nano-remediation in presence of other hazardous contaminants in seawater and on the eco-friendly nature of the NPs. However, to improve the understanding of other climate change factor such as pH and salinity on interactive effect on Hg before and after the nano-remediation process (in presence of other hazardous contaminants) further toxicity studies are imperative and should be carried out. Moreover, new nanomaterials should be developed to remove other hazardous contaminants such as As and Cd from seawater and the efficiency of the new material should be checked by combining both chemical and ecotoxicological approach to get a complete picture of the water treatment process.

8.1 REFERENCES

Arora S, Rajwade JM, Paknikar KM (2012) Nanotoxicology and *in vitro* studies: The need of the hour. Toxicol. Appl. Pharmacol 258:151–165.

Britto RS, Garcia ML, Rocha AM, Flores JA, Pinheirc MVB, Monserrat JM, Ferreira JLR (2012) Effects of carbon nanomaterials fullerene C60 and fullerol C60(OH)18–22 on gills of fish Cyprinus carpio (Cyprinidae) exposed to ultraviolet radiation. Aquatic Toxicology 114–115, 15:80–87

Xiu M, Pan L, Jin Q (2014). Bioaccumulation and oxidative damage in juvenile scallop Chlamys farreri exposed to benzo[a]pyrene, benzo[b]fluoranthene and chrysene. Ecotoxicol Environ Saf. 107:103-10